

# Influence of drought and recovery on fungal communities and fine-roots associated to European beech and Norway spruce considering inter- and intraspecific tree mixture

Jasmin Ute Danzberger

Vollständiger Abdruck der von der TUM School of Life Sciences der Technischen Universität München zur Erlangung einer

Doktorin der Naturwissenschaften (Dr. rer. nat.)

genehmigten Dissertation.

Vorsitz: Prof. Dr. Johannes Kollmann

Prüfende der Dissertation:

1. apl. Prof. Dr. Karin Pritsch
2. Prof. Dr. J. Philipp Benz
3. Prof. Dr. Tamir Klein

Die Dissertation wurde am 19.03.2024 bei der Technischen Universität München eingereicht und durch die TUM School of Life Sciences am 25.07.2024 angenommen.

*“For my dreams I hold my life  
For wishes I behold my night  
The truth at the end of time  
Losing faith makes a crime”*

Tuomas Holopainen (Nightwish), Sleeping Sun

## I Summary

Forests cover around one-third of the land area of our planet and impact the global climate through various means, including the storage of approximately 45% of terrestrial carbon. However extreme and frequent droughts resulting from climate change have far-reaching consequences for forests, even leading to forest dieback. Nevertheless, trees have developed strategies to withstand periods of drought. For example, increased fine-root growth has been shown to increase water uptake when drought occurs. Yet, with prolonged drought, root mortality increases. Drought reactions differ between tree species. While beech, for example, shows a high carbon turnover during drought and continuously produces new fine-roots of short life span, spruce relies on carbon preservation through mechanisms such as maintaining its roots with a protective suberin layer. Moreover, the mixture of tree species can positively influence the performance of trees in mild to moderate droughts if their traits, for example rooting depth, are complementary. Ectomycorrhizal (ECM) fungi can provide the tree with root-inaccessible water and make nutrients available to the plant while receiving photosynthetic products from the plant. With the onset of drought, the proportion of fungal species classified as long- and medium-distance exploration types, which might have better access to soil water reserves, increases. However, fungal species differ in their drought resistance, which can lead to changes in the fungal community during drought.

In this dissertation, five questions are considered, which, with the help of two experiments, should lead to a better understanding of fungus-tree interactions in beech and spruce under drought and rewatering:

1. Are fungal communities in drought-prone regions better adapted to dry periods compared to communities in moist regions and thus less affected by drought?
2. Are seedlings less affected by drought when growing in soils with drought-adapted fungal communities and interspecific root interaction?
3. How do the fine-root systems of mature beech and spruce recover within three months upon drought release after five years of repeated summer drought?

4. Do root-associated fungal communities connected to beech and spruce recover after rewatering to resemble their pre-drought composition?
5. How does a species mixture of beech and spruce affect the fine-root recovery of both trees and the respective root-associated fungal communities compared to single species?

To address questions 1 and 2, a greenhouse experiment was set up, in which beech (1 year) and spruce (2 years) seedlings were planted in soils originating from different regions characterized by varying rainfall histories. Seedlings were established in inter- and intraspecific mixture, subjected to a two-month drought, and labelled with  $^{13}\text{C}$ -enriched  $\text{CO}_2$  at the end of the drought period. Before and after drought, the fungal communities in the soils were assessed, and after the drought, those on the roots as well. To assess growth, the biomass of roots, stems and leaves of seedlings were measured before and after the drought, in addition to the mycorrhization, the number of vital tips, taproot length and root branching were determined at harvest. The  $^{13}\text{C}$ -content was determined in all organs to identify differences in C allocation under drought.

During the experimental drought, the fungal community associated with beech as well as spruce fine-roots changed the least in dry region soils and the most in moist region soils, indicating an adaption of the fungal communities to the climatic conditions of the region. Moreover, the prevailing ECM taxa in both dry region soil and root samples, regardless of drought or control conditions, were classified as long-distance and medium-distance exploration types. However, a better performance of the seedlings in the soils from dry regions could not be shown. Differences in the root architecture of the seedlings in the different soils (described by taproot length, root branching intensity, number of vital root tips and degree of mycorrhization) suggest that the architecture of the root system plays a critical role in the drought tolerance of the seedlings, especially in beech. Nonetheless, the colonisation of roots with ECM fungi can affect the root system architecture and thus influence

the seedlings' drought performance. A positive effect when beech and spruce seedlings grew together in mixture could not be observed.

To address questions 3, 4 and 5, mature beech and spruce trees at forest stand level were irrigated after five years of an experimental summer drought and the spruce trees of one plot pair were labelled with  $^{13}\text{C}$ -depleted  $\text{CO}_2$  within the Kranzberg roof (KROOF) experiment. Over a period from one week before to three months after irrigation, growth, vitality and mycorrhization of beech and spruce fine-roots were investigated using mesh bags. The root-associated fungal communities in the different interaction zones (beech neighbouring beech (BB), beech neighbouring spruce (Bmix), spruce neighbouring beech (Smix) and spruce neighbouring spruce (SS)) were investigated using fine-roots from soil cores. After rewatering, spruce prioritised fine-root growth. Moreover, an extensive portion of the photoassimilates synthesised during the rewatering phase was rapidly transported into the growing fine-roots after drought release, improving water uptake. However, the proportion of these new photoassimilates found in the mycorrhizae resembled those of the non-droughted control over the same period, suggesting that the symbiosis in terms of sink strength was unaffected by the drought as long as the corresponding roots were vital. Yet, it is possible that the time between the colonisation of new growing roots with ECM fungi and full mycorrhiza formation led to an asynchrony in C allocation between fine-root growth and mycorrhizae. The recovery of the fine-root system differed between beech and spruce. While in beech new fine-roots were formed, suberised fine-roots in spruce were reactivated and grew as good as the control roots. Yet, the longevity and vitality of these reactivated spruce fine-roots were reduced. The fungal communities associated with both tree species did not change significantly within three months, indicating a stable and adapted community that can tolerate significant fluctuations in soil moisture. However, the composition of the fungal communities appeared to be dependent on the species specific responses of trees to drought and rewatering. Furthermore, a large proportion of fungi assigned to saprotrophs were also reported to have a secondary root-associated lifestyle. This secondary lifestyle might enhance their ability to withstand

drought by benefiting from enhanced nutrient availability resulting from increased root exudation and consistent soil moisture in the rhizosphere during drought. A mixture effect regarding root regeneration could only be detected on individual measurement days, with lower vitality and reduced growth observed in spruce roots within the mixture. The species richness of root-associated fungi, though, was highest in the mixture, which could be due to the soil heterogeneity in this zone and the associated niche diversity. In addition, the tree mixture seemed to have a positive effect on the abundance of spruce-specific ECM fungi, as it was higher in the species mixture than in monospecific spruce interaction.

Based on these results, the five initial questions concerning the reaction of fungal communities and fine-roots during drought and recovery can now be answered. I was able to show that fungal communities in drought-adapted soils were less affected by drought than those in soils from moister regions. Nevertheless, it appears that plant growth during drought was likely more responsive to taproot length, root branching intensity and degree of mycorrhization than long-term adaption in fungal symbiosis. Yet, it cannot be excluded that fungi influenced the seedlings' drought tolerance by for example exudation of fungal hormones affecting seedling growth including root architecture. Hence, a possible contribution of fungi on seedlings' drought tolerance needs further investigation, including other microbial groups and their interplay with root-associated fungi, as well as specific root-fungus interactions. After 5 years of repeated droughts, fine-root systems were able to recover, and their recovery was prioritised above all other organs in terms of C transport and allocation. Nevertheless, the fungal communities established during the drought conditions were stable for the first three months after rewatering. Their composition, however, was strongly linked to the tree species-specific drought and recovery responses. Tree species mixture had no clear influence on the recovery of the fine-root system, but increased fungal diversity. The focus of this study is primarily on the initial phases of recovery, leaving the long-term consequences and the relationship between root growth and fungi uncertain, necessitating further investigation. With the rising occurrence and duration of droughts, there

is a need to determine whether the trees undergoing recovery can endure future droughts, providing insights into forest dynamics under changing climate conditions.

## II Zusammenfassung

Wälder bedecken etwa ein Drittel der Landfläche unseres Planeten und beeinflussen das globale Klima unter anderem dadurch, dass sie etwa 45 % des terrestrischen Kohlenstoffs speichern. Doch extreme und häufige Dürreperioden infolge des Klimawandels haben weitreichende Folgen für die Wälder und können sogar zum Waldsterben führen. Bäume haben jedoch Strategien entwickelt, um Dürreperioden zu überstehen. So hat sich beispielsweise gezeigt, dass ein verstärktes Feinwurzelwachstum die Wasseraufnahme bei Trockenheit erhöht. Bei längerer Trockenheit jedoch nimmt die Wurzelsterblichkeit zu. Die Reaktionen auf Trockenheit unterscheiden sich von Baumart zu Baumart. Während die Buche beispielsweise bei Trockenheit einen hohen Kohlenstoffumsatz aufweist und ständig neue Feinwurzeln mit kurzer Lebensdauer produziert, setzt die Fichte auf Kohlenstoffhaltung, indem sie beispielsweise die Wurzeln mit einer schützenden Suberinsschicht versieht. Auch die Mischung von Baumarten kann sich positiv auf die Leistung von Bäumen bei leichter bis mittlerer Trockenheit auswirken, wenn sich ihre Eigenschaften, z. B. die Durchwurzelungstiefe, ergänzen. Ektomykorrhizapilze (ECM) können den Baum über ihre dünnen Hyphen mit für die Wurzeln unzugänglichem Wasser versorgen und der Pflanze Nährstoffe zur Verfügung stellen, während sie von der Pflanze Photosyntheseprodukte erhalten. Mit Beginn der Trockenheit steigt der Anteil der Pilzarten, die als Lang- und Mittelstrecken-Explorationstypen eingestuft werden und einen besseren Zugang zu den Wasserreserven im Boden haben. Allerdings unterscheiden sich Pilzarten in ihrer Trockenheitsresistenz, was zu Veränderungen in der Pilzgemeinschaft während der Trockenheit führen kann.

In dieser Dissertation werden fünf Fragen untersucht, die mit Hilfe von zwei Experimenten zu einem besseren Verständnis der Pilz-Baum-Interaktionen bei Buche und Fichte unter Trockenheit und Wiederbewässerung führen sollen:

1. Sind Pilzgemeinschaften in trockenheitsgefährdeten Regionen bereits an Trockenperioden angepasst und daher weniger von Trockenheit betroffen?



2. Sind Sämlinge weniger von Trockenheit betroffen, wenn sie in Böden mit an Trockenheit angepassten Pilzgemeinschaften und interspezifischen Wurzelinteraktionen wachsen?
3. Wie erholen sich die Feinwurzelsysteme ausgewachsener Buchen und Fichten nach fünf Jahren wiederholter Sommertrockenheit innerhalb von drei Monaten nach der Trockenheit?
4. Erholen sich die wurzelassoziierten Pilzgemeinschaften von Buche und Fichte nach der Wiederbewässerung und ähneln ihrer Zusammensetzung vor der Trockenheit?
5. Wie wirkt sich eine Artenmischung aus Buche und Fichte auf die Erholung der Feinwurzeln beider Bäume und der jeweiligen wurzelassoziierten Pilzgemeinschaften im Vergleich zu einzelnen Arten aus?

Zur Beantwortung der Fragen 1 und 2 wurde ein Gewächshausexperiment durchgeführt, bei dem einjährige Buchen- und zweijährige Fichtensämlinge in Böden aus verschiedenen Regionen mit unterschiedlichen Niederschlagsverläufen gepflanzt wurden. Die Sämlinge wurden in einer inter- und intraspezifischen Mischung gepflanzt, einer zweimonatigen Trockenheit ausgesetzt und am Ende der Dürreperiode mit  $^{13}\text{C}$ -angereichertem  $\text{CO}_2$  markiert. Vor und nach der Trockenheit wurden die Pilzgemeinschaften in den Böden und nach der Trockenheit auch die auf den Wurzeln bestimmt. Darüber hinaus wurde die Biomasse der Wurzeln, des Stammes und der Blätter vor und nach der Trockenheit bestimmt und die Mykorrhizierung, die Anzahl der vitalen Spitzen, die Länge der Hauptwurzel und die Wurzelverzweigung bei der Ernte ermittelt. In allen Organen wurde der  $^{13}\text{C}$ -Gehalt bestimmt, um Unterschiede in der C-Verteilung unter Trockenstress zu identifizieren.

Während der experimentellen Trockenheit veränderte sich die Pilzgemeinschaft, die mit den Feinwurzeln von Buchen und Fichten assoziiert war, in den Böden der Trockenregion am wenigsten und in den Böden der Feuchtregion am meisten, was auf eine Anpassung der Pilzgemeinschaften an die klimatischen Bedingungen der Region hindeutet. So wurden die vorherrschenden ECM-Taxa sowohl in den Boden- als auch in den Wurzelproben der

Trockenregion, unabhängig von den Trockenheits- oder Kontrollbedingungen, als Langstrecken- und Mittelstrecken-Explorationstypen eingestuft. Eine bessere Trockentoleranz der Sämlinge in den Böden aus Trockengebieten konnte jedoch nicht nachgewiesen werden. Die Unterschiede in der Wurzelarchitektur der Sämlinge in den verschiedenen Böden (beschrieben durch die Länge der Hauptwurzel, die Intensität der Wurzelverzweigung, die Anzahl der vitalen Wurzelspitzen und den Grad der Mykorrhizierung) lassen vermuten, dass die Architektur des Wurzelsystems eine entscheidende Rolle für die Trockentoleranz der Sämlinge spielt, insbesondere bei Buche. Die Besiedlung der Wurzeln mit ECM-Pilzen kann sich jedoch auf die Architektur des Wurzelsystems und damit auf die Trockenheitsleistung der Sämlinge auswirken. Ein positiver Mischungseffekt von Buchen- und Fichtensämlingen konnte nicht beobachtet werden.

Zur Beantwortung der Fragen 3, 4 und 5 wurden ausgewachsene Buchen und Fichten auf Waldbestandsebene nach fünf Jahren experimenteller Sommertrockenheit bewässert und die Fichten eines Parzellenpaares im Rahmen des „Kranzberg-Roof“ (KROOF) Experiments mit <sup>13</sup>C-abgereichertem CO<sub>2</sub> markiert. In einem Zeitraum von einer Woche vor der Bewässerung bis drei Monate danach wurden Wachstum, Vitalität und Mykorrhizierung der Buchen- und Fichtenfeinwurzeln mit Hilfe von Netzbeuteln untersucht. Die wurzellozierten Pilzgemeinschaften in den verschiedenen Interaktionszonen (Buche neben Buche (BB), Buche neben Fichten (Bmix), Fichte neben Buche (Smix) und Fichte neben Fichte (SS)) wurden anhand von Boden-Bohrkernen untersucht.

Nach der Wiederbewässerung begünstigte die Fichte das Feinwurzelnwachstum, um die Wasseraufnahme zu verbessern. Zu diesem Zweck wurde ein großer Teil der während der Wiederbewässerungsphase synthetisierten Photoassimilate nach der Trockenheit rasch in die wachsenden Feinwurzeln transportiert, welche die Wasseraufnahme verbessern. Der Anteil dieser neuen Photoassimilate, die in den Mykorrhizen gefunden wurden, ähnelte jedoch dem der Kontrollgruppe ohne Trockenheit im gleichen Zeitraum, was darauf hindeutet, dass die Symbiose in Bezug auf die Senkenstärke durch die Trockenheit nicht beeinträchtigt wurde,

solange die entsprechenden Wurzeln vital waren. Es ist jedoch möglich, dass die Zeit zwischen der Besiedlung neu wachsender Wurzeln mit ECM-Pilzen und der vollständigen Mykorrhizabildung zu einer Asynchronie in der C-Allokation zwischen Feinwurzelwachstum und Mykorrhiza führte.

Die Erholung des Feinwurzelsystems verlief bei Buche und Fichte unterschiedlich. Während bei der Buche neue Feinwurzeln gebildet wurden, wurden bei der Fichte suberisierte Feinwurzeln reaktiviert und wuchsen genauso gut wie die Kontrollwurzeln. Die Langlebigkeit und Vitalität dieser reaktivierten Wurzeln war jedoch geringer als in den Kontrollen. Die Pilzgemeinschaften veränderten sich innerhalb von drei Monaten nicht wesentlich, was auf eine stabile, angepasste Gemeinschaft hinweist, die Schwankungen der Bodenfeuchtigkeit tolerieren kann. Allerdings schien die Zusammensetzung der Pilzgemeinschaften von der Reaktion des Baumes auf Trockenheit und Wiederbewässerung abhängig zu sein. Darüber hinaus wies ein großer Teil der Pilze, die den Saprotrophen zugeordnet werden, auch eine sekundäre, wurzellozierte Lebensweise auf. Diese sekundäre Lebensweise könnte ihre Widerstandsfähigkeit gegenüber Trockenheit erhöhen, da sie von der verbesserten Nährstoffverfügbarkeit infolge der verstärkten Wurzelexsudation und der konstanten Bodenfeuchtigkeit in der Rhizosphäre während der Trockenheit profitiert. Ein Mischungseffekt in Bezug auf die Wurzelregeneration konnte nur an einzelnen Messtagen festgestellt werden, wobei eine geringere Vitalität und ein geringeres Wachstum der Fichtenwurzeln innerhalb der Mischung beobachtet wurden. Der Artenreichtum der wurzellozierten Pilze war in der Mischung am höchsten, was auf die Bodenheterogenität in dieser Zone und die daraus resultierende Nischenvielfalt zurückzuführen sein könnte. Darüber hinaus schien sich die Baummischung positiv auf die Häufigkeit fichtenspezifischer Ektomykorrhizapilze auszuwirken, da sie in der Buche-Fichte Mischung höher ist als in der monospezifischen Fichteninteraktion.

Auf der Grundlage dieser Ergebnisse können die fünf anfänglichen Fragen zur Reaktion von Pilzgemeinschaften und Feinwurzeln während der Trockenheit und der Erholung nun

beantwortet werden. Ich konnte zeigen, dass Pilzgemeinschaften in trockenheitsangepassten Böden weniger von Trockenheit beeinflusst werden als die in Böden aus feuchteren Regionen. Dennoch scheint es, dass das Pflanzenwachstum während der Trockenheit eher von der Länge der Hauptwurzel, der Intensität der Wurzelverzweigung und dem Grad der Mykorrhizierung abhing als von der langfristigen Anpassung der Pilzsymbiose. Es kann allerdings nicht ausgeschlossen werden, dass Pilze die Trockentoleranz der Sämlinge beeinflusst haben, zum Beispiel durch pilzbedingte Veränderungen der Genexpression, die das Wachstum der Sämlinge und die Wurzelarchitektur beeinflussen. Daher muss ein möglicher Beitrag von Pilzen zur Trockentoleranz von Sämlingen weiter untersucht werden, auch im Hinblick auf andere mikrobielle Gruppen und ihr Zusammenspiel mit wurzelassoziierten Pilzen sowie auf spezifische Wurzel-Pilz-Interaktionen. Nach fünf Jahren wiederholter Trockenheit konnten sich die Feinwurzelsysteme erholen, und ihre Erholung hatte in Bezug auf den C-Transport und die Verteilung Vorrang vor allen anderen Organen. Dennoch waren die während der Trockenheit entstandenen Pilzgemeinschaften in den ersten drei Monaten nach der Wiederbewässerung stabil. Ihre Zusammensetzung stand jedoch in engem Zusammenhang mit den baumartenspezifischen Trockenheits- und Erholungsreaktionen. Die Baumartenmischung hatte keinen eindeutigen Einfluss auf die Erholung des Feinwurzelsystems, erhöhte aber die Pilzvielfalt. Der Schwerpunkt dieser Studie liegt in erster Linie auf den ersten Phasen der Erholung, so dass die langfristigen Folgen und die Beziehung zwischen Wurzelwachstum und Pilzen ungewiss bleiben und weitere Untersuchungen erforderlich sind. Angesichts des zunehmenden Auftretens und der Dauer von Dürren muss festgestellt werden, ob die Bäume, die sich erholen, künftige Dürren überstehen können, was Einblicke in die Walddynamik unter veränderten Klimabedingungen ermöglicht.

## III Table of contents

I Summary.....	3
II Zusammenfassung.....	8
IV List of abbreviations.....	16
V List of figures.....	18
VI List of tables.....	20
VII List of included articles.....	21
VIII List of included manuscripts.....	21
IX List of not included articles.....	21
1. Introduction.....	22
1.1 Forests and drought.....	22
1.1.1 Root system.....	24
1.1.2 European beech and Norway spruce.....	26
1.1.2 Mixture effects.....	27
1.2 Soils.....	28
1.3 Fungi.....	30
1.3.1 Fungi and drought.....	32
1.4 Drought release.....	34
1.4.1 Drought release effects on tree roots.....	35
1.4.2 Drought release effects in soil.....	35
1.4.3 Drought release effects on soil and root fungi.....	36
1.5 Objectives of the thesis.....	37
2 Material and methods.....	41

2.1 Greenhouse experiment: beech and spruce seedlings growing in soils with different precipitation histories were exposed to drought.....	41
2.1.1 Soil characteristics .....	41
2.1.2 Plant growth and greenhouse settings.....	42
2.1.3 Drought treatment, <sup>13</sup> CO <sub>2</sub> labelling and harvest .....	43
2.1.4 Sampling.....	44
2.1.5 Fine-root parameter .....	44
2.2 KROOF rewatering experiment in a mature forest site.....	44
2.2.1 Setup of the KROOF experiment.....	45
2.2.2 Rewatering and <sup>13</sup> CO <sub>2</sub> labelling.....	46
2.2.3 Sampling.....	47
2.2.4 Fine-root parameters.....	48
2.2 Nucleic acid extraction and fungal ITS sequencing .....	49
2.3 Bioinformatics and statistical methods .....	50
2.3.1 DNA-sequence data analysis.....	50
2.3.2 Statistics .....	50
3 Publications, manuscripts and additional results .....	52
3.1 Acclimation in root architecture rather than long-term adaption of fungal symbiosis mitigates drought effect on European beech seedlings (manuscript).....	53
3.2 High resilience of carbon transport in long-term drought-stressed mature Norway spruce trees within 2 weeks after drought release (Article I).....	55
3.3 Dynamics of initial C allocation after drought release in mature Norway spruce - Increased belowground allocation of current photoassimilates covers only half of the C used for fine-root growth (Article II).....	57

3.4 Drought legacy effects on fine-root-associated fungal communities are modulated by root interactions between tree species (Article III).....	59
3.5 Additional results not presented in the manuscript and articles (all results in appendix) .....	61
4 General discussion.....	63
4.1 Are fungal communities in drought-prone regions better adapted to dry periods compared to communities in moist regions and thus less affected by drought?.....	63
4.2 Are seedlings less affected by drought when growing in soils with drought-adapted fungal communities and interspecific root interaction? .....	67
4.3 How do the fine-root systems of mature beech and spruce recover within three months upon drought release after five years of repeated summer drought? .....	69
4.4 Do root-associated fungal communities connected to beech and spruce recover after rewatering to resemble their pre-drought composition? .....	74
4.5 How does a species mixture of beech and spruce affect the fine-root recovery of both trees and the respective root-associated fungal communities compared to single species? .....	77
5 Conclusions and outlook .....	77
6 References.....	81
7. Danksagung .....	103
8. Appendix.....	104

## IV List of abbreviations

<b>&lt;</b>	Is lower than	<b>ECM</b>	Ectomycorrhizal
<b>=</b>	Equal	<b>FDA</b>	Fluorescein-Diacetate
<b>&gt;</b>	Is higher than	<b>F<sub>label</sub></b>	Fraction of labelled carbon
<b>%</b>	Per cent	<b>g</b>	Gram
<b>(r)DNA</b>	(ribosomal) Deoxyribonucleic acid	<b>Gt</b>	Gigaton
<b>°C</b>	Degree Celcius	<b>H</b>	Hydrogen
<b>µl</b>	Microliter	<b>h</b>	Hour(s)
<b>ABA</b>	Abscisic acid	<b>H<sub>2</sub>O</b>	Water
<b>am</b>	Ante meridiem	<b>IR</b>	Intermediate region soil
<b>ANOVA</b>	Analysis of variance	<b>ITS</b>	Internal transcribed spacer
<b>BB</b>	Beech neighbouring beech	<b>KARST.</b>	Hermann Karsten
<b>Bmix</b>	Beech neighbouring spruce	<b>KH<sub>2</sub>PO<sub>4</sub></b>	Potassium dihydrogen phosphate
<b>bp</b>	Basepairs	<b>klux</b>	Kilolux
<b>C</b>	Carbon	<b>km<sup>2</sup></b>	Square kilometre
<b>cDNA</b>	Complementary DNA	<b>kPa</b>	Kilopascal
<b>CET</b>	Central European time	<b>KROOF</b>	Kranzberg roof experiment
<b>cm</b>	Centimetre	<b>l</b>	Liter
<b>C<sub>new</sub></b>	Recent photoassimilates	<b>L.</b>	Carl von Linné
<b>CO<sub>2</sub></b>	Carbondioxide	<b>LfL</b>	Bayerische Landesanstalt für Landwirtschaft
<b>contC<sub>new</sub></b>	Contribution of C <sub>new</sub>	<b>LWF</b>	Bayerische Landesanstalt für Wald und Forstwirtschaft
<b>CTR</b>	Carbon transport rate	<b>m</b>	Meter
<b>d</b>	Day(s)		
<b>DR</b>	Dry region soil		



<b>m a.s.l.</b>	Meter above sea level	<b>pm</b>	Post meridiem
<b>min</b>	Minute(s)	<b>pmol</b>	Picomol
<b>MIX</b>	Mixed culture	<b>PPFD</b>	Photosynthetic photon flux density
<b>mm</b>	Milimeter	<b>RNA</b>	Ribonucleic acid
<b>MR</b>	Moist region soil	<b>rpm</b>	Rounds per minute
<b>MPa</b>	Megapascal	<b>S</b>	Sulfur
<b>N</b>	Nitrogen	<b>se</b>	Standard error
<b>Na<sub>2</sub>HPO<sub>4</sub></b>	Sodium dihydrogen phosphate	<b>Smix</b>	Spruce neighbouring beech
<b>ng</b>	Nanogram	<b>SS</b>	Spruce neighbouring spruce
<b>nM</b>	Nanomolar	<b>SWC</b>	Soil water content
<b>NSC</b>	Non-structural carbohydrates	<b>TDR</b>	Time Domain Reflectometry
<b>OTU</b>	Operational taxonomic unit	<b>UV</b>	Ultraviolet
<b>P</b>	Phosphorous	<b>vol %</b>	Volume percent
<b>p</b>	Probability of error	<b>w/v</b>	Weight/volume
<b>PCR</b>	Polymerase chain reaction	<b>δ</b>	Delta
<b>PERMANOVA</b>	Permutational multivariate analysis of variance		
<b>pH</b>	Pondus hydrogenii; Potential of hydrogen		

## V List of figures

**Figure 1:** Setup of the greenhouse experiment. Soils of different regions of Bavaria/ Germany were taken to a depth of 30 cm in beech-spruce mixture stands along a precipitation gradient and beech as well as spruce grown in respective pots with inter- or intraspecific root contact. A two-month drought was applied to half of the seedlings whereby before and after drought soil samples were taken for fungal ITS sequencing. After drought, the seedlings were labelled with  $^{13}\text{C}$  enriched  $\text{CO}_2$  for two days. At harvest, above- and belowground parameters of the seedlings were determined and fungal ITS sequencing performed with fine-root samples... 38

**Figure 2:** a) Planting scheme of beech (circles) and spruce (triangles) in pots containing soil from the (DR, red), the intermediate region (IR, yellow), and the moist region (MR, blue), with inter- or intraspecific root contact. b) Seedlings in the fumigation tent with LED lamps to compensate for any potential light reduction caused by the tent and ensure photosynthesis. .... 43

**Figure 3:** a) Arrangement of the experimental plots 1 to 12 at the Kranzberg Forest Roof (KROOF) site. CO refers to controls and TE to rewetted former drought plots, SS indicates the spruce monospecific area, BB the beech monospecific area and MIX the mixture. Boxes display corresponding pairs. Plots in red boxes have not been sampled. Plots in the blue box have additionally been  $^{13}\text{C}$ -labelled during the rewetting. b) illustrates the temperature (line) and precipitation (bars) within the sampling period, c) the soil water content in 0 – 7 cm of control and rewatered plots; different line types indicate the different watering campaigns: solid = first (I, plots 7, 8), dashed = second (II, plots 3, 4, 11, 12), and dotted = third (III, plots 5, 6). Black arrows and roman numbers mark the starting day of the respective watering campaign: I = 25.06.2019, II = 04.07.2019, III = 10.07.2019. Ribbons = standard errors. The figure was modified from article III..... 46

**Figure 4:** Setup of the rewatering experiment at Kranzberg Forest. One plot consisted of mature beech and spruce trees and three interaction zones: beech neighbouring beech (BB), beech neighbouring spruce (MIX) and spruce neighbouring spruce (SS). Root samples were

taken via soil cores and mesh bags on different days with respect to the watering event. Parallel to the watering, spruce trees were labelled with <sup>13</sup>C depleted CO<sub>2</sub>. Fine-roots from soil cores were taken for fungal ITS sequencing and biomass determination, fine-roots and mycorrhizal tips of mesh bags were used for δ<sup>13</sup>C measurements and tracing fine-root parameters. The figure was modified from article III. .... 48

**Figure 5:** Example of fine-root harvest and sample processing. a) excavated mesh bag including a fine-root on harvest day. b) spruce fine-root of a drought plot before drought release and c) the same root at harvest 35 days after watering. d) fluorescent root tip stained with fluorescein-diacetate for vitality analysis..... 49

**Figure 6:** Summed up relative abundances of rDNA-based soil and root-associated fungal communities according to trophic mode and ECM fungal exploration type grouped by soil types (DR = dry region soil, IR = intermediate region soil, MR = moist region soil) and treatment (CO = control, D = drought). a) shows the trophic modes of soil and root-associated fungal communities whereby blue represents ectomycorrhizal fungi, yellow parasites, grey pathogens and red saprotrophs. b) illustrates the abundance of ectomycorrhizal exploration types of soil and root-associated ectomycorrhizal fungi. Blue portrays contact types, yellow long-distance types, grey medium-distance types and red short-distance types. This figure was modified from manuscript I. .... 64

**Figure 7:** Overview of carbon (C) allocation in spruce after drought release. The C sink activity a) describes the summed-up amount of C used by a tree in each organ within 28 days after drought release. b) illustrates the allocation of newly assimilated C (C<sub>new</sub>) in each organ. The grey bar plots indicate the allocation above- and belowground. c) reflects the percentage of to fine-roots allocated C<sub>new</sub> concerning the total fine-root C demand. Blue emphasizes control trees and red rewatered trees. n.s. = not significant, \* indicates p < 0.05, \*\* p < 0.01, \*\*\* p < 0.001. The figure was modified from article II. .... 73

**Figure 8:** a) Non-metric multidimensional scaling (NMDS) plot of root-associated fungal community composition. Each plot shows samples from one sampling date relative to the day of rewatering in a shared coordinate system (i.e., the same ordination). Ellipses represent 95%

confidence intervals. Stress = 0.18. b) Summed up relative abundance of trophic modes after watering in control and rewatered plots, in each of three tree rooting zones: beech monospecific (BB), spruce monospecific (SS) and mixture (MIX). The figure was modified from article III..... 74

**Figure 9:** Overview of the response to rewatering of the studied belowground organs and C transport in mature beech and spruce within the first three month, taking into account a mixture of tree species..... 78

## VI List of tables

**Table 1:** General drought effects on tree fine-root traits. ↑ indicates a positive effect, ↗ a predominantly positive trend, ↓ indicates a negative effect, ↘ indicates a predominantly negative trend, → indicates predominantly no effect. Adjusted from Brunner et al. (2015). 25

**Table 2:** Soil texture and nutrient content of the different region soils. DR = dry region soil, IR = intermediate region soil and MR = moist region soil. Table adjusted from manuscript I. ... 42

## VII List of included articles

- I. Hikino, K., **Danzberger, J.**, Riedel, V. P., Rehschuh, R., Ruehr, N. K., Hesse, B. D., Lehmann, M. M., Buegger, F., Weikl, F., Pritsch, K., & Grams, T. E. E. (2021). High resilience of carbon transport in long-term drought-stressed mature Norway spruce trees within 2 weeks after drought release. *Global Change Biology*, 00, 1–16.
- II. Hikino, K.\*, **Danzberger, J.\***, Riedel, V. P., Hesse, B. D., Hafner, B. D., Gebhardt, T., Rehschuh, R., Ruehr, N. K., Brunn, M., Bauerle, T. L., Landhäusser, S. M., Lehmann, M. M., Rötzer, T., Pretzsch, H., Buegger, F., Weikl, F., Pritsch, K., & Grams, T. E. E. (2022). Dynamics of initial carbon allocation after drought release in mature Norway spruce — increased belowground allocation of current photoassimilates covers only half of the carbon used for fine-root growth. *Global Change Biology*, 00, 1–17.

\* Authors contributed equally to this work

- III. **Danzberger, J.**, Werner, R., Mucha, J., Pritsch, K., Weikl, F. (2023). Drought legacy effects on fine-root-associated fungal communities are modulated by root interactions between tree species. *Frontiers in Forests and Global Change*.

## VIII List of included manuscripts

- I. **Danzberger, J.\***, Hikino, K.\*, Landhäusser, S. M., Buegger, F., Hesse, B. D., Meyer, S., Weikl, F., Grams, T. E.E., Pritsch, K. (submitted). Acclimation in root architecture rather than long-term adaption of fungal symbiosis mitigates drought effect on European beech seedlings

\* Authors contributed equally to this work

## IX List of not included articles

- I. Mucha J., **Danzberger J.**, Werner R., Pritsch K., Weikl F. (2024). Effects of rewatering on soil fungi and soil enzymes in a spruce-beech forest after a 5-year experimental drought. *Plant and Soil*.

# 1. Introduction

## 1.1 Forests and drought

Forests cover 31 % of Earth's land surface and store around 45 % of the terrestrial carbon (C) (Bonan 2008). They absorb 1.2 Gt of C annually, offsetting up to 20 % of anthropogenic carbon emissions (Liu et al. 2015; Friedlingstein et al. 2019). Furthermore, they play a role in surface cooling and global water distribution by promoting cloud formation and precipitation through evapotranspiration (Bonan 2008; Gupta et al. 2018; Sheil 2018). Hence, forests have a very high impact on the global C cycle and the world's climate (Bonan 2008; Lal et al. 2018). Temperate forests cover parts of North America, Central Europe, Eastern China and Japan leading to a total coverage area of 10.4 million km<sup>2</sup>, which constitutes around 6 % of all ecosystems on the planet and 22 % of all forests (de Gouvenain and Silander 2017; McCarragher and Rigg 2020). Their climate is characterised by strong seasonality in temperature and precipitation leading to periods of tree growth and dormancy (de Gouvenain and Silander 2017; McCarragher and Rigg 2020). As a result of climate change, extreme events such as long droughts and heavy rainfall are becoming more frequent, which, among other things, can reduce forest diversity and productivity (Ratcliffe et al. 2017; Ammer 2019) and are thought to significantly driving forest dieback (Allen et al. 2010, 2015; Anderegg et al. 2013). In the first quarter of the 21<sup>st</sup> century, drought years in Central Europe accumulated with consecutive extreme years such as 2003, 2015, 2018 and 2019 (Asner et al. 2016; Schuldt et al. 2020; Büntgen et al. 2021). According to the latest report of the Intergovernmental Panel on Climate Change (IPCC 2021), the global temperature in 2100 might rise by 1.8 °C in a best-case scenario while in a worst-case scenario, it is predicted to rise by 3.3 to 5.7 °C. Even the best-case scenario poses enormous challenges for trees within a very short time. It is difficult for trees to adapt to rapidly changing environmental conditions due to their long life cycles (Allen et al. 2015). Hence, the 2018 drought caused an early defoliation of trees in Central Europe (Schuldt et al. 2020; Rohner et al. 2021). Prolonged or consecutive droughts are shown to cause long-lasting changes in stem and canopy structure (Carnicer et al. 2011).

Furthermore, it makes trees more prone to bark-beetle infestations which were especially devastating for Norway spruce (*Picea abies* (L.) Karst.) (Jactel et al. 2012; Netherer et al. 2019; Schuldt et al. 2020). The drought-caused damage and mortality of deciduous tree saplings differs between species, so a ranking was created by Beloiu et al. (2022): *S. aucuparia* > *P. avium* > *C. betulus* > *F. alnus* > *Q. robur* > *U. glabra* > *S. nigra* > *C. avellana* > *Crataegus spp.* > *A. pseudoplatanus* > *F. excelsior* > *Q. petraea* > *B. pendula* > *F. sylvatica* > *A. campestre*. Generally, it has been shown that conifer forests suffer greater damage than deciduous forests (Beloiu et al. 2022).

High temperature and low humidity lead to enhanced water evaporation by the tree. To counteract increased water loss and thus prevent hydraulic failure, some tree species reduce their stomatal conductance with decreasing soil water potential which is referred to as isohydric regulation (McDowell et al. 2008). This, however, ceases photosynthesis and thus leads to lower productivity (Ciais et al. 2005). During long-lasting droughts, however, this could lead to C starvation (Manzoni et al. 2012; Sevanto et al. 2014). To avoid C starvation, anisohydric species, in contrast, maintain a higher stomatal conductance to ensure a high C gain also under drought while risking hydraulic failure caused by high evaporation (McDowell et al. 2008). Thus, tree drought survival not only depends on a sufficient water supply but also the availability of C within the whole tree (Sala et al. 2010; Ruehr et al. 2019; Hartmann et al. 2020). Hence, the C allocation is shown to change with drought revealing a higher allocation to root growth (structural carbon) and C storage (non-structural C) (Meier and Leuschner 2008; Gaul et al. 2008; Poorter et al. 2012; Blessing et al. 2015; Hommel et al. 2016; Chuste et al. 2020). Furthermore, some studies have shown that in trees of different developmental stages, the transport of photoassimilates is restricted under drought (Adams et al. 2017; Hesse et al. 2018; Sevanto 2018). Changes in the phloem, which is responsible for the transport of photosynthates in trees, have also been observed. Thus, increased viscosity and thinner pipes have been revealed (Woodruff and Ryan 2014; Sevanto 2014, 2018; Hesse et al. 2018). Yet, external factors such as soil properties influence the trees' drought survival. For example, silty

soils or soils with silt:clay:loam mixture retain water more efficiently than sandy soils which have the least soil water holding capacity (Piedallu et al. 2011), but roots in sandy soils were shown to grow deeper (Schenk and Jackson 2002; Zhou et al. 2020).

### 1.1.1 Root system

Compared to aboveground organs, studies on the impact of drought on belowground organs such as the rooting system, which forms the bridge between soil and plant, are rarer. Roots are estimated to make up 20 - 40 % of the complete tree biomass, with coarse-roots being responsible for a stable anchorage in the soil as well as water and nutrient conduction (Brunner et al. 2015). On the other hand, fine-roots (<2mm diameter) are necessary for water and nutrient uptake and form the symbiotic interaction zone, making them a crucial factor for drought survival (Körner 2019). When drought emerges, fine-root growth has been shown to increase the water uptake and thus avoid drought stress. It is proposed that roots send signals to the shoots via the phytohormone abscisic acid (ABA) when water scarcity occurs, resulting in stomatal closure as well as a decrease in leaf growth (Hamanishi and Campbell 2011). ABA has also been shown to play a role as a growth-regulating hormone, delaying leaf and root development in ABA-insensitive poplars (Arend et al. 2009). Under normal conditions, a low ABA concentration in the roots promotes root growth (Sharp et al. 2000). Under drought, however, the ABA concentration is increased and inhibits root growth (Nakashima and Yamaguchi-Shinozaki 2013) leading to a decreasing root biomass during drought (Joslin et al. 2000; Leuschner et al. 2004; Ruehr et al. 2009; Herzog et al. 2014). There is also evidence that an increased ABA concentration in the roots leads to a higher formation of water channels (so-called aquaporins) in the root, which regulate water uptake and distribution (Brunner et al. 2015). With drought severity, root mortality increases (Gaul et al. 2008) and the root lifespan decreases in the absence of hydraulic redistribution (Bauerle et al. 2008; Eissenstat and McCormack 2013). It has also been shown that the vascular diameter of roots decreases under severe drought which is associated with reduced hydraulic conductivity (Eldhuset et al. 2013) and that fine-roots eventually perish under prolonged drought (Gaul et al. 2008). During



severe drought, very fine-roots ( $\leq 0.5$  mm) of beech seedlings were found to undergo a molecular remodelling leading to a decrease of enzymes related to the C metabolism which decelerated the consumption of energy resources (Domingo et al. 2023). Some tree species (e.g. Norway spruce) suberise their fine-roots to reduce water loss and increase water-use efficiency (Steudle 2002; Baxter et al. 2009). Table 1 gives an overview of drought effects on tree fine-roots in general (Brunner et al. 2019).

However, drought responses at the fine-root level vary between tree species. For instance, as shown in Table 1, the lifespan of roots generally decreases, although it tends to increase in Norway spruce, while remaining unchanged in European beech (Zwetsloot and Bauerle 2021). Nikolova et al. (2020) report, that beech and spruce follow different ecological strategies. While beech follows a “fast” strategy with rapid C turnover, reflected in the continuous formation of short-lived, absorptive fine-roots with a high, specific fine-root area and high respiratory activity, spruce follows a “slow” strategy with long-term C storage. For this purpose, long-living spruce fine-roots are suberised and the respiratory activity is downgraded.

**Table 1:** General drought effects on tree fine-root traits.  $\uparrow$  indicates a positive effect,  $\nearrow$  a predominantly positive trend,  $\downarrow$  indicates a negative effect,  $\searrow$  indicates a predominantly negative trend,  $\rightarrow$  indicates predominantly no effect. Adjusted from Brunner et al. (2015).

Root trait categories	Root traits	Effect of drought
<b>Growth</b>	Biomass	$\downarrow$
	Lifespan	$\searrow$
	Mortality	$\nearrow$
	Production	$\searrow$
	Turnover rate	$\searrow$
<b>Architecture</b>	Branching	$\rightarrow$

	Length	↘
	Rooting depth	↑
	Tip frequency	↘
<b>Morphology</b>	Diameter	↘
	Root area index (RAI)	→
	Root tissue density (RTD)	→
	Specific root length	→
<b>Anatomy</b>	Conduits	↗
<b>Biotic</b>	Mycorrhizae	↗
<b>Biochemical</b>	Suberin/ Aliphatics	→
<b>Physiological</b>	Abscisic acid (ABA)	↑
	Exudates	↘
	Respiration	↓
<b>Molecular</b>	Aquaporins	↗

### 1.1.2 European beech and Norway spruce

Two dominating species in European temperate forests to date are European beech (*Fagus sylvatica* L.) and Norway spruce (*Picea abies* (L.) KARST.) (Brus et al. 2012), from here onwards referred to as beech and spruce, respectively. Beech is predominant in around 16 % of German forests (BMEL 2014) whereby the natural distribution covers large parts of Europe. It has a heart-shaped rooting system and is categorised as a rather anisohydric species. During drought, it has a high C turnover which results in a permanent production of thin, absorptive fine-roots with high respiration suggesting an effective resource exploitation (Nikolova et al.

2020). Norway spruce, an evergreen conifer, is predominant in around 26 % of German forests (BMEL 2014) but is native to subalpine and boreal areas. Because of its importance to the timber industry, it has been grown in monocultures in Central Europe outside its natural range (Forster et al. 2019). Spruce is categorised as a rather isohydric species with a plate-shaped, shallow rooting system. In contrast to beech, spruce preserves C during drought which is shown in fine-root suberisation (Nikolova et al. 2020) which aids to prevent the loss of water and nutrients but also hinders the movement of water and nutrients into the plant (Steudle 2002). Additionally, it reduces respiration (Nikolova et al. 2020). Both tree species form symbioses with ectomycorrhizal (ECM) fungi as detailed below (1.3).

### 1.1.2 Mixture effects

One approach in forest management to counter climate change caused damage to forests is mixing tree species (Zhang et al. 2012; Forrester 2015; Pretzsch et al. 2015). There is evidence that higher species diversity can mitigate the destructive effect of droughts in forests (Liu et al. 2022). Beloiu et al. (2022) demonstrated that tree diversity increased forest health during the drought years of 2015, 2019, and 2020, with mixed forests exhibiting greater resistance than monocultures during the 2018 drought. Consequently, species mixtures can enhance resource availability (Ammer 2016). Furthermore, research has indicated that spruce thrives better in nutrient-poor soil when interplanted with beech (Pretzsch et al. 2010), as beech utilizes nutrients from deeper soil layers and enhances spruce's nutrient status through litter fall. On nutrient-rich soils, however, it was shown that beech profits from a mixture with spruce which is suggested to reduce beech's intraspecific competition (Pretzsch et al. 2010). Moreover, beech grows better in dry stands when it is growing together with coniferous trees leading to improved water exploitation of deeper soil layers (Grossiord et al. 2014b) and better water use (González de Andrés et al. 2018). Spruce profits from a mixture with deep-rooting beech in a dry environment due to hydraulic redistribution (Hafner et al. 2017; Rukh et al. 2020). Additionally, beech fine-roots had a longer lifespan under drought when growing

in a mixture with spruce compared to beech in monoculture while fine-root longevity in spruce was not affected by tree mixture (Zwetsloot and Bauerle 2021).

Positive mixture effects are more likely if the species growing in mixture have complementary traits such as different rooting depths to optimize water uptake strategies (Haberstroh and Werner 2022). Conversely, no positive effect in water uptake was demonstrated when similar traits were present, for example, when mixing two conifers with similar root systems (Grossiord et al. 2014b). Drought severity can affect the mixing effect of different species. While there are mainly positive or even neutral mixing effects during mild droughts, the observations of positive effects decrease with drought severity until negative effects even predominate under severe drought (Haberstroh and Werner 2022). In many studies, deciduous trees, in particular, seem to benefit during drought when growing along with conifers (Grossiord et al. 2014a; Bello et al. 2019; Magh et al. 2019; Torquato et al. 2020) while conifers were often negatively affected in mixture with increasing drought stress (Rascher et al. 2011; Grossiord et al. 2013, 2015; Rodríguez-Robles et al. 2020) even if their resource use is complementary. Thus, deep-rooting beech can be very competitive when admixed with spruce, pushing spruce to root in the upper soil layers, which may leave spruce, already shallow-rooted as it is, even more susceptible to drought as the upper soil layers dry out faster (Schume et al. 2004; Goisser et al. 2016). Also, the productivity of both, beech and spruce, was shown to decrease during heavy drought (Pretzsch et al. 2012).

## 1.2 Soils

Forest soils are often referred to as the “growth medium of trees”, whose properties define the growth intensity of trees (von Wilpert 2022). Indeed, soil texture, for instance, has a tremendous impact on tree growth behaviour. Thus, seedlings growing in sandy soils have been reported to have a higher root:shoot ratio compared to seedlings growing in sandy loam soils, indicating that the plants in sandy soils produced more roots (Meijer et al. 2011). Also Bezemer et al. (2006) reported that the plant-soil feedback in restored chalk soil was different from sandy loam soil in grasslands. Furthermore, the amount of soil organic matter, defined

as “all organic materials found in soils irrespective of origin or state of decomposition” (Baldock and Skjemstad 1999) mainly consisting of C, hydrogen (H), oxygen (O), nitrogen (N), phosphorous (P) and sulphur (S) (Krull et al. 2004), strongly affects physical (stabilisation of soil structure), chemical (buffering and pH changes) and biological (supply of substrate and nutrients for microbes) soil properties and thus the soil fertility (Krull et al. 2004; Raison and Khanna 2011). A high content of soil organic matter is often associated with better plant nutrition, enhanced water holding capacity, increased porosity and earlier soil warming in spring (Lal 2002; Krull et al. 2004) but this depends on the needs of the respective organisms relying on the soil. Soil can also affect the drought response of trees. It was shown that soil acidity can affect the drought effects of young oaks and oak saplings (Kuster et al. 2013; Hu et al. 2015). Moreover, trees with a medium, more balanced nutrient regime showed significantly higher resistance and resilience to extreme droughts (Schmied et al. 2023) and trees in shallow, well-drained soil grow less than trees on deep, silty soil and are more drought-sensitive (Rehshuh et al. 2017). Soils are not merely growth media that hold water and nutrients for trees, they are dynamic systems and habitats for a multitude of organisms. Estimates suggest there may be up to 10 billion living microbes in a single gram of soil (Rosselló-Mora and Amann 2001; Torsvik and Øvreås 2002). Biogeochemical cycles such as C, N, P and S, which are essential for multiple ecosystem functions (e.g. plant growth stimulation, effect on the soil’s chemical and physical structure), are controlled by the soil microbiome (Van Elsas et al. 2019). The plants and soil organisms are in consistent interaction which is called the “plant-soil feedback” (Bever et al. 1997; Bever 2003; Van der Putten 2003) and is considered a major driver of plant community assembly and functioning. When soil dries, not only plant roots do lose contact with the surrounding soil leading to reduced water and nutrient uptake (Carminati et al. 2009) but also soil microbes are severely stressed. Soil microbes, amongst them fungi, rapidly adapt to the osmotic conditions in their surrounding which requires a strategy to stay hydrated in desiccated soil (Schimel 2018). Furthermore, dry soil makes the dissolution, diffusion and transport of substrates to the microbes more difficult (Schimel 2018). Hence, precipitation history (Cavender-Bares et al. 2009), soil temperature

(Domisch et al. 2002) and nutrient addition (Avis et al. 2003) have been shown to alter the fungal community structure. The significance of fungi in forest ecosystems and their reaction to drought will be worked out in detail in the following chapter (1.3).

### 1.3 Fungi

With an estimate of 2.5 million species, fungi are the second-largest kingdom after animal invertebrates with an estimate of 8.5 million species (Niskanen et al. 2023). However, only 6.2 % (115.000) of the species have been described to date. Fungi are essential to nearly all life on Earth, playing a crucial role in supporting terrestrial plants through improved nutrient absorption, immune response stimulation, and enhanced stress resistance, ecosystem functioning by particularly the degradation of natural polymers and even have a widespread impact on humanity, serving as a source of bioactive compounds like antibiotics and immunosuppressants (Antonelli et al. 2023; Prescott et al. 2023; Niskanen et al. 2023). Within forest ecosystems, fungi have a significant role as plant symbionts, decomposers of organic material, and a food source for wildlife (Marcot 2017). Fungal lifestyles can be classified into saprotrophic, pathogenic and symbiotrophic, which all have individual roles in biogeochemical cycles (Baldrian and Kohout 2017). Saprotrophic fungi, the largest group, decompose insoluble organic matter such as lignocellulose and chitin by secretion of extracellular enzymes making them a central player in carbon cycling (Hartl et al. 2012; Baldrian and Kohout 2017). Furthermore, the decomposition of plant-derived organic material is a major process to reveal nutrients other than C, which can be absorbed by plant roots (Lundell et al. 2014). The biomass of degradable deadwood reaches up to 67 Gt in manageable forests (FAO 2010), thus, in forests especially wood- and litter-decaying fungi are of importance. Degradation rates, however, can be affected by changes in the topsoil temperature and litter quality (Zhang et al. 2008; Prescott 2010; Lundell et al. 2014). Visually, four patterns of fungal degradation can be distinguished which are all major wood component degrading white rot (e.g. hardwood decaying *Phanerochaete chrysosporium* and litter decaying *Agrocybe praecox*), cell wall carbohydrates degrading brown rot (e.g. *Laetiporus sulphureus*), cell wall carbohydrates

degrading soft rot (e.g. *Trichoderma spp.*, *Penicillium spp.*) as well as wood resins and wax degrading blue stain (e.g. *Ophiostoma piceae*) (Lundell et al. 2014; Zabel and Morrell 2020; Langer et al. 2021; Mäkelä et al. 2021). The latter, however, is regarded as less important for wood organic C cycling due to their lacking ability to degrade (hemi-) cellulose and lignin. In recent studies, it has been shown that saprotrophic fungi can develop additional root-associated lifestyles (Tedersoo and Smith 2013; Smith et al. 2017; Baldrian and Kohout 2017) and even exhibit symbiotic traits (Jumpponen 2001; Kohler et al. 2015; Almario et al. 2017). Pathotrophic fungi cause tree diseases which have negative effects on development and growth (García-Guzmán and Heil 2014). Symbiotrophs endorse the supply of minerals and water to the trees while obtaining photosynthetically derived carbohydrates (van der Heijden et al. 2015). This group contains mycorrhizal fungi, which form a symbiotic association with plant roots (Smith and Read 2008). Fossil evidence indicates the presence of mycorrhizas in some of the earliest land plants dating back approximately 400 million years (Suz et al. 2018). Mycorrhizal fungi can be categorised into arbuscular mycorrhizal fungi, which colonise 78 % of plant species, including herbs, shrubs, trees, and ferns, orchid mycorrhizal fungi, specific to Orchidaceae (10 % of plant species), ectomycorrhizal fungi, which colonise 2.2 % of plant species, particularly woody species, and ericoid mycorrhizal fungi, which colonise Ericaceae (1.5 % of plant species) (Suz et al. 2018). Ectomycorrhizal fungi prevail in temperate forests (Tedersoo et al. 2014) colonizing around 95 % of tree roots and forming ectomycorrhizae with tree species in the Pinaceae such as *P. abies*, Fagales such as *F. sylvatica*, and others (Courty et al. 2010; Becquer et al. 2019). Ectomycorrhizae are characterized by the presence of a hyphal mantle formed by the fungus and a Hartig net where hyphae grow in the intercellular space of the apoplast of the root epidermis or cortical cells without penetrating them (Kottke and Oberwinkler 1986). In the Hartig net, the symbiotic exchange of water, nutrients and C in the form of sugar between fungus and plant takes place. Extraradical hyphae can grow from the hyphal mantle and thus enlarge soil exploration and nutrient and water uptake to different degrees. These structures are classified into exploration types (Agerer 2001) describing the degree of soil exploration ranging from contact types having a smooth mantle surface with

only a few, short (< 0.5 mm) extraradical hyphae to long-distance types that form congregations of parallel hyphae, so-called rhizomorphs, which are cable-like structures that can pervade the soil. It is shown that the ectomycorrhizal hyphae network is used as an “underground highway” for trading nutrients and C with and between plants (Klein et al. 2016). The symbiosis with ectomycorrhizal fungi increases the area of water absorption in the tree through fungal hyphae and enables access to soil water that the roots could not obtain by themselves (Bornyasz et al. 2005; Lehto and Zwiazek 2011). Also, improved hydraulic conductivity has been shown in mycorrhizal plants compared to non-mycorrhizal ones (Lee et al. 2010). Furthermore, it is discussed that ECM fungi enhance the expression of aquaporins, which improves water transport (Brunner et al. 2015). In forests, the composition of the ECM fungal community has been shown to affect tree growth, with rapid growth associated with ECM communities that harbour high inorganic but low organic nitrogen acquisition gene proportions and contact exploration types (Anthony et al. 2022). Moreover, it has been demonstrated that seedlings inoculated with microbial communities from arid regions survived dry periods better, but this could have been associated rather with the composition of arbuscular than ECM fungi (Allsup et al. 2023). During drought, ECM fungi were found to increase growth of Chinese red pine seedlings by improving the seedlings hydraulic function and increasing C storage (Wang et al. 2021), and transferring water between oak seedlings (Egerton-Warburton et al. 2007), both increasing the trees’ drought survival.

### 1.3.1 Fungi and drought

The drought response of fungi differs between species (Richard et al. 2011) and is influenced by different factors. Kerner et al. (2012) analysed the proteome of *Cenococcum geophilum*, an ectomycorrhizal fungus that is well known to tolerate drought, and found 15 highly abundant proteins associated with fungal drought response, including so-called heat shock proteins. These heat shock proteins help other proteins to fold under extreme conditions, stabilise them preventing degradation and accelerate degradation of non-functioning proteins (Wang et al. 2004). Twelve of these proteins were differently abundant when the fungus experienced



drought stress indicating an adjustment in protein expression to environmental changes. Late embryogenesis abundant (LEA) domain containing proteins, that are related to drought stress tolerance (Oliveira et al. 2007), were only present in drought-stressed fungi (Kerner et al. 2012). Furthermore, some ectomycorrhizal fungal species such as *Suillus bovinus* and *Rhizopogon luteolus* form isolated chords from hydrophobic mycelium for efficient water transport only having a small proportion of hydrophilic mycelium which might be responsible for water absorption (Unestam and Sun 1995). Also, a proportion of dark pigmented melanin in the hyphae mantle can increase the fungal drought tolerance (Fernandez and Koide 2013). It was shown that the production of melanin in *Aspergillus niger* increased with a stress gradient of increasing UV-radiation, temperature and desiccation (Singaravelan et al. 2008) and inhibition of melanin production in *C. geophilum* significantly reduced the fungal drought tolerance (Fernandez and Koide 2013). Moreover, fungi with root interaction were less affected than free-living soil fungi likely because they can profit from root exudates and better water availability (Castaño et al. 2018).

In most studies addressing the composition of fungal communities during drought, changes in composition have been demonstrated. Richard et al. (2011) found that during a five-year consecutive drought, the community composition of ECM fungi changed without a decrease in species richness or diversity. Furthermore, an analysis of similarity by Cavender-Bares et al. (2009) revealed that the composition of ECM fungi communities differed significantly along a soil moisture gradient. Similarly, Nickel et al. (2018) reported a change in the ECM fungal community over three years of consecutive summer drought with an increase of species with long rhizomorphs, complementing Castaño et al. (2023), who found that on pine seedlings under drought, ECM fungi with long-distance exploration types and hydrophobic mycelia were dominating taxa. Contrary, in a mature forest, Castaño et al. (2018) reported an increase in the abundance of species with short-distance exploration type in a dry environment while in moist environments species with long-distance exploration type were dominating.

At species level, observations on beech trees indicated that the abundance of the predominant ECM species, *Byssocorticium atrovirens*, and *Lactarius subdulcis* remained unaffected by drought (Shi et al. 2002). Conversely, the less abundant but growth-promoting *Xerocomus chrysenteron* increased in response to drought (Shi et al. 2002).

#### 1.4 Drought release

Different studies have shown the effects of dry periods to vary between species in both young and mature trees. Among young trees in forests of central Germany, rowan (*Sorbus aucuparia* L.) was shown to regenerate faster, albeit with lower vitality, after a drought year than young beeches, which recovered fully (Beloïu et al. 2020, 2022). Adult beech trees, on the other hand, recovered quickly after a dry year (Kunz et al. 2018). Recent studies also showed that a drought legacy phase with continued reduced growth and incomplete recovery can last up to four years after drought (Anderegg et al. 2015), and tree recovery time increases with tree size (Trugman et al. 2018). The drought damage on the canopy of coniferous forests was higher than in deciduous forests leading to a higher extent of recovery in coniferous forests (Beloïu et al. 2022). Repair processes after a dry phase include the establishment of new xylem, embolism refilling and the restoration of carbon stores (Brodersen and McElrone 2013; Galiano et al. 2017; Ruehr et al. 2019; Rehschuh and Ruehr 2022). The recovery of tree species differs according to the drought severity and the tree mixture (Haberstroh and Werner 2022). It has been shown that under moderate drought, the tree mixture has a positive effect on at least one species in mixture by regenerating faster than in monoculture. Under severe drought, however, the regeneration of tree species in mixture can be delayed or even reduced compared to trees growing in monoculture (Magh et al. 2019; Rodríguez-Robles et al. 2020; Haberstroh et al. 2021; Haberstroh and Werner 2022). It has also been shown that root production, microbial activity and soil respiration were stimulated at the end of a dry season (Hagedorn et al. 2016; Brunner et al. 2019; Joseph et al. 2020; Gao et al. 2021; Werner et al. 2021). Despite the importance of roots as water and nutrient-absorbing organs and their

interaction with soil fungi, little is known about the recovery of fine-root systems and root-associated fungal communities.

#### 1.4.1 Drought release effects on tree roots

In a mature pine forest, a sudden rise of the soil water availability was observed to increase the belowground metabolic activity and deplete the amount of soluble sugars in the roots during the first three days, resulting in a strongly increased assimilate transport into the rhizosphere (Joseph et al. 2020). In beech seedlings, a high belowground C allocation was observed in mycorrhizal roots, microbial biomass and soil respiration after watering, indicating a high priority of root metabolism restoration (Hagedorn et al. 2016). After a severe drought period, very fine-roots in beech seedlings displayed increased root growth and low starch concentrations, indicating that these roots relied on their starch reserves to recommence growth (Domingo et al. 2023). Furthermore, it was observed that in mature beech trees water uptake shifts from shallow roots to roots in deeper soil and was decreased during drought, which quickly recovered after drought release and returned to shallow roots within three weeks (Gessler et al. 2022).

#### 1.4.2 Drought release effects in soil

A frequently observed phenomenon directly after drought release is a pulse-like increase in soil CO<sub>2</sub> efflux, which is known as the Birch effect (Birch 1958; Kim et al. 2012; Göransson et al. 2013). The mechanisms of the Birch effect are still unclear. Yet, several studies propose that the C derives from the microbial biomass (e.g. Kieft et al. 1987; Fierer and Schimel 2003; Slessarev et al. 2020). One common hypothesis is the accumulation of compatible osmolytes in membrane-bound cells of microorganisms during drought to prevent dehydration (Malik et al. 2019; Roy Chowdhury et al. 2019; Slessarev et al. 2020). During irrigation, the cells must quickly eliminate these enriched osmolytes to prevent membrane rupture. Thus, among others, proline, glutamine, glycine betaine and trehalose are released into the surrounding soil (Kempf and Bremer 1998; Halverson et al. 2000; Welsh 2000; Warren 2019), which can be rapidly assimilated and mineralised by other microorganisms (Barnard et al. 2020). Joseph et

al. (2020) report an increase of new photoassimilates in soil respiration and soil microbial biomass in a mature pine forest after irrigation indicating an increase in belowground metabolic activity. However, the large CO<sub>2</sub> pulse after rapid drought release is likely to result from all, biological, physical and chemical mechanisms, and needs further investigations (Barnard et al. 2020). Together with soil respiration also nitrogen mineralisation increased with drought release likely due to an immediate but short mobilisation of amino acids and a high degradation of N-rich substrates by microbes (Saetre and Stark 2005; Leitner et al. 2017).

#### 1.4.3 Drought release effects on soil and root fungi

To date, not much is known about the effects of drought release on soil and root-associated fungi, although it is an important component in understanding forest recovery. In general, the reaction of the soil fungal communities to drought and rewet was compared with that of the bacterial communities (Bapiri et al. 2010; Yuste et al. 2011; Barnard et al. 2015, 2020; de Vries et al. 2018). Hence in grassland soils, the fungal growth remained unaffected after drying-rewetting cycles while bacterial growth decreased (Bapiri et al. 2010) and potentially active soil fungal communities revealed little response to drought and wet-up compared to bacteria (Barnard et al. 2015). Furthermore, grassland soil fungal co-occurrence networks were proven to be more stable during desiccation and subsequent recovery than bacterial networks (de Vries et al. 2018). Fungal richness, however, was shown to increase after drought but resembled controls again one week after rewetting (de Vries et al. 2018). In forest soils, the fungal diversity was less sensitive to changes in soil moisture, temperature and plant activity than the bacterial diversity and fungal communities were able to adapt to environmental changes during the seasons (Yuste et al. 2011). Barnard et al. (2020) propose that the lower sensitivity of fungi to changes in soil water content compared to bacteria is due to their hyphal structure and frequent mutualistic strategies (De Boer et al. 2005). Yet, the effect of drought release on root-associated fungal communities in forests is still critically understudied and is addressed in this thesis.

## 1.5 Objectives of the thesis

This work focuses on the interplay between soil and root-associated fungi and tree drought response and recovery. The first part of this work aims to address two key questions: 1) whether fungal communities in drought-prone regions are better adapted to dry periods compared to those in moist regions and are thus less affected by drought and 2) whether seedlings are less affected by drought when growing in soils with drought-adapted fungal communities and interspecific root interaction. Therefore, the influence of natural precipitation history on the drought response of soil and root-associated fungal communities and beech and spruce seedlings was investigated (manuscript I). Based on the findings that microbial communities adapt over time to soil properties such as soil moisture and temperature, and that fungal symbioses can improve a plant's water supply during drought, I hypothesized that the fungal communities in soils of a dry region were already drought-adapted. Accordingly, plants associated with the soil microbes of the dry region would benefit from their adaptation and be less affected by drought than those associated with fungi of the moist region. Furthermore, tree species mixture has been shown to positively influence the performance of trees in mild to moderate droughts. Thus, I hypothesized that beech and spruce seedlings would benefit from interspecific root interaction and be less affected by drought. For this purpose, beech and spruce seeds were planted and raised in soils from beech-spruce mixture stands along a natural precipitation gradient within Bavaria and exposed to a two-month drought followed by three days of  $^{13}\text{CO}_2$  labelling to trace the allocation of new photoassimilates. Soil samples for fungal community analysis were taken before and after drought and root samples for root-associated fungal community analysis with the harvest after drought. To provide insight into belowground responses to drought, various root system parameters, such as mycorrhization, branching, and root depth, were also determined with harvest (Figure 1).

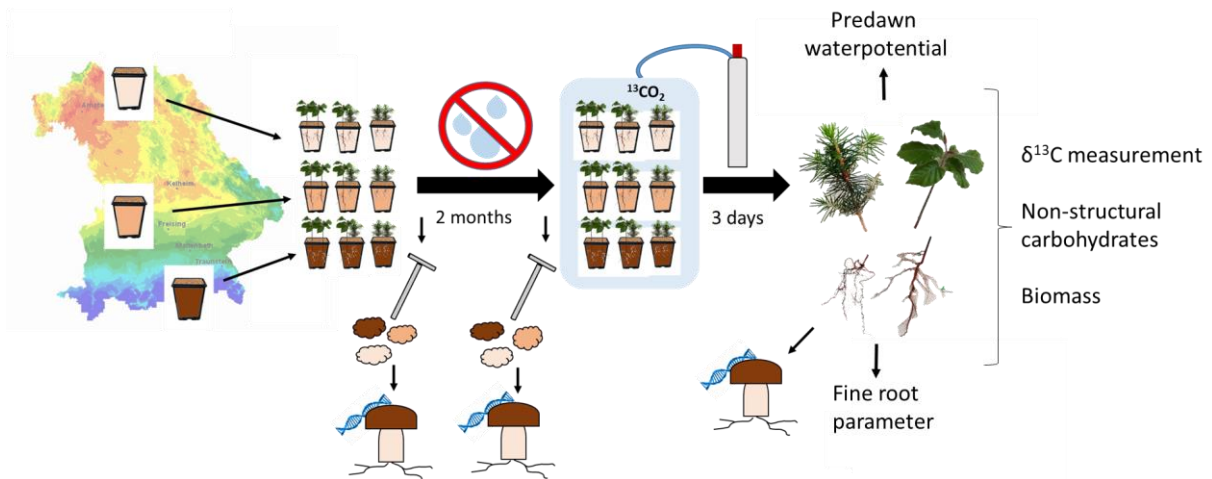


**Figure 1:** Setup of the greenhouse experiment. Soils of different regions of Bavaria/ Germany were taken to a depth of 30 cm in beech-spruce mixture stands along a precipitation gradient and beech as well as spruce grown in respective pots with inter- or intraspecific root contact. A two-month drought was applied to half of the seedlings whereby before and after drought soil samples were taken for fungal ITS sequencing. After drought, the seedlings were labelled with  $^{13}\text{C}$  enriched  $\text{CO}_2$  for two days. At harvest, above- and belowground parameters of the seedlings were determined and fungal ITS sequencing performed with fine-root samples.

The second part of this thesis focuses on belowground drought recovery in a mature beech and spruce forest site and is divided into, first, the transport and distribution of C throughout the spruce tree (articles I and II) with special interest given in this thesis to the root system. In this part the objective is to investigate 3) how the fine-root systems of mature beech and spruce recover within three months upon drought release after five years of repeated summer drought. Based on the need for water to restore all tree functions and an increased root production after drought release, the hypothesis here was that with respect to both, C transport and allocation, the regeneration of the water-absorbing fine-root system is a high priority. For this reason, spruce trees on one recovering and the accompanying control plot were labelled with  $^{13}\text{C}$ -enriched  $\text{CO}_2$  for two weeks starting with the watering event. Samples of different above- and belowground organs were taken in a period of 4 weeks after the watering, including mycorrhizal and non-mycorrhizal fine-root tips, and the arrival time of newly assimilated C as well as the total C demand and allocation of new photoassimilates was determined.

A second aspect was the recovery of root-associated fungal communities with consideration of the recovery of tree species-specific fine-root systems and tree species mixture (article III). This section aims to address the key questions: 4) whether root-associated fungal communities linked to beech and spruce recover after rewatering to resemble their pre-drought composition and 5) how a species mixture of beech and spruce affects the fine-root recovery of both trees and the respective root-associated fungal communities compared to single species. The findings that the fungal community composition changes with drought and the soil heterogeneity of tree species mixture positively affects fungal communities lead to the hypotheses that after watering the communities will undergo a change and resemble the control communities, and that tree mixture has a positive effect on fungal diversity and fine-root regeneration. Therefore, fine-roots were taken on all recovering and control plots in a period of one week before and up to three months after the watering via soil cores and mesh bags including all tree root interaction zones: beech neighbouring beech (BB), beech neighbouring spruce (Bmix, when beech roots could be separated from spruce, otherwise MIX), spruce neighbouring beech (Smix, when spruce roots could be separated from beech, otherwise MIX) and spruce neighbouring spruce (SS). Root-associated fungal communities were determined by ITS sequencing. Fine-root parameters such as root vitality, root growth, biomass and mycorrhization were determined to assess fine-root recovery strategies of beech and spruce.

To gain a comprehensive understanding of how forest ecosystems in Central Europe may develop under climate change, it is crucial to understand how dominant tree species react to recurrent droughts and their ability to recover. Achieving a full understanding of tree drought reactions and recovery requires combining knowledge about aboveground and belowground reactions, including tree-associated and soil fungi as important members of forest soils. The findings of this thesis contribute to a better understanding of how drought affects fungal communities in forest soils with varying precipitation histories, and subsequently could influence the responses of European beech and Norway spruce seedlings to drought.

Additionally, these results shed light on post-drought C transport and allocation throughout mature spruce trees, as well as the dynamics of the fine-root systems of mature beech and spruce and their associated fungi.



## 2 Material and methods

This section provides an overview of the experimental setups and summarises the main methods used. Specific methods used in the different experiments are described in detail in the respective articles and manuscripts.

### 2.1 Greenhouse experiment: beech and spruce seedlings growing in soils with different precipitation histories were exposed to drought

To determine the influence of natural precipitation history on soil and root-associated fungal communities and the rooting system of beech seedlings, soils of three regions along a natural precipitation gradient in Bavaria were chosen: Arnstein, Kranzberg and Wasserburg.

#### 2.1.1 Soil characteristics

Arnstein (9°58'37.3"E; 49°54'10.8"N; 330 m.a.s.l.) represents a naturally dry region with an average rainfall of 310 mm during the vegetation period and an average temperature of 14 °C. The soil's parent material is valley sediment. Soil from this region will be referred to as "dry region soil" (DR). Kranzberg (11°39'39.6"E; 48°25'8.4"N; 490 m.a.s.l.) characterises a medium moist forest site with an average rainfall of 480 mm during the vegetation period and an average temperature of 13.8 °C. The soil derives from loess over tertiary sediments, in the following referred to as "intermediate region soil" (IR). Wasserburg (12°04'22.8"E; 48°08'31.2"N; 620 m.a.s.l.) represents a moist region having an average rainfall of 640 mm during the vegetation period and an average temperature of 13.9 °C. Wasserburg soil derives from Würm glacier moraines. It will be referred to as "moist region soil" (MR).

For the greenhouse experiment from manuscript I, 20 cm topsoil excluding litter from mixed stands of all three sites was collected and amixed with 30 vol % quartzite sand to equalize the field capacity (DR = 21.6 %, IR = 21.8 %, MR = 21.1 %, determined at 33 kPa). To exclude nutrient deficiencies and determine the exact texture of the soils, soil samples were sent to the Bayerische Landesanstalt für Landwirtschaft (LfL) for analysis (Table 2).

**Table 2:** Soil texture and nutrient content of the different region soils. DR = dry region soil, IR = intermediate region soil and MR = moist region soil. Table adjusted from manuscript I.

	<b>DR</b>	<b>IR</b>	<b>MR</b>
<b>Coarse sand [%]</b>	28.60	33.40	49.90
<b>Coarse silt [%]</b>	21.20	22.70	10.90
<b>Medium sand [%]</b>	1.50	4.00	7.60
<b>Medium silt [%]</b>	18.60	15.00	8.20
<b>Fine sand [%]</b>	1.80	4.50	9.40
<b>Fine silt [%]</b>	5.60	4.20	4.10
<b>Clay [%]</b>	22.70	16.20	10.00
<b>Soil organic matter [%]</b>	5.20 ± 0.29	5.80 ± 2.25	7.08 ± 1.35
<b>C [%]</b>	2.40	1.48	5.00
<b>N [%]</b>	0.16	0.12	0.23
<b>Al [μmol/g]</b>	3.85	35.34	44.74
<b>Ca [μmol/g]</b>	88.52	29.51	30.06
<b>Fe [μmol/g]</b>	0.05	0.33	3.09
<b>K [μmol/g]</b>	2.09	1.40	0.82
<b>Mg [μmol/g]</b>	13.93	12.80	11.46
<b>Mn [μmol/g]</b>	1.51	1.03	0.18
<b>Na [μmol/g]</b>	4.06	3.10	4.17
<b>P [μmol/g]</b>	0.02	0.03	0.03

### 2.1.2 Plant growth and greenhouse settings

Spruce seeds were sown in the respective pots in 2018 and beech seeds in 2019 (Figure 2a) and grown for one year under sufficient watering (field capacity 20 - 25 % volumetric soil water content, SWC). To ensure controlled experimental conditions, seedlings were kept in a greenhouse with UV-transparent glass and air-conditioned cabins. Cabin temperature was

thus synchronized to outside temperature during the experiment and measured automatically four times per hour together with air moisture and light intensity. The mean temperature from 22.05.2020 – 31.08.2020 was  $20 \pm 6$  °C, mean air humidity was  $68 \pm 8$  % during this period and mean light intensity was  $1.3 \pm 3$  klux.

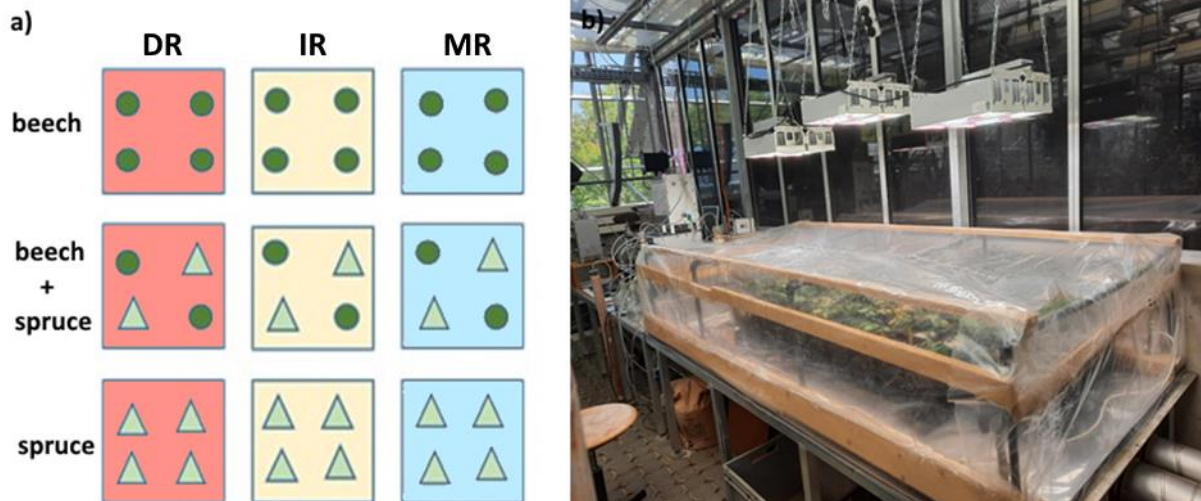


**Figure 2:** a) Planting scheme of beech (circles) and spruce (triangles) in pots containing soil from the (DR, red), the intermediate region (IR, yellow), and the moist region (MR, blue), with inter- or intraspecific root contact. b) Seedlings in the fumigation tent with LED lamps to compensate for any potential light reduction caused by the tent and ensure photosynthesis.

### 2.1.3 Drought treatment, $^{13}\text{C}_2$ labelling and harvest

In May and June 2020, an 8-week drought was applied to the seedlings. According to the relationship between plant or soil water potential and SWC determined in pre-experiments, the target SWC of each pot was defined as 20 % (close to the field capacity) for controls and 12 % for drought treatment for all three soils. Three days before harvest, the seedlings were fumigated with  $^{13}\text{C}$ -enriched  $\text{CO}_2$  for 72 h while the plants were kept in a transparent, airtight fumigation tent (Figure 2b). To ensure photosynthesis and compensate for light reduction by the tent, LED lights were installed above the tent providing c.  $350 \mu\text{mol m}^{-2} \text{s}^{-1}$  photosynthetic photon flux density (PPFD) from 6 am to 4 pm. During harvest, the seedlings were cut 1 cm above the soil and predawn plant water potential was measured using a Scholander pressure bomb (mod. 1505D, PMS Instrument Co., Albany, OR, USA) before sunrise (2 am – 5 am).

#### 2.1.4 Sampling

Soil samples were taken before and after the drought treatment with a soil corer (diameter 5 mm, length 20 cm) and immediately frozen until DNA extraction. After harvest, the rooting system was excavated from the soil, pictures were taken on graph paper and the root system separated into coarse-roots (> 2 mm) and fine-roots (< 2 mm). Single mycorrhizal and non-mycorrhizal fine-root tips were taken, dried and analysed by isotope ratio mass spectrometry (IRMS; delta V Advantage; Thermo Fisher Scientific) coupled to an Elemental Analyzer (Euro EA; Eurovector). After weighing the total fine-root fresh weight, one-third of the fine-roots were immediately frozen for fungal DNA analysis, and two-thirds were weighted again, dried and ground for biomass and non-structural carbohydrate (NSC) measurements akin to the procedure for leaves, stems and coarse-roots.

#### 2.1.5 Fine-root parameter

To gain insights into the root systems of the different treatments and tree species, the following fine-root parameters were measured: number of vital, dead and mycorrhizal root tips, biomass, taproot length and branching intensity. The number of vital, dead and mycorrhizal root tips was counted after harvest. To identify mycorrhizal root tips, attention was paid to the growth form, tip shape, colour and presence of a hyphal mantle and external hyphae. The taproot length of seedlings was measured based on pictures of the root system on harvest day with the software ImageJ (version 1.53a, National Institute of Health, USA). Branching intensity was determined by counting the lateral roots and dividing it by the taproot length.

#### 2.2 KROOF rewatering experiment in a mature forest site

To determine the belowground drought recovery in mature beech and spruce trees concerning the fine-root system and root-associated fungal communities, the plots at the experimental site Kranzberg were rewatered after five consecutive years of experimental summer drought.

### 2.2.1 Setup of the KROOF experiment

The rewatering experiment (articles I, II, III) took place at the 0.5 ha mature forest site Kranzberg forest. Soil parameters of this site were described in chapter 2.1.1. In 2010, the experimental area was divided into 12 plots of 110 to 200 m<sup>2</sup>. Each plot contained three to four trees of European beech (*Fagus sylvatica* L.) as well as Norway spruce (*Picea abies* (L.) KARST.). Each plot was divided into three interaction zones: beech neighbouring beech (BB), beech neighbouring spruce (MIX) and spruce neighbouring spruce (SS) (Goisser et al. 2016; Nickel et al. 2018). Water transport from the plot exterior was prevented by trenching the plots to a one-metre depth and installing waterproof tarpaulin in the trenches. Vertical water transport was naturally prevented by a layer of clay at a depth of approx. 1 m (Grams et al. 2021). In 2013, 6 plots were equipped with under-canopy roofs for throughfall exclusion and 6 control plots where control and throughfall exclusion plots were arranged pairwise (Figure 3a). After four years of recovery from trenching, the throughfall exclusion experiment was started at the beginning of the 2014 growing season. From then on, the roofs closed automatically during rainfall. Thus, rain was excluded from the TE plots for five consecutive years (2014 - 2018) during the growing season (March - November). A weather station on the site recorded air temperature at 2 m and precipitation every 10 minutes (Figure 3b). The volumetric soil water content at different depths (0 - 7 cm, 10 – 30cm, 30 – 50 cm and 50 – 70 cm) was determined with time-domain reflectometers (TDR 100, Campbell Scientific Inc., Logan, Utah, USA) (Figure 3c).

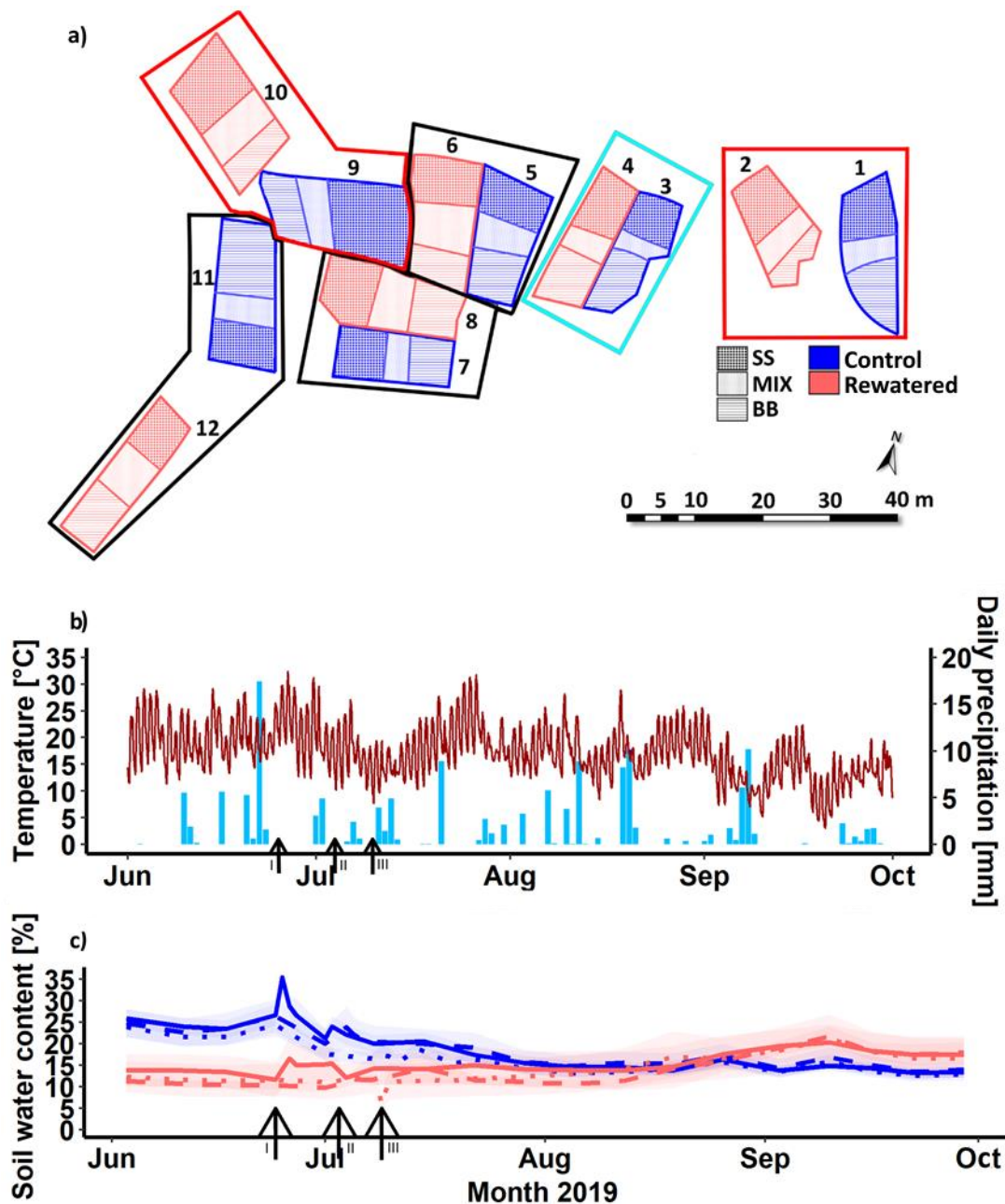


**Figure 3:** a) Arrangement of the experimental plots 1 to 12 at the Kranzberg Forest Roof (KROOF) site. CO refers to controls and TE to rewetted former drought plots, SS indicates the spruce monospecific area, BB the beech monospecific area and MIX the mixture. Boxes display corresponding pairs. Plots in red boxes have not been sampled. Plots in the blue box have additionally been  $^{13}\text{C}$ -labelled during the rewetting. b) illustrates the temperature (line) and precipitation (bars) within the sampling period, c) the soil water content in 0 – 7 cm of control and rewatered plots; different line types indicate the different watering campaigns: solid = first (I, plots 7, 8), dashed = second (II, plots 3, 4, 11, 12), and dotted = third (III, plots 5, 6). Black arrows and roman numbers mark the starting day of the respective watering campaign: I = 25.06.2019, II = 04.07.2019, III = 10.07.2019. Ribbons = standard errors. The figure was modified from article III.

### 2.2.2 Rewatering and $^{13}\text{CO}_2$ labelling

In 2019, the SWC of the rewatered plots was raised back to that of the controls via controlled drip irrigation. For this, on average  $12849 \pm 2801$  l were supplied to the plots via perforated tubes covering the plots at 20 cm intervals for 40 h to initiate the recovery phase (Grams et

al. 2021). The predawn water potential of the rewatered trees recovered from  $-0.93 \pm 0.03$  MPa to  $-0.69 \pm 0.05$  MPa (CO  $-0.61 \pm 0.02$  MPa) after seven days, indicating that the trees were no longer water limited (Grams et al. 2021). In parallel with irrigation, spruce trees in plots 3 and 4 were labelled with  $^{13}\text{C}$ -depleted  $\text{CO}_2$  for 14 days. For this purpose, perforated PVC tubes were suspended from the crown tip over the entire crown area, through which labelled  $\text{CO}_2$  was pumped from 5 am to 7 pm.

### 2.2.3 Sampling

Fine-root samples of mature beech and spruce were taken in two different ways (Figure 4). The roots for monitoring C allocation, fine-root growth, vitality and mycorrhization were taken via mesh bags. For this, individual fine-roots from the upper soil layer (0-5 cm (control) and 0-10 cm (rewatered)) that were still connected to the tree were excavated in April 2019 and carefully put into 1/3 with surrounded soil-filled mesh bags (12.5 cm x 6.5 cm, mesh width 80  $\mu\text{m}$ , open area of 29 %) (Figure 5a). These fine-roots were harvested on days -7, 10, 17, 28, 35, 42 and 89. For  $\delta^{13}\text{C}$  measurements, additional fine-roots were collected daily on the plots for two weeks after rewatering started to get a higher time resolution.

Fine-roots for fungal community analysis and biomass determination were taken via soil cores (diameter 1.4 cm, 25 cm depth). For each interaction zone of each plot, 10 cores were taken on days -7, 6, 18, 41 and 84 and their dark organic topsoil layer (2 - 12 cm, on average 9.38 cm) was pooled to ensure a high representation of the respective zone in the sample. Fine-roots were carefully separated from the soil with sterile tweezers.

In this work, two plot pairs (1/2 and 9/10) were not sampled because in 2015 during a bark beetle infestation, the spruces of plots 2 and 10 died. To maintain the balance between control and rewatered plots, the corresponding plots 1 and 9 were also excluded.

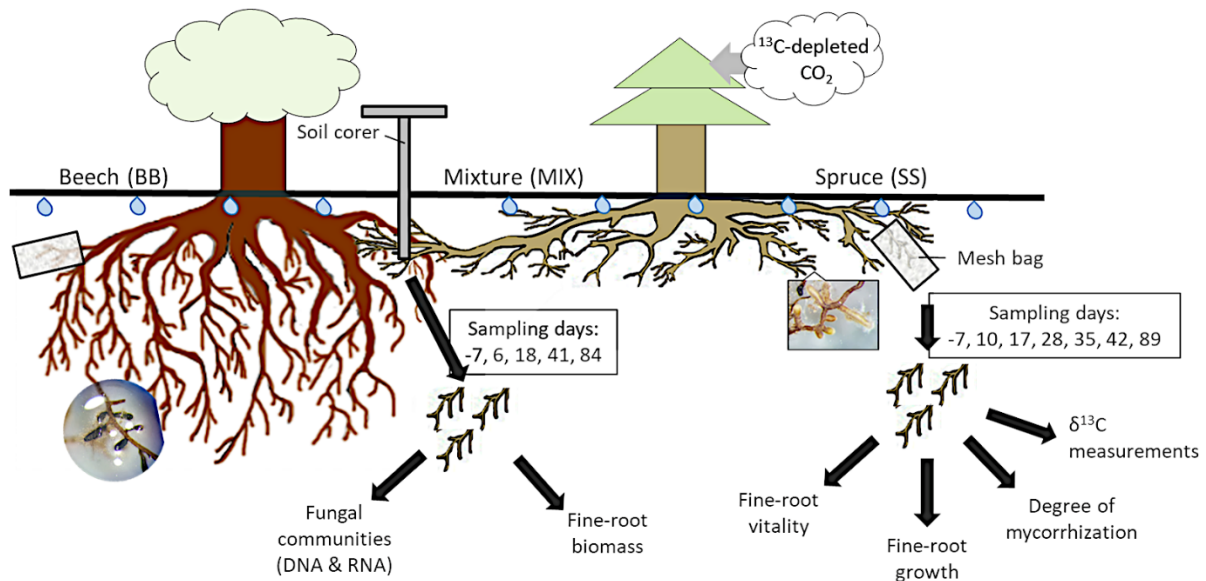


**Figure 4:** Setup of the rewatering experiment at Kranzberg Forest. One plot consisted of mature beech and spruce trees and three interaction zones: beech neighbouring beech (BB), beech neighbouring spruce (MIX) and spruce neighbouring spruce (SS). Root samples were taken via soil cores and mesh bags on different days with respect to the watering event. Parallel to the watering, spruce trees were labelled with  $^{13}\text{C}$  depleted  $\text{CO}_2$ . Fine-roots from soil cores were taken for fungal ITS sequencing and biomass determination, fine-roots and mycorrhizal tips of mesh bags were used for  $\delta^{13}\text{C}$  measurements and tracing fine-root parameters. The figure was modified from article III.

## 2.2.4 Fine-root parameters

To follow the fine-root growth in mature trees, pictures of the excavated fine-roots were taken before putting them into mesh bags (Figure 5b) and on the respective harvest day (Figure 5c). The total root length before and after watering was measured on the pictures with the software ImageJ (version 1.53a, National Institute of Health, USA). The initial length of a fine-root was then subtracted from the length after harvest and corrected by the growth determined at day -7 to exclude pre-experimental growth. According to the method of Qian et al. (1998), the vitality of mesh bag derived fine-roots was assigned using fluorescein-diacetate (FDA). Thus, the fluorescence intensity of root meristem, central cylinder, Hartig net (if root tip is mycorrhizal) or root cortex (if root tip non-mycorrhizal) and hyphal mantle of stained root tip slices was evaluated by eye using a fluorescent microscope (Axioplan, Zeiss, Oberkochen, Germany) (Figure 5d). To estimate the degree of mycorrhization, the total number of roots and of mycorrhizal root tips was counted for each mesh bag root. For fine-



root biomass, 30 mg of root powder was dried and the biomass per cm<sup>3</sup> of soil was determined using the soil volume of the soil cores.

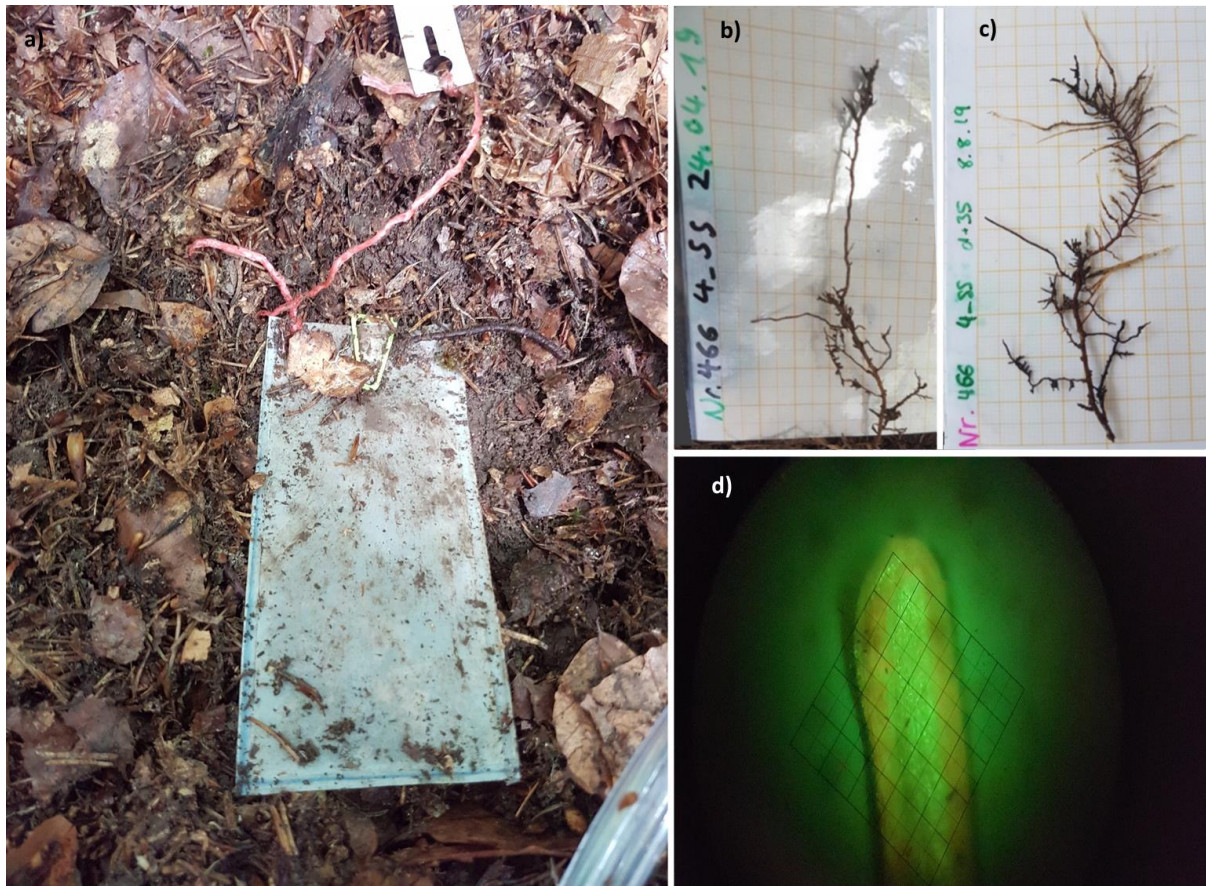


**Figure 5:** Example of fine-root harvest and sample processing. a) excavated mesh bag including a fine-root on harvest day. b) spruce fine-root of a drought plot before drought release and c) the same root at harvest 35 days after watering. d) fluorescent root tip stained with fluorescein-diacetate for vitality analysis.

## 2.2 Nucleic acid extraction and fungal ITS sequencing

For all root and soil samples in both experiments, the same methods for DNA extraction and sequencing were used and therefore are described here only once. Due to its high degree of interspecific variability, conserved primer sites and multiple copies in the genome (Blaalid et al. 2013), the fungal ITS2 rDNA region was amplified and sequenced for fungal species identification. The DNA of all root and soil samples was extracted using the DNeasy PowerSoil Pro Kit (Qiagen, Hilden, Germany) and the DNeasy PowerSoil Kit (Qiagen, Hilden, Germany), respectively. For the KROOF rewating experiment, in addition to DNA, less stable RNA was extracted using the ZymoBIOMICS DNA/RNA Miniprep Kit (Zymo Research, Irvine, California,

USA) to determine community changes after drought release thus reflecting only the metabolically active fungi and excluding remaining molecules of dead organisms. Extracted RNA was then transcribed to cDNA and treated like the DNA samples afterwards. The ITS amplicon was isolated by polymerase chain reaction (PCR) in triplicates with primer mixtures described by (Tedersoo et al. 2014), containing Illumina adapter sequences for Illumina Miseq sequencing. To identify the different samples, each sample received an individual combination of Illumina's custom indexing primers that was added to the adapter sequences. The samples were then sequenced on a Miseq v3chemistry, 600 cycles flow cell (Illumina, San Diego, CA, USA).

### 2.3 Bioinformatics and statistical methods

Here, a summary is given on the generally used bioinformatic and statistical analyses used. Specific analyses are detailed in the respective manuscripts.

#### 2.3.1 DNA-sequence data analysis

Raw sequence data (provided in FASTQ format) were prepared for further analysis using the automated pipeline for fungal ITS sequences PIPITS v2.7 (Gweon et al. 2015). There, the sequences were quality filtered, the ITS2 region extracted and sequences below 100 bp excluded. The remaining sequences were then assigned to Operational Taxonomic Units (OTUs) with 97 % sequence similarity. The taxonomic classification was achieved using the Ribosomal Database Project (RDP) classifier, which compares the sequences with those supplied by the UNITE database. Further fungal traits were then assigned by matching the genus level of the taxonomic output with the FungalTraits database (Pölme et al. 2020).

#### 2.3.2 Statistics

For statistics and graphic illustration, the software R (version 4.0.2, RCore Team, 2021) and RStudio (version 1.4.1717, RStudio Inc.) were used. Sequencing data were randomly rarefied with 1.000 repetitions using GNUniFrac (Chen et al. 2012) to a sample depth of 10.000 or 6.000. Taxa that occurred less than 10 times were removed. The R package vegan (Oksanen et al. 2019) was used to calculate Bray-Curtis dissimilarity between the samples and

multivariate testing to determine the effects of treatment, soil types, tree interactions and in case of roots tree species by permutational multivariate analysis of variance (PERMANOVA). The package phyloseq (McMurdie and Holmes 2013) was used to produce ordinations and calculate abundances.

To statistically analyse single factors, the data were tested for normal distribution using the Shapiro-Wilk test. Normally distributed datasets were analysed using an analysis of variance (ANOVA) or a linear mixed model. If normality of the data failed ( $p < 0.05$ ), either a nonparametric aligned rank transform for nonparametric factorial ANOVAs (ART-ANOVA) for multifactorial comparisons or Kruskal-Wallis test for one-factorial comparisons was performed. Depending on the previous statistical testing method, Tukey's honest significance test, Dunn test or paired PERMANOVA were used for post-hoc analysis, the latter two with Bonferroni-adjustment. Samples were considered significantly different when  $p < 0.05$ .

### 3 Publications, manuscripts and additional results

In this work, the interaction between soil/root-associated fungi and tree drought response and recovery was investigated. This section provides a summary of the results, which are further detailed in the respective manuscript and articles attached. The influence of soils with distinct precipitation histories on the drought response of fungal communities and beech seedlings is summarised in 3.1. The belowground drought recovery in mature beech and spruce was approached in three different aspects: recovery of the C transport system in spruce (3.2), C allocation within the whole spruce tree (3.3) and the recovery of root-associated fungal communities with respect to the fine-root system of beech and spruce (3.4). Additional results on spruce seedlings, which were omitted from manuscript I (and thus chapter 3.1) are presented separately in chapter 3.5.

### 3.1 Acclimation in root architecture rather than long-term adaption of fungal symbiosis mitigates drought effect on European beech seedlings (manuscript)

Danzberger, J. \*, Hikino, K. \*, Landhäusser, S.M., Hesse, B.D., Meyer, S., Buegger, F., Weigl, F., Grams, T.E.E., Pritsch, K.

\*These authors have contributed equally to this work and share the first authorship

To determine whether fungal communities in drought-prone regions were better adapted to dry periods and thus less affected by drought and whether plants grow better in drought-adapted soils, an artificial drought phase of two months was simulated in a greenhouse experiment. Fungal community composition was determined in soils before and after drought and in roots with tree harvest after drought by fungal ITS sequencing. Furthermore, seedling growth, biomass of leaves, stem and roots, as well as photosynthetic activity were recorded along with the fine-root morphology. Additionally, the C allocation to the different organs was traced by  $^{13}\text{C}$  labelling. The abundance of different fungal traits as well as dominating species changed the most in moist region samples and least in dry region samples. According to predawn plant water potential measurements, MR plants were the least drought-stressed. Their roots grew significantly deeper into the soil in drought-treated pots having the least root branches while DR plants rooted shallow with high branching intensity. Following the plant water potential, growth and photosynthesis were more affected by drought in DR and IR plants. Also, the allocation of newly synthesised C ( $C_{\text{new}}$ ) followed the plant water potential where the amount of  $C_{\text{new}}$  increased in leaves in DR and IR plants during drought and decreased belowground while in MR plants the same amount of  $C_{\text{new}}$  is transferred belowground in control and drought treated samples. These results confirm the hypothesis that previously adapted fungal communities are less affected by drought. However, drought stress of beech seedlings seems to depend to a high extend on the root architecture but a fungal influence on root architecture cannot be excluded.

### Contribution:

I wrote the paper draft together with Kyohsuke Hikino and we share the first authorship. Both of us planned and conducted the experiment and did the sampling together with the co-authors. My responsibility lay in root and soil sampling, ITS sequencing and analyses, measuring fine-root parameters and the respective data analysis. Both first authors prepared the samples for  $\delta^{13}\text{C}$  measurements which were carried out by Franz Buegger. I interpreted the results together with the co-authors.

### 3.2 High resilience of carbon transport in long-term drought-stressed mature Norway spruce trees within 2 weeks after drought release (Article I)

Hikino, K., Danzberger, J., Riedel, V. P., Rehschuh, R., Ruehr, N. K., Hesse, B. D., Lehmann, M. M., Buegger, F., Weikl, F., Pritsch, K., Grams, T. E. E. (2021). *Global Change Biology*.

To investigate the recovery of carbon transport rates in approximately 70-year-old Norway spruce (*Picea abies* [L.] KARST.) after 5 years of recurrent summer drought, a continuous whole tree  $^{13}\text{C}$ -labelling experiment was conducted in parallel with irrigation. The timing of the arrival of current photoassimilates in key C sinks was determined by tracking  $^{13}\text{C}$  labelling in the stem and soil  $\text{CO}_2$  output and in the tips of living fine-roots. In the first week after rewatering, aboveground C transport rates (CTR) from crown to trunk base were still 50% lower ( $0.16 \pm 0.01 \text{ m h}^{-1}$ ) in formerly drought-stressed trees compared to controls ( $0.30 \pm 0.06 \text{ m h}^{-1}$ ). On the contrary, the belowground CTR (from the base of the trunk to the soil  $\text{CO}_2$  efflux) were already similar between treatments (about  $0.03 \text{ m h}^{-1}$ ). After two weeks, the aboveground C transport of the formerly drought-stressed trees recovered and resembled the controls. Moreover, the regrowth of water-absorbing fine-roots after drought release was reinforced by a faster uptake of  $^{13}\text{C}$  in the formerly drought-stressed trees (within  $12 \pm 10$  hours after arrival at the trunk base) compared to the controls ( $73 \pm 10$  hours). Thus, the C transport system within the whole tree ranging from crown to soil  $\text{CO}_2$  efflux fully recovered within two weeks after drought release, demonstrating a high resilience to recurring summer droughts in mature spruce and is an important criterion for the restoration of other tree functions and productivity. The immediate recovery of the belowground CTR in comparison to aboveground, along with the fast uptake of new photoassimilates by recovering fine-roots compared to the controls, support the hypothesis that the regeneration of the water-absorbing fine-roots after drought release is a high priority.

## Contributions:

As co-author I wrote those parts of the introduction, material and methods, results and discussion that deal with ectomycorrhizae and fine-roots. Furthermore, I sampled and processed mycorrhizal and fine-root samples, did the respective data analysis. I interpreted the entire results together with all co-authors.



### 3.3 Dynamics of initial C allocation after drought release in mature Norway spruce - Increased belowground allocation of current photoassimilates covers only half of the C used for fine-root growth (Article II)

Hikino, K. \*, Danzberger, J. \*, Riedel, V. P., Hesse, B. D., Hafner, B. D., Gebhardt, T., Rehschuh, R., Ruehr, N. K., Brunn, M., Bauerle, T. L., Landhäusser, S. M., Lehmann, M. M., Rötzer, T., Pretzsch, H., Buegger, F., Weigl, F., Pritsch, K., Grams, T. E. E. (2022). *Global Change Biology*.

\* Kyohsuke Hikino and Jasmin Danzberger contributed equally to this work and share the first authorship.

After drought, tree recovery also depends on an adequate C allocation to the sink organs. Within this article, the dynamics of C sink activity at the whole tree level together with the allocation of recent photoassimilates ( $C_{\text{new}}$ ) and stored C in mature Norway spruce were determined after drought release. We used the same experiment as above (3.1), i.e. a continuous, whole tree  $^{13}\text{C}$  labelling in parallel with controlled irrigation after five years of experimental summer drought. The use of  $C_{\text{new}}$  for growth and  $\text{CO}_2$  efflux was followed along branches, trunks, coarse and fine-roots, ectomycorrhizae and root exudates to soil  $\text{CO}_2$  efflux after drought. Regarding the aboveground organs, branch efflux notably showed the most significant difference between recovering trees ( $558 \pm 86 \text{ g C tree}^{-1} 28 \text{ days}^{-1}$ ) and controls ( $1205 \pm 131 \text{ g C tree}^{-1} 28 \text{ days}^{-1}$ ). In contrast, belowground, the C sink activity of fine-root growth in recovering trees was with  $965 \pm 136 \text{ g C tree}^{-1} 28 \text{ days}^{-1}$  seven times higher than in control trees ( $136 \pm 12 \text{ g C tree}^{-1} 28 \text{ days}^{-1}$ ). The allocation of  $C_{\text{new}}$  in recovering trees towards aboveground sinks was 19 % lower than in controls, whereas it was 19 % higher in recovering trees towards belowground sinks compared to controls and with the highest difference in fine-root growth (recovering:  $18 \pm 4 \%$ , control:  $1 \pm 0 \%$ ). Nonetheless, only half of the C used for new fine-root growth consisted of  $C_{\text{new}}$ , while the other half originated from stored C. These results indicate a low precedence of aboveground sinks during recovery of mature spruce trees compared to belowground sinks, which additionally to chapter 3.2 reinforce the

hypothesis of a prioritised recovery of the water-absorbing fine-roots after drought release. Furthermore, these findings underscore the importance of both the availability of carbon stores and the allocation of newly assimilated photoassimilates to facilitate the repair and regrowth of functional tissues.

#### Contributions:

I wrote the paper draft together with Kyohsuke Hikino, both sharing the first authorship. We collaboratively designed the experiment, carried out the experimental procedures, and conducted the sampling together with the co-authors. I processed fine-root and mycorrhizal samples, prepared them for  $\delta^{13}\text{C}$  measurement, determined fine-root growth and analysed them. Furthermore, I interpreted the results together with the co-authors.

### 3.4 Drought legacy effects on fine-root-associated fungal communities are modulated by root interactions between tree species (Article III)

Danzberger, J., Werner, R., Mucha, R., Pritsch, K., Weigl, F. (2023). *Frontiers in Forests and Global Change*.

To gain a detailed insight into belowground recovery, the relationship between root-associated fungal community composition and tree species-specific fine-root regeneration in mature European beech and Norway spruce was assessed in the same rewatering experiment. During the recovery phase from five years of experimental summer drought, the root-associated fungal community composition was tracked by ITS sequencing at DNA and RNA level for three months along with fine-root parameters in monospecific and mixed tree interaction zones. The dynamics of fine-root recovery contrasted between beech and spruce. Beech primarily generated new fine-roots, while spruce reactivated dormant fine-roots with a similar growth but shorter lifespan compared to controls. However, no distinct impact of tree species mixture on fine-root recovery could be identified. The root-associated fungal communities showed no significant response to rewatering within the first three months after rewatering. Nevertheless, the abundance of fungal trophic modes and single fungal species within root-associated fungal communities significantly differed between beech and spruce. Beech had a higher abundance of ECM fungi, while spruce showed a greater prevalence of saprotrophs. This difference is likely influenced by tree species-specific drought responses, such as fine-root suberisation in spruce and continuous fine-root production in beech. A high number of saprotrophic fungal species were associated to a secondary, root-associated lifestyle. A higher species richness and increase of ECM fungi on roots with interspecific root contact after drought indicate a positive effect of tree species mixture.

These results suggest, that structure of the fungal community after rewatering was lastingly influenced by the previous drought, but its composition highly depends on the development of tree-specific root systems and habitat heterogeneity. Moreover, a facultative root-

associated lifestyle of saprotrophic fungi could support fungal survival during drought. These results do not support the hypothesis that fungal communities will undergo a change and resemble the control communities within the initial phase of recovery after drought release. However, it remains unclear whether there will be a recovery in the longer term. Furthermore, while the hypothesis that tree species mixture has a positive effect on fungal diversity and fine-root regeneration was supported for fungal diversity, it was not supported for fine-root regeneration.

#### Contributions:

I wrote the paper, developed the outline and performed the experimental work and statistical analysis with the help of Ramona Werner and Fabian Weigl. I planned the experiment together with the co-authors and interpreted the results together with the co-authors.

### 3.5 Additional results not presented in the manuscript and articles (all results in appendix)

To thoroughly assess whether seedlings are less affected by drought in soils with drought-adapted fungal communities and interspecific root interactions, spruce seedlings were studied alongside beech seedlings as part of the greenhouse experiment (as described in chapter 3.1 and manuscript I). Spruce seedlings were grown either in monoculture or in mixed-culture pots with beech, and subjected to a two-month drought. As with beech in manuscript I, seedling growth, leaf, stem, and root biomass were measured, alongside fine-root morphology and allocation of new photoassimilates. Fungal community composition was analysed in soils both before and after drought, as well as in roots collected during the post-drought harvest, using fungal ITS sequencing. The predawn water potential in spruce seedlings was significantly lower in drought-treated seedlings across all soils, indicating water stress, though the severity of this stress did not vary between soil types. Relative stem and root biomass growth was not affected by drought, although seedlings in IR soil displayed stunted growth and higher mortality. Drought caused changes in C allocation in spruce seedlings growing in DR soil, with reduced C directed to the roots and increased allocation to the leaves compared to control seedlings. Under drought conditions, spruce seedlings in DR soil exhibited a significant increase in taproot length and a reduction in the degree of mycorrhization, while seedlings in other soils showed no such drought effects. Soil fungal communities differed significantly between the various soil types but did not differ between control and drought treatments. In contrast, root fungal communities showed significant differences between both treatments and soils. In the roots of drought-treated seedlings, the abundance of saprotrophic fungi increased at the expense of ECM fungi, particularly in DR and MR soils. Species mixture had no effect on either fine-root morphology or the composition of fungal communities.

### Contribution:

I planned and conducted the experiment together with Kyohsuke Hikino. My responsibility lay in root and soil sampling, ITS sequencing, measuring fine-root parameters and the respective data analysis. Kyohsuke and I prepared the samples for  $\delta^{13}\text{C}$  measurements which were carried out by Franz Buegger. I have interpreted these results as part of this doctoral thesis.

## 4 General discussion

In this work, the influence of naturally drought-adapted soils and fungal communities on the drought resistance of beech and spruce seedlings, the belowground recovery of mature beech and spruce and their root-associated fungal communities after repeated summer drought and the influence of tree species mixture on recovery have been investigated.

In this general discussion, I combine the results from all studies and discuss them in the context of the research questions and hypotheses stated previously. Detailed discussions of the individual studies can be found in the respective articles and manuscripts (appendix).

### 4.1 Are fungal communities in drought-prone regions better adapted to dry periods compared to communities in moist regions and thus less affected by drought?

To determine whether fungal communities in soils from dry regions are less affected by drought phases than those from moist regions, beech and spruce seedlings were grown in different soils with inter- and intraspecific root contact and exposed to a two-month drought as part of the greenhouse experiment.

Differences between the fungal community composition associated with beech and spruce roots were observed (Appendix Figure A5), which can be attributed to the host species preference of the ECM fungi in particular (Tedersoo et al. 2008, 2010; Ding et al. 2011).

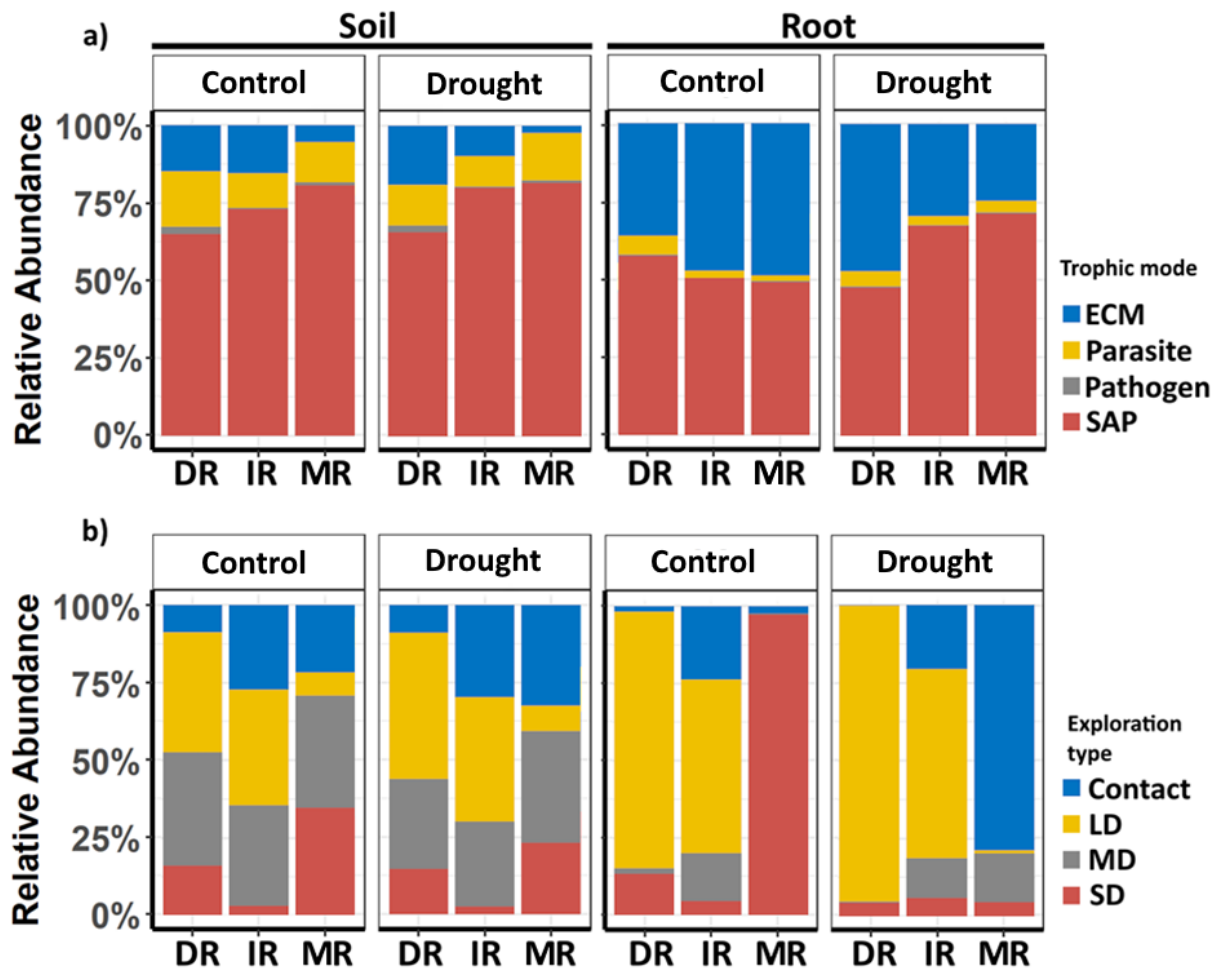


*Figure 6: Summed up relative abundances of rDNA-based soil (left panels) and root-associated fungal communities (right panels) according to trophic mode and ECM fungal exploration type grouped by soil types (DR = dry region soil, IR = intermediate region soil, MR = moist region soil) and treatment (CO = control, D = drought). a) shows the trophic modes of soil and root-associated fungal communities whereby blue represents ectomycorrhizal fungi, yellow parasites, grey pathogens and red saprotrophs. b) illustrates the abundance of ectomycorrhizal exploration types of soil and root-associated ectomycorrhizal fungi. Blue portrays contact types, yellow long-distance types, grey medium-distance types and red short-distance types. This figure was modified from manuscript I.*

The fungal communities obtained from soil as well as root samples varied across the different soils even before the drought experiment in both beech and spruce pots, indicating an adaption of the fungal communities to the different soils along the precipitation gradient (Cavender-Bares et al. 2009; Huang et al. 2021). In the soil samples, saprotrophic fungi predominated across all three soil types in both beech (manuscript I, Figure 6a) and spruce (Appendix Figure A6a). Compared to soil samples, the abundance of ECM fungi is higher in root samples of beech as well as spruce seedlings, whereby in beech in all soils as well as



spruce in DR, saprotrophs and ECM fungi were detected in more or less equal proportions (approximately 50:50 according to read counts). Saprotrophs gain their C mainly from the decay of organic matter (Talbot et al. 2013, 2015) allowing a more free-living lifestyle compared to ECM fungi, which rather depend on their host's C supply (Lindahl and Tunlid 2015) and thus need direct host contact. This could explain the different proportions of saprotrophs and ECM fungi in soil compared to root samples. Furthermore, the abundance of ECM fungi grouped by their assigned exploration types revealed higher shares of long- and medium-distance types in DR and IR compared to MR in soil and root samples of beech (Figure 6b) and spruce (Appendix Figure A6b). It is assumed that ECM fungi with long- or medium-distance exploration types are more effective at transporting water compared to short-distance or contact types (Brownlee et al. 1983; Agerer 2001). A closer look at the fungal species composition further strengthened this observation of community adaption to the soils in both soil and root samples for beech as well as spruce. Hence, for example, drought-tolerating *Melanogaster* sp. (beech and spruce soil and root; Frey et al., 2021; Izzo et al., 2005) and *Cortinarius* sp. (spruce soil; (Bödeker et al. 2014; Boczoń et al. 2021)) were highly abundant in DR but less in MR.

With application of the experimental drought, the proportions of trophic modes did not change much in soil fungal communities associated to beech and spruce in all soils (Figure 6a, Appendix Figure A6a) while the abundance of saprotrophs in root-associated fungal communities linked to beech and spruce increased especially in MR compared to controls. Hence, the abundance of saprotrophic fungi also increases in DR in spruce seedlings during drought, which could be due to a lower root plasticity compared to beech (Schall et al. 2012) and root dormancy with decreased mycorrhization (Feil et al. 1988). These results indicate a more stable community of soil fungi during drought compared to the fungal community associated to roots, which was also observed in grassland fungal communities during drought (Fu et al. 2022) and supports earlier findings of drought resistant soil fungal communities (de Vries et al. 2012, 2018). It is possible that root-associated fungi react to changes in the quality

and quantity of root exudates (Warembourg et al. 2003; Williams and de Vries 2020; Lozano et al. 2021) caused by the host's species-specific drought response (Lozano et al. 2021). During drought, the abundances of ECM fungi with different exploration types in DR soil and root samples (and in beech IR as well) remained unchanged. However, in MR, contact types became the most abundant fungal exploration type in both beech and spruce roots, compared to controls. This is in line with the observed rise in the prevalence of contact types during extended drought periods (Castaño et al. 2018, article III), which can potentially be attributed to their relatively lower carbon costs for maintenance (Lehto and Zwiazek 2011). ECM fungi on tree seedlings were shown to be rapidly supplied by recent photoassimilates (Heinonsalo et al. 2004) and less by C reserves (Druebert et al. 2009). Nevertheless, no reduction in the allocation of new photoassimilates to belowground was observed in MR beech seedlings with drought (manuscript I) which could justify such a drastic change in fungal species abundance in favour of fungal species classified as contact type.

On species level, the composition of the most abundant ECM fungi underwent the most changes in MR during drought compared to controls of beech and spruce in soil and root samples. Therefore, the proportion of *Amanita* sp., a drought tolerant (Querejeta et al. 2009) species classified as contact type, increased substantially with drought, while other species decreased strongly compared to control. Hence, the drastic shift in MR in beech to contact types during drought is likely driven by a high increase of *Amanita* sp.. *Amanita muscaria* has been shown to up- and downregulate PIP genes in plants (Marjanović et al. 2005), coding for Aquaporins which are essential for water uptake. The increase of *Amanita* sp. during drought might indicate that this species could also have a positive influence on water uptake.

In summary, these results revealed that fungal communities sourced from naturally dry regions underwent comparatively fewer changes during a drought period in beech and spruce, unlike fungal communities from naturally moist regions. Overall, the respective hypothesis that fungal communities in soils originating from a dry region were drought-adapted and thus less affected by drought than fungal communities from a moist region could be confirmed.

#### 4.2 Are seedlings less affected by drought when growing in soils with drought-adapted fungal communities and interspecific root interaction?

Multiple studies have indicated that the mixture of beech and spruce trees in dry regions can lead to mutual benefits for both species (e.g. González de Andrés et al., 2018; Grossiord et al., 2014a; Hafner et al., 2017; Rukh et al., 2020). In this experiment, however, it was not possible to detect any positive mixing effects for either beech or spruce. Most studies that reported positive mixture effects on beech and spruce focused on mature trees, but studies examining beech and spruce seedlings remain scarce. As such, Kozovits et al. (2005) observed that beech seedlings exhibited a smaller size when grown alongside spruce, compared to seedlings growing in monoculture. Nonetheless, the root system remained unaffected by the reduced growth. Conversely, Bebre et al. (2021) noted a slightly increased biomass production in beech seedlings when planted in mixture with spruce, albeit statistically insignificant.

The predawn leaf water potential of beech and spruce seedlings was notably reduced during drought in comparison to controls across all soil types, which implies that all drought treated seedlings experienced drought stress. Unexpectedly, the difference in predawn water potential between control and drought treated beech seedlings was considerably less pronounced in MR compared to DR and IR, even though MR harboured the least drought-adapted fungal communities (manuscript I). The reduction of the predawn leaf water potential of spruce seedlings with drought has been similar in all soils (Appendix Figure A1). According to Allsup et al. (2023), seedlings of different tree genera, associating with either arbuscular or ECM fungi, that were inoculated with microbial communities from dry regions revealed an enhanced drought resistance. However, this benefit was primarily attributed to an increase in diversity of arbuscular fungi and thus only detected in seedling genera associated with arbuscular fungi and was not detectable in ECM fungi-associated seedlings. Additionally, Herol et al. (2023, Preprint) described, that with the onset of drought, a positive effect of ECM fungi on Aleppo pine seedling growth was greatly diminished or even non-existent under competition. As both, beech and spruce are ECM-associated species, and considering the

application of drought, the findings of this thesis confirm the results of these studies. Seedlings grown in soils with drought-tolerant fungal communities did not show an improved drought tolerance according to their predawn leaf water potential and relative stem and root growth (manuscript I, Appendix Figures A1, A2).

Remarkable was the observed difference in the root systems of beech and spruce seedlings across the different soils (manuscript I, Appendix Figure A4). Notably, in beech seedlings, the taproot length in MR exceeded that in DR, with a comparatively lower branching intensity, whereas in spruce, the taproot length was the largest in DR.

Moreover, in DR soil, the length of spruce taproots significantly increased compared to the other soils (Appendix Figure A4a). This increase was accompanied by a notable decrease in the level of mycorrhization within the same soil (Appendix Figure A4d). A similar trend was detected in beech, where the degree of mycorrhization tended to be lowest in MR (additionally indicated by the lowest sequencing reads in MR; data not shown), coinciding with the highest taproot length in MR (manuscript I). This suggests a pattern where reduced mycorrhization coincides with a greater taproot lengths. This contrasts with the findings of Pena et al. (2013), who reported longer roots and a higher specific root length in mycorrhizal beech seedlings compared to non-mycorrhizal seedlings. On the other hand, a study on Scots pine seedlings revealed a higher shoot/root ratio and lower root biomass in mycorrhizal seedlings compared to non-mycorrhizal seedlings (Colpaert et al. 1996). In their experimental setup using a semi-hydroponic system, Colpaert et al. (1996) ruled out enhanced nutrient uptake or growth as explanations for the increased shoot/root ratio. Instead, they attributed this phenomenon to the mycorrhizal infection itself, suggesting a redistribution of carbon allocation from root growth to fungal growth. In the present study, the allocation of new photoassimilates to the fine-roots of beech seedlings was slightly lower in MR compared to the more mycorrhizal DR and IR (manuscript I). In DR spruce seedlings, the C allocation to fine-roots decreased significantly under drought conditions when the degree of mycorrhization declined (Appendix Figures A3, A4d). Moreover, ECM fungi were found to produce and exude

compounds similar to plant hormones, such as auxins, which can initiate root modifications (Chanclud and Morel 2016). Thus, plants interacting with mycorrhizal fungi had a higher concentration of auxin (Barker and Tagu 2000; Meixner et al. 2005; Chanclud and Morel 2016), which, in high concentrations, has been shown to inhibit root growth (Tanimoto 2005). Therefore, it is possible that with lower mycorrhization, the root systems of MR beech and DR spruce were less restricted in growth by fungal hormones.

Nevertheless, it was noticed that both control and drought treated spruce seedlings within IR were smaller compared to those in DR and MR and had a higher mortality. Soil nutrient analysis (manuscript I) indicated a slightly lower concentration of N and C within IR, but no deficiency. Conversely, beech seedlings had no reduced growth in this soil compared to DR and MR. Neither the soil nor the roots of these IR spruce seedlings showed a higher abundance of parasitic or pathogenic fungal species, and the identified species of parasitic or pathogenic fungal was not different between IR, DR, and MR. Hence, it is possible that another, non-fungal pathogen, such as bacteria or viruses, may have infected these seedlings and was not detected in this study.

In summary, these findings indicate that the structure of the root system plays a critical role in seedlings' drought tolerance, particularly in the case of beech. Previous adaption of the fungal communities, however, did not increase the seedlings' drought tolerance, neither did interspecific root interaction. Yet, the results suggest that the degree of mycorrhization influenced the root architecture and carbon allocation, and thus was associated with drought tolerance. However, the hypothesis that seedlings growing in dry region soil would benefit from the association with drought-adapted fungi and tree species mixture needs to be rejected.

#### 4.3 How do the fine-root systems of mature beech and spruce recover within three months upon drought release after five years of repeated summer drought?

While most studies on forest drought recovery focus on aboveground organs, little is known about the fine-roots and root-associated fungal communities, despite both play a crucial role

in tree survival as they are in charge of water and nutrient absorption (cf. article III). After a strong reduction of beech and spruce fine-root growth during drought on the same experimental site (Nickel et al. 2018; Zwetsloot and Bauerle 2021), a high priority of fine-root growth after drought release in mature trees was determined in this work, underpinning the requirement to restore the essential functions of fine-roots for resource uptake (Bardgett et al. 2014; Solly et al. 2018; Germon et al. 2020). After drought release, the fine-root biomass increased in both, beech and spruce, indicating increased root growth (article III). Increased fine-root production and fine-root biomass were also shown for other coniferous trees after watering (Olesinski et al. 2011; Brunner et al. 2019). However, the recovery of the root systems of both tree species differed from each other (article III). During drought, beech was shown to constantly produce new, thin fine-roots and have older ones die, while fine-roots in spruce became increasingly suberised to prevent water and nutrient loss (Nikolova et al. 2020). Also, after rewatering, the root systems of the two tree species differed in their recovery. Beech fine-roots established before the watering event had only low vitality compared to control roots and both controls and recovering roots showed no longitudinal growth. In spruce, before watering established fine-roots were reactivated and grew as well as in controls – similar to Scots pine (Joseph et al. 2020) – even though their vitality was lowered, suggesting reduced longevity (Gaul et al. 2008). Increased growth, however, requires a higher C usage to build up new cell walls. In this work, a seven times higher C sink activity in spruce (article II, Figure 7a), which describes the C demand, was reported in fine-root growth of recovering trees compared to controls. The trees might preferentially allocate C to the organ which supplies the tree with the growth-limiting resource – water during drought - according to the optimal partitioning theory (Bloom et al. 1985). With water, a high amount of dissolved nutrients are taken up needed for repair processes and growth (Gessler et al. 2017). New photoassimilates in recovering trees arrived in the roots five times faster (article I) and were allocated to the fine-roots to a higher extent (article II, Figure 7b) than in controls. The belowground C transport rate of recovering spruce trees was already resembling controls in the first week (article I), whereas it took two weeks for the aboveground C transport rate

to recover. This finding suggests that the root phloem transport recovered fast and fully thus enabling fine-root growth and resulting water absorbance (Poorter et al. 2012). Also in young beech and mature Scots pine, a preferred C allocation to the rooting system was shown after drought release (Hagedorn et al. 2016; Joseph et al. 2020; Gao et al. 2021). In the present study, the majority of the carbon demand for fine-root growth in control trees is met by new photoassimilates, consistent with findings in other tree species such as American sweetgum (Lynch et al. 2013) and oak (Langley et al. 2002). In contrast, in recovering trees, over half of the carbon supply used for root growth is derived from carbon stores (article II, Figure 7c). Furthermore, the concentration of starch in this experiment decreased in fine-roots within the first week after watering together with an increase of sugars in NSCs suggesting that C stores were mobilised for fine-root growth. A study on Chinese fir saplings also showed a higher reduction of NSC pools in fine-roots than in aboveground tissues after drought release (Yang et al. 2016). The fast incorporation time and preferred allocation of C in fine-roots of recovering trees following a highly increased C demand supports the theory that sink activity controls source activity and not vice versa, which is discussed in the literature (Fatichi et al. 2014; Körner 2015). The C allocation to mycorrhizae did not differ between recovering and control spruces (article II) indicating that the symbiosis between fungi and plant roots is not affected by drought in terms of sink strength as long as the fine-roots are still vital (Fuchslueger et al. 2014; Nickel et al. 2018). Furthermore, the suberisation of spruce fine-roots during drought can be a barrier for ECM colonisation (Brundrett 2002; Sharda and Koide 2008) which would result in a need for new colonisation of growing roots after rewatering. Indeed, the mycorrhization in spruce fine-roots increased from day 28 after watering (article III) which is the time needed for full mycorrhizal development (Ineichen and Wiemken 1992). This can lead to an asynchrony in C allocation between fine-root growth and ectomycorrhizae, whereby the allocation of newly assimilated C to newly formed ectomycorrhizae might peak at a later time point than in fine-root growth and thus was not covered during our study period of four weeks. Mycorrhization of beech fine-roots, however, strongly correlated with fine-root

vitality (article III) indicating that fungal partners in addition to environmental factors also strongly rely on surviving root tips during drought (Shi et al., 2002; Weigl et al., 2023, Preprint).

Alltogether, these results suggest a fast recovery of the fine-root systems in both beech and spruce. In spruce, this involved a fast restoration of the belowground carbon transport rate and a substantial allocation of new photoassimilates to recovering fine-roots. In both species, fine-root recovery immediately started after drought release, but with different strategies between beech (continuous fine-root production) and spruce (fine-root reactivation). Hence, the hypothesis that the regeneration of the water-absorbing fine-root system is a high priority can be confirmed.



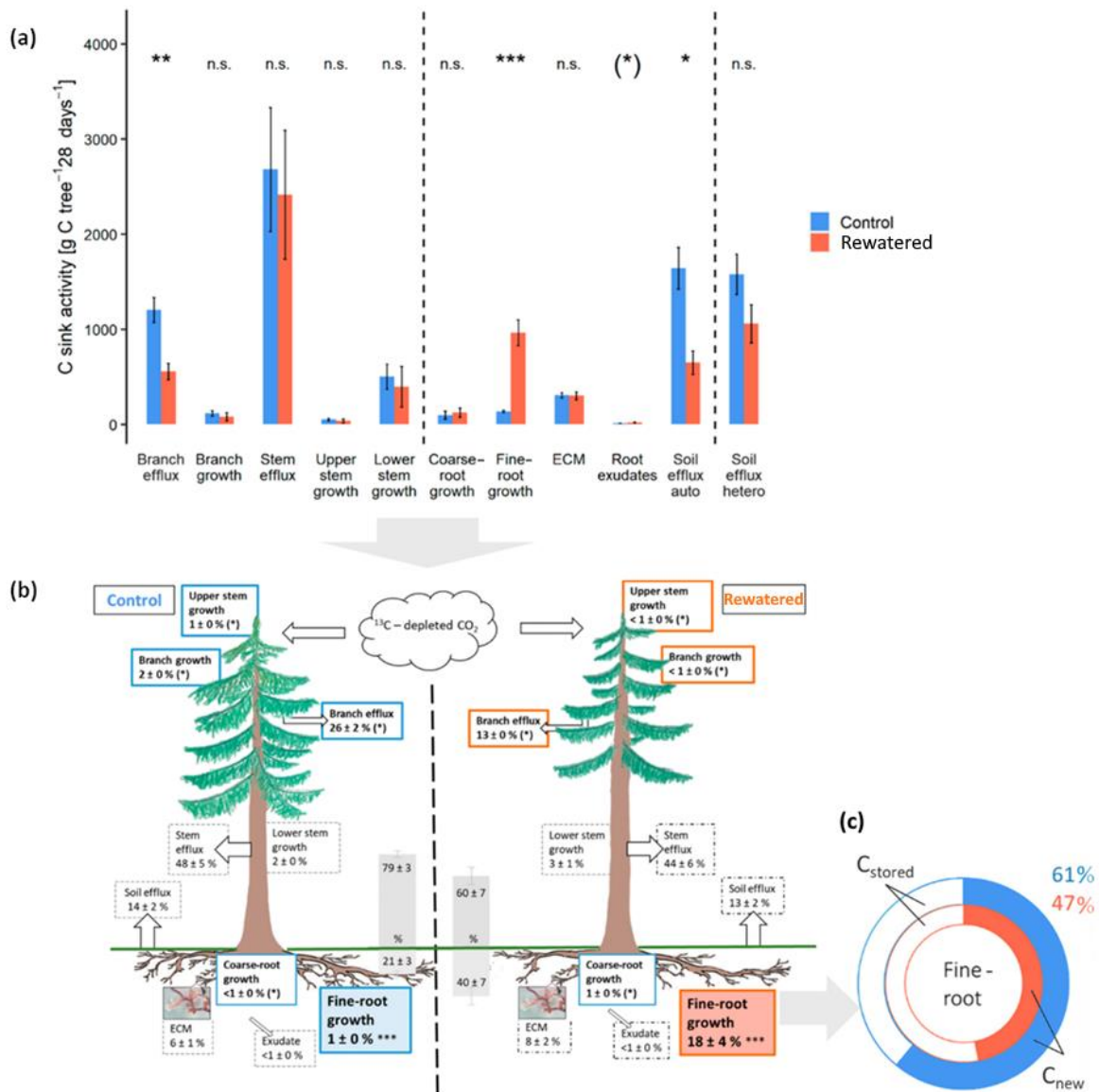


**Figure 7:** Overview of carbon (C) allocation in spruce after drought release. The C sink activity a) describes the summed-up amount of C used by a tree in each organ within 28 days after drought release. b) illustrates the allocation of newly assimilated C (C<sub>new</sub>) in each organ. The grey bar plots indicate the allocation above- and belowground. c) reflects the percentage of to fine-roots allocated C<sub>new</sub> concerning the total fine-root C demand. Blue emphasizes control trees and red rewatered trees. n.s. = not significant, \* indicates  $p < 0.05$ , \*\*  $p < 0.01$ , \*\*\*  $p < 0.001$ . The figure was modified from article II.

#### 4.4 Do root-associated fungal communities connected to beech and spruce recover after rewatering to resemble their pre-drought composition?

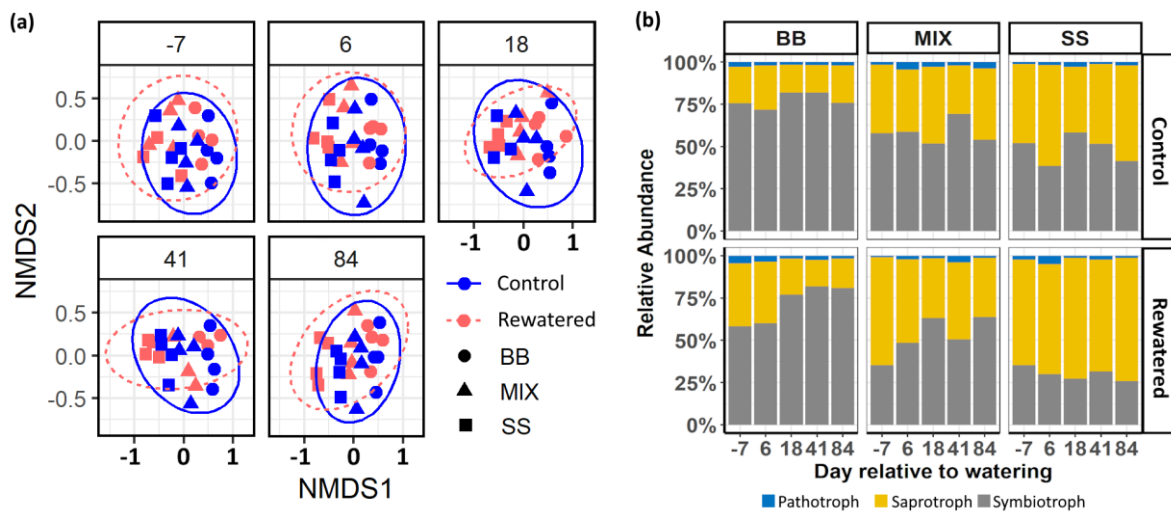


**Figure 8:** a) Non-metric multidimensional scaling (NMDS) plot of root-associated fungal community composition. Each plot shows samples from one sampling date relative to the day of rewatering in a shared coordinate system (i.e., the same ordination). Ellipses represent 95% confidence intervals. Stress = 0.18. b) Summed up relative abundance of trophic modes after watering in control and rewatered plots, in each of three tree rooting zones: beech monospecific (BB), spruce monospecific (SS) and mixture (MIX). The figure was modified from article III.

The community composition of root-associated fungal communities linked to beech as well as spruce did not significantly change after drought release (article III, Figure 8a) which could indicate that during the years of consecutive summer drought, fungal communities have established with tolerance to fluctuations in soil moisture. This is also supported by the observation that a large proportion of the most common mycorrhizal fungi in this study were classified as drought-resistant and the most common saprotrophs as fungi with a secondary, root-associated lifestyle. In bare soil of the same plots, only 5 out of 52 saprotrophic genera were assigned to secondary root-associated lifestyles after rewatering (Mucha et al. 2024). The root exudation of beech and spruce in the upper soil layers increased with desiccation as long as the roots were vital and soil contact was given (Brunn et al. 2022), which may give the fungi considerable advantages over free-living saprotrophic fungi without root association. Smith et al. (2017) discovered that among 201 tested saprotrophic, wood-decaying fungal species, 17% exhibited occasional colonization of roots. Saprotrophy to biotrophy transition is

suggested to be a central trend in evolution of ECM fungi (Kariman et al., 2018) and therefore saprotrophic fungi with secondary root-associated lifestyle could be an indication for the development of new ECM fungal species (Baldrian et al., 2017). This transition is proposed to be relatively "easy" and/or highly positively selected (Baldrian et al., 2017), given that it occurred at least 80 times in various lineages throughout evolution (e.g. Matheny & Hibbett 2009, Tedersoo et al. 2010, Brundrett & Tedersoo 2018, Kohler et al., 2015, Lebreton et al., 2021). Moreover, fungal adaptations to rapidly changing environmental conditions can happen fast due to the ability of fungi for interspecific hybridisation, (Steensels et al., 2021, Wrzosek et al. 2017, Schardl et al., 2003). Hence, a development from saprotrophic fungi to new symbiotrophs during ongoing changing climate is possible but requires further investigation. After rewatering, C sink activity and the allocation of new photoassimilates to root exudates increased in spruce compared to controls (Article II), potentially continuing to support fungal species with root-associated lifestyles. Additionally, compared to controls, the quantity of new photoassimilates in spruce-associated ectomycorrhizae remained unchanged after rewatering (article II) and increased in beech (Hagedorn et al. 2016). These findings suggest that root-fungal associations were maintained at a high level or even primed to enhance water and nutrient uptake.

However, the composition of fungal communities differed significantly between beech and spruce. Many studies have shown that the host species influences the composition of fungal communities to a large extent (Ishida et al. 2007; Dickie 2007; Tedersoo et al. 2012; Bogar and Kennedy 2013; Nacke et al. 2016; Otsing et al. 2021) – also under drought (Nickel et al. 2018). On beech roots, ECM fungi were predominant in both treatments while on spruce roots during drought and after drought release, saprotrophic fungi were the most abundant (article III, Figure 8b), which can be explained by beech and spruce species-specific drought reactions (Nikolova et al. 2020), and recovery patterns of the fine-root systems (this study). In beech, fine-root production was shown to continue during drought (Nikolova et al. 2020) and after recovery (article III), which enables colonisation by ECM fungi. In contrast, the suberisation of

spruce roots during drought prevents ECM colonisation (Brundrett 2002; Sharda and Koide 2008) and favours the proliferation of saprotrophic fungi with root-associated traits. After drought release, these root-associated saprotrophs were the fungi in closest proximity to reactivated and freshly growing fine-roots, making them the probable initial colonisers (Bruns 1995). Fast colonisation by saprotrophs could negatively affect later colonising ECM fungi sharing the same niche (“priority effect”) (Kennedy 2010; Kvaschenko et al. 2017). Furthermore, the abundance of the most prominent fungal species did not change after watering (article III). These fungal species included many saprotrophic species with facultative root-associated lifestyles and drought-resistant ECM suggesting a drought adaptation of the fungal communities. In comparison, fungal species in the surrounding soil less frequently had a reported root-associated lifestyle reflecting a separation of the habitats (Goldmann et al. 2016). Also, the soil respiration and C allocation to soil respiration during and after the drought were low (article II; Nikolova et al., 2009) indicating a reduced microbial activity. It is possible, that drought-adapted communities established a better C use efficiency with time leading to reduced respiration with the number of repetitive droughts (Evans and Wallenstein 2012; de Nijs et al. 2019; Canarini et al. 2021).

Overall, these results indicate that the composition of root-associated fungal communities related to beech and spruce remained unchanged during the initial phase after rewatering, suggesting an adaptation to soil moisture fluctuations during drought. Drought-resistant ECM fungi and root-associated saprotrophs were dominant on both beech and spruce roots. Specifically, ECM fungi were predominant on beech roots, while saprotrophic fungi prevailed on spruce roots, reflecting the tree species-specific responses to the previous drought and rewatering. The hypothesis that fungal communities would return to the control status after rewatering had to be declined at least within the initial period of three months.

#### 4.5 How does a species mixture of beech and spruce affect the fine-root recovery of both trees and the respective root-associated fungal communities compared to single species?

Concerning the recovery of the fine-root system, a tree mixture effect was low and only significant on individual measuring days (article III). Thus, vitality and growth were occasionally lower on spruce roots in mixture than in monospecific interaction. Beech was shown to be more competitive under drought than spruce (Schmid 2002; Zwetsloot et al. 2019) which could explain these occurrences. However, no positive mixture effect on vitality and growth of beech roots could be identified on those days, possibly due to the low responsiveness of beech fine-roots established prior to rewatering. Nevertheless, tree mixture has been shown to increase fungal diversity, partly due to increased soil heterogeneity and the resulting creation of new niches (Conn and Dighton 2000; Aponte et al. 2010; Gao et al. 2013; Tedersoo et al. 2016). Also in this experiment, higher species richness of root-associated fungi was detected in both control and drought treated seedlings in mixture. Furthermore, the abundance of ECM fungi, which also contained spruce-specific species, increased in the mixture after irrigation and exceeded the ECM abundance in spruce monoculture, suggesting that spruce-associated ECM fungi benefitted from admixture with beech. This is consistent with observations that ECM communities associated to spruce are influenced by neighbouring trees of different species (Hubert and Gehring 2008; Otsing et al. 2021). Overall, the hypothesis that tree mixture has a positive effect could not be confirmed for fine-root regeneration but for the abundance of spruce-specific ECM fungi.

## 5 Conclusions and outlook

In this study, I investigated the effects of drought and recovery on fungal communities and fine-roots of beech and spruce trees. Regarding drought effects, I found that fungal communities in soils adapted to drought were less affected compared to those in moister regions. This suggests that as severe droughts become more frequent due to climate change, fungal community structures may change more significantly in regions without a history of

drought. However, the response of beech and spruce seedlings to drought appears to depend more on the flexibility of root architecture rather than on fungal community composition. Nonetheless, the results do not exclude a potential contribution of fungi to seedlings' drought tolerance and suggest the need for further studies, including other groups of microorganisms and their interactions with root-associated fungi, as well as specific root-fungus interactions. While this study focused on seedlings in a controlled environment, different responses under natural conditions and with varying tree age might occur. This study emphasises the importance of evaluating tree specific drought effects on in relation to root-associated microorganisms.

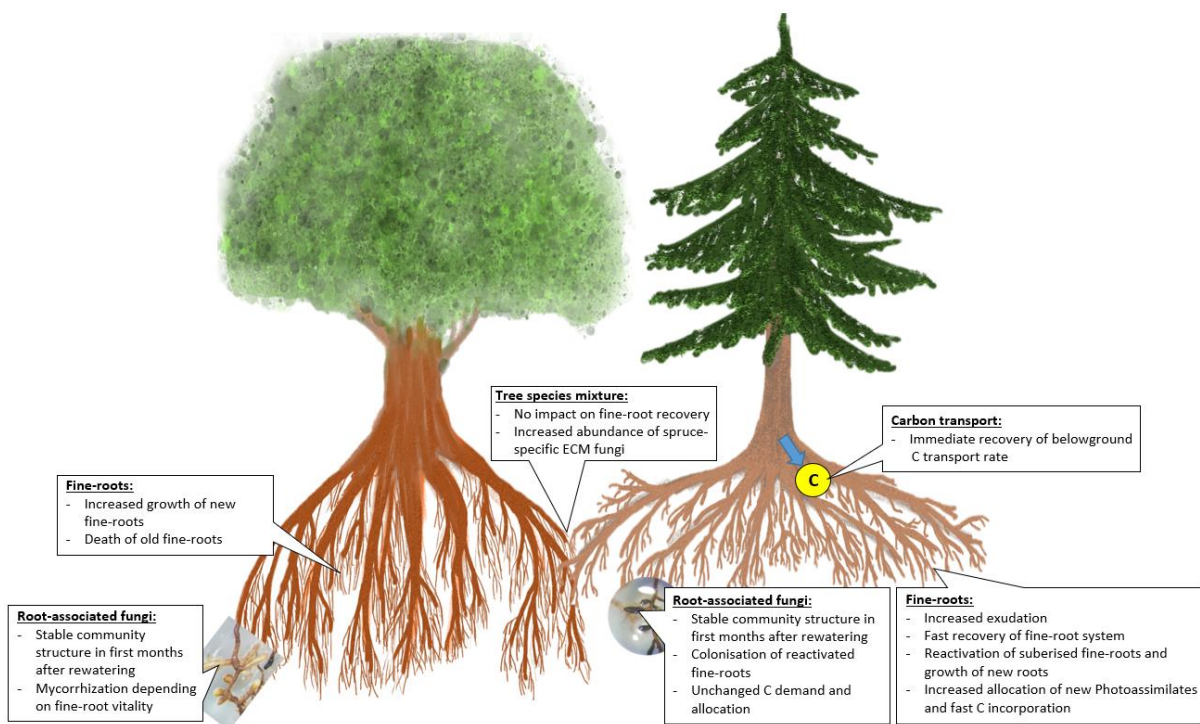


**Figure 9:** Overview of the response to rewatering of the studied belowground organs and C transport in mature beech and spruce within the first three months, taking into account a mixture of tree species.

As part of the KROOF experiment, this study provides insights into the recovery of root-associated fungal communities and fine-root systems in mature beech and spruce trees, as well as C allocation in spruce and the recovery of its carbon transport system (Figure 9). The composition of root fungal communities remained stable in the initial period after rewatering but was significantly influenced by species-specific responses to previous drought and the

restoration of fine-root systems after drought. A positive tree mixture effect of increased total fungal OTU richness underlines the role of diversification in forests from a belowground perspective. However, the study's three-month duration was too short to capture fungal community and fine-root system resilience, emphasizing the need for longer-term investigations to assess the full functional capacity of forest ecosystems post-drought. Comparisons between soil and root-associated fungal species in both experiments provide further evidence, that an association between saprotrophic fungi and roots may not be an exception but possibly a survival strategy driven by increased competitive pressure under drought conditions. Given the fast environmental changes and fungal capacity for rapid evolution, a simplistic classification into distinct classes such as saprotroph and symbiotroph may not fully capture their dynamic nature to change lifestyles. Hence, I suggest considering potential secondary fungal lifestyles and habitat environments in fungal analysis. Furthermore, continuous surveillance of fungal species with root-associated secondary lifestyles, especially at the genetic level, could shed light on the emergence and evolution of novel symbionts.

Monitoring C sink activity, allocation of new phototassimilates and recovery of the C transport system of whole spruce trees after rewatering, the recovery of belowground organs, especially fine-root growth, was highly prioritised to aboveground organs. Furthermore, belowground carbon sink activity was primarily supported by stored carbon. Long-term recovery of carbon uptake and allocation to sinks is expected once the water-absorbing root system is fully restored. The altered C allocation towards belowground sinks may have long-lasting effects on stem growth, emphasizing the necessity for long-term observation of biomass partitioning to understand the enduring consequences of drought on spruce forest productivity and C storage dynamics. Although the main focus of this study was on C allocation after rewatering in mature spruce, a similar trend was observed in young beech (Hagedorn et al. 2016). Despite the distinct recovery strategies of fine-root systems in beech and spruce, the overall prioritisation on fine-root system recovery over other organs appears to be a strategy shared

across species. The future impact of climate change is expected to result in increased frequency and prolonged durations of drought. Consequently, trees undergoing recovery from dry periods are likely to face recurrent drought challenges. To gain a more comprehensive understanding of future forest development, it is essential to investigate whether trees that have recovered once can successfully recover from subsequent drought events.



## 6 References

- Adams HD, Zeppel MJB, Anderegg WRL, et al (2017) A multi-species synthesis of physiological mechanisms in drought-induced tree mortality. *Nat Ecol Evol* 1:1285–1291. <https://doi.org/10.1038/s41559-017-0248-x>
- Agerer R (2001) Exploration types of ectomycorrhizae. *Mycorrhiza* 11:107–114. <https://doi.org/10.1007/s005720100108>
- Allen CD, Breshears DD, McDowell NG (2015) On underestimation of global vulnerability to tree mortality and forest die-off from hotter drought in the Anthropocene. *Ecosphere* 6:. <https://doi.org/10.1890/ES15-00203.1>
- Allen CD, Macalady AK, Chenchouni H, et al (2010) A global overview of drought and heat-induced tree mortality reveals emerging climate change risks for forests. *For Ecol Manag* 259:660–684. <https://doi.org/10.1016/j.foreco.2009.09.001>
- Allsup CM, George I, Lankau RA (2023) Shifting microbial communities can enhance tree tolerance to changing climates. *Science* 380:835–840. <https://doi.org/10.1126/science.adf2027>
- Almario J, Jeena G, Wunder J, et al (2017) Root-associated fungal microbiota of nonmycorrhizal *Arabis alpina* and its contribution to plant phosphorus nutrition. *Proc Natl Acad Sci U S A* 114:E9403–E9412. <https://doi.org/10.1073/pnas.1710455114>
- Ammer C (2019) Diversity and forest productivity in a changing climate. *New Phytol* 221:50–66. <https://doi.org/10.1111/nph.15263>
- Ammer C (2016) Unraveling the Importance of Inter- and Intraspecific Competition for the Adaptation of Forests to Climate Change. In: *Progress in Botany Vol. 78*. pp 345–367
- Anderegg WRL, Kane JM, Anderegg LDL (2013) Consequences of widespread tree mortality triggered by drought and temperature stress. *Nat Clim Change* 3:30–36. <https://doi.org/10.1038/nclimate1635>
- Anderegg WRL, Schwalm C, Biondi F, et al (2015) Pervasive drought legacies in forest ecosystems and their implications for carbon cycle models. *Science* 349:528–532. <https://doi.org/10.1126/science.aab1833>
- Anthony MA, Crowther TW, van der Linde S, et al (2022) Forest tree growth is linked to mycorrhizal fungal composition and function across Europe. *ISME J* 1–10. <https://doi.org/10.1038/s41396-021-01159-7>
- Antonelli A, Fry C, Smith RJ, et al (2023) *State of the World’s Plants and Fungi, 2023*.
- Aponte C, García LV, Marañón T, Gardes M (2010) Indirect host effect on ectomycorrhizal fungi: Leaf fall and litter quality explain changes in fungal communities on the roots of co-occurring Mediterranean oaks. *Soil Biol Biochem* 42:788–796. <https://doi.org/10.1016/j.soilbio.2010.01.014>

- Arend M, Schnitzler JP, Ehling B, et al (2009) Expression of the Arabidopsis mutant *abi1* gene alters abscisic acid sensitivity, stomatal development, and growth morphology in gray poplars. *Plant Physiol* 151:2110–2119. <https://doi.org/10.1104/pp.109.144956>
- Asner GP, Brodrick PG, Anderson CB, et al (2016) Progressive forest canopy water loss during the 2012–2015 California drought. *Proc Natl Acad Sci U S A* 113:E249–E255. <https://doi.org/10.1073/pnas.1523397113>
- Avis PG, McLaughlin DJ, Dentinger BC, Reich PB (2003) Long-term increase in nitrogen supply alters above- and below-ground ectomycorrhizal communities and increases the dominance of *Russula* spp. in a temperate oak savanna. *New Phytol* 160:239–253. <https://doi.org/10.1046/j.1469-8137.2003.00865.x>
- Baldock J, Skjemstad J (1999) Soil organic carbon / soil organic matter. In: *Soil analysis: an interpretation manual*. CSIRO Publishing, pp 159–170
- Baldrian P, Kohout P (2017) Interactions of saprotrophic fungi with tree roots: can we observe the emergence of novel ectomycorrhizal fungi? *New Phytol* 215:511–513. <https://doi.org/10.1111/nph.14665>
- Bapiri A, Bååth E, Rousk J (2010) Drying-Rewetting Cycles Affect Fungal and Bacterial Growth Differently in an Arable Soil. *Microb Ecol* 60:419–428. <https://doi.org/10.1007/s00248-010-9723-5>
- Bardgett RD, Mommer L, De Vries FT (2014) Going underground: Root traits as drivers of ecosystem processes. *Trends Ecol Evol* 29:692–699. <https://doi.org/10.1016/j.tree.2014.10.006>
- Barker SJ, Tagu D (2000) The roles of auxins and cytokinins in mycorrhizal symbioses. *J Plant Growth Regul* 19:144–154. <https://doi.org/10.1007/s003440000021>
- Barnard RL, Blazewicz SJ, Firestone MK (2020) Rewetting of soil: Revisiting the origin of soil CO<sub>2</sub> emissions. *Soil Biol Biochem* 147:107819. <https://doi.org/10.1016/j.soilbio.2020.107819>
- Barnard RL, Osborne CA, Firestone MK (2015) Changing precipitation pattern alters soil microbial community response to wet-up under a Mediterranean-type climate. 946–957. <https://doi.org/10.1038/ismej.2014.192>
- Bauerle TL, Richards JH, Smart DR, Eissenstat DM (2008) Importance of internal hydraulic redistribution for prolonging the lifespan of roots in dry soil. *Plant Cell Environ* 071120025334002-??? <https://doi.org/10.1111/j.1365-3040.2007.01749.x>
- Baxter I, Hosmani PS, Rus A, et al (2009) Root Suberin Forms an Extracellular Barrier That Affects Water Relations and Mineral Nutrition in Arabidopsis. *PLoS Genet* 5:e1000492. <https://doi.org/10.1371/journal.pgen.1000492>

- Bebre I, Riebl H, Annighöfer P (2021) Seedling growth and biomass production under different light availability levels and competition types. *Forests* 12:.. <https://doi.org/10.3390/f12101376>
- Becquer A, Guerrero-Galán C, Eibensteiner JL, et al (2019) The ectomycorrhizal contribution to tree nutrition. *Adv Bot Res* 89:77–126. <https://doi.org/10.1016/bs.abr.2018.11.003>
- Bello J, Vallet P, Perot T, et al (2019) How do mixing tree species and stand density affect seasonal radial growth during drought events? *For Ecol Manag* 432:436–445. <https://doi.org/10.1016/j.foreco.2018.09.044>
- Beloiu M, Stahlmann R, Beierkuhnlein C (2022) Drought impacts in forest canopy and deciduous tree saplings in Central European forests. *For Ecol Manag* 509:.. <https://doi.org/10.1016/j.foreco.2022.120075>
- Beloiu M, Stahlmann R, Beierkuhnlein C (2020) High recovery of saplings after severe drought in temperate deciduous forests. *Forests* 11:1–17. <https://doi.org/10.3390/F11050546>
- Bever JD (2003) Soil community feedback and the coexistence of competitors: Conceptual frameworks and empirical tests. *New Phytol* 157:465–473. <https://doi.org/10.1046/j.1469-8137.2003.00714.x>
- Bever JD, Westover KM, Antonovics J (1997) Incorporating the Soil Community into Plant Population Dynamics: The Utility of the Feedback Approach. *J Ecol* 85:561. <https://doi.org/10.2307/2960528>
- Bezemer TM, Lawson CS, Hedlund K, et al (2006) Plant species and functional group effects on abiotic and microbial soil properties and plant-soil feedback responses in two grasslands. *J Ecol* 94:893–904. <https://doi.org/10.1111/j.1365-2745.2006.01158.x>
- Birch HF (1958) The effect of soil drying on humus decomposition and nitrogen availability. *Plant Soil* 10:9–31. <https://doi.org/10.1007/BF01343734>
- Blaalid R, Kumar S, Nilsson RH, et al (2013) ITS1 versus ITS2 as DNA metabarcodes for fungi. *Mol Ecol Resour* 13:218–224. <https://doi.org/10.1111/1755-0998.12065>
- Blessing CH, Werner RA, Siegwolf R, Buchmann N (2015) Allocation dynamics of recently fixed carbon in beech saplings in response to increased temperatures and drought. *Tree Physiol* 35:585–598. <https://doi.org/10.1093/treephys/tpv024>
- Bloom AJ, Chapin FS, Mooney HA (1985) RESOURCE LIMITATION IN PLANTS-AN ECONOMIC ANALOGY
- BMEL (2014) The forest in Germany. Selected results of the third National Forest Inventory [Der Wald in Deutschland. Ausgewählte Ergebnisse der dritten Bundeswaldinventur.]. 3. Ed.:56

- Boczoń A, Hilszczańska D, Wrzosek M, et al (2021) Drought in the forest breaks plant–fungi interactions. *Eur J For Res* 140:1301–1321. <https://doi.org/10.1007/s10342-021-01409-5>
- Bödeker ITM, Clemmensen KE, Boer W de, et al (2014) Ectomycorrhizal *Cortinarius* species participate in enzymatic oxidation of humus in northern forest ecosystems. *New Phytol* 203:245–256. <https://doi.org/10.1111/nph.12791>
- Bogar LM, Kennedy PG (2013) New wrinkles in an old paradigm: Neighborhood effects can modify the structure and specificity of *Alnus*-associated ectomycorrhizal fungal communities. *FEMS Microbiol Ecol* 83:767–777. <https://doi.org/10.1111/1574-6941.12032>
- Bonan GB (2008) Forests and Climate Change: Forcings, Feedbacks, and the Climate Benefits of Forests. *Science* 320:1444–1449. <https://doi.org/10.1126/science.1155121>
- Bornyas MA, Graham RC, Allen MF (2005) Ectomycorrhizae in a soil-weathered granitic bedrock regolith: Linking matrix resources to plants. *Geoderma* 126:141–160. <https://doi.org/10.1016/j.geoderma.2004.11.023>
- Brodersen CR, McElrone AJ (2013) Maintenance of xylem network transport capacity: A review of embolism repair in vascular plants. *Front Plant Sci* 4:1–11. <https://doi.org/10.3389/fpls.2013.00108>
- Brownlee C, Duddridge JA, Malibari A, Read DJ (1983) The structure and function of mycelial systems of ectomycorrhizal roots with special reference to their role in forming inter-plant connections and providing pathways for assimilate and water transport. In: *Tree Root Systems and Their Mycorrhizas*. Springer, Dordrecht, pp 433–443
- Brundrett MC (2002) Coevolution of roots and mycorrhizas of land plants. *New Phytol* 154:275–304. <https://doi.org/10.1046/j.1469-8137.2002.00397.x>
- Brunn M, Hafner BD, Zwetsloot MJ, et al (2022) Carbon allocation to root exudates is maintained in mature temperate tree species under drought. *New Phytol* 965–977. <https://doi.org/10.1111/nph.18157>
- Brunner I, Herzog C, Dawes MA, et al (2015) How tree roots respond to drought. *Front Plant Sci* 6:547. <https://doi.org/10.3389/fpls.2015.00547>
- Brunner I, Herzog C, Galiano L, Gessler A (2019) Plasticity of fine-root traits under long-term irrigation of a water-limited scots pine forest. *Front Plant Sci* 10:. <https://doi.org/10.3389/fpls.2019.00701>
- Bruns TD (1995) Thoughts on the processes that maintain local species diversity of ectomycorrhizal fungi. *Plant Soil* 170:63–73. <https://doi.org/10.1007/BF02183055>
- Brus DJ, Hengeveld GM, Walvoort DJJ, et al (2012) Statistical mapping of tree species over Europe. *Eur J For Res* 131:145–157. <https://doi.org/10.1007/s10342-011-0513-5>

- Büntgen U, Urban O, Krusic PJ, et al (2021) Recent European drought extremes beyond Common Era background variability. *Nat Geosci* 14:190–196. <https://doi.org/10.1038/s41561-021-00698-0>
- Canarini A, Schmidt H, Fuchslueger L, et al (2021) Ecological memory of recurrent drought modifies soil processes via changes in soil microbial community. *Nat Commun* 12:1–14. <https://doi.org/10.1038/s41467-021-25675-4>
- Carminati A, Vetterlein D, Weller U, et al (2009) When Roots Lose Contact. *Vadose Zone J* 8:805–809. <https://doi.org/10.2136/vzj2008.0147>
- Carnicer J, Coll M, Ninyerola M, et al (2011) Widespread crown condition decline, food web disruption, and amplified tree mortality with increased climate change-type drought. *Proc Natl Acad Sci U S A* 108:1474–1478. <https://doi.org/10.1073/pnas.1010070108>
- Castaño C, Lindahl BD, Alday JG, et al (2018) Soil microclimate changes affect soil fungal communities in a Mediterranean pine forest. *New Phytol* 220:1211–1221. <https://doi.org/10.1111/nph.15205>
- Castaño C, Suarez-Vidal E, Zas R, et al (2023) Ectomycorrhizal fungi with hydrophobic mycelia and rhizomorphs dominate in young pine trees surviving experimental drought stress. *Soil Biol Biochem* 178:. <https://doi.org/10.1016/j.soilbio.2022.108932>
- Cavender-Bares J, Izzo A, Robinson R, Lovelock CE (2009) Changes in ectomycorrhizal community structure on two containerized oak hosts across an experimental hydrologic gradient. *Mycorrhiza* 19:133–142. <https://doi.org/10.1007/s00572-008-0220-3>
- Chanclud E, Morel JB (2016) Plant hormones: a fungal point of view. *Mol Plant Pathol* 17:1289–1297. <https://doi.org/10.1111/mpp.12393>
- Chen J, Bittinger K, Charlson ES, et al (2012) Associating microbiome composition with environmental covariates using generalized UniFrac distances. *Bioinformatics* 28:2106–2113. <https://doi.org/10.1093/bioinformatics/bts342>
- Chuste PA, Maillard P, Bréda N, et al (2020) Sacrificing growth and maintaining a dynamic carbohydrate storage are key processes for promoting beech survival under prolonged drought conditions. *Trees - Struct Funct* 34:381–394. <https://doi.org/10.1007/s00468-019-01923-5>
- Ciais P, Reichstein M, Viovy N, et al (2005) Europe-wide reduction in primary productivity caused by the heat and drought in 2003. *Nature* 437:529–533. <https://doi.org/10.1038/nature03972>
- Colpaert JV, Van Laere A, Van Assche JA (1996) Carbon and nitrogen allocation in ectomycorrhizal and non-mycorrhizal *Pinus sylvestris* L seedlings. *Tree Physiol* 16:787–793. <https://doi.org/10.1093/treephys/16.9.787>

- Conn C, Dighton J (2000) Litter quality influences on decomposition, ectomycorrhizal community structure and mycorrhizal root surface acid phosphatase activity. *Soil Biol Biochem* 32:489–496. [https://doi.org/10.1016/S0038-0717\(99\)00178-9](https://doi.org/10.1016/S0038-0717(99)00178-9)
- Courty PE, Buée M, Diedhiou AG, et al (2010) The role of ectomycorrhizal communities in forest ecosystem processes: New perspectives and emerging concepts. *Soil Biol Biochem* 42:679–698. <https://doi.org/10.1016/j.soilbio.2009.12.006>
- De Boer W, Folman LB, Summerbell RC, Boddy L (2005) Living in a fungal world: Impact of fungi on soil bacterial niche development. *FEMS Microbiol Rev* 29:795–811. <https://doi.org/10.1016/j.femsre.2004.11.005>
- de Gouvenain RC, Silander JA (2017) Temperate Forests ☆. In: Reference Module in Life Sciences. Elsevier, pp 1–44
- de Nijs EA, Hicks LC, Leizeaga A, et al (2019) Soil microbial moisture dependences and responses to drying–rewetting: The legacy of 18 years drought. *Glob Change Biol* 25:1005–1015. <https://doi.org/10.1111/gcb.14508>
- de Vries FT, Griffiths RI, Bailey M, et al (2018) Soil bacterial networks are less stable under drought than fungal networks. *Nat Commun* 9:. <https://doi.org/10.1038/s41467-018-05516-7>
- de Vries FT, Liiri ME, Bjørnlund L, et al (2012) Land use alters the resistance and resilience of soil food webs to drought. *Nat Clim Change* 2:276–280. <https://doi.org/10.1038/nclimate1368>
- Dickie IA (2007) Host preference, niches and fungal diversity. *New Phytol* 174:230–233. <https://doi.org/10.1111/j.1469-8137.2007.02055.x>
- Ding Q, Liang Y, Legendre P, et al (2011) Diversity and composition of ectomycorrhizal community on seedling roots: the role of host preference and soil origin. *Mycorrhiza* 21:669–680. <https://doi.org/10.1007/s00572-011-0374-2>
- Domingo G, Vannini C, Marsoni M, et al (2023) A multifaceted approach to reveal the very-fine root's response of *Fagus sylvatica* seedlings to different drought intensities. *Physiol Plant* 175:1–15. <https://doi.org/10.1111/ppl.13934>
- Domisch T, Finér L, Lehto T, Smolander A (2002) Effect of soil temperature on nutrient allocation and mycorrhizas in Scots pine seedlings. *Plant Soil* 243:253. <https://doi.org/10.1023/A:1019943426535>
- Druebert C, Lang C, Valtanen K, Polle A (2009) Beech carbon productivity as driver of ectomycorrhizal abundance and diversity. *Plant Cell Environ* 32:992–1003. <https://doi.org/10.1111/j.1365-3040.2009.01983.x>
- Egerton-Warburton LM, Querejeta JI, Allen MF (2007) Common mycorrhizal networks provide a potential pathway for the transfer of hydraulically lifted water between plants. *J Exp Bot* 58:1473–1483. <https://doi.org/10.1093/jxb/erm009>

- Eissenstat DM, McCormack ML (2013) Root Water Uptake and Water Flow in the Soil–Root Domain. In: *Plant Roots*. CRC Press, pp 368–385
- Eldhuset TD, Nagy NE, Volařík D, et al (2013) Drought affects tracheid structure, dehydrin expression, and above- and belowground growth in 5-year-old Norway spruce. *Plant Soil* 366:305–320. <https://doi.org/10.1007/s11104-012-1432-z>
- Evans SE, Wallenstein MD (2012) Soil microbial community response to drying and rewetting stress: Does historical precipitation regime matter? *Biogeochemistry* 109:101–116. <https://doi.org/10.1007/s10533-011-9638-3>
- FAO (2010) *Global Forest Resources Assessment 2010: Main report*. Rome, Italy
- Fatichi S, Leuzinger S, Körner C (2014) Moving beyond photosynthesis: From carbon source to sink-driven vegetation modeling. *New Phytol* 201:1086–1095. <https://doi.org/10.1111/nph.12614>
- Feil W, Kottke I, Oberwinkler F (1988) The effect of drought on mycorrhizal production and very fine root system development of Norway spruce under natural and experimental conditions. *Plant Soil* 108:221–231. <https://doi.org/10.1007/BF02375652>
- Fernandez CW, Koide RT (2013) The function of melanin in the ectomycorrhizal fungus *Cenococcum geophilum* under water stress. *Fungal Ecol* 6:479–486. <https://doi.org/10.1016/j.funeco.2013.08.004>
- Fierer N, Schimel JP (2003) A Proposed Mechanism for the Pulse in Carbon Dioxide Production Commonly Observed Following the Rapid Rewetting of a Dry Soil. *Soil Sci Soc Am J* 67:798. <https://doi.org/10.2136/sssaj2003.0798>
- Forrester DI (2015) Transpiration and water-use efficiency in mixed-species forests versus monocultures: Effects of tree size, stand density and season. *Tree Physiol* 35:289–304. <https://doi.org/10.1093/treephys/tpv011>
- Forster M, Falk W, Reger B (2019) *Klima – Boden – Baumartenwahl*
- Frey B, Walthert L, Perez-Mon C, et al (2021) Deep Soil Layers of Drought-Exposed Forests Harbor Poorly Known Bacterial and Fungal Communities. *Front Microbiol* 12:. <https://doi.org/10.3389/fmicb.2021.674160>
- Friedlingstein P, Jones MW, O’Sullivan M, et al (2019) Global Carbon Budget 2019. *Earth Syst Sci Data* 11:1783–1838. <https://doi.org/10.5194/essd-11-1783-2019>
- Fu W, Chen B, Jansa J, et al (2022) Contrasting community responses of root and soil dwelling fungi to extreme drought in a temperate grassland. *Soil Biol Biochem* 169:108670. <https://doi.org/10.1016/j.soilbio.2022.108670>
- Fuchslueger L, Bahn M, Fritz K, et al (2014) Experimental drought reduces the transfer of recently fixed plant carbon to soil microbes and alters the bacterial community

- composition in a mountain meadow. *New Phytol* 201:916–927. <https://doi.org/10.1111/nph.12569>
- Galiano L, Timofeeva G, Saurer M, et al (2017) The fate of recently fixed carbon after drought release: towards unravelling C storage regulation in *Tilia platyphyllos* and *Pinus sylvestris*. *Plant Cell Environ* 40:1711–1724. <https://doi.org/10.1111/pce.12972>
- Gao C, Shi NN, Liu YX, et al (2013) Host plant genus-level diversity is the best predictor of ectomycorrhizal fungal diversity in a Chinese subtropical forest. *Mol Ecol* 22:3403–3414. <https://doi.org/10.1111/mec.12297>
- Gao D, Joseph J, Werner RA, et al (2021) Drought alters the carbon footprint of trees in soils—tracking the spatio-temporal fate of <sup>13</sup>C-labelled assimilates in the soil of an old-growth pine forest. *Glob Change Biol* 27:2491–2506. <https://doi.org/10.1111/gcb.15557>
- García-Guzmán G, Heil M (2014) Life histories of hosts and pathogens predict patterns in tropical fungal plant diseases. *New Phytol* 201:1106–1120. <https://doi.org/10.1111/nph.12562>
- Gaul D, Hertel D, Borken W, et al (2008) Effects of experimental drought on the fine root system of mature Norway spruce. *For Ecol Manag* 256:1151–1159. <https://doi.org/10.1016/j.foreco.2008.06.016>
- Germon A, Laclau JP, Robin A, Jourdan C (2020) Tamm Review: Deep fine roots in forest ecosystems: Why dig deeper? *For Ecol Manag* 466:.. <https://doi.org/10.1016/j.foreco.2020.118135>
- Gessler A, Bächli L, Rouholahnejad Freund E, et al (2022) Drought reduces water uptake in beech from the drying topsoil, but no compensatory uptake occurs from deeper soil layers. *New Phytol* 233:194–206. <https://doi.org/10.1111/nph.17767>
- Gessler A, Schaub M, McDowell NG (2017) The role of nutrients in drought-induced tree mortality and recovery. *New Phytol* 214:513–520. <https://doi.org/10.1111/nph.14340>
- Goisser M, Geppert U, Rötzer T, et al (2016) Does belowground interaction with *Fagus sylvatica* increase drought susceptibility of photosynthesis and stem growth in *Picea abies*? *For Ecol Manag* 375:268–278. <https://doi.org/10.1016/j.foreco.2016.05.032>
- Goldmann K, Schröter K, Pena R, et al (2016) Divergent habitat filtering of root and soil fungal communities in temperate beech forests. *Sci Rep* 6:1–10. <https://doi.org/10.1038/srep31439>
- González de Andrés E, Camarero JJ, Blanco JA, et al (2018) Tree-to-tree competition in mixed European beech–Scots pine forests has different impacts on growth and water-use efficiency depending on site conditions. *J Ecol* 106:59–75. <https://doi.org/10.1111/1365-2745.12813>



- Göransson H, Godbold DL, Jones DL, Rousk J (2013) Bacterial growth and respiration responses upon rewetting dry forest soils: Impact of drought-legacy. *Soil Biol Biochem* 57:477–486. <https://doi.org/10.1016/j.soilbio.2012.08.031>
- Grams TEE, Hesse BD, Gebhardt T, et al (2021) The Kroof experiment: realization and efficacy of a recurrent drought experiment plus recovery in a beech/spruce forest. *Ecosphere* 12:. <https://doi.org/10.1002/ecs2.3399>
- Grossiord C, Forner A, Gessler A, et al (2015) Influence of species interactions on transpiration of Mediterranean tree species during a summer drought. *Eur J For Res* 134:365–376. <https://doi.org/10.1007/s10342-014-0857-8>
- Grossiord C, Gessler A, Granier A, et al (2014a) Impact of interspecific interactions on the soil water uptake depth in a young temperate mixed species plantation. *J Hydrol* 519:3511–3519. <https://doi.org/10.1016/j.jhydrol.2014.11.011>
- Grossiord C, Granier A, Gessler A, et al (2014b) Does Drought Influence the Relationship Between Biodiversity and Ecosystem Functioning in Boreal Forests? *Ecosystems* 17:394–404. <https://doi.org/10.1007/s10021-013-9729-1>
- Grossiord C, Granier A, Gessler A, et al (2013) Forest Ecology and Management The influence of tree species mixture on ecosystem-level carbon accumulation and water use in a mixed boreal plantation. *For Ecol Manag* 298:82–92. <https://doi.org/10.1016/j.foreco.2013.03.001>
- Gupta SK, Ram J, Singh H (2018) Comparative Study of Transpiration in Cooling Effect of Tree Species in the Atmosphere. *J Geosci Environ Prot* 06:151–166. <https://doi.org/10.4236/gep.2018.68011>
- Gweon HS, Oliver A, Taylor J, et al (2015) PIPITS: An automated pipeline for analyses of fungal internal transcribed spacer sequences from the Illumina sequencing platform. *Methods Ecol Evol* 6:973–980. <https://doi.org/10.1111/2041-210X.12399>
- Haberstroh S, Caldeira MC, Lobo-do-Vale R, et al (2021) Nonlinear plant–plant interactions modulate impact of extreme drought and recovery on a Mediterranean ecosystem. *New Phytol* 231:1784–1797. <https://doi.org/10.1111/nph.17522>
- Haberstroh S, Werner C (2022) The role of species interactions for forest resilience to drought. *Plant Biol*. <https://doi.org/10.1111/plb.13415>
- Hafner BD, Tomasella M, Häberle KH, et al (2017) Hydraulic redistribution under moderate drought among English oak, European beech and Norway spruce determined by deuterium isotope labeling in a split-root experiment. *Tree Physiol* 37:950–960. <https://doi.org/10.1093/treephys/tpx050>
- Hagedorn F, Joseph J, Peter M, et al (2016) Recovery of trees from drought depends on belowground sink control. *Nat Plants* 2:16111. <https://doi.org/10.1038/nplants.2016.111>

- Halverson LJ, Jones TM, Firestone MK (2000) Release of Intracellular Solutes by Four Soil Bacteria Exposed to Dilution Stress. *Soil Sci Soc Am J* 64:1630–1637. <https://doi.org/10.2136/sssaj2000.6451630x>
- Hamanishi ET, Campbell MM (2011) Genome-wide responses to drought in forest trees. *Forestry* 84:273–283. <https://doi.org/10.1093/forestry/cpr012>
- Hartl L, Zach S, Seidl-Seiboth V (2012) Fungal chitinases: Diversity, mechanistic properties and biotechnological potential. *Appl Microbiol Biotechnol* 93:533–543. <https://doi.org/10.1007/s00253-011-3723-3>
- Hartmann H, Bahn M, Carbone M, Richardson AD (2020) Plant carbon allocation in a changing world – challenges and progress: introduction to a Virtual Issue on carbon allocation: Introduction to a virtual issue on carbon allocation. *New Phytol* 227:981–988. <https://doi.org/10.1111/nph.16757>
- Heinonsalo J, Hurme K-R, Sen & R (2004) Recent 14 C-labelled assimilate allocation to Scots pine seedling root and mycorrhizosphere compartments developed on reconstructed podzol humus, E-and B-mineral horizons
- Herol L, Avidar M, Yirmiahu S, et al (2023) Context-dependent benefits of ectomycorrhizal fungi on Aleppo pine seedling performance under drought and interplant competition. <https://www.researchsquare.com>. Accessed 24 Nov 2023
- Herzog C, Steffen J, Graf Pannatier E, et al (2014) Nine years of irrigation cause vegetation and fine root shifts in a water-limited pine forest. *PLoS ONE* 9:. <https://doi.org/10.1371/journal.pone.0096321>
- Hesse BD, Goisser M, Hartmann H, Grams TEE (2018) Repeated summer drought delays sugar export from the leaf and impairs phloem transport in mature beech. *Tree Physiol* 39:192–200. <https://doi.org/10.1093/treephys/tpy122>
- Hommel R, Siegwolf R, Zavadlav S, et al (2016) Impact of interspecific competition and drought on the allocation of new assimilates in trees. *Plant Biol Stuttg Ger* 18:785–796. <https://doi.org/10.1111/plb.12461>
- Hu B, Simon J, Günthardt-Goerg MS, et al (2015) Changes in the dynamics of foliar N metabolites in oak saplings by drought and air warming depend on species and soil type. *PLoS ONE* 10:1–21. <https://doi.org/10.1371/journal.pone.0126701>
- Huang Q, Jiao F, Huang Y, et al (2021) Response of soil fungal community composition and functions on the alteration of precipitation in the grassland of Loess Plateau. *Sci Total Environ* 751:. <https://doi.org/10.1016/j.scitotenv.2020.142273>
- Hubert NA, Gehring CA (2008) Neighboring trees affect ectomycorrhizal fungal community composition in a woodland-forest ecotone. *Mycorrhiza* 18:363–374. <https://doi.org/10.1007/s00572-008-0185-2>

- Ineichen K, Wiemken V (1992) Changes in the fungus-specific, soluble-carbohydrate pool during rapid and synchronous ectomycorrhiza formation of *Picea abies* with *Pisolithus tinctorius*
- IPCC (2021) Climate Change 2021 The Physical Science Basis Summary for Policymakers Working Group I Contribution to the Sixth Assessment Report of the Intergovernmental Panel on Climate Change
- Ishida TA, Nara K, Hogetsu T (2007) Host effects on ectomycorrhizal fungal communities: Insight from eight host species in mixed conifer-broadleaf forests. *New Phytol* 174:430–440. <https://doi.org/10.1111/j.1469-8137.2007.02016.x>
- Izzo AD, Meyer M, Trappe JM, et al (2005) Hypogeous Ectomycorrhizal Fungal Species on Roots and in Small Mammal Diet in a Mixed-Conifer Forest. *For Sci* 51:243–254
- Jactel H, Petit J, Desprez-Loustau ML, et al (2012) Drought effects on damage by forest insects and pathogens: A meta-analysis. *Glob Change Biol* 18:267–276. <https://doi.org/10.1111/j.1365-2486.2011.02512.x>
- Joseph J, Gao D, Backes B, et al (2020) Rhizosphere activity in an old-growth forest reacts rapidly to changes in soil moisture and shapes whole-tree carbon allocation. *Proc Natl Acad Sci U S A* 117:24885–24892. <https://doi.org/10.1073/pnas.2014084117>
- Joslin JD, Wolfe MH, Hanson PJ (2000) Effects of altered water regimes on forest root systems. *New Phytol* 147:117–129. <https://doi.org/10.1046/j.1469-8137.2000.00692.x>
- Jumpponen A (2001) Dark septate endophytes - Are they mycorrhizal? *Mycorrhiza* 11:207–211. <https://doi.org/10.1007/s005720100112>
- Kempf B, Bremer E (1998) Uptake and synthesis of compatible solutes as microbial stress responses to high-osmolality environments. *Arch Microbiol* 170:319–330. <https://doi.org/10.1007/s002030050649>
- Kennedy P (2010) Ectomycorrhizal fungi and interspecific competition: Species interactions, community structure, coexistence mechanisms, and future research directions. *New Phytol* 187:895–910. <https://doi.org/10.1111/j.1469-8137.2010.03399.x>
- Kerner R, Delgado-Eckert E, Del Castillo E, et al (2012) Comprehensive proteome analysis in *Cenococcum geophilum* Fr. as a tool to discover drought-related proteins. *J Proteomics* 75:3707–3719. <https://doi.org/10.1016/j.jprot.2012.04.039>
- Kieft TL, soroker E, firestone MK (1987) Microbial biomass response to a rapid increase in water potential when dry soil is wetted. *Soil Biol Biochem* 19:119–126. [https://doi.org/10.1016/0038-0717\(87\)90070-8](https://doi.org/10.1016/0038-0717(87)90070-8)
- Kim DG, Vargas R, Bond-Lamberty B, Turetsky MR (2012) Effects of soil rewetting and thawing on soil gas fluxes: A review of current literature and suggestions for future research. *Biogeosciences* 9:2459–2483. <https://doi.org/10.5194/bg-9-2459-2012>

- Klein T, Siegwolf RTW, Körner C (2016) Belowground carbon trade among tall trees in a temperate forest. *Science* 352:342–344. <https://doi.org/10.1126/science.aad6188>
- Kohler A, Kuo A, Nagy LG, et al (2015) Convergent losses of decay mechanisms and rapid turnover of symbiosis genes in mycorrhizal mutualists. *Nat Genet* 47:410–415. <https://doi.org/10.1038/ng.3223>
- Körner C (2019) No need for pipes when the well is dry—a comment on hydraulic failure in trees. *Tree Physiol* 39:695–700. <https://doi.org/10.1093/treephys/tpz030>
- Körner C (2015) Paradigm shift in plant growth control. *Curr Opin Plant Biol* 25:107–114. <https://doi.org/10.1016/j.pbi.2015.05.003>
- Kottke I, Oberwinkler F (1986) Mycorrhiza of forest trees - structure and function. *Trees* 1:. <https://doi.org/10.1007/BF00197021>
- Kozovits AR, Matyssek R, Blaschke H, et al (2005) Competition increasingly dominates the responsiveness of juvenile beech and spruce to elevated CO<sub>2</sub>/O<sub>3</sub> concentrations throughout two subsequent growing seasons. *Glob Change Biol* 11:1387–1401. <https://doi.org/10.1111/j.1365-2486.2005.00993.x>
- Krull ES, Skjemstad JO, Baldock JA (2004) Functions of Soil Organic Matter and the Effect on Soil Properties
- Kunz J, Löffler G, Bauhus J (2018) Minor European broadleaved tree species are more drought-tolerant than *Fagus sylvatica* but not more tolerant than *Quercus petraea*. *For Ecol Manag* 414:15–27. <https://doi.org/10.1016/j.foreco.2018.02.016>
- Kuster TM, Arend M, Bleuler P, et al (2013) Water regime and growth of young oak stands subjected to air-warming and drought on two different forest soils in a model ecosystem experiment. *Plant Biol* 15:138–147. <https://doi.org/10.1111/j.1438-8677.2011.00552.x>
- Kyaschenko J, Clemmensen KE, Hagenbo A, et al (2017) Shift in fungal communities and associated enzyme activities along an age gradient of managed *Pinus sylvestris* stands. *ISME J* 11:863–874. <https://doi.org/10.1038/ismej.2016.184>
- Lal R (2002) Soil carbon dynamics in cropland and rangeland. *Environ Pollut* 116:353–362. [https://doi.org/10.1016/S0269-7491\(01\)00211-1](https://doi.org/10.1016/S0269-7491(01)00211-1)
- Lal R, Smith P, Jungkunst HF, et al (2018) The carbon sequestration potential of terrestrial ecosystems. *J Soil Water Conserv* 73:145A-152A. <https://doi.org/10.2489/jswc.73.6.145A>
- Langer GJ, Bußkamp J, Terhonen E, Blumenstein K (2021) Fungi inhabiting woody tree tissues. In: *Forest Microbiology*. Elsevier, pp 175–205

- Langley JA, Drake BG, Hungate BA (2002) Extensive belowground carbon storage supports roots and mycorrhizae in regenerating scrub oaks. *Oecologia* 131:542–548. <https://doi.org/10.1007/s00442-002-0932-6>
- Lee SH, Calvo-Polanco M, Chung GC, Zwiazek JJ (2010) Role of aquaporins in root water transport of ectomycorrhizal jack pine (*Pinus banksiana*) seedlings exposed to NaCl and fluoride. *Plant Cell Environ* 33:769–780. <https://doi.org/10.1111/j.1365-3040.2009.02103.x>
- Lehto T, Zwiazek JJ (2011) Ectomycorrhizas and water relations of trees: a review. *Mycorrhiza* 21:71–90. <https://doi.org/10.1007/s00572-010-0348-9>
- Leitner S, Minixhofer P, Inselsbacher E, et al (2017) Short-term soil mineral and organic nitrogen fluxes during moderate and severe drying–rewetting events. *Appl Soil Ecol* 114:28–33. <https://doi.org/10.1016/j.apsoil.2017.02.014>
- Leuschner C, Hertel D, Schmid I, et al (2004) Stand fine root biomass and fine root morphology in old-growth beech forests as a function of precipitation and soil fertility. *Plant Soil* 258:43–56. <https://doi.org/10.1023/B:PLSO.0000016508.20173.80>
- Lindahl BD, Tunlid A (2015) Ectomycorrhizal fungi - potential organic matter decomposers, yet not saprotrophs. *New Phytol.* 205:1443–1447
- Liu D, Wang T, Peñuelas J, Piao S (2022) Drought resistance enhanced by tree species diversity in global forests. *Nat Geosci* 15:800–804. <https://doi.org/10.1038/s41561-022-01026-w>
- Liu YY, Van Dijk AIJM, De Jeu RAM, et al (2015) Recent reversal in loss of global terrestrial biomass. *Nat Clim Change* 5:470–474. <https://doi.org/10.1038/nclimate2581>
- Lozano YM, Aguilar-Trigueros CA, Roy J, Rillig MC (2021) Drought induces shifts in soil fungal communities that can be linked to root traits across 24 plant species. *New Phytol* 232:1917–1929. <https://doi.org/10.1111/nph.17707>
- Lundell TK, Mäkelä MR, de Vries RP, Hildén KS (2014) Genomics, lifestyles and future prospects of wood-decay and litter-decomposing basidiomycota. Elsevier Ltd.
- Lynch DJ, Matamala R, Iversen CM, et al (2013) Stored carbon partly fuels fine-root respiration but is not used for production of new fine roots. *New Phytol* 199:420–430. <https://doi.org/10.1111/nph.12290>
- Magh, Bonn, Grote, et al (2019) Drought Superimposes the Positive Effect of Silver Fir on Water Relations of European Beech in Mature Forest Stands. *Forests* 10:897. <https://doi.org/10.3390/f10100897>
- Mäkelä MR, Hildén KS, Kuuskeri J (2021) Fungal Lignin-Modifying Peroxidases and H<sub>2</sub>O<sub>2</sub>-Producing Enzymes. In: Zaragoza Ó, Casadevall A (eds) *Encyclopedia of Mycology*. Elsevier, pp 247–259

- Malik AA, Swenson T, Weihe C, et al (2019) Physiological adaptations of leaf litter microbial communities to long-term drought. *bioRxiv*. <https://doi.org/10.1101/631077>
- Manzoni S, Schimel JP, Porporato A (2012) Responses of soil microbial communities to water stress: Results from a meta-analysis. *Ecology* 93:930–938. <https://doi.org/10.1890/11-0026.1>
- Marcot BG (2017) A review of the role of fungi in wood decay of forest ecosystems. U.S. Department of Agriculture, Forest Service, Pacific Northwest Research Station, Portland, OR
- Marjanović Ž, Uehlein N, Kaldenhoff R, et al (2005) Aquaporins in poplar: What a difference a symbiont makes! *Planta* 222:258–268. <https://doi.org/10.1007/s00425-005-1539-z>
- McCarragher S, Rigg LS (2020) Temperate forest ecosystems. In: *International Encyclopedia of Geography*. Wiley, pp 1–15
- McDowell N, Pockman WT, Allen CD, et al (2008) Mechanisms of plant survival and mortality during drought: Why do some plants survive while others succumb to drought? *New Phytol* 178:719–739. <https://doi.org/10.1111/j.1469-8137.2008.02436.x>
- McMurdie PJ, Holmes S (2013) Phyloseq: An R Package for Reproducible Interactive Analysis and Graphics of Microbiome Census Data. *PLoS ONE* 8:. <https://doi.org/10.1371/journal.pone.0061217>
- Meier IC, Leuschner C (2008) Belowground drought response of European beech: Fine root biomass and carbon partitioning in 14 mature stands across a precipitation gradient. *Glob Change Biol* 14:2081–2095. <https://doi.org/10.1111/j.1365-2486.2008.01634.x>
- Meijer SS, Holmgren M, Van Der Putten WH (2011) Effects of plant-soil feedback on tree seedling growth under arid conditions. *J Plant Ecol* 4:193–200. <https://doi.org/10.1093/jpe/rtr011>
- Meixner C, Ludwig-Müller J, Miersch O, et al (2005) Lack of mycorrhizal autoregulation and phytohormonal changes in the supernodulating soybean mutant nts1007. *Planta* 222:709–715. <https://doi.org/10.1007/s00425-005-0003-4>
- Mucha J, Danzberger J, Werner R, et al (2024) Effects of rewatering on soil fungi and soil enzymes in a spruce-beech forest after a 5-year experimental drought. *Plant Soil*. <https://doi.org/10.1007/s11104-024-06564-3>
- Nacke H, Goldmann K, Schöning I, et al (2016) Fine spatial scale variation of soil microbial communities under European beech and Norway spruce. *Front Microbiol* 7:. <https://doi.org/10.3389/fmicb.2016.02067>
- Nakashima K, Yamaguchi-Shinozaki K (2013) ABA signaling in stress-response and seed development. *Plant Cell Rep* 32:959–970. <https://doi.org/10.1007/s00299-013-1418-1>

- Netherer S, Panassiti B, Pennerstorfer J, Matthews B (2019) Acute Drought Is an Important Driver of Bark Beetle Infestation in Austrian Norway Spruce Stands. *Front For Glob Change* 2:1–21. <https://doi.org/10.3389/ffgc.2019.00039>
- Nickel UT, Weigl F, Kerner R, et al (2018) Quantitative losses vs. qualitative stability of ectomycorrhizal community responses to 3 years of experimental summer drought in a beech–spruce forest. *Glob Change Biol* 24:e560–e576. <https://doi.org/10.1111/gcb.13957>
- Nikolova PS, Bauerle TL, Häberle KH, et al (2020) Fine-Root Traits Reveal Contrasting Ecological Strategies in European Beech and Norway Spruce During Extreme Drought. *Front Plant Sci* 11:. <https://doi.org/10.3389/fpls.2020.01211>
- Nikolova PS, Raspe S, Andersen CP, et al (2009) Effects of the extreme drought in 2003 on soil respiration in a mixed forest. *Eur J For Res* 128:87–98. <https://doi.org/10.1007/s10342-008-0218-6>
- Niskanen T, Lücking R, Dahlberg A, et al (2023) Pushing the Frontiers of Biodiversity Research: Unveiling the Global Diversity, Distribution, and Conservation of Fungi. *Annu Rev Environ Resour* 48:149–176. <https://doi.org/10.1146/annurev-environ-112621-090937>
- Oksanen AJ, Blanchet FG, Friendly M, et al (2019) Vegan. In: *Encyclopedia of Food and Agricultural Ethics*. Springer Netherlands, Dordrecht, pp 2395–2396
- Olesinski J, Lavigne MB, Krasowski MJ (2011) Effects of soil moisture manipulations on fine root dynamics in a mature balsam fir (*Abies balsamea* L. Mill.) forest. *Tree Physiol* 31:339–348. <https://doi.org/10.1093/treephys/tpr006>
- Oliveira E, Amara I, Bellido D, et al (2007) LC-MS/MS identification of *Arabidopsis thaliana* heat-stable seed proteins: Enriching for LEA-type proteins by acid treatment. *J Mass Spectrom* 42:1485–1495. <https://doi.org/10.1002/jms.1292>
- Otsing E, Anslan S, Ambrosio E, et al (2021) Tree Species Richness and Neighborhood Effects on Ectomycorrhizal Fungal Richness and Community Structure in Boreal Forest. *Front Microbiol* 12:. <https://doi.org/10.3389/fmicb.2021.567961>
- Pena R, Simon J, Rennenberg H, Polle A (2013) Ectomycorrhiza affect architecture and nitrogen partitioning of beech (*Fagus sylvatica* L.) seedlings under shade and drought. *Environ Exp Bot* 87:207–217. <https://doi.org/10.1016/j.envexpbot.2012.11.005>
- Piedallu C, Gégout JC, Bruand A, Seynave I (2011) Mapping soil water holding capacity over large areas to predict potential production of forest stands. *Geoderma* 160:355–366. <https://doi.org/10.1016/j.geoderma.2010.10.004>
- Pölme S, Abarenkov K, Henrik Nilsson R, et al (2020) FungalTraits: a user-friendly traits database of fungi and fungus-like stramenopiles. *Fungal Divers* 105:. <https://doi.org/10.1007/s13225-020-00466-2>

- Poorter H, Niklas KJ, Reich PB, et al (2012) Biomass allocation to leaves, stems and roots: Meta-analyses of interspecific variation and environmental control. *New Phytol* 193:30–50. <https://doi.org/10.1111/j.1469-8137.2011.03952.x>
- Prescott CE (2010) Litter decomposition: What controls it and how can we alter it to sequester more carbon in forest soils? *Biogeochemistry* 101:133–149. <https://doi.org/10.1007/s10533-010-9439-0>
- Prescott TAK, Hill R, Mas-Claret E, et al (2023) Fungal Drug Discovery for Chronic Disease: History, New Discoveries and New Approaches. *Biomolecules* 13:986. <https://doi.org/10.3390/biom13060986>
- Pretzsch H, Block J, Dieler J, et al (2010) Comparison between the productivity of pure and mixed stands of Norway spruce and European beech along an ecological gradient. *Ann For Sci* 67:712–712. <https://doi.org/10.1051/forest/2010037>
- Pretzsch H, del Río M, Ammer C, et al (2015) Growth and yield of mixed versus pure stands of Scots pine (*Pinus sylvestris* L.) and European beech (*Fagus sylvatica* L.) analysed along a productivity gradient through Europe. *Eur J For Res* 134:927–947. <https://doi.org/10.1007/s10342-015-0900-4>
- Pretzsch H, Dieler J, Seifert T, Rötzer T (2012) Climate effects on productivity and resource-use efficiency of Norway spruce (*Picea abies* [L.] Karst.) and European beech (*Fagus sylvatica* [L.]) in stands with different spatial mixing patterns. *Trees - Struct Funct* 26:1343–1360. <https://doi.org/10.1007/s00468-012-0710-y>
- Qian XM, Kottke I, Oberwinkler F (1998) Activity of different ectomycorrhizal types studied by vital fluorescence. *Plant Soil* 199:91–98. <https://doi.org/10.1023/A:1004226220283>
- Querejeta JL, Egerton-Warburton LM, Allen MF (2009) Topographic position modulates the mycorrhizal response of oak trees to interannual rainfall variability. *Ecology* 90:649–662. <https://doi.org/10.1890/07-1696.1>
- Raison RJ, Khanna PK (2011) Possible Impacts of Climate Change on Forest Soil Health. 257–285. [https://doi.org/10.1007/978-3-642-20256-8\\_12](https://doi.org/10.1007/978-3-642-20256-8_12)
- Rascher KG, Große-Stoltenberg A, Máguas C, Werner C (2011) Understorey Invasion by *Acacia longifolia* Alters the Water Balance and Carbon Gain of a Mediterranean Pine Forest. *Ecosystems* 14:904–919. <https://doi.org/10.1007/s10021-011-9453-7>
- Ratcliffe S, Wirth C, Jucker T, et al (2017) Biodiversity and ecosystem functioning relations in European forests depend on environmental context. *Ecol Lett* 20:1414–1426. <https://doi.org/10.1111/ele.12849>
- Rehshuh R, Mette T, Menzel A, Buras A (2017) Soil properties affect the drought susceptibility of Norway spruce. *Dendrochronologia* 45:81–89. <https://doi.org/10.1016/j.dendro.2017.07.003>



- Rehseh R, Ruehr NK (2022) Diverging responses of water and carbon relations during and after heat and hot drought stress in *Pinus sylvestris*. *Tree Physiol* 42:1532–1548. <https://doi.org/10.1093/treephys/tpab141>
- Richard F, Roy M, Shahin O, et al (2011) Ectomycorrhizal communities in a Mediterranean forest ecosystem dominated by *Quercus ilex*: Seasonal dynamics and response to drought in the surface organic horizon. *Ann For Sci* 68:57–68. <https://doi.org/10.1007/s13595-010-0007-5>
- Rodríguez-Robles U, Arredondo JT, Huber-Sannwald E, et al (2020) Coupled plant traits adapted to wetting/drying cycles of substrates co-define niche multidimensionality. *Plant Cell Environ* 43:2394–2408. <https://doi.org/10.1111/pce.13837>
- Rohner B, Kumar S, Liechti K, et al (2021) Tree vitality indicators revealed a rapid response of beech forests to the 2018 drought. *Ecol Indic* 120:106903. <https://doi.org/10.1016/j.ecolind.2020.106903>
- Rosselló-Mora R, Amann R (2001) The species concept for prokaryotes. *FEMS Microbiol Rev* 25:39–67. [https://doi.org/10.1016/S0168-6445\(00\)00040-1](https://doi.org/10.1016/S0168-6445(00)00040-1)
- Roy Chowdhury T, Lee J-Y, Bottos EM, et al (2019) Metaphenomic Responses of a Native Prairie Soil Microbiome to Moisture Perturbations. *mSystems* 4:. <https://doi.org/10.1128/msystems.00061-19>
- Ruehr NK, Grote R, Mayr S, Arneith A (2019) Beyond the extreme: Recovery of carbon and water relations in woody plants following heat and drought stress. *Tree Physiol* 39:1285–1299. <https://doi.org/10.1093/treephys/tpz032>
- Ruehr NK, Offermann CA, Gessler A, et al (2009) Drought effects on allocation of recent carbon: From beech leaves to soil CO<sub>2</sub> efflux. *New Phytol* 184:950–961. <https://doi.org/10.1111/j.1469-8137.2009.03044.x>
- Rukh S, Poschenrieder W, Heym M, Pretzsch H (2020) Drought Resistance of Norway Spruce (*Picea abies* [L.] Karst) and European Beech (*Fagus sylvatica* [L.]) in Mixed vs. Monospecific Stands and on Dry vs. Wet Sites. From Evidence at the Tree Level to Relevance at the Stand Level. *Forests* 11:639. <https://doi.org/10.3390/f11060639>
- Saetre P, Stark JM (2005) Microbial dynamics and carbon and nitrogen cycling following re-wetting of soils beneath two semi-arid plant species. *Oecologia* 142:247–260. <https://doi.org/10.1007/s00442-004-1718-9>
- Sala A, Piper F, Hoch G (2010) Physiological mechanisms of drought-induced tree mortality are far from being resolved. *New Phytol* 186:274–281. <https://doi.org/10.1111/j.1469-8137.2009.03167.x>
- Schall P, Lödige C, Beck M, Ammer C (2012) Biomass allocation to roots and shoots is more sensitive to shade and drought in European beech than in Norway spruce seedlings. *For Ecol Manag* 266:246–253. <https://doi.org/10.1016/j.foreco.2011.11.017>

- Schenk HJ, Jackson RB (2002) The global biogeography of roots. *Ecol Monogr* 72:311–328. [https://doi.org/10.1890/0012-9615\(2002\)072\[0311:TGBOR\]2.0.CO;2](https://doi.org/10.1890/0012-9615(2002)072[0311:TGBOR]2.0.CO;2)
- Schimel JP (2018) Life in dry soils: Effects of drought on soil microbial communities and processes. *Annu Rev Ecol Evol Syst* 49:409–432. <https://doi.org/10.1146/annurev-ecolsys-110617-062614>
- Schmid I (2002) The influence of soil type and interspecific competition on the fine root system of Norway spruce and European beech
- Schmied G, Hilmers T, Mellert KH, et al (2023) Nutrient regime modulates drought response patterns of three temperate tree species. *Sci Total Environ* 868:161601. <https://doi.org/10.1016/j.scitotenv.2023.161601>
- Schuldt B, Buras A, Arend M, et al (2020) A first assessment of the impact of the extreme 2018 summer drought on Central European forests. *Basic Appl Ecol* 45:86–103. <https://doi.org/10.1016/j.baae.2020.04.003>
- Schume H, Jost G, Hager H (2004) Soil water depletion and recharge patterns in mixed and pure forest stands of European beech and Norway spruce. *J Hydrol* 289:258–274. <https://doi.org/10.1016/j.jhydrol.2003.11.036>
- Sevanto S (2018) Drought impacts on phloem transport. *Curr Opin Plant Biol* 43:76–81. <https://doi.org/10.1016/j.pbi.2018.01.002>
- Sevanto S (2014) Phloem transport and drought. *J Exp Bot* 65:1751–1759. <https://doi.org/10.1093/jxb/ert467>
- Sevanto S, McDowell NG, Dickman LT, et al (2014) How do trees die? A test of the hydraulic failure and carbon starvation hypotheses. *Plant Cell Environ* 37:153–161. <https://doi.org/10.1111/pce.12141>
- Sharda JN, Koide RT (2008) Can hypodermal passage cell distribution limit root penetration by mycorrhizal fungi? *New Phytol* 180:696–701. <https://doi.org/10.1111/j.1469-8137.2008.02600.x>
- Sharp RE, LeNoble ME, Else MA, et al (2000) Endogenous ABA maintains shoot growth in tomato independently of effects on plant water balance: Evidence for an interaction with ethylene. *J Exp Bot* 51:1575–1584. <https://doi.org/10.1093/jexbot/51.350.1575>
- Sheil D (2018) Forests, atmospheric water and an uncertain future: the new biology of the global water cycle. *For Ecosyst* 5:19. <https://doi.org/10.1186/s40663-018-0138-y>
- Shi L, Guttenberger M, Kottke I, Hampp R (2002) The effect of drought on mycorrhizas of beech (*Fagus sylvatica* L.): Changes in community structure, and the content of carbohydrates and nitrogen storage bodies of the fungi. *Mycorrhiza* 12:303–311. <https://doi.org/10.1007/s00572-002-0197-2>

- Singaravelan N, Grishkan I, Beharav A, et al (2008) Adaptive melanin response of the soil fungus *Aspergillus niger* to UV radiation stress at “Evolution Canyon”, Mount Carmel, Israel. *PLoS ONE* 3:2–6. <https://doi.org/10.1371/journal.pone.0002993>
- Slessarev EW, Lin Y, Jiménez BY, et al (2020) Cellular and extracellular C contributions to respiration after wetting dry soil. *Biogeochemistry* 147:307–324. <https://doi.org/10.1007/s10533-020-00645-y>
- Smith GR, Finlay RD, Stenlid J, et al (2017) Growing evidence for facultative biotrophy in saprotrophic fungi: data from microcosm tests with 201 species of wood-decay basidiomycetes. *New Phytol* 215:747–755. <https://doi.org/10.1111/nph.14551>
- Smith SE, Read DJ (2008) *Mycorrhizal Symbiosis*. Academic Press, San Diego, CA, USA
- Solly EF, Brunner I, Helmisaari HS, et al (2018) Unravelling the age of fine roots of temperate and boreal forests. *Nat Commun* 9:1–8. <https://doi.org/10.1038/s41467-018-05460-6>
- Steudle E (2002) Transport of Water in Plants. *Environ Control Biol* 40:29–37. <https://doi.org/10.2525/ecb1963.40.29>
- Suz LM, Sarasan V, Wearn JA, et al (2018) Positive plant–fungal interactions. In: *State of the World’s Fungi*. Royal Botanic Gardens, Kew, pp 32–39
- Talbot JM, Bruns TD, Smith DP, et al (2013) Independent roles of ectomycorrhizal and saprotrophic communities in soil organic matter decomposition. *Soil Biol Biochem* 57:282–291. <https://doi.org/10.1016/j.soilbio.2012.10.004>
- Talbot JM, Martin F, Kohler A, et al (2015) Functional guild classification predicts the enzymatic role of fungi in litter and soil biogeochemistry. *Soil Biol Biochem* 88:441–456. <https://doi.org/10.1016/j.soilbio.2015.05.006>
- Tanimoto E (2005) Regulation of Root Growth by Plant Hormones—Roles for Auxin and Gibberellin. *Crit Rev Plant Sci* 24:249–265. <https://doi.org/10.1080/07352680500196108>
- Tedersoo L, Bahram M, Cajthaml T, et al (2016) Tree diversity and species identity effects on soil fungi, protists and animals are context dependent. *ISME J* 10:346–362. <https://doi.org/10.1038/ismej.2015.116>
- Tedersoo L, Bahram M, Ryberg M, et al (2014) Global biogeography of the ectomycorrhizal /sebacina lineage (Fungi, Sebaciniales) as revealed from comparative phylogenetic analyses. *Mol Ecol* 23:4168–4183. <https://doi.org/10.1111/mec.12849>
- Tedersoo L, Bahram M, Toots M, et al (2012) Towards global patterns in the diversity and community structure of ectomycorrhizal fungi. *Mol Ecol* 21:4160–4170. <https://doi.org/10.1111/j.1365-294X.2012.05602.x>

- Tedersoo L, Jairus T, Horton BM, et al (2008) Strong host preference of ectomycorrhizal fungi in a Tasmanian wet sclerophyll forest as revealed by DNA barcoding and taxon-specific primers. *New Phytol* 180:479–490. <https://doi.org/10.1111/j.1469-8137.2008.02561.x>
- Tedersoo L, Sadam A, Zambrano M, et al (2010) Low diversity and high host preference of ectomycorrhizal fungi in Western Amazonia, a neotropical biodiversity hotspot. *ISME J* 4:465–471. <https://doi.org/10.1038/ismej.2009.131>
- Tedersoo L, Smith ME (2013) Lineages of ectomycorrhizal fungi revisited: Foraging strategies and novel lineages revealed by sequences from belowground. *Fungal Biol Rev* 27:83–99. <https://doi.org/10.1016/j.fbr.2013.09.001>
- Torquato PR, Will RE, Zhang B, Zou CB (2020) Stand-Level Transpiration Increases after Eastern Redcedar (*Juniperus virginiana* L.) Encroachment into the Midstory of Oak Forests. *Forests* 11:901. <https://doi.org/10.3390/f11090901>
- Torsvik V, Øvreås L (2002) Microbial diversity and function in soil: from genes to ecosystems. *Curr Opin Microbiol* 5:240–5. [https://doi.org/10.1016/s1369-5274\(02\)00324-7](https://doi.org/10.1016/s1369-5274(02)00324-7)
- Trugman AT, Detto M, Bartlett MK, et al (2018) Tree carbon allocation explains forest drought-kill and recovery patterns. *Ecol Lett* 21:1552–1560. <https://doi.org/10.1111/ele.13136>
- Unestam T, Sun YP (1995) Extramatrical structures of hydrophobic and hydrophilic ectomycorrhizal fungi. *Mycorrhiza* 5:301–311. <https://doi.org/10.1007/BF00207402>
- van der Heijden MGA, Martin FM, Selosse MA, Sanders IR (2015) Mycorrhizal ecology and evolution: The past, the present, and the future. *New Phytol* 205:1406–1423. <https://doi.org/10.1111/nph.13288>
- Van der Putten WH (2003) PLANT DEFENSE BELOWGROUND AND SPATIOTEMPORAL PROCESSES IN NATURAL VEGETATION. *Ecology* 84:2269–2280. <https://doi.org/10.1890/02-0284>
- Van Elsas JD, Trevors JT, Rosado AS, Nannipieri P (2019) *Modern Soil Microbiology*, Third Edition. CRC Press
- von Wilpert K (2022) Forest Soils—What’s Their Peculiarity? *Soil Syst* 6:. <https://doi.org/10.3390/soilsystems6010005>
- Wang J, Zhang H, Gao J, et al (2021) Effects of ectomycorrhizal fungi (*Suillus variegatus*) on the growth, hydraulic function, and non-structural carbohydrates of *Pinus tabulaeformis* under drought stress. *BMC Plant Biol* 21:1–13. <https://doi.org/10.1186/s12870-021-02945-3>
- Wang W, Vinocur B, Shoseyov O, Altman A (2004) Role of plant heat-shock proteins and molecular chaperones in the abiotic stress response. *Trends Plant Sci* 9:244–252. <https://doi.org/10.1016/j.tplants.2004.03.006>

- Warembourg FR, Roumet C, Lafont F (2003) Differences in rhizosphere carbon-partitioning among plant species of different families. *Plant Soil* 256:347–357. <https://doi.org/10.1023/A:1026147622800>
- Warren CR (2019) Isotope pool dilution reveals rapid turnover of small quaternary ammonium compounds. *Soil Biol Biochem* 131:90–99. <https://doi.org/10.1016/j.soilbio.2019.01.004>
- Weigl FC, Grams TEE, Pritsch K (2023) Responses of root-associated fungal communities of mature beech and spruce during five years of experimental drought. *Ecology*
- Welsh DT (2000) Ecological significance of compatible solute accumulation by micro-organisms: From single cells to global climate. *FEMS Microbiol Rev* 24:263–290. [https://doi.org/10.1016/S0168-6445\(99\)00038-8](https://doi.org/10.1016/S0168-6445(99)00038-8)
- Werner C, Meredith LK, Ladd SN, et al (2021) Ecosystem fluxes during drought and recovery in an experimental forest. *Science* 374:1514–1518. <https://doi.org/10.1126/science.abj6789>
- Williams A, de Vries FT (2020) Plant root exudation under drought: implications for ecosystem functioning. *New Phytol* 225:1899–1905. <https://doi.org/10.1111/nph.16223>
- Woodruff DR, Ryan M (2014) The impacts of water stress on phloem transport in Douglas-fir trees. *Tree Physiol* 34:5–14. <https://doi.org/10.1093/treephys/tpt106>
- Yang Q, Zhang W, Li R, et al (2016) Different responses of non-structural carbohydrates in above-ground tissues/organs and root to extreme drought and re-watering in Chinese fir (*Cunninghamia lanceolata*) saplings. *Trees - Struct Funct* 30:1863–1871. <https://doi.org/10.1007/s00468-016-1419-0>
- Yuste JC, Peñuelas J, Estiarte M, et al (2011) Drought-resistant fungi control soil organic matter decomposition and its response to temperature. *Glob Change Biol* 17:1475–1486. <https://doi.org/10.1111/j.1365-2486.2010.02300.x>
- Zabel RA, Morrell JJ (2020) Chemical changes in wood caused by decay fungi. *Wood Microbiol* 215–244. <https://doi.org/10.1016/b978-0-12-819465-2.00008-5>
- Zhang D, Hui D, Luo Y, Zhou G (2008) Rates of litter decomposition in terrestrial ecosystems: global patterns and controlling factors. *J Plant Ecol* 1:85–93. <https://doi.org/10.1093/jpe/rtn002>
- Zhang Y, Chen HYH, Reich PB (2012) Forest productivity increases with evenness, species richness and trait variation: A global meta-analysis. *J Ecol* 100:742–749. <https://doi.org/10.1111/j.1365-2745.2011.01944.x>
- Zhou Y, Wigley BJ, Case MF, et al (2020) Rooting depth as a key woody functional trait in savannas. *New Phytol* 227:1350–1361. <https://doi.org/10.1111/nph.16613>

Zwetsloot MJ, Bauerle TL (2021) Repetitive seasonal drought causes substantial species-specific shifts in fine-root longevity and spatio-temporal production patterns in mature temperate forest trees. *New Phytol.* <https://doi.org/10.1111/nph.17432>

Zwetsloot MJ, Goebel M, Paya A, et al (2019) Specific spatio-temporal dynamics of absorptive fine roots in response to neighbor species identity in a mixed beech-spruce forest. *Tree Physiol* 39:1867–1879. <https://doi.org/10.1093/treephys/tpz086>

## 7. Danksagung

Ein großer Dank geht an meine Betreuerin Prof. Dr. Karin Pritsch, die mir die Möglichkeit gegeben hat, an diesem faszinierenden Thema zu forschen und mich in jeder Phase der Promotion unterstützt hat. Auch großer Dank geht an Dr. Fabian Weigl für die gute Zusammenarbeit im Labor und im Feld, sowie für die Unterstützung in der Bioinformatik und in R. Desweiteren möchte ich Kyohsuke Hikino danken für die gute Zusammenarbeit, die zahlreichen, aufschlussreichen Diskussionen und die vielen gemeinsamen Arbeitsstunden im Gewächshaus. Unsere Gewächshaus-Playlist wird mir immer in bester Erinnerung bleiben 😊. Ein weiteres großes Dankeschön geht an Franz Buegger für all den Rat in Sachen Technik und Isotopen, sein handwerkliches Geschick im Feld und beim Bau des Labelling-Zeltes und dafür, dass ich bei jeglichen technischen Problemen zu ihm kommen durfte. Auch bei Prof. Dr. Simon Landhäuser und Prof. Dr. Thorsten Grams möchte ich mich bedanken für alle anregenden Diskussionen, die sehr geholfen haben, die Ergebnisse aus einer anderen Perspektiven zu betrachten. All die Arbeit in der Vorbereitung, im Feld und im Labor wäre nicht zu bewältigen gewesen ohne die Unterstützung zahlreicher Helferchen: Ramona Werner, Laura Pohlenz, Valentin Kugler, Sarah Kristen, Isabelle Pitzen, Tina Kiedeisch und Selina Schulz. Neben der Unterstützung im Labor hatten Elke Gerstner und Barbara „Bärbel“ Groß immer ein offenes Ohr und aufmunternde Worte. Ich möchte meiner Familie danken, allen voran meinen Eltern und Victor Beccari, dass sie stets für mich da waren, an mich geglaubt und mich stets unterstützt haben. Vielen Dank an meine Freunde, dass ihr immer ein offenes Ohr habt und jeden erdenklichen Unfug mitmacht.

Ohne euch wäre diese Arbeit so nicht möglich gewesen!

## 8. Appendix

- Additional results
- Manuscript I (submitted)
- Article I (published)
- Article II (published)
- Article III (published)



## Additional results not presented in the manuscript and articles

To fully address whether seedlings are less affected by drought in soils with drought-adapted fungal communities and interspecific root interaction, both beech seedlings (BB; described in chapter 3.1 and manuscript I) and spruce seedlings were studied as part of the greenhouse experiment, although spruce seedlings were not addressed in manuscript I. The results relating to spruce and interspecific root interaction are described in this chapter. 40 spruce seedlings grew in 10 monoculture pots consisting of four seedlings per pot only having intraspecific root contact (SS), 20 spruce seedlings grew in 10 mixed culture pots consisting of two beech and two spruce seedlings having interspecific root contact (Bmix for beech roots and Smix for spruce).

### Spruce drought stress, relative growth and allocation of new photoassimilates

The otherwise unpublished data on plant physiology presented in this section were provided by Kyohsuke Hikino and have been included in this thesis with his permission. Inclusion of these data provides a broader perspective on the seedlings' drought responses across the different soils and the interpretation of all results.

The predawn plant water potential in spruce seedlings was significantly lower in drought treated compared to control seedlings in all soils (Figure A1), indicating that drought-treated seedlings experienced water stress. Nonetheless, there were no differences in the extent of drought stress between the soils.

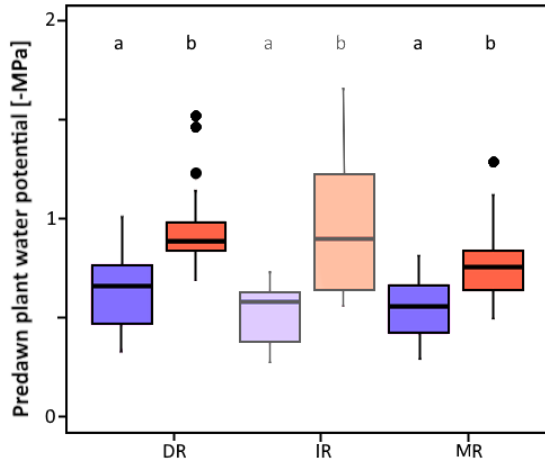


**Figure A1:** Predawn plant water potential on the day of harvest. Blue colour displays the controls and red colour the drought treated seedlings. Due to reduced replicates in IR, these results are displayed in a lighter colour. Lowercase letters indicate significant differences among the groups according to Tukey-HSD. The figure was provided by Kyohsuke Hikino and adjusted by me.

The relative biomass growth of both stems and roots showed no differences between control and drought seedlings (Figure A2a, b) within their respective soils.

Nevertheless, spruce seedlings growing in IR soil showed stunted growth in the controls as well as under drought (Figure A2a, b) of the monoculture and the mixed culture and were more prone to needle discolouration and mortality compared to seedlings growing in DR and MR soils (personal observation). For this reason, the number of seedling replicates in IR is reduced and the corresponding results should be considered with caution as indicated by lighter colours in Figures A1, A2, A3, A4, A6.

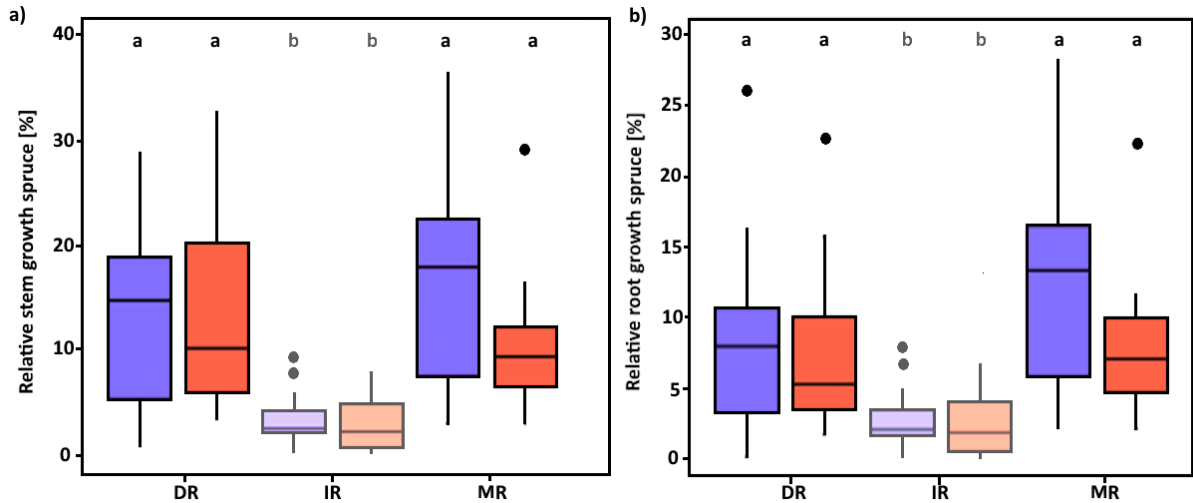


**Figure A2:** a) Relative stem and b) root biomass growth during the drought treatment of 8 weeks. Dry region (DR), intermediate region (IR) and moist region (MR) soil. Blue colour displays the controls and red colour the drought treated seedlings. Due to reduced replicates in IR, these results are displayed in a lighter colour. Lowercase letters indicate significant differences among the groups according to Tukey-HSD. The figure was provided by Kyohsuke Hikino and adjusted by me.

The allocation of newly assimilated C in spruce seedlings only changed significantly in DR with the application of drought, with a reduced C allocation to the roots but a higher allocation in leaves in drought treated compared to control seedlings (Figure A3).

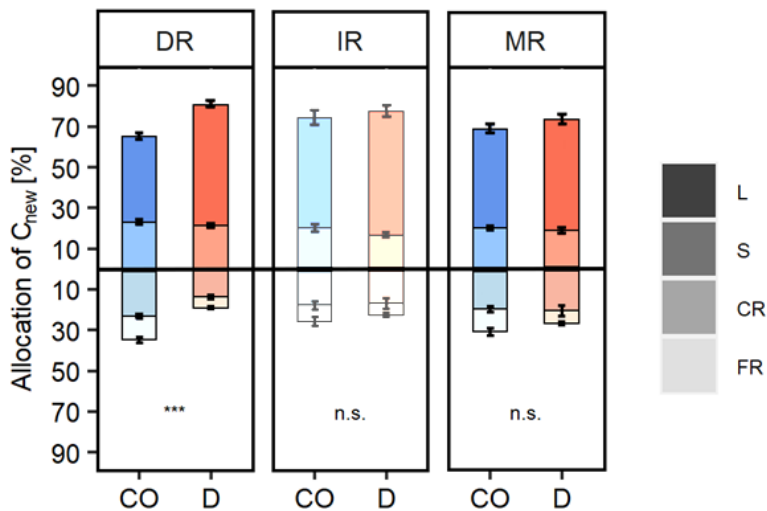


**Figure A3:** Allocation of newly assimilated C ( $C_{new}$ ) in leaf (L), stem (S), coarse-roots (CR), and fine-roots (FR) after three days of labelling under control (CO) and drought (D) treatments. Dry region (DR), intermediate region (IR) and moist region (MR) soil. Due to reduced replicates in IR, these results are displayed in a lighter colour. The asterisk indicates significant differences

in the ratio of belowground to total  $C_{new}$  between CO and D plants according to Tukey-HSD: \*\*\*,  $p < 0.001$ , n.s.: not significant. The figure was provided by Kyohsuke Hikino and adjusted by me.

## Root morphology in beech and spruce seedlings with inter- and intraspecific root interaction after experimental drought

All measured root parameters, including taproot length, root branching intensity, percentage of vital tips, and the degree of mycorrhization, differed significantly between control and drought treated, inter- and intraspecific root interaction, as well as soil type (Table A1).

**Table A1:** The influence of treatment (treat), root interaction (RI) and soil on Taproot length, branching intensity, vital tips and degree of mycorrhization. Significance was tested by ANOVA and indicated by bold numbers.

	Taproot length		Branching intensity		Vital tips		Mycorrhization	
	F	p	F	p	F	p	F	p
<i>Treat</i>	53.76	<b>&lt; 0.001</b>	45.91	<b>&lt; 0.001</b>	511.72	<b>&lt; 0.001</b>	59.79	<b>&lt; 0.001</b>
<i>RI</i>	112.1	<b>&lt; 0.001</b>	94.43	<b>&lt; 0.001</b>	79.54	<b>&lt; 0.001</b>	8.11	<b>&lt; 0.001</b>
<i>Soil</i>	3.28	<b>0.04</b>	6.70	<b>0.001</b>	53.57	<b>&lt; 0.005</b>	8.52	<b>&lt; 0.001</b>
<i>Treat x RI</i>	9.27	<b>&lt; 0.001</b>	19.02	<b>&lt; 0.001</b>	23.82	0.07	0.34	0.79
<i>Treat x Soil</i>	2.11	0.13	1.82	0.16	62.12	<b>0.002</b>	3.58	<b>0.03</b>
<i>RI x Soil</i>	27.46	<b>&lt; 0.001</b>	6.41	<b>&lt; 0.001</b>	87.65	<b>&lt; 0.001</b>	3.57	<b>0.002</b>
<i>Treat x RI x Soil</i>	1.64	0.13	2.54	<b>0.02</b>	25.61	<b>0.02</b>	2.96	<b>0.01</b>

Nonetheless, a post-hoc Tukey HSD test demonstrated that within the different soils and treatments no root parameter displayed a significant difference between root interactions of a single tree species (e.g., BB and Bmix in DR control), except for branching intensity between BB and Bmix in DR control (Table A2). Consequently, in the following paragraph no further distinction was made between inter- and intraspecific root interaction, but solely between spruce control and drought treated. The root parameters of beech have been documented in manuscript I, and have shown that in DR and MR, seedlings had longer taproots and lower branching intensity during drought. Furthermore, the number of vital tips of beech seedlings

decreased in DR and IR soils, but not significantly and the degree of mycorrhization tended to decline in IR and MR soils.

**Table A2:** Post-hoc Tukey HSD test for taproot length, branching intensity, vital tips and degree of mycorrhization on inter- and intraspecific root interactions of beech and spruce within the soils (DR: dry region, IR: intermediate region, MR: moist region) and control (CO)/ drought treated (D). The tests were performed with Bonferroni adjustment.

		Taproot length	Branching intensity	Vital tips	Mycorrhization
		P <sub>adj</sub>	P <sub>adj</sub>	P <sub>adj</sub>	P <sub>adj</sub>
DR CO	<i>Bmix – BB</i>	1.00	<b>0.03</b>	1.00	1.00
	<i>Smix – SS</i>	1.00	1.00	1.00	1.00
DR D	<i>Bmix – BB</i>	1.00	1.00	1.00	1.00
	<i>Smix – SS</i>	1.00	1.00	1.00	1.00
IR CO	<i>Bmix – BB</i>	1.00	0.96	1.00	0.97
	<i>Smix – SS</i>	1.00	0.86	1.00	1.00
IR D	<i>Bmix – BB</i>	1.00	1.00	1.00	0.89
	<i>Smix – SS</i>	1.00	1.00	1.00	1.00
MR	<i>Bmix – BB</i>	0.18	1.00	1.00	0.89
CO	<i>Smix – SS</i>	1.00	1.00	1.00	1.00
MR D	<i>Bmix – BB</i>	1.00	1.00	0.99	1.00
	<i>Smix – SS</i>	1.00	0.99	1.00	1.00

In DR, the spruce seedlings had a significantly higher taproot length compared to IR and MR (Figure A4a), with even longer roots in drought treated compared to control seedlings. Conversely, no difference in taproot length was observed between controls and drought treated seedlings in IR and MR. However, the branching intensity remained similar across all soil types and between control and drought treated (Figure A4b). Furthermore, when compared to control seedlings, the percentage of vital root tips (Figure A4c) decreased in

drought treated seedlings within DR and IR, while the degree of mycorrhization (Figure A4d) decreased solely in DR.

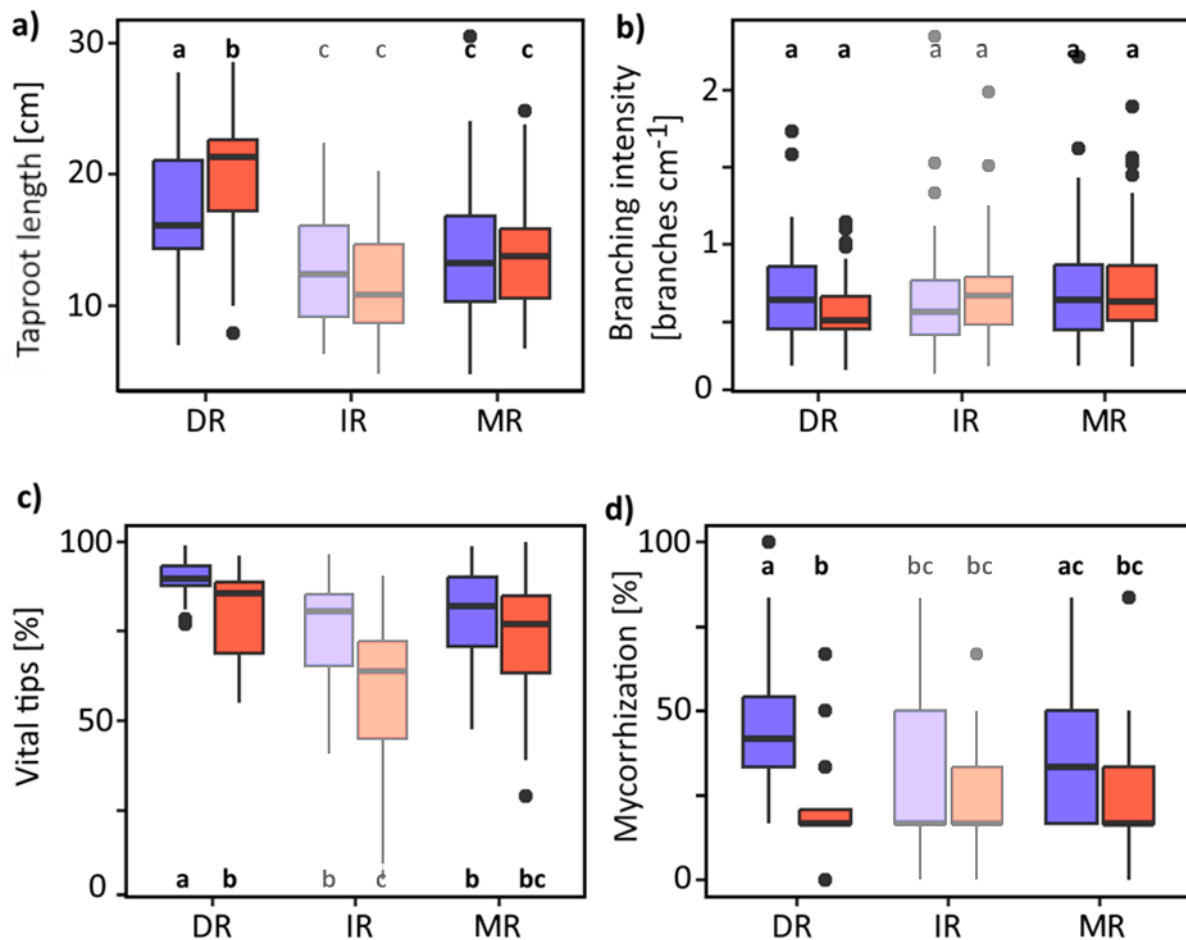


**Figure A4:** Fine-root traits including taproot length (a), branching intensity (b), percentage of vital root tips (c) and degree of mycorrhization (d). Blue boxes represent controls and red boxes drought treatment. Due to reduced replicates in IR, these results are displayed in a lighter colour. Lowercase letters indicate significant differences among the groups according to Dunn-test.

Root and soil derived fungal community compositions in spruce seedlings with inter- and intraspecific root interaction after experimental drought

The composition of fungal communities (Figure A5) did not significantly differ between spruce seedlings planted either in monoculture or in a mixture, as indicated by both the soil samples ( $p = 0.24$ ,  $R^2 = 0.01$ , PERMANOVA) and the root samples ( $p = 0.17$ ,  $R^2 = 0.02$ , PERMANOVA). Nonetheless, the fungal community composition differed significantly between roots of beech seedlings and spruce seedlings ( $p < 0.001$ ,  $R^2 = 0.11$ , PERMANOVA). Additionally, the fungal

community composition differed significantly between the soil regions in soil samples ( $p < 0.001$ ,  $R^2 = 0.61$ , PERMANOVA) as well as root samples ( $p < 0.001$ ,  $R^2 = 0.47$ , PERMANOVA). Moreover, no significant distinctions were noted between the samples taken before the drought treatment and the control samples taken after the drought treatment ( $p = 0.14$ ,  $R^2 = 0.02$ , PERMANOVA). Consequently, pre-drought samples were excluded from further analysis, and root interaction was not further considered.

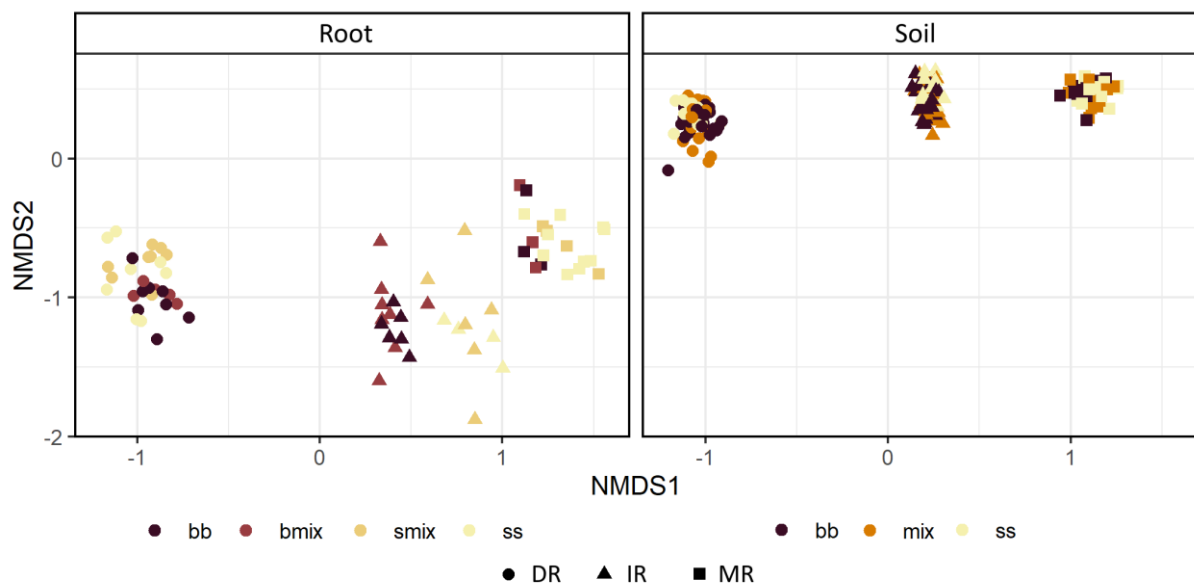


**Figure A5:** Non-metric multidimensional scaling (NMDS) plot of root-associated (left panel) and soil fungal community composition (right panel) in a shared coordinate system (i.e., the same ordination). The colours represent the different root interactions (inter- and intraspecific), the shapes the different soil regions (DR = dry region, IR = intermediate region, MR = moist region). Stress = 0.12.

Regarding the soil samples, Shannon Index and species richness displayed significant differences between control and drought treated, whereas species richness differed among the soils (Table A3), with most species counts identified in DR controls. On the other hand, within the root samples, the Shannon and Simpson Indices, species richness, and Evenness did not exhibit significant differences between control and drought treated. However, all diversity metrics, except Evenness, displayed differences between the soils (Table A3), with the highest values recorded in DR.

**Table A3:** Soil and root associated fungal alpha-diversity based on rDNA displayed by Shannon Index, Simpson Index, species richness and Pielou's Evenness summarized by treatment (treat) and region soil (DR = drought region, IR = intermediate region, MR = moist region). Values are displayed as means  $\pm$  standard error. The influence of treatment and soil on fungal diversity was tested using either ANOVA or Scheirer-Ray-Hare-Test (\*). Bold numbers indicate significances and df degrees of freedom.

<b>Soil fungal communities</b>										
<i>Treat</i>	<i>Soil</i>	<i>Shannon Index</i>		<i>Simpson Index</i>		<i>species richness</i>		<i>Pielou's Evenness</i>		
<i>Control</i>	DR	4.80 $\pm$ 0.31		0.98 $\pm$ 0.01		602.00 $\pm$ 32.56		0.75 $\pm$ 0.05		
<i>Control</i>	IR	4.69 $\pm$ 0.14		0.97 $\pm$ 0.01		539.00 $\pm$ 67.80		0.75 $\pm$ 0.01		
<i>Control</i>	MR	4.49 $\pm$ 0.09		0.97 $\pm$ 0.00		453.25 $\pm$ 42.41		0.73 $\pm$ 0.01		
<i>Drought</i>	DR	4.60 $\pm$ 0.55		0.96 $\pm$ 0.05		533.50 $\pm$ 30.64		0.73 $\pm$ 0.08		
<i>Drought</i>	IR	4.35 $\pm$ 0.26		0.96 $\pm$ 0.01		491.25 $\pm$ 55.98		0.70 $\pm$ 0.04		
<i>Drought</i>	MR	4.30 $\pm$ 0.13		0.96 $\pm$ 0.01		428.00 $\pm$ 22.82		0.71 $\pm$ 0.01		
		<i>Shannon Index</i>		<i>Simpson Index*</i>		<i>species richness</i>		<i>Pielou's Evenness</i>		
		df	F	p	H	p	F	p	F	p
<i>Treat</i>		1	6.57	<b>0.02</b>	31.14	0.08	10.52	<b>0.004</b>	4.09	<b>0.05</b>
<i>Soil</i>		2	2.80	0.08	27.04	0.26	16.75	<b>&lt; 0.001</b>	0.62	0.55
<i>Treat x Soil</i>		2	0.22	0.80	15.23	0.47	0.49	0.62	0.27	0.76

<b>Root fungal communities</b>										
<i>Treat</i>	<i>Soil</i>	<i>Shannon Index</i>		<i>Simpson Index</i>		<i>species richness</i>		<i>Pielou's Evenness</i>		
<i>Control</i>	DR	4.03 $\pm$ 0.09		0.96 $\pm$ 0		331.62 $\pm$ 14.63		0.69 $\pm$ 0.01		
<i>Control</i>	IR	3.44 $\pm$ 0.12		0.94 $\pm$ 0.01		199.86 $\pm$ 11.32		0.65 $\pm$ 0.02		
<i>Control</i>	MR	3.88 $\pm$ 0.09		0.94 $\pm$ 0.01		325.00 $\pm$ 17.08		0.67 $\pm$ 0.01		
<i>Drought</i>	DR	4.00 $\pm$ 0.11		0.95 $\pm$ 0.01		340.87 $\pm$ 21.47		0.69 $\pm$ 0.01		
<i>Drought</i>	IR	3.55 $\pm$ 0.07		0.94 $\pm$ 0.01		242.00 $\pm$ 26.58		0.65 $\pm$ 0.02		
<i>Drought</i>	MR	3.71 $\pm$ 0.12		0.94 $\pm$ 0.01		278.55 $\pm$ 23.16		0.66 $\pm$ 0.01		
		<i>Shannon Index</i>		<i>Simpson Index*</i>		<i>species richness</i>		<i>Pielou's Evenness</i>		
		df	F	p	H	p	F	p	F	p



<i>Treat</i>	1	0.05	0.82	0.09	0.76	0.74	0.39	0.04	0.83
<i>Soil</i>	2	10.35	< <b>0.001</b>	63.53	<b>0.04</b>	17.14	< <b>0.001</b>	3.02	<b>0.06</b>
<i>Treat x Soil</i>	2	0.56	0.58	0.02	1.00	2.02	0.15	0.02	0.98

The soil fungal communities differed significantly only between the soils ( $p < 0.001$ ,  $R^2 = 0.61$ , PERMANOVA) but not between control and drought. Across both control and drought conditions, saprotrophic fungi were predominant in all three soils (Figure A6a). Within the ECM fungal species, species classified as medium-distance exploration types were highly prevalent in all three soils (Figure A6b). Although the abundances remained unchanged with drought in DR and IR, the abundance of contact types increased in MR soil.

At species level, the most abundant identified soil saprotrophic species showed no differences between control and drought within all three soils. Specifically, in DR, it was *Penicillium* sp. (control: 24 %, drought: 30 %) and *Mortierella* sp. (control: 13 %, drought: 13 %); in IR, *Solicoccozyma terricola* (control: 17 %, drought: 18 %), and in MR it was both, *S. terricola* (control: 16 %, drought: 17 %) and *Oidiodendron chlamydosporicum* (control: 13 %, drought: 16 %). Regarding the soil ECM fungal species, the most abundant identified species remained unchanged between control and drought treatment in DR (*Amphinema byssoides* control: 49 %, drought: 24 %) and IR (*Cortinarius* sp. control: 38 %, drought: 34 % and *Rhizopogon* sp. control: 17 %, drought: 20 %), whereas in MR, it was *Tylospora asterophora* (24 %) and *Lactarius* sp. (24 %) in the control and *Amanita* sp. (20 %) and *Piloderma sphaerosporum* (14 %) in the drought treatment.

The fungal communities revealed from the root samples showed significant differences between treatments ( $p = 0.02$ ,  $R^2 = 0.03$ , PERMANOVA) and soils ( $p < 0.001$ ,  $R^2 = 0.47$ , PERMANOVA).

Within the root-associated fungal communities, saprotrophic fungi were predominant in controls of IR and MR (Figure A6a), while in DR the proportion of saprotrophic and ECM fungi was around 45 % each. In roots of drought treated seedlings, the abundance of saprotrophs

increased at the expense of ECM fungi compared to controls in DR and MR soils. ECM fungi were further distinguished according to different exploration types (Figure A6b). In DR soil, medium-distance types were predominant and increased further during drought. While in IR soil long-distance types and in MR soil medium- and short-distance types were highly abundant in controls, and their abundance decreased with drought in IR soil in favour of especially contact types.

Regarding the abundance of root fungal species, *Penicillium* sp. (23 %) and *Oidiodendron* sp. (20 %) were the most prevalent saprotrophic species in DR controls, with *Penicillium* sp. further increasing under drought (51 %). In IR soil, *Phialocephala* sp. (30 %) dominated in controls, whereas *Penicillium* sp. (16 %) along with *Phialocephala* sp. (15 %) prevailed during drought. *Oidiodendron rhodogenum* (control: 20 %, drought: 19 %) and another *Oidiodendron* sp. (control: 17 %, drought: 14 %) were the most commonly identified saprotrophic species in both control and drought treatments of MR soil. Regarding ECM fungi, *Amphinema byssoides* (control: 47 %, drought: 67 %) appeared to be the most abundant species in roots of both control and drought treatments in DR soil. *Melanogaster* sp. (50 %) dominated in IR soil controls, whereas *Clavulina* sp. (41 %) was predominant in the drought treatment. Species abundances also changed in MR soil with drought, with *Tylospora asterophora* (34 %) and *Piloderma sphaerosporum* (31 %) being prevalent in control, and *Amanita* sp. (38 %) and *Melanogaster* sp. (16 %) under drought.

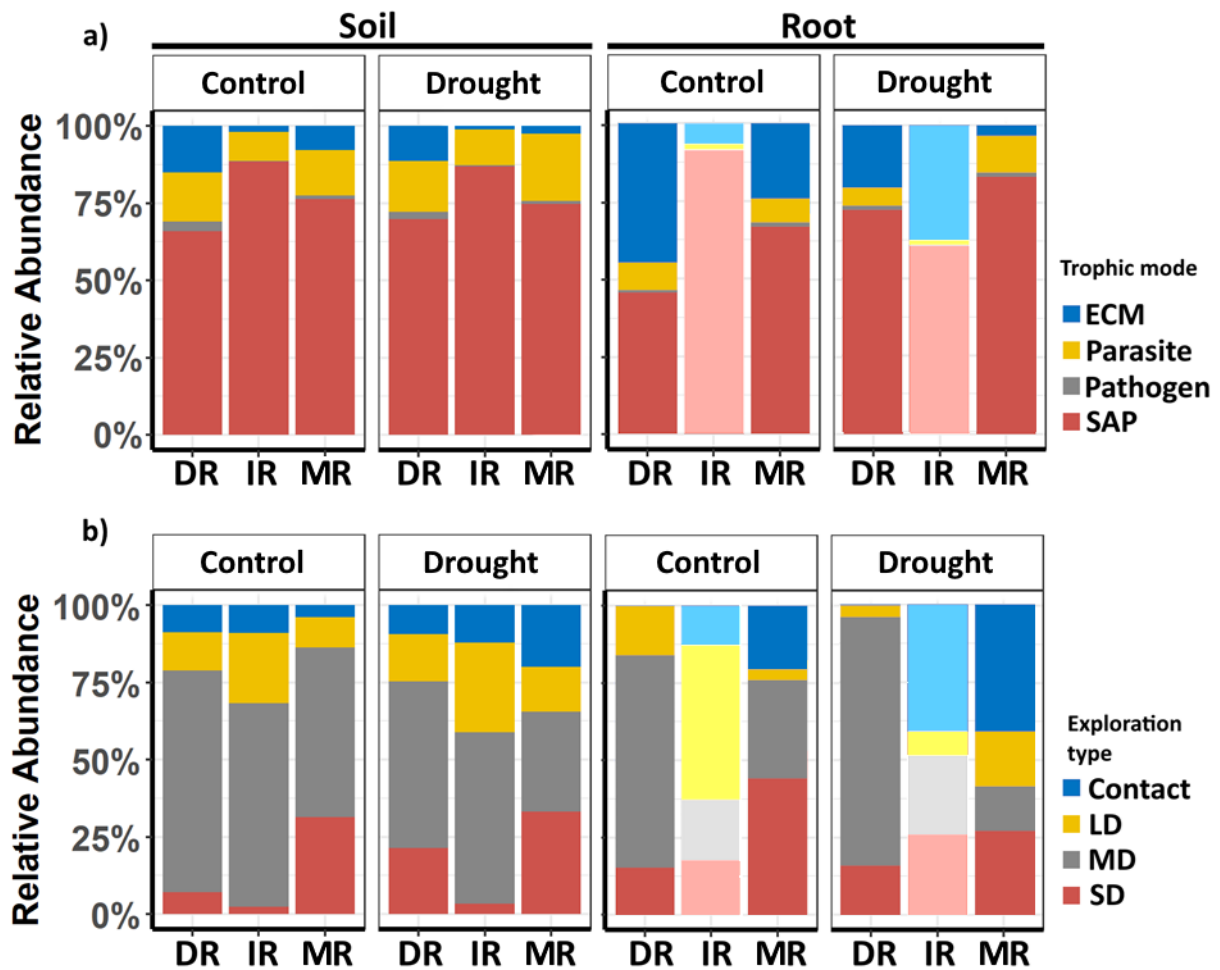


*Figure A6: Summed up relative abundances of rDNA-based soil (left panels) and root-associated fungal communities (right panels) according to a) trophic mode (blue: ectomycorrhizal fungi (ECM), yellow: parasites, grey: pathogens, red: saprotrophs (SAP)) and b) ECM fungal exploration type (blue: contact types, yellow: long-distance types (LD), grey: medium-distance types (MD), red: short-distance types (SD)) grouped by soil types (DR = dry region soil, IR = intermediate region soil, MR = moist region soil) and treatment. Due to reduced replicates in IR, these results are displayed in a lighter colour.*

Manuscript I: Acclimation in root architecture rather than long-term adaptation of fungal symbiosis mitigates drought effect on European beech seedlings

Jasmin Danzberger\*, Kyohsuke Hikino\*, Simon M. Landhusser, Benjamin D. Hesse, Sophie Meyer, Franz Buegger, Fabian Weikl, Thorsten E.E. Grams, Karin Pritsch

\*These authors have contributed equally to this work and share the first authorship

1 Acclimation in root architecture rather than long-term adaptation of  
2 fungal symbiosis mitigates drought effect on European beech seedlings  
3

4 **Author's names**

5 Jasmin Danzberger<sup>1,2,3\*</sup>, Kyohsuke Hikino<sup>1,3\*</sup>, Simon M. Landhäusser<sup>4</sup>, Benjamin D. Hesse<sup>1,5</sup>, Sophie Meyer<sup>1</sup>,  
6 Franz Buegger<sup>2</sup>, Fabian Weigl<sup>1</sup>, Thorsten E.E. Grams<sup>1</sup>, Karin Pritsch<sup>2</sup>

7 \*These authors have contributed equally to this work and share the first authorship

8 **Corresponding authors:**

9 Jasmin Danzberger; jasmin.danzberger@slu.se

10 Kyohsuke Hikino; kyohsuke.hikino@slu.se

11 **Author's affiliation**

12 <sup>1</sup> Technical University of Munich, TUM School of Life Sciences, Professorship for Land Surface-Atmosphere  
13 Interactions, Ecophysiology of Plants, 85354 Freising, Germany

14 <sup>2</sup> Helmholtz Zentrum München - German Research Center for Environmental Health (GmbH), Research  
15 Unit Environmental Simulation, 85764 Neuherberg, Germany

16 <sup>3</sup> Swedish University of Agricultural Sciences (SLU), Department of Forest Ecology and Management,  
17 Umeå, Sweden

18 <sup>4</sup> University of Alberta, Department of Renewable Resources, Edmonton, AB, T6G 2E3, Canada

19 <sup>5</sup> University of Natural Resources and Life Sciences, Department of Integrative Biology and Biodiversity  
20 Research, Institute of Botany, Gregor-Mendel-Straße 33, 1180 Vienna, Austria.

21 **ORCID**

22 Jasmin Danzberger - <https://orcid.org/0000-0002-1683-7345>

23 Kyohsuke Hikino - <https://orcid.org/0000-0002-6981-3988>

24 Simon M. Landhäusser - <https://orcid.org/0000-0002-4466-1607>

- 25 Benjamin D. Hesse - <https://orcid.org/0000-0003-1113-9801>
- 26 Franz Buegger - <https://orcid.org/0000-0003-3526-4711>
- 27 Fabian Weikl - <https://orcid.org/0000-0003-3973-6341>
- 28 Thorsten E. E. Grams - <https://orcid.org/0000-0002-4355-8827>
- 29 Karin Pritsch - <https://orcid.org/0000-0001-6384-2473>

## 30 Abstract

31 The composition of fungal communities in soils is known to impact tree performance. However, fungal  
32 communities differ among regions with different precipitation histories and may change during drought.

33 To determine the influence of soil origin and associated climate adaptation of fungal communities on plant  
34 drought responses, beech (*Fagus sylvatica* (L.)) seedlings were established from seed and grown in three  
35 different soils with similar water retention property taken from a natural precipitation gradient. One year  
36 after the establishment, the seedlings were exposed to a two-month drought from late May to mid-August  
37 with predawn water potentials of about  $-1.5$  MPa. At the end of the drought period, a whole-plant  $^{13}\text{C}$   
38 labelling was performed. Before and after the drought period, soil and root fungal community  
39 composition, root architecture, seedling biomass and growth, carbon relations and leaf physiology were  
40 determined.

41 The impact of drought on the composition of the fungal communities was the lowest in soils from dry  
42 regions, which suggests a natural adaptation of the fungal communities to a dry environment.  
43 Nevertheless, in contrast to our expectations, the seedlings grown in soil originating from dry regions were  
44 most affected by drought. This was demonstrated by a lower predawn water potential, probably due to  
45 shorter root systems with higher root branching compared to those grown in moist region soils where a  
46 greater taproot length was observed.

47 Thus, we conclude that the drought response of beech seedlings depends on different rooting patterns  
48 when growing in soils of different origins, rather than soil adapted fungal communities.

49 **Key words:** *Fagus sylvatica*, fungal communities, precipitation gradient, root system, carbon relations

## 50 Introduction

51 In European temperate forests, European beech (*Fagus sylvatica* (L.)) is a predominant tree species with  
52 a known drought sensitivity in both, the seedling (Lendzion and Leuschner 2008; Gebauer et al. 2020; Beloiu et  
53 al. 2022) and the mature tree stage (Arend et al. 2022; Frei et al. 2022; Schmied et al. 2023), which raises  
54 concerns about the species' future role in forests (Rennenberg et al. 2004; Geßler et al. 2007; Leuschner 2020).

55 Change in stomatal aperture (closure) is generally seen as a first quick physiological response to drought  
56 (Choat et al. 2018), however, beech is considered a more anisohydric species that will maintain its  
57 photosynthetic activity under increasing drought, which makes it more prone to water loss (Leuschner  
58 2020). Other slower responses relate to shifts in carbon (C) allocation to increased belowground structural  
59 growth (Meier and Leuschner 2008; Hommel et al. 2016) and increase in non-structural carbon (NSC)  
60 concentrations (Blessing et al. 2015; Chuste et al. 2020), leading to osmotic adjustments at the cellular and  
61 organ level (Tomasella et al. 2018; Leuschner et al. 2019). This preferential allocation belowground can  
62 generally lead to an increase in root to shoot ratios (as observed at global scale, (Poorter et al. 2012; Tumber-  
63 Dávila et al. 2022)). While root morphological characteristics such as architecture and rooting depth play  
64 significant roles for water uptake and can potentially mitigate drought effects (Brunner et al. 2015;  
65 Brinkmann et al. 2019; Clément et al. 2019; Germon et al. 2020; Kahmen et al. 2022), increased solute  
66 concentrations, such as soluble sugars, in the root system can keep the water potential of roots lower  
67 than that of soil and therefore maintain root water uptake under drought (Meier et al. 1992; Aaltonen et  
68 al. 2017; Nikolova et al. 2020).

69 Previous studies have also investigated the variation in drought responses and the potential adaptation  
70 of beech selected from different provenances (Leuschner 2020; Petrik et al. 2022), or along climatic  
71 gradients in mature forests (Nahm et al. 2007; Meier and Leuschner 2008). Typically, although not always,  
72 provenances of beech from dry regions appeared to be more adapted to dry conditions, e.g. less mortality  
73 and less growth reduction under drought, compared to those from moister regions (Leuschner 2020 and  
74 references therein). All these studies, however, focused only on the plant response and did not explore  
75 possible linkages with edaphic conditions of the soils from these locations. Soil properties such as soil type  
76 (Contran et al. 2013; Thiel et al. 2014; Buhk et al. 2016; Liu et al. 2017) and microbial communities (Fitzpatrick et  
77 al. 2018; Meisner et al. 2018) can have tremendous direct and indirect impacts on plants and their responses.  
78 For example, it has been shown that seedlings inoculated with microbial communities originating from  
79 arid regions had higher drought tolerance (Allsup et al. 2023). Ectomycorrhizal (ECM) fungi are known to  
80 improve the plant hydraulic function as well as increase the C storage (Wang et al. 2021) and transfer water

81 between trees (Egerton-Warburton et al. 2007). However, little is known about the linkage between naturally  
82 drought adapted soil microbiomes and the drought resistance of plants (Körner 2011).

83 Recent studies highlight the importance of soil and root-associated fungi for plant performance (Gundale  
84 et al. 2014; Anthony et al. 2022) particularly under stress conditions (Lehto and Zwiazek 2011; Kivlin et al. 2013;  
85 Lata et al. 2018; Porter et al. 2020; Allsup et al. 2023). Fungal species can be assigned to different trophic  
86 modes: saprotrophic, symbiotrophic, and pathotrophic (*sensu* Nguyen et al. 2016a), or as fungi with  
87 unknown ecological role (Tedersoo and Smith 2013; Nguyen et al. 2016a; Unuk et al. 2019) as well as animal- or  
88 mycoparasites (Nguyen et al. 2016a; Pöhlme et al. 2020). Saprotrophic fungi are often referred to as “free-  
89 living fungi” (e.g. Castaño et al. 2018) because, unlike ECM fungi, they do not form symbiotic relationships  
90 with host plants and obtain their nutrients by decomposing organic material in the soil (e.g. Nguyen et al.  
91 2016b). Hence, they are suspected to be more sensitive to environmental changes such as drought (Castaño  
92 et al. 2018). However, some saprotrophic fungal species can additionally establish interactions with plants,  
93 for example by living as root endophytes (Pöhlme et al. 2020) or by forming hyphal mantle and Hartig net-  
94 like structures on the roots similar to ECM fungi (Smith et al. 2017) and thus compete for niches with ECM  
95 fungi. Ectomycorrhizal fungi can grow extraradical hyphae from the hyphal mantle, which are classified  
96 by their extension into the surrounding soil as contact, short-distance, medium-distance, and long-  
97 distance exploration types (Agerer 2001; Weigt et al. 2012). Under drought, several studies showed that the  
98 abundance of ECM fungi decreased (Lozano et al. 2021; Castaño et al. 2023) and their composition changed  
99 (Shi et al. 2002; Swaty et al. 2004; Richard et al. 2011; Nickel et al. 2018). Thus, abundances of short- and  
100 medium-distance explorers decreased, while the number of long-distance explorers increased (Nickel et  
101 al. 2018), which enlarge the water absorbing area and explore the soil for water with their rhizomorphs  
102 (Mohan et al. 2014; Brunner et al. 2015; Nickel et al. 2018; Castaño et al. 2023). Precipitation history has been  
103 shown to alter the fungal community structure leading to more drought-resistant fungal species in dry  
104 regions that were not present in more humid regions (Cavender-Bares et al. 2009). However, it is still poorly  
105 understood how drought events affect fungal communities in soils with different precipitation histories  
106 and how those subsequently impact specific plant drought responses.

107 Therefore, the present study focused on soils with different precipitation histories and their effect on (i)  
108 root-associated fungal communities and (ii) drought responses of beech seedlings. We hypothesized that  
109 a fungal community associated with soils from dry regions is better adapted to drought and thus less  
110 affected (fungal community shows less change) to a subsequent drought event compared to that from  
111 moist regions. Further, we hypothesized that seedlings that were established and grown in a soil from a



112 dry region show better acclimation to drought at the fine root level than those grown in a moist region  
113 soil, i.e., longer taproot length and/or higher root to shoot ratio, and that this acclimation of the root  
114 system and the adaptation of the associated fungi collectively mitigate drought effects on beech.

## 115 Methods

### 116 Experimental setup

117 Soils from three regions in Bavaria, Germany, were collected in mixed beech (*Fagus sylvatica* L.) - spruce  
118 (*Picea abies* (L.) KARST.) stands along a natural precipitation gradient ranging from a dry region (DR) in the  
119 north (Gramschatz Forest close to Arnstein: 49.903° (N), 9.977° (E); 330 m.a.s.l.) with average rainfall of  
120 310 mm (1971 – 2000) during the growing season between May and October, over an intermediate region  
121 (IR) (Kranzberg Forest close to Freising: 48.419° (N), 11.661° (E); 490 m.a.s.l.) with average rainfall of 480  
122 mm, to a moist region (MR) in the south (Großhaager Forest close to Wasserburg: 48.142° (N), 12.073°  
123 (E); 620 m.a.s.l.) with average rainfall of 640 mm during the growing season (Pretzsch et al. 2014). All  
124 locations have a long-term average temperature of 13.8 – 14.0 °C during the growing season (1971 – 2000)  
125 (Pretzsch et al. 2014). Soil characteristics of the different regions are listed in Table S1 in supplements. At  
126 each site, 20 cm of the top layer excluding litter were taken, sieved to 1 cm and mixed with 30 vol%  
127 quartzite sand to equalize soil water retention properties. To ensure that the soil-sand-mixture (from here  
128 onwards termed “soil”) included enough nutrients for the seedlings throughout the experiment phase,  
129 soil nutrient content was analyzed (Table S2). The nitrogen concentration of all soils (0.1 – 0.2 %) showed  
130 no deficiency (> 0.08 %). Soil organic matter before the drought treatment (Table S2) was determined by  
131 weighing 5 g of soil of each region (n = 3) first after drying at 70 °C for 72 hours and then again after 3  
132 hours at 500 °C.

133 In spring 2019, beech (*Fagus sylvatica* L.) was seeded (4 seeds, seed source HkG 81024 Alpenvorland, a  
134 moist region) in 20-40 pots per soil region (17×17×20 cm (depth), in total 90 pots) and grown for one year  
135 under well-watered conditions in an unheated greenhouse. For that, all pots were regularly watered to  
136 field capacity (equivalent to c. 21.5 % volumetric soil water content (SWC)). In the spring 2020, 20 pots  
137 from each region were selected and 10 pots with 4 seedlings each were assigned to either a control or a  
138 drought treatment (n = 10) according to similar seedling sizes. Within each region, control and drought  
139 treatment pots had similar root collar diameter and height, thus similar initial seedling biomass (Fig. 3a  
140 for initial biomass). Two months before applying the drought treatment (spring 2020), all pots were  
141 transferred to another greenhouse with UV transparent glass and temperature-controlled conditions to

142 keep the experiment conditions as natural as possible. Greenhouse temperature was synchronized with  
143 outside temperature conditions during the experiment and climatic variables were measured  
144 automatically four times per hour, including air humidity and photosynthetic photon flux density (PPFD).  
145 The mean temperature during the study period (May, 22<sup>nd</sup> 2020 – August, 31<sup>st</sup> 2020) was  $20 \pm 6$  °C, vapour  
146 pressure deficit was  $0.82 \pm 0.8$  kPa and mean PPFD during the daytime (6 am – 8 pm) was  $208 \mu\text{mol m}^{-2} \text{s}^{-1}$   
147 (Fig. S1). The maximum PPFD was reached between 10-11 am with up to  $1500 \mu\text{mol m}^{-2} \text{s}^{-1}$ . The pots  
148 were randomly arranged and re-arranged every two weeks to minimize potential spatial differences in air  
149 circulation, light, temperature and neighbouring effects in the greenhouse. No fertilizer or plant  
150 protection agents were used during the experiment.

### 151 Pre-drought experiments

152 Relationship between soil water potential and SWC was established for each region soil (Fig. S2) using a  
153 pressure plate method (Richards 1941; Wang et al. 2015), whereby the curves did not significantly differ  
154 among region soils (tested after logarithmic transformation of soil water potential). The average field  
155 capacity determined was 21.6 %, 21.8 %, and 21.1 % SWC, for DR, IR, and MR soil, respectively.

156 In addition, the relationship between predawn plant water potential ( $\Psi_{\text{PD}}$ ) and SWC was measured with  
157 extra pots that were not selected for the drought treatment, using a Scholander pressure chamber (mod.  
158 1505D, PMS Instrument Co., Albany, OR, USA) and Time Domain Reflectometry (TDR100, Campbell  
159 Scientific, Logan, CT, USA, measured at the center of the pot using 10 cm probes), respectively. According  
160 to the relationship between  $\Psi_{\text{PD}}$  and the SWC (Fig. S2), the target SWC of each pot was defined as 20 %  
161 (close to the field capacity) for control and 12 % (expecting predawn plant water potentials of  $-1$  to  $-1.5$   
162 MPa) for drought treatment for all three region soils. Prior to the drought treatment, the initial weight of  
163 each pot at the SWC of 20 % ( $-0.006$  MPa, based on the relationship between soil water potential and  
164 SWC) was noted and SWC was maintained in all pots by watering them every other day to their respective  
165 initial weight.

### 166 Drought treatment

167 At the end of May, after the beech had flushed and the shoots had expanded, the drought treatment was  
168 superimposed on the drought group. The drought treatment lasted for eight weeks. To make the intensive  
169 harvest work at the end of the study manageable, pots were randomly assigned to one of three groups  
170 staggered with different drought starting times one week apart (drought start on May 25<sup>th</sup>, June 1<sup>st</sup>, and  
171 June 8<sup>th</sup>, 2020, respectively). All treatment combinations were equally distributed in each time group and

172 the phenological stages of the seedlings were not different among the different starting times. While the  
173 control pots were watered every other day to maintain a SWC of 20 %, the pots assigned to the drought  
174 treatment were watered on the same day but with only half the amount of water to gradually dry the soil  
175 to 12 % SWC (3-4 weeks), at which the SWC was then maintained until the harvest (Fig. 1a). Only for  
176 drought pots SWC was measured with TDR sensors before every watering, and the pot weight was  
177 recorded (Galvez et al. 2011). On hot days SWC was measured daily and seedlings were additionally watered  
178 off schedule with about half the amount of water loss to avoid a lethal drought.

### 179 Leaf gas exchange

180 CO<sub>2</sub> assimilation rates (A) at a CO<sub>2</sub> concentration of 400 ppm and leaf stomatal conductance to water  
181 vapour (g<sub>s</sub>) were measured before applying the drought and during the 4<sup>th</sup> and 7<sup>th</sup> week of the drought  
182 treatment, using an open gas exchange system LI-6800 (Li-Cor Inc., Lincoln, NE, USA). One fully expanded  
183 leaf was randomly selected for each plant and the same leaf was measured consistently, excluding newly  
184 produced leaves during the drought treatment. During the measurement, the PPFD was set to 500 μmol  
185 m<sup>-2</sup> s<sup>-1</sup>, the leaf temperature to 25 °C, and the relative humidity to around 60 %.

### 186 <sup>13</sup>C labelling

187 In the last (8<sup>th</sup>) week of the drought treatment, three days before harvest, all pots were labelled with <sup>13</sup>C-  
188 CO<sub>2</sub> for three consecutive days. Leaf samples for the pre-labelling background were collected from  
189 randomly chosen three pots per treatment (n = 3) before the labelling (Table S3). Pots were then located  
190 in a transparent tent with a volume of c. 1300 L. The target C isotope composition in the tent during the  
191 labelling was set to 20 atom% <sup>13</sup>C to make sure that the expected natural difference in the isotopic  
192 signature among organs (leaf, stem, coarse root, and fine root) (~ 1 ‰, Ruehr et al. 2009) would be  
193 negligible (< 1 % of the isotopic signature in the samples after labelling), since pre-labelling sampling was  
194 only possible for leaves to avoid destructive samplings. The labelling started at 4 am and ended at 8 pm  
195 each day. LED lights were used from 6 am to 4 pm to ensure photosynthetic activity (c. 350 μmol m<sup>-2</sup> s<sup>-1</sup>  
196 PPFD). Four electronic fans were used for homogeneous distribution of labelled air in the tent. The  
197 atmospheric CO<sub>2</sub> concentration and δ<sup>13</sup>C in the tent were continuously monitored during the labelling  
198 using cavity ring-down spectroscopy (CRDS, ESP-1000; PICARRO, see Table S4). Direct diffusion of <sup>13</sup>CO<sub>2</sub>  
199 into the soil likely happened but was not relevant for the study since only plant bulk tissues were  
200 considered. Temperature, Vapour Pressure Deficit, and PPFD were also monitored throughout the  
201 labelling days (Table S4).

## 202 Soil and seedling sampling

203 Soil samples were taken before (initial) and after the drought treatment using a soil corer (diameter: 5  
204 mm, length: 20 cm). At each measurement time, three soil cores were randomly taken per pot, combined  
205 and instantly frozen at -80 °C.

206 At the end of the study,  $\Psi_{PD}$  was measured before sunrise (2 am – 5 am CET). Immediately after, SWC of  
207 each pot was recorded with TDR sensors, and the seedlings were separated into leaves, stem, coarse roots  
208 (> 2mm), and fine roots (< 2mm) and their fresh weights were recorded. Prior to drying, the leaf samples  
209 were scanned (Epson Perfection 4990 Photo, Epson Deutschland GmbH, Meerbusch, Germany) to  
210 determine the leaf area and calculate the specific leaf are (SLA) based on the leaf dry weight. The degree  
211 of mycorrhization was determined from the fine root samples by root tip counting and expressing the  
212 number of mycorrhized tips as a ratio of the total vital tips (Danzberger et al. 2023). Each root system was  
213 photographed on graph paper. Two thirds of the fine roots were directly frozen at -80 °C for DNA  
214 extraction (see below). The remaining fine root samples and the other leaf, stem, and coarse root samples  
215 were oven dried at 64 °C for 72 h to determine their dry weight, and ground for later analyses using a ball  
216 mill (MM400, Retsch, Haan, Germany). The dry weight of the fine roots that were frozen for DNA  
217 extraction was calculated using their fresh weight and the ratio of the dry to fresh weight of the respective  
218 fine roots (determined from the remaining one third of the fine roots).

## 219 Growth and biomass

220 Basal stem diameter and height of each plant were determined before the onset of the drought treatment  
221 and at the end of the study directly before the harvest. Basal stem diameter was recorded twice  
222 perpendicular to each other, and the average was used. To ensure measurement consistency the stem  
223 was marked 1 cm above the soil.

224 Since initial destructive seedling samples could not be obtained before the onset of drought due to sample  
225 limitations, we estimated the initial biomass for each seedling using allometric functions based on the  
226 final harvest data of the control seedlings (nls function in R, package: stats, version: 3.6.1, Fig. 3a). First,  
227 an allometric function for estimating stem biomass was developed using stem diameter and height as  
228 input parameters individually for each soil. The calculated stem biomass corresponded well to the  
229 measured stem biomass according to linear regression ( $p < 0.001$ ,  $R^2 = 0.84$ ).

$$230 \quad \text{Stem biomass [mg]} = a * \text{height [cm]} * \text{diameter [mm]}^2 + b$$

231 Whereby  $a$  and  $b$  are the coefficient determined by the function. Using these coefficients together with  
232 stem diameter and height before the onset of the drought treatment, the initial stem biomass was  
233 calculated. Then, using final harvest data of the control seedlings, relationship between total root biomass  
234 (i.e. combined coarse and fine roots) and stem biomass was developed with a linear regression (lm  
235 function in R). The calculated root biomass agreed well with the measured root biomass according to  
236 linear regression ( $p < 0.001$ ,  $R^2 = 0.61$ ). It was not possible to determine the initial biomass of coarse and  
237 fine roots separately, because no or only weak relationships existed between both root types and stem  
238 biomass. Finally, initial total root biomass before the onset of the drought was calculated from the initial  
239 stem biomass using the relationship.

240 Relative stem growth during the drought treatment of 8 weeks were calculated for each seedling by  
241 subtracting the estimated initial biomass from the measured final biomass at the harvest.

$$242 \text{ Relative stem biomass growth [\%]} = \frac{\text{Stem biomass at harvest [mg]} - \text{initial stem biomass [mg]}}{\text{initial stem biomass [mg]}} * 100$$

#### 243 Taproot length and branching intensity

244 The taproot length expresses the length from the stem base to the root tip at the end of the taproot.  
245 Therefore, the root systems from images taken at the harvest were measured using the program ImageJ  
246 (version 1.53a, National Institute of Health, USA). In parallel, the number of all branches (McCormack et al.  
247 2015) was counted and divided by the total length of the respective fourth-order root to gain a  
248 comparative parameter (“branching intensity”).

#### 249 Analysis of stable C isotopic composition ( $\delta^{13}\text{C}$ ) and allocation of newly assimilated C

250 Stable C isotopic composition ( $\delta^{13}\text{C}$ ) of leaf, stem, coarse root, and fine root samples were determined  
251 with an isotope ratio mass spectrometer (IRMS, delta V Advantage; Thermo Fisher Scientific) coupled to  
252 an Elemental Analyzer (Euro EA; Eurovector).

253  $^{13}\text{C}$  derived from the newly assimilated C ( $^{13}\text{C}_{\text{excess}}$  in  $\mu\text{g}$ ) was calculated for each plant organ using  $\delta^{13}\text{C}$   
254 converted to atom%, C content, and biomass at the harvest (Ruehr et al. 2009).

$$255 \quad {}^{13}\text{C}_{\text{excess}} = 1000 \cdot \frac{\text{atom}\%_s - \text{atom}\%_{\text{pre}}}{100} \cdot B \cdot \frac{\text{C}\%}{100}$$

256 Whereby  $\text{atom}\%_s$  and  $\text{atom}\%_{\text{pre}}$  are atom% of the samples at the harvest and before the labeling,  
257 respectively.  $B$  gives the biomass at the harvest (mg), and  $\text{C}\%$  the percentage of carbon in the sample.

258 Finally,  $^{13}\text{C}_{\text{excess}}$  in each organ was summed up for each plant and expressed as a relative allocation among  
259 the organs.

#### 260 Non-structural carbohydrates (NSC)

261 Total soluble sugars were extracted from ground leaf, stem, coarse root, and fine root samples in 80 %  
262 hot ethanol, followed by a phenol-sulfuric assay to determine their concentration colorimetrically  
263 (Landhäusser et al. 2018). Six seedlings from 6 different pots were randomly chosen for each treatment  
264 ( $n = 6$ ). Starch concentration was determined after an  $\alpha$ -amylase and amyloglucosidase digestion followed  
265 by a peroxide-glucose oxidase/o-dianisidine reaction and concentrations were expressed as percent of  
266 sample dry weight. Using the concentration data and the biomass of leaves, stems, coarse and fine roots  
267 at harvest, sugar and starch content for each sample tissue were calculated. Finally, after combining the  
268 content of sugar and starch for coarse and fine roots, it was expressed as a ratio of the sugar and starch  
269 content in roots (belowground) to the total content (leaf, stem, coarse, and fine roots all combined) for  
270 each seedling.

#### 271 DNA extraction, library preparation, sequencing and bioinformatics

272 Frozen fine root systems ( $n = 10$  per soil and treatment) were ground in liquid nitrogen. DNA of 250 mg  
273 root powder per sample as well as 250 mg soil ( $n = 6$  per soil, treatment and sampling time) were extracted  
274 according to the DNeasy PowerSoil Pro Kit (Qiagen, Hilden, Germany) protocol and diluted to 5 ng /  $\mu\text{L}$ .  
275 For high-throughput sequencing, a polymerase chain reaction (PCR) was performed in triplicates with  
276 primer mixtures for the ITS2 rDNA as described by Tedersoo et al. (2015), containing Illumina dual adapter  
277 sequences for Miseq sequencing (protocol Part # 15044223; Illumina, San Diego, CA, USA, Table S5).  
278 Library preparation was performed as described in Danzberger et al. (2023) and Method S1 in  
279 supplements.

280 The sequence data from the sequencing was provided in FASTQ format and prepared for further analysis  
281 using the fungal analysis pipeline PIPITS v2.7 (Gweon et al. 2015). In a first step, read pairs were joined and  
282 the sequences were filtered for quality based on the pipeline's default settings. Afterwards, the fungal  
283 ITS2 sequences were extracted using ITSx (Bengtsson-Palme et al. 2013) and sequences below 100 bp  
284 excluded. The remaining sequences were assigned to OTUs based on 97 % sequence identity using  
285 VSEARCH (Rognes et al. 2016) and chimeras removed using the UNITE CHIME reference dataset (Nilsson et  
286 al. 2015). Taxonomic classification relied on RDP Classifier (Wang et al. 2007) comparing sequences with  
287 those in the UNITE database (Kõljalg et al. 2013). Further fungal traits such as "fungal trophic mode",

288 “ectomycorrhizal exploration types” (Agerer 2001), and saprotrophic “primary” and “secondary” lifestyle  
289 were assigned by matching the genus level of the taxonomic output with the FungalTraits database (Pöhlme  
290 et al. 2020).

## 291 Statistical analysis

292 For statistics and graphic illustration, the software R (version 4.0.2, RCore Team, 2021) and RStudio  
293 (version 1.4.1717, RStudio Inc.) were used. Sequencing data were randomly rarefied (average of 1.000  
294 repetitions) using “Rarefy” in *GUniFrac* (Chen et al. 2012) to a depth of 6.000 (soil samples) and 5.000  
295 (root samples) sequences per sample. Taxa that occurred less than 10 times were removed. Bray-Curtis  
296 dissimilarities between samples were calculated using “vegdist” in the R package *vegan* (Oksanen et al.  
297 2019). The function “diversity” in the same package was applied to determine the Shannon–Wiener  
298 Diversity Index (“Shannon Index”) and Simpson’s Index of Diversity (“Simpson Index”), and “specnumber”  
299 to determine species richness. Thereupon, evenness was calculated by Shannon Index/log(species count).

300 All the datasets were analysed using a linear mixed model using treatment (control and drought) and  
301 region soil (DR, IR, and MR) as fixed effects and start of the drought (separated into three groups) as a  
302 random effect (package: nlme, version: 3.1-151). For the data of biomass, growth, fine root architecture,  
303 and allocation of newly assimilated C, average values of each pot were calculated before applying linear-  
304 mixed model ( $n = 10$ ). Normality of the residuals (Shapiro test/ qq-plots) and homogeneity of variances  
305 (Levene test) were tested for every model. If any fixed factor was significant, post-hoc test with Tukey  
306 correction (package: emmeans, version: 2.30-0) was performed. Correlations of fine root parameters were  
307 determined with Pearson correlation (“cor.test” in stats). For sequence data, multivariate homogeneity  
308 of group dispersions was tested using the function “betadisper” in *vegan*. To test the effects of treatment  
309 and soil region, soil- and root-community data were analysed comparatively with a permutational  
310 multivariate analysis of variance (PERMANOVA) using “adonis” (package *vegan*), whereby all models were  
311 run with 9.999 permutations. If significant differences between the levels of a factor occurred, a multilevel  
312 pairwise comparisons of permutational multivariate analysis of variance (pairwise PERMANOVA;  
313 *pairwise.adonis*; (Martinez Arbizu 2020)) with Bonferroni p-value correction was applied. The functions  
314 “prune\_taxa” and “transform\_sample\_counts” from the package *phyloseq* (version 1.36.0; McMurdie &  
315 Holmes, 2013) were used to assess relative abundances of fungal trophic modes and exploration types.  
316 Data in text and tables are given as the mean  $\pm$  1SE, unless stated otherwise.

## 317 Results

### 318 Efficacy of the drought treatment

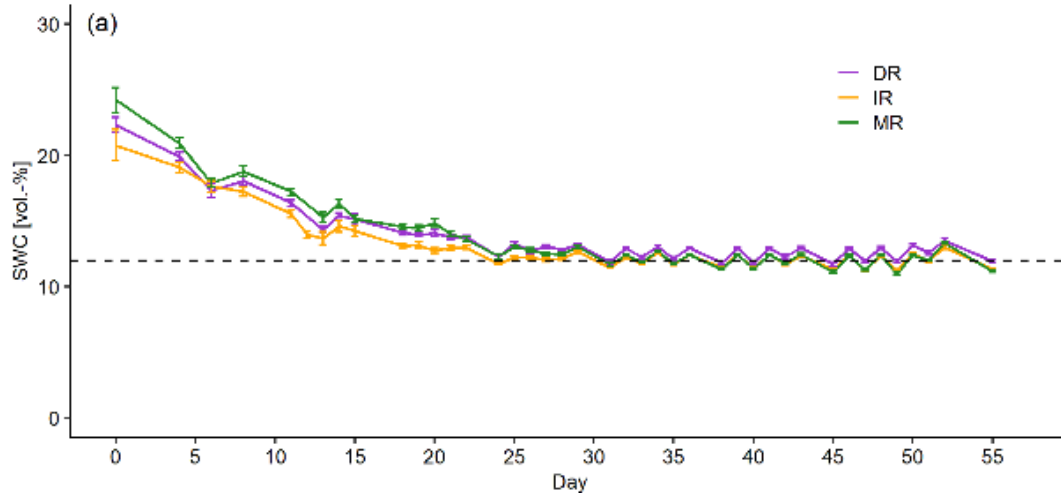
319 Soil moisture in the drought treatment was equally low for all region soils (Fig. 1a). Soil water content  
320 (SWC) of drought pots gradually decreased after the start of the drought treatment and reached the target  
321 SWC of 12 vol.-% after 3-4 weeks. The mean SWC at the end of the drought treatment was  $11.8 \pm 0.3$  vol.-  
322 % in DR,  $11.3 \pm 0.2$  in IR, and  $10.9 \pm 0.3$  in MR soil (Fig. 1b), which was significantly lower than that of  
323 controls with around 20 % (treatment  $p < 0.001$ , Table S6).

324 While SWC of drought pots was significantly lower than that of controls in all region soils,  $\Psi_{PD}$  of drought  
325 seedlings was only significantly lower in DR and IR soils (treatment x region soil  $p < 0.001$ , Fig. 1c). Despite  
326 the similar SWC and its relationship with soil water potential in of all three region soils, drought treated  
327 seedlings growing in MR soil showed similar  $\Psi_{PD}$  to the controls, and thus significantly higher  $\Psi_{PD}$  ( $-0.84 \pm$   
328  $0.10$  MPa) than drought seedlings growing in DR and IR soil (with c.  $-1.90$  MPa), while  $\Psi_{PD}$  of control  
329 seedlings were similar in all region soils ( $-0.56$  MPa on average).

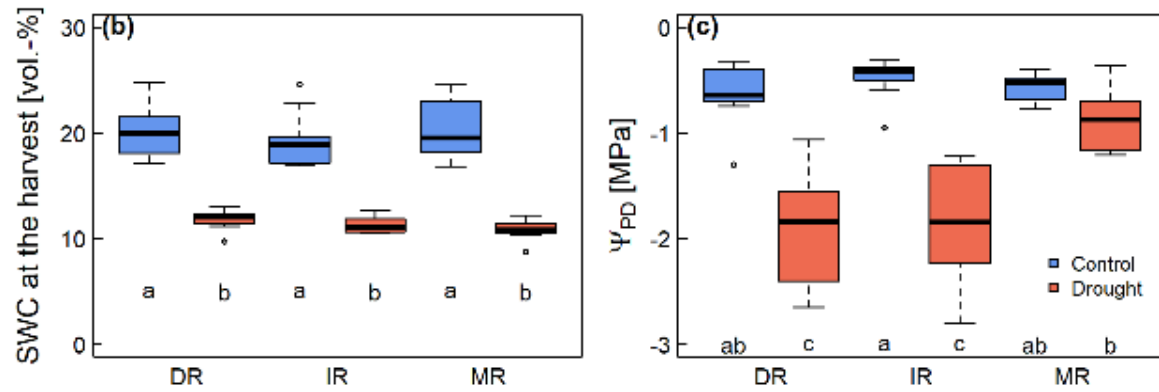
330 Net carbon assimilation rates and stomatal conductance showed similar patterns as  $\Psi_{PD}$  (Fig. 1d,e).  
331 Drought treatment significantly reduced both parameters, while the extent of the decrease was different  
332 among region soils (treatment x region soil  $p < 0.001$  Table S6). While assimilation rates and stomatal  
333 conductance of DR and IR seedlings were reduced by  $>75$  % under drought compared to controls, the  
334 decrease in MR seedlings were only 20 % for assimilation rates and 47 % for stomatal conductance.

335

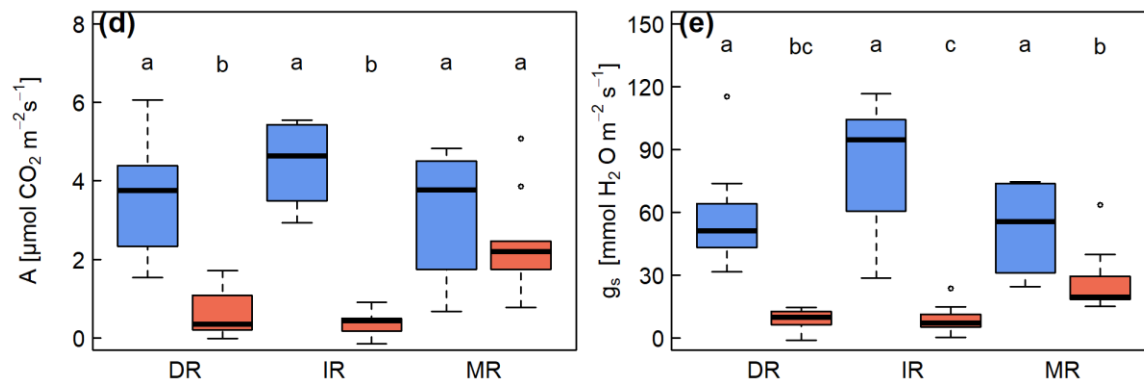




336



337



338

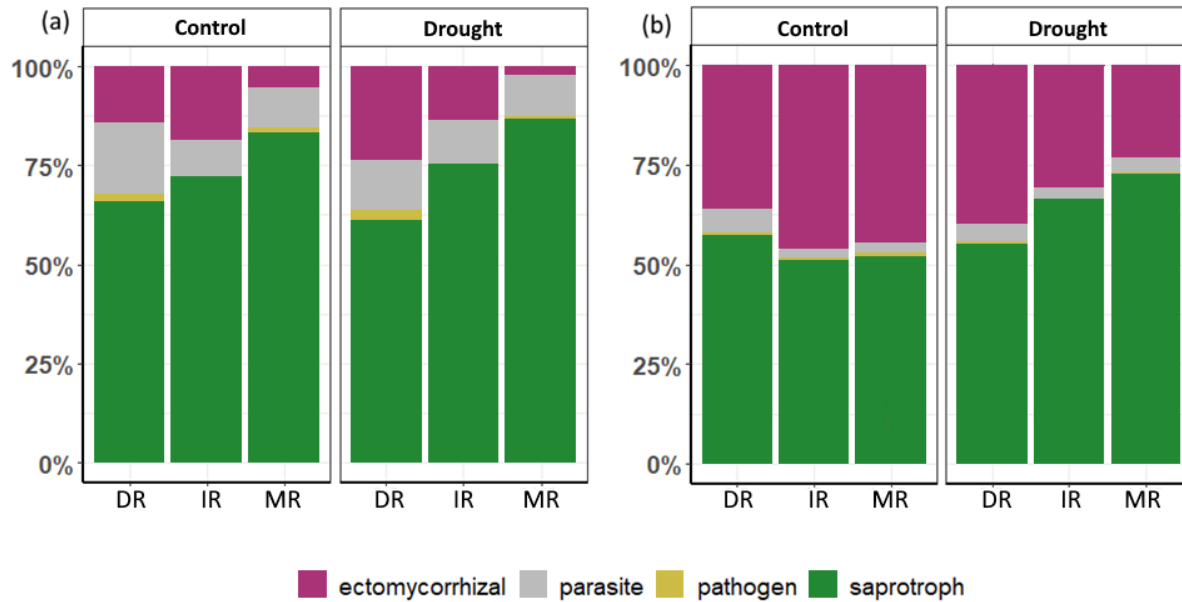
339 **Fig. 1 a)** Soil water content (SWC, in vol.%) of drought pots with dry region (DR, purple), intermediate region (IR, yellow) and moist  
 340 region (MR, green) soil during the drought treatment of 56 days (8 weeks). **b)** SWC of control (blue) and drought (red) pots at the  
 341 harvest. **c)** Predawn plant water potential ( $\Psi_{PD}$ ) at the day of harvest. **d)** Mean net carbon assimilation rates ( $A$ ) and **e)** stomatal  
 342 conductance ( $g_s$ ) during 4th and 7th week. Lowercase letters indicate significant differences among the groups according to post-  
 343 doc test.

#### 344 Fungal community composition

345 10 root samples and 13 soil samples have been excluded from further analyses due to a low sequencing  
346 depth. For further analysis, 2571 OTUs originating from root samples, and 2299 OTUs from soil samples  
347 were left. Because soil fungal community composition did not significantly change between pre-drought  
348 and post-drought controls during the two-month drought treatment ( $p = 0.34$ ,  $R^2 = 0.02$ , PERMANOVA),  
349 the pre-drought samples have been excluded and only the post-drought samples in both treatments have  
350 been compared.

351 The soil fungal community composition only differed significantly between the three different region soils  
352 ( $p < 0.001$ ,  $R^2 = 0.62$ , PERMANOVA) but was not significantly influenced by drought treatment within the  
353 different region soils. All alpha-diversity metrics were highest in DR soil (Table S7). Saprotrophic fungi  
354 were the most abundant group in all region soils (Fig. 2a) and their abundance increased from DR to IR to  
355 MR soil with no significant effect of drought treatment. The composition of the saprotrophic fungal  
356 community differed significantly between the different region soils ( $p < 0.001$ ,  $R^2 = 0.71$ , PERMANOVA).  
357 Similarly to saprotrophs, the ECM fungal community was significantly affected by the soil region ( $p < 0.001$ ,  
358  $R^2 = 0.34$ , PERMANOVA) but not by drought treatment. The proportion of ECM fungi within the soil fungal  
359 community was higher in DR and IR compared to MR soil (Fig. 2a).

360 In contrast to the soil fungal community composition, the root-associated fungal community composition  
361 was affected by both, region soil ( $p < 0.001$ ,  $R^2 = 0.50$ , PERMANOVA) and drought ( $p = 0.002$ ,  $R^2 = 0.06$ ,  
362 PERMANOVA). None of the diversity metrics of root-associated fungi were affected by drought treatment,  
363 but Shannon diversity, species richness and Evenness were significantly influenced by region soil (Table  
364 S7). PERMANOVA indicated that region soil and treatment significantly affected both, root-associated  
365 saprotrophic (region soil  $p = 0.0001$ ,  $R^2 = 0.48$ ; drought  $p = 0.0031$ ,  $R^2 = 0.05$ ) and ECM fungal communities  
366 (region soil  $p = 0.0001$ ,  $R^2 = 0.26$ ; drought  $p = 0.0031$ ,  $R^2 = 0.05$ ). In controls, saprotrophic and ECM fungi  
367 made up around 50 % each in IR and MR roots, while in DR roots the abundance of saprotrophs was  
368 slightly higher than of ECM fungi (Fig. 2b). The relative abundance of saprotrophs increased with drought  
369 treatment in IR and MR roots accompanying a decrease of ECM fungi. In DR roots, however, abundance  
370 changes were minimal. For both soil and root-associated fungal communities, “region soil” had a higher  
371 effect size compared to “drought treatment”.



372

373 **Fig. 2** Relative abundances of ectomycorrhizal (pink), parasite (grey), pathogenic (gold) and saprotrophic (green) fungi in soil (a)  
 374 and roots (b) in controls and during drought separated by different soils (dry region = DR, intermediate region = IR, moist region  
 375 = MR)

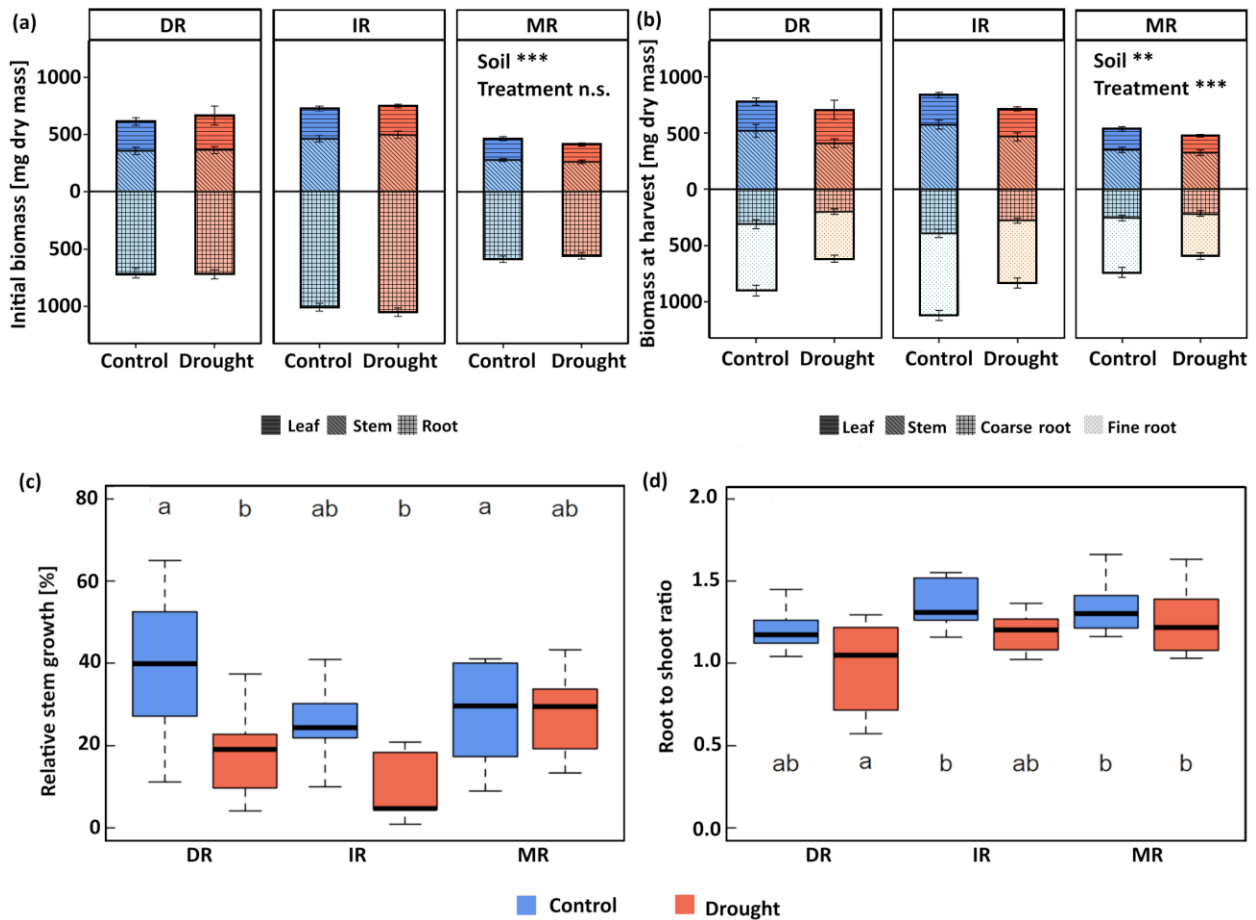
376 The most abundant soil saprotrophic species differed between the region soils but were not affected by  
 377 drought treatment in any region soil (Table S8). Among the ECM species (Table S9), it was noticeable that  
 378 in both, DR and IR, drought tolerant *Melanogaster* sp. was by far the most abundant species, which did  
 379 not change during drought. In MR, however, the abundance of fungal species changed with drought  
 380 treatment. While *Lactarius* sp., *Amanita* sp. and *Hebeloma radicosum* were predominant in controls,  
 381 *Amanita* sp. and *Hydnotrya tulasnei*, were the most common species in the drought treatment. *Lactarius*  
 382 sp., on the other hand, only accounted for 4% in the drought treatment compared to 24.2% in controls.

383 Among root-associated saprotrophs (Table S10), *Oidiodendron* sp., a species with primary saprotrophic  
 384 and secondary root-endophytic lifestyle, was highly abundant in each region soil in controls and under  
 385 drought. With drought, the abundance of *Penicillium* sp. increased in root samples from DR and IR, but  
 386 not in MR soils. Among ECM fungi (Table S11), *Melanogaster* sp. was by far the most abundant species in  
 387 DR and IR roots in both, controls and drought. In MR, however, the abundance of species changed  
 388 drastically with drought. While *Sebacina* sp. made up 96 % of all ECM species in MR controls, it decreased  
 389 to only 0.1 % under drought. The abundance of drought tolerating *Amanita* sp. in MR on the other hand  
 390 increased from 0.4 % in controls to 78 % under drought, and *Theleophora terrestris*, another drought  
 391 tolerating species, made up 15 % of all ECM species in MR during drought, while it was not detected in  
 392 controls.

393 ECM exploration types (Fig. S3) were dominated by long- and medium-distance types in DR and IR soils  
394 and roots in both controls and during drought, whereby a high share of long-distance explorers was  
395 covered by *Melanogaster* sp.. In MR soils and roots, however, short- and medium distance explorers were  
396 predominating in controls, while during drought, the strong increase of *Amanita* sp. and *Hydnotrya*  
397 *tulasnei* represented a dominance of contact types.

### 398 Biomass and growth of seedlings

399 Initial plant biomass (Fig. 3a) and biomass of control plants at the harvest (Fig. 3b) were the highest in IR  
400 soil and the lowest in the MR soil (region soil  $p < 0.001$ , Table S6). Drought treatment significantly reduced  
401 the relative stem growth (Fig. 3c, treatment  $p < 0.05$ , Table S6), which led to a significantly lower biomass  
402 of drought treated seedlings at the harvest compared to the controls (treatment  $p < 0.01$ , Fig. 3b, Table  
403 S6). Reduction of the relative stem growth under drought was higher in DR (from  $40 \pm 6\%$  in control to  $20$   
404  $\pm 4\%$  in drought seedlings,  $p = 0.07$  according to post-hoc test, Fig. 3c) and in IR seedlings (from  $25 \pm 3\%$   
405 in control to  $10 \pm 4\%$  in drought,  $p = 0.4$ ) compared to MR seedlings (from  $32 \pm 7\%$  in control to  $28 \pm 3\%$   
406 in drought,  $p > 0.9$ ). Root to shoot ratio (Fig. 3d) significantly decreased under drought (treatment  $p <$   
407  $0.01$ , Table S6), while the ratio was significantly higher in IR and MR seedlings compared to DR seedlings  
408 (region soil  $p < 0.01$ , Table S6). Specific leaf area (SLA) was not affected by drought treatment, although it  
409 was significantly higher in IR compared to DR and MR seedlings (region soil  $p < 0.05$ , Table S6, Fig. S4).



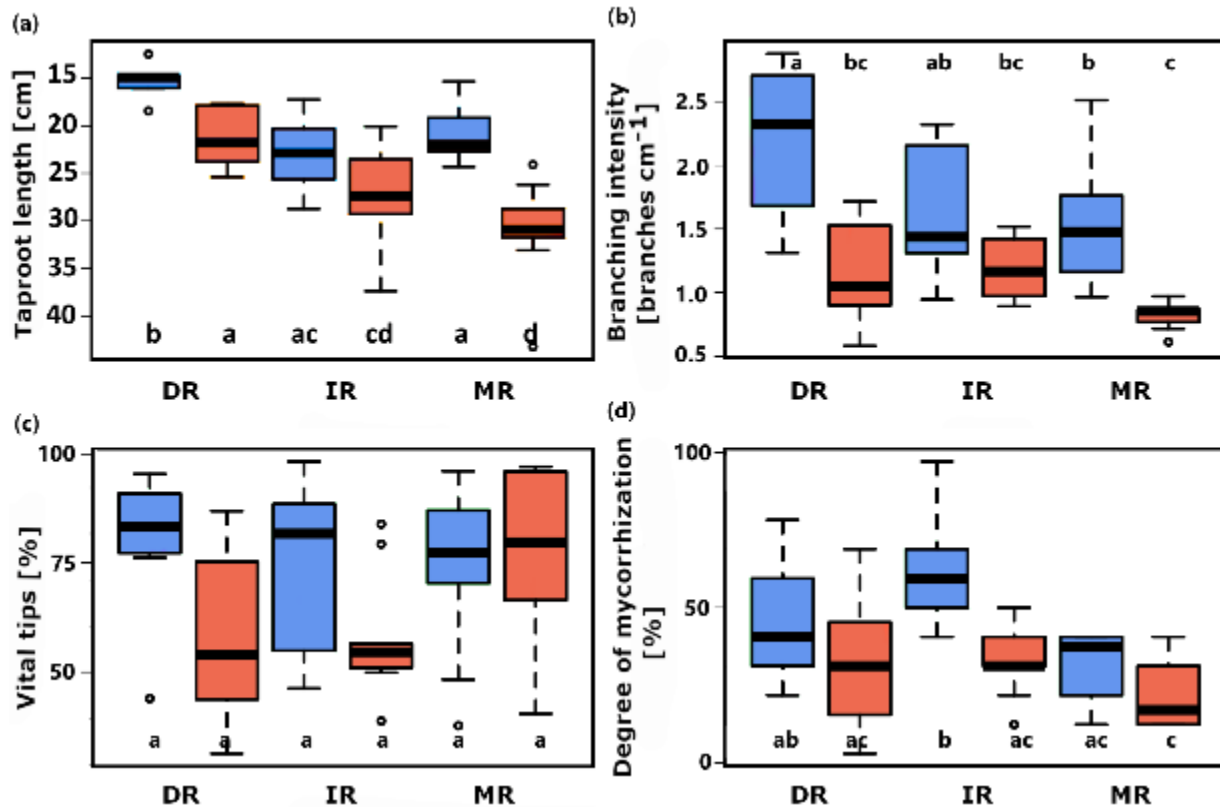
410

411 *Fig. 3 a) Initial biomass of leaf, stem, and root (coarse- and fine-root combined) before the onset of the drought treatment. All*  
 412 *pots were equally assigned to control (blue) and drought (red) treatments according to the diameter and height. b) Biomass at*  
 413 *the harvest separately in leaf, stem, coarse root, and fine root under control and drought treatment. c) Relative stem growth*  
 414 *during the drought treatment of 8 weeks. d) Ratio of root to shoot biomass at the harvest. Dry region (DR), intermediate region*  
 415 *(IR) and moist region (MR) soil. Asterisks indicate significant differences of total biomass among treatments and region soils. \*\*\*,*  
 416 *p<0.001, \*\*, p<0.01, n.s.; not significant. Lowercase letters indicate significant differences among the groups according to post-*  
 417 *hoc test*

## 418 Fine root architecture

419 The root architecture described by taproot length, branching intensity, vital tips and degree of  
 420 mycorrhization differed between the treatments and except vital tips between region soils (Table S6).  
 421 With drought, seedlings in DR and MR were rooting significantly longer (Fig. 4a) and had a lower branching  
 422 intensity (Fig. 4b). Furthermore, branching intensity was negatively correlated with taproot length ( $p <$   
 423  $0.001$ ,  $r = -0.5$ ) indicating that as taproot length increased, the number of branches per cm declined. The  
 424 number of vital tips tended to decrease in DR and IR, but not significantly (Fig. 4c). The degree of

425 mycorrhization, however, declined with drought in IR and MR soils whereby the decrease was not  
 426 significant in MR (Fig. 4d). Nevertheless, a decline of mycorrhization in MR soil was supported by a low  
 427 number of sequence reads in MR drought samples.



428

429 *Fig. 4 Fine root architecture including taproot length (a), branching intensity (b), percentage of vital root tips (c) and degree of*  
 430 *mycorrhization (d). Blue boxes represent controls and red boxes drought treatment. Dry region (DR), intermediate region (IR) and*  
 431 *moist region (MR) soil. Lowercase letters indicate significant differences among the groups according to post-hoc test.*

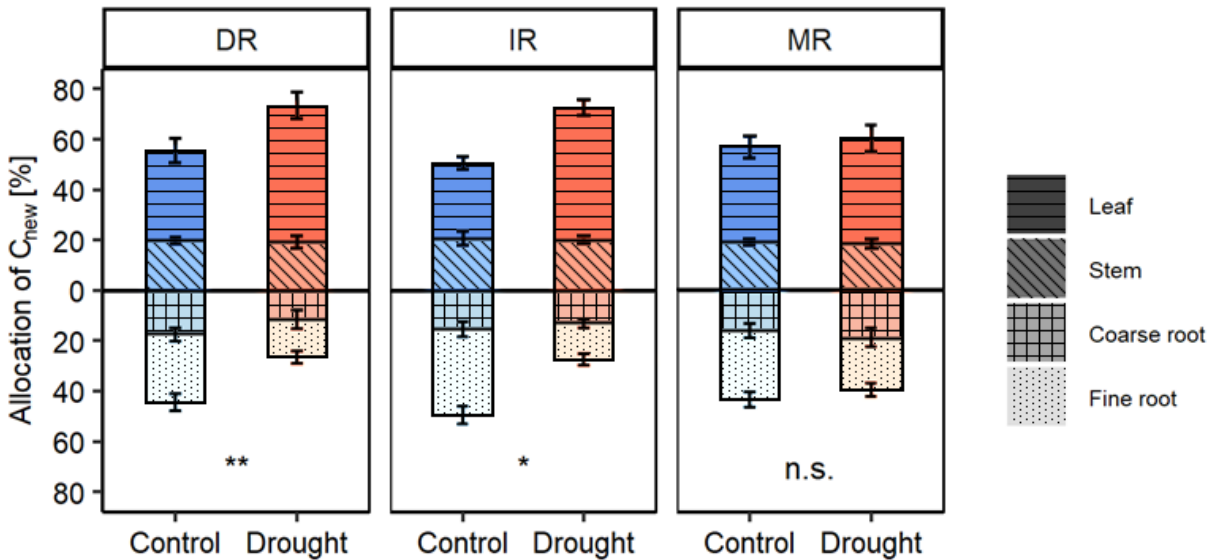
432

### 433 Allocation of newly assimilated C

434 Control seedlings allocated similar amounts of newly assimilated C to belowground organs in all region  
 435 soils ( $47 \pm 3\%$  of total newly assimilated C, Fig. 5), while drought effects were different among region soils  
 436 (treatment x region soil  $p < 0.05$ , Table S6). Drought significantly reduced the belowground allocation of  
 437 newly assimilated C in DR and IR seedlings. Here, more newly assimilated C remained in the leaves ( $54 \pm$   
 438  $5\%$  and  $53 \pm 3\%$  of total newly assimilated C) compared to control plants with  $36 \pm 5\%$  and  $30 \pm 2\%$  in

439 the leaves, respectively. In contrast, similar amounts of newly assimilated C were allocated belowground  
 440 in MR seedlings under both control and drought treatments ( $46 \pm 3\%$ ).

441



442

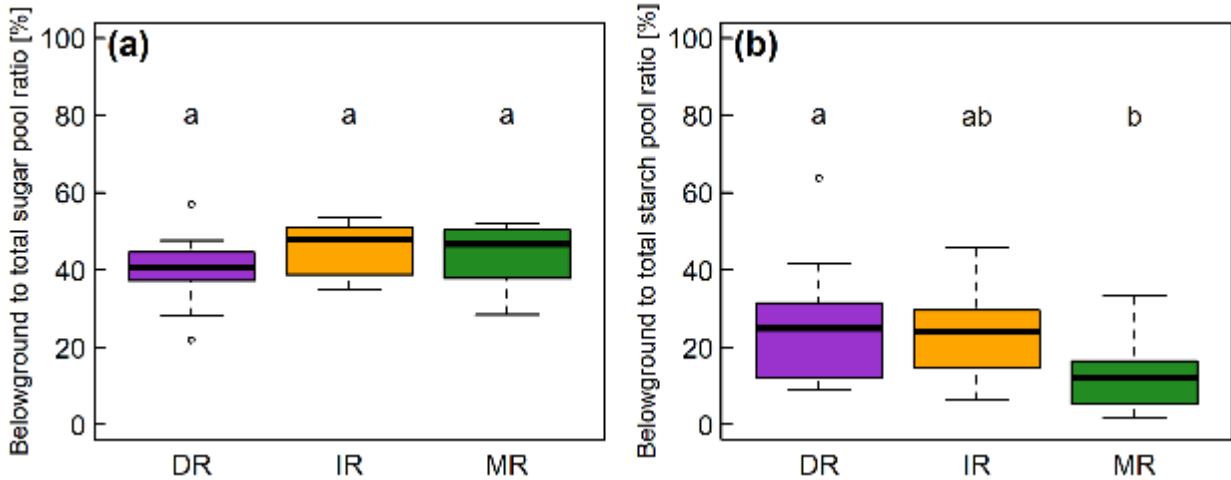
443 **Fig. 5** Allocation of newly assimilated C ( $C_{new}$ ) in leaf, stem, coarse roots, and fine roots after three days of labelling under control  
 444 (blue) and drought (red) treatments. Dry region (DR), intermediate region (IR) and moist region (MR) soil. The asterisk indicates  
 445 significant differences in the ratio of belowground to total  $C_{new}$  between control and drought plants according to post-hoc test:  
 446 \*\*,  $p < 0.01$ , \*,  $p < 0.05$ , n.s.; not significant

#### 447 NSC concentration and pools

448 Sugar concentration of control seedlings was similar in all organs among the three region soils (Fig. S5,  
 449 except for coarse root, where DR seedlings showed lower sugar concentration compared to the IR  
 450 seedlings). Under drought, sugar concentration significantly increased in all organs of DR and IR seedlings  
 451 (Fig. S5), while MR seedlings only increased their sugar concentration in the stem. Starch concentration  
 452 in the leaf significantly increased in IR seedlings under drought, while it decreased in MR seedlings (Fig.  
 453 S6, treatment x region soil  $p < 0.05$ , Table S6). Starch concentration in stems and coarse roots displayed  
 454 only an effect of region soil in DR seedlings showing lower concentrations than the IR and MR seedlings  
 455 ( $p < 0.05$ , Table S6). Starch concentration in fine roots was similar in all seedlings under both control and  
 456 drought treatments.

457 Ratios of belowground to total sugar pools varied between 40 - 45 % in the seedlings growing in different  
 458 region soils (Fig. 6a); however, the ratio did not differ among seedlings growing in the different region

459 soils and were not affected by drought (Table S6). For starch the ratio of the belowground to the total  
460 starch pool was also not affected by drought (Table S6), but plants grown in DR soil had a significantly  
461 higher ratio compared to seedlings grown in MR soil (region soil  $p < 0.05$  Table S6; Fig 6b).



462  
463 *Fig. 6 Ratio of belowground (root) sugar and starch content to the total sugar (a) and starch (b) pools (leaf, stem, coarse, and fine*  
464 *roots all combined), in dry region (DR, purple), intermediate region (IR, yellow) and moist region (MR, green) soil. Lowercase letters*  
465 *indicate significant differences among the groups according to post-hoc test*

## 466 Discussion

467 The present study aimed to elucidate the effects of soils with different long-term precipitation histories  
468 on soil and root-associated fungal community composition and beech seedling performance in response  
469 to a drought.

### 470 Fungal communities in dry region soil were less affected by drought

471 Before the onset of drought, soil fungal communities differed among the region soils and they did not  
472 significantly change in controls during the two months. While saprotrophic fungi were predominant in all  
473 three region soils, they were more abundant in MR soil compared to IR and DR (Fig. 2a), which could  
474 reflect the higher content of soil organic matter in MR soil (Talbot et al. 2013, 2015). In addition, the root-  
475 associated fungal community composition differed significantly between the region soils suggesting an  
476 adaptation of fungal communities to soil moisture over time, which has previously been shown for ECM  
477 fungi along a soil moisture gradient (Cavender-Bares et al. 2009). Likewise, Canarini et al. (2021) stated that  
478 soil microbial communities were more drought tolerant after repeated long-term drought forming an  
479 ecological memory in the soil, which could enhance the resilience of ecosystem functioning. A more in-



480 depth look at the species composition reinforced the presumption of community adaptation. Among the  
481 saprotrophs in soil and root samples, *Penicillium* sp., *Mortierella* sp., and *Oidiodendron* sp. were  
482 dominating. Of these, *Penicillium* sp. was found in earlier studies mainly when low soil moisture prevailed  
483 (Ridout et al. 2017). *Mortierella* sp. and *Oidiodendron* sp. have been classified as species with secondary  
484 root-associated or root-endophytic lifestyle (Pöhlme et al. 2020), that may help the fungi surviving dry  
485 periods (Smith et al. 2017). While a high occurrence of drought-tolerant ECM fungal species such as  
486 *Melanogaster* (Izzo et al. 2005; Frey et al. 2021), have been detected in DR and IR in both controls and during  
487 drought, this was not the case in MR.

488 While there was no effect of the drought treatment on the soil fungal communities, there was a drought  
489 effect on the root-associated fungal communities. This indicates that soil fungal communities might be  
490 more stable compared to root-associated fungal communities during a short-term drought event (de Vries  
491 et al. 2012, 2018; Fu et al. 2022). This is in line with several other studies which found that soil fungal  
492 communities are largely unaffected by droughts of different durations and severities (Bastida et al. 2019;  
493 Liu et al. 2020; Wilhelm et al. 2022). A possible explanation could be that root-associated fungi responded to  
494 the seedlings' reaction to drought (Lozano et al. 2021) such as increased exudation (Karst et al. 2017; Williams  
495 and de Vries 2020; Brunn et al. 2022) or changed root architecture (Nikolova et al. 2020). Soil fungi, on the  
496 other hand, are not in direct contact with the root and might therefore be less influenced by these  
497 responses.

498 With drought, the root-associated fungal community composition changed most in MR and least in DR  
499 soils when considering the abundance of different trophic modes, fungal exploration types and species  
500 abundances, which support a natural adaptation of fungal communities to soil moisture deficits in the DR  
501 soil. In root samples (Fig. 2b), the relative abundance of saprotrophic and ECM fungi in controls was  
502 around 50 % each in all region soils, but with drought the relative abundance of saprotrophs increased in  
503 IR and the most in MR roots. This supports our hypothesis for root associated fungi that fungal  
504 communities in DR are least affected. This is in line with a study by Lozano et al. (2021), who found that the  
505 abundance of saprotrophic fungi increased during drought, while it decreased for mutualist fungi. As  
506 described above, an altered exudation during drought could also attract saprotrophs (Sun and Fries 1992).  
507 Furthermore, some saprotrophic species have been identified to have a secondary, root-associated  
508 lifestyle (Tedersoo and Smith 2013; Smith et al. 2017), which enables them to occupy multiple ecological  
509 niches (Selosse et al. 2018) and thus compete with ECM fungi. Adaptation to drought and the resulting  
510 mitigated response to further drought was also reflected at the species level of root-associated fungi.

511 While in DR and IR root-associated communities *Melanogaster* sp. made up the vast majority in both  
512 control and drought treatments, there was a drastic change in species abundance in MR. Here, the  
513 abundance of *Amanita* sp., a drought-tolerant fungus (Querejeta et al. 2003) classified as contact  
514 exploration type (Agerer 2001), increased extremely under drought compared to controls. This complies  
515 with an increase in the abundance of contact types under prolonged drought (Castaño et al. 2018), and may  
516 be explained by their lower carbon costs to sustain (Lehto and Zwiazek 2011). In this experiment, however,  
517 no significant difference in the supply of new photoassimilates to roots was detected between controls  
518 and drought treated plants in MR soil (Fig. 5). *Amanita* can lead to up- and downregulation of PIP genes  
519 in plants (Marjanović et al. 2005b), which code for aquaporins that are essential for water uptake. One could  
520 speculate about the benefit of a potential fungal mediated upregulated PIP gene expression in seedling  
521 growth during drought, thus favouring fungal niche occupation, but substantiating evidence and thus  
522 further research is necessary.

523 In total, the fungal communities in DR soil roots were least affected by drought treatment, while those in  
524 MR soil roots underwent the greatest changes, confirming our first hypothesis that fungal communities in  
525 DR soil are less affected by drought. In soil fungal communities, however, no changes have been observed.

#### 526 [Beech grown in dry region soil were less acclimated to drought at fine root level](#)

527 While fungal communities in DR soil appear to be better adapted to drought compared to those in MR  
528 soil, seedlings grown in DR soil did not show any better acclimation in fine root architecture, contrasting  
529 with our second hypothesis. Rather, seedlings grown in MR soil had a longer root system and lower  
530 branching intensity than those grown in DR and IR soil (Fig. 4a,b). This may result from slight differences  
531 in soil texture with a higher sand proportion in MR compared to DR soil, since fine root growth rate is  
532 higher in sand than in clay soil for beech (Weemstra et al. 2017). Potentially, seed origin (Alpenvorland,  
533 moist region) could have genetically contributed to differences in drought responses based on the  
534 different selection pressures of habitats, i.e. possible advantages in MR soil compared to in DR soil.  
535 However, this is unlikely the main effect in our study, since our seed source when grown in moist as well  
536 as dry region soils showed a similar plasticity in fine roots under drought. This is supported by a previous  
537 study across Europe reporting no effect of local adaptation on survival of beech seedlings (Muffler et al.  
538 2021). Under drought, seedlings in both DR and MR soils significantly increased taproot length with a  
539 parallel decrease in branching, whereby the fine roots in MR soil rooted longest compared to the plants  
540 growing in IR and DR soils. Longer and deeper growing roots with less branching have been identified as  
541 active drought response in seedlings (Meijer et al. 2011; Asefa et al. 2022). As observed in mature European

542 beech forests (Hodge 2004; Wambsganss et al. 2021), beech seedlings showed a high morphological plasticity  
543 in roots (towards faster foraging strategy) to cope with drought. Furthermore, although the root to shoot  
544 ratio decreased under drought in all region soils (Fig. 3d), contrary to the global observations (Poorter et  
545 al. 2012; Tumber-Dávila et al. 2022), it was significantly higher in MR compared to DR seedlings.

546 All in all, these results provide no support for our second hypothesis, that seedlings grown in DR soil would  
547 be better acclimated to dry conditions at the fine root level compared to those grown in MR soil.

#### 548 [Acclimation in fine root rather than adaptation in fungal community composition mitigated](#) 549 [drought effect on beech seedlings](#)

550 It is often discussed that a mycorrhizal symbiosis can improve the drought performance in tree seedlings  
551 (e.g. Querejeta et al. 2003; Marjanović et al. 2005a; Bréda et al. 2006; Wang et al. 2021). In the present study,  
552 however, even though the root fungal communities appear to be adapted to low SWC, a relative  
553 improvement of seedling growth during drought was not observed in DR soil. Seedlings growing in MR soil  
554 were least stressed during the drought while having the least adapted fungal community and lowest  
555 degree of mycorrhization, indicating that mycorrhization only had a minor contribution on seedling plant  
556 water uptake (Steudle and Heydt 1997; Buchenau et al. 2022). However, the root architecture of the  
557 seedlings also differed substantially in the different soils and under drought conditions and may have  
558 contributed more to the better performance of the MR seedlings under drought than the fungal  
559 community composition. These results are similar to the findings by Moser et al. (2015), that root  
560 architecture rather than ECM colonisation is crucial for drought resistance of *Pinus sylvestris*. Kipfer et al.  
561 (2012) also found that a symbiosis with ECM fungi did not provide additional support during desiccation.  
562 Allsup et al. (2023) found that an inoculation of seedlings with fungal communities from dry regions  
563 enhances the plant drought survival, but this applied only to arbuscular mycorrhizal fungi while ECM fungi  
564 had no significant effect on the seedlings' drought performance. ECM fungi influence root growth by  
565 regulating fungal and host growth hormones (Fitter 1987; Hetrick 1991; Navarro-Ródenas et al. 2013;  
566 Calvo-Polanco et al. 2019; de Freitas Pereira et al. 2023). Therefore, it is possible that the more sparsely  
567 fungus-colonised roots in MR were less inhibited by fungi in their growth and were thus able to grow  
568 longer into the soil. As a result, these seedlings in MR showed a higher  $\Psi_{PD}$  during drought (Fig. 1c). Thus,  
569 less stress in the MR seedlings led to their better photosynthesis and growth (Fig. 1,3). We are aware that  
570 the average taproot length was longer than the depth of the pots (> 20 cm) and we don't know how the  
571 taproots were growing inside pots. However, we assume that the taproot after 20 cm were growing at  
572 the bottom of the pots where the highest water availability can be expected. Therefore, it is likely that

573 the longest taproot length of MR seedlings contributed to their better water uptake and higher  $\Psi_{PD}$  by  
574 larger soil exploration. Differences in soil texture are unlikely the cause for the different  $\Psi_{PD}$ , since the  
575 relationship between soil water potential and the SWC were similar among three region soils (Fig. S2).  
576 Furthermore, smaller initial biomass and leaf area of MR seedlings (Fig. 3a) are probably caused by the  
577 higher C/N ratio of MR soil compared to the other region soils and can be a potential cause for less drought  
578 effects through less water use, in addition to the root architecture. However, this is unlikely since SWC  
579 measurements before the regular watering showed similar values (Fig. 1a) and the amount of added water  
580 was similar in all three region soils. Allocation of newly assimilated C to belowground sinks decreased  
581 under drought following the decrease in  $\Psi_{PD}$ , as observed in previous studies in beech seedlings (Ruehr et  
582 al. 2009; Zang et al. 2014) and other species (Poorter et al. 2012). Although allocation of newly assimilated C  
583 belowground is important for the maintenance and growth of roots (Blessing et al. 2016; Hommel et al. 2016;  
584 Hikino et al. 2022), less C was transferred there in DR and IR seedlings under drought, thus no acclimation  
585 was observed in C allocation contrary to our second hypothesis. This is likely due to delayed sugar export  
586 from leaves and/or reduced phloem transport (Zang et al. 2014; Hesse et al. 2018). Although roots are  
587 important for long-term reserve storage in some species (Blessing et al. 2016; Wiley et al. 2019; Montague et  
588 al. 2022) and stored reserves (particularly starch) are used for root growth (Wang et al. 2018; Tang et al.  
589 2022; Domingo et al. 2023), allocation to NSC reserve pools did not shift to belowground organs under  
590 drought in our study which is contrary to observations in other species (Galvez et al. 2011, 2013; Chuste  
591 et al. 2020). This might be due to a shorter duration or lower intensity of drought in the present study  
592 compared to their studies. Although the ratio of belowground to total starch pool was significantly higher  
593 in DR compared to MR plants (Fig. 6a), these reserves were not used during drought and thus did likely  
594 not contribute to the mitigation of drought, maintaining or even increasing reserves in roots (Galvez et al.  
595 2011, 2013). However, sugar concentration increased under drought in all organs including coarse and fine  
596 roots (Fig. S5) which is correlated with the decreased  $\Psi_{PD}$  (Fig. 1c). Similar increases in sugar  
597 concentrations were observed in previous drought experiments with beech seedlings (Liu et al. 2017; Pflug  
598 et al. 2018; Tomasella et al. 2019; Chuste et al. 2020). Contrary to the growth reduction under drought, other  
599 C sinks such as osmoregulation appear to be up-regulated, which was observed in other studies (Sala et al.  
600 2012; Dietze et al. 2014; Chuste et al. 2020).

601 Above all, the results indicate that MR seedlings, which showed some acclimation to drought at the fine  
602 root level, experienced the least drought stress during this experiment. Additionally, the fungal  
603 community associated with MR seedlings significantly changed towards more drought-tolerant species.

604 These findings support our third hypothesis, stating that the root system including root and associated  
605 fungi can mitigate drought effects on plants.

## 606 Conclusion

607 A changing climate with more frequent and severe droughts challenges global forests. Hence, it is essential  
608 to evaluate which factors can positively impact tree survival. The results of this study suggest that the  
609 drought stress response of beech seedlings appears to depend more strongly on the plasticity of root  
610 architecture rather than on fungal community composition even if soil fungal communities are adapted  
611 to drought conditions. However, a fungal contribution to the seedlings' drought performance cannot be  
612 excluded completely and needs to be studied further by e.g. including other groups of microorganisms  
613 and their interactions with root-associated fungi, as well as specific root-fungus interactions. Since this  
614 study explores these relationships on seedlings in a rather artificial environment, we cannot preclude  
615 differing responses that will occur under natural conditions and that vary with tree age (Hartmann et al.  
616 2018). Nevertheless, this study pinpoints the need to evaluate the effects of drought on trees in the  
617 context of root associated microorganisms.

## 618 Acknowledgements

619 We would like to thank Sarah Kristen and Isabella Pitzen for their support with watering plants, daily SWC  
620 measurements and root architecture analysis, and Thomas Feuerbach for setting up and maintaining the  
621 measurement and <sup>13</sup>C labelling equipment. We also appreciate supports during the intensive harvests by  
622 Elke Gerstner, Barbara Groß and Joseph Heckmair. Furthermore, we thank Tina Kiedeisch for a helping  
623 hand during DNA extraction and sequencing preparation. We also thank Pak Chow for NSC quantification  
624 measurements, Franziska Bucka for a support with pressure plates, and Uwe Blum for performing soil  
625 nutrient measurements. We also thank Benjamin D. Hafner for his generous pre-submission review.

## 626 Declarations

### 627 Funds

628 The project was funded by the German Research Foundation (DFG) through grants GR 1881/5-1,  
629 MA1763/10-1, PR555/2-1, PR292/22-1 and by the Bavarian State Ministries of the Environment and  
630 Consumer Protection as well as Food, Agriculture and Forestry (W047/Kroof II).

## 631 Author contribution statement

632 KP and TEEG originally designed the experiment, and JD and KH finalized the experimental design. All  
633 authors contributed to the sample and the data collection. JD and KH analyzed, interpreted the data,  
634 and wrote the manuscript with support from all authors. All authors revised and edited the manuscript.  
635 JD and KH contributed equally.

## 636 Conflict of interest

637 The authors declare that there is no conflict of interest.

## 638 Data availability

639 The raw sequencing data presented in this study are openly available in in the NCBI Sequence Read  
640 Archive and included in the BioProject with accession number PRJNA1063582. All other data presented in  
641 this study are available in this article and the respective supplementary information.

642

## 643 References

644

- 645 Aaltonen H, Linden A, Heinonsalo J, et al (2017) Effects of prolonged drought stress on Scots pine  
646 seedling carbon allocation. *Tree Physiol* 37:418–427. <https://doi.org/10.1093/treephys/tpw119>
- 647 Agerer R (2001) Exploration types of ectomycorrhizae. *Mycorrhiza* 11:107–114.  
648 <https://doi.org/10.1007/s005720100108>
- 649 Allsup CM, George I, Lankau RA (2023) Shifting microbial communities can enhance tree tolerance to  
650 changing climates. *Science* 380:835–840. <https://doi.org/10.1126/science.adf2027>
- 651 Anthony MA, Crowther TW, van der Linde S, et al (2022) Forest tree growth is linked to mycorrhizal  
652 fungal composition and function across Europe. *ISME J* 1–10. <https://doi.org/10.1038/s41396-021-01159-7>
- 653
- 654 Arend M, Link RM, Zahnd C, et al (2022) Lack of hydraulic recovery as a cause of post-drought foliage  
655 reduction and canopy decline in European beech. *New Phytol* 234:1195–1205.  
656 <https://doi.org/10.1111/nph.18065>
- 657 Asefa M, Worthy SJ, Cao M, et al (2022) Above- and below-ground plant traits are not consistent in  
658 response to drought and competition treatments. *Ann Bot* 1–12.  
659 <https://doi.org/10.1093/aob/mcac108>

- 660 Bastida F, López-Mondéjar R, Baldrian P, et al (2019) When drought meets forest management: Effects  
661 on the soil microbial community of a Holm oak forest ecosystem. *Sci Total Environ* 662:276–286.  
662 <https://doi.org/10.1016/j.scitotenv.2019.01.233>
- 663 Beloiu M, Stahlmann R, Beierkuhnlein C (2022) Drought impacts in forest canopy and deciduous tree  
664 saplings in Central European forests. *For Ecol Manag* 509:.  
665 <https://doi.org/10.1016/j.foreco.2022.120075>
- 666 Bengtsson-Palme J, Ryberg M, Hartmann M, et al (2013) Improved software detection and extraction of  
667 ITS1 and ITS2 from ribosomal ITS sequences of fungi and other eukaryotes for analysis of  
668 environmental sequencing data. *Methods Ecol Evol* 4:914–919. <https://doi.org/10.1111/2041-210X.12073>
- 670 Blessing CH, Barthel M, Gentsch L, Buchmann N (2016) Strong coupling of shoot assimilation and soil  
671 respiration during drought and recovery periods in beech as indicated by natural abundance  $\delta^{13}$   
672 C measurements. *Front Plant Sci* 7:1–12. <https://doi.org/10.3389/fpls.2016.01710>
- 673 Blessing CH, Werner RA, Siegwolf R, Buchmann N (2015) Allocation dynamics of recently fixed carbon in  
674 beech saplings in response to increased temperatures and drought. *Tree Physiol* 35:585–598.  
675 <https://doi.org/10.1093/treephys/tpv024>
- 676 Bréda N, Huc R, Granier A, Dreyer E (2006) Temperate forest trees and stands under severe drought: a  
677 review of ecophysiological responses, adaptation processes and long-term consequences. *Ann  
678 For Sci* 63:625–644. <https://doi.org/10.1051/forest:2006042>
- 679 Brinkmann N, Eugster W, Buchmann N, Kahmen A (2019) Species-specific differences in water uptake  
680 depth of mature temperate trees vary with water availability in the soil. *Plant Biol* 21:71–81.  
681 <https://doi.org/10.1111/plb.12907>
- 682 Brunn M, Hafner BD, Zwetsloot MJ, et al (2022) Carbon allocation to root exudates is maintained in  
683 mature temperate tree species under drought. *New Phytol* 965–977.  
684 <https://doi.org/10.1111/nph.18157>
- 685 Brunner I, Herzog C, Dawes MA, et al (2015) How tree roots respond to drought. *Front Plant Sci* 6:547.  
686 <https://doi.org/10.3389/fpls.2015.00547>
- 687 Buchenau N, van Kleunen M, Wilschut RA (2022) Direct and legacy-mediated drought effects on plant  
688 performance are species-specific and depend on soil community composition. *Oikos* 2022:.  
689 <https://doi.org/10.1111/oik.08959>
- 690 Buhk C, Kämmer M, Beierkuhnlein C, et al (2016) On the influence of provenance to soil quality  
691 enhanced stress reaction of young beech trees to summer drought. *Ecol Evol* 6:8276–8290.  
692 <https://doi.org/10.1002/ece3.2472>
- 693 Calvo-Polanco M, Armada E, Zamarreño AM, et al (2019) Local root ABA/cytokinin status and aquaporins  
694 regulate poplar responses to mild drought stress independently of the ectomycorrhizal fungus  
695 *Laccaria bicolor*. *J Exp Bot* 70:6437–6446. <https://doi.org/10.1093/jxb/erz389>

- 696 Canarini A, Schmidt H, Fuchslueger L, et al (2021) Ecological memory of recurrent drought modifies soil  
697 processes via changes in soil microbial community. *Nat Commun* 12:1–14.  
698 <https://doi.org/10.1038/s41467-021-25675-4>
- 699 Castaño C, Lindahl BD, Alday JG, et al (2018) Soil microclimate changes affect soil fungal communities in  
700 a Mediterranean pine forest. *New Phytol* 220:1211–1221. <https://doi.org/10.1111/nph.15205>
- 701 Castaño C, Suarez-Vidal E, Zas R, et al (2023) Ectomycorrhizal fungi with hydrophobic mycelia and  
702 rhizomorphs dominate in young pine trees surviving experimental drought stress. *Soil Biol  
703 Biochem* 178:. <https://doi.org/10.1016/j.soilbio.2022.108932>
- 704 Cavender-Bares J, Izzo A, Robinson R, Lovelock CE (2009) Changes in ectomycorrhizal community  
705 structure on two containerized oak hosts across an experimental hydrologic gradient.  
706 *Mycorrhiza* 19:133–142. <https://doi.org/10.1007/s00572-008-0220-3>
- 707 Chen J, Bittinger K, Charlson ES, et al (2012) Associating microbiome composition with environmental  
708 covariates using generalized UniFrac distances. *Bioinformatics* 28:2106–2113.  
709 <https://doi.org/10.1093/bioinformatics/bts342>
- 710 Choat B, Brodribb TJ, Brodersen CR, et al (2018) Triggers of tree mortality under drought. *Nature*  
711 558:531–539. <https://doi.org/10.1038/s41586-018-0240-x>
- 712 Chuste PA, Maillard P, Bréda N, et al (2020) Sacrificing growth and maintaining a dynamic carbohydrate  
713 storage are key processes for promoting beech survival under prolonged drought conditions.  
714 *Trees - Struct Funct* 34:381–394. <https://doi.org/10.1007/s00468-019-01923-5>
- 715 Clément C, Pierret A, Maeght JL, et al (2019) Linking tree-rooting profiles to leaf phenology: a first  
716 attempt on *Tectona Grandis* Linn F. *Trees - Struct Funct* 33:1491–1504.  
717 <https://doi.org/10.1007/s00468-019-01876-9>
- 718 Contran N, Günthardt-Goerg MS, Kuster TM, et al (2013) Physiological and biochemical responses of  
719 *Quercus pubescens* to air warming and drought on acidic and calcareous soils. *Plant Biol*  
720 15:157–168. <https://doi.org/10.1111/j.1438-8677.2012.00627.x>
- 721 Danzberger J, Werner R, Mucha J, et al (2023) Drought legacy effects on fine-root-associated fungal  
722 communities are modulated by root interactions between tree species. *Front For Glob Change*  
723 6:1–16. <https://doi.org/10.3389/ffgc.2023.1197791>
- 724 de Freitas Pereira M, Cohen D, Auer L, et al (2023) Ectomycorrhizal symbiosis prepares its host locally  
725 and systemically for abiotic cue signaling. *Plant J.* <https://doi.org/10.1111/tpj.16465>
- 726 de Vries FT, Griffiths RI, Bailey M, et al (2018) Soil bacterial networks are less stable under drought than  
727 fungal networks. *Nat Commun* 9:. <https://doi.org/10.1038/s41467-018-05516-7>
- 728 de Vries FT, Liiri ME, Bjørnlund L, et al (2012) Land use alters the resistance and resilience of soil food  
729 webs to drought. *Nat Clim Change* 2:276–280. <https://doi.org/10.1038/nclimate1368>
- 730 Dietze MC, Sala A, Carbone MS, et al (2014) Nonstructural carbon in woody plants. *Annu Rev Plant Biol*  
731 65:667–687. <https://doi.org/10.1146/annurev-arplant-050213-040054>



- 732 Domingo G, Vannini C, Marsoni M, et al (2023) A multifaceted approach to reveal the very-fine root's  
733 response of *Fagus sylvatica* seedlings to different drought intensities. *Physiol Plant* 175:1–15.  
734 <https://doi.org/10.1111/ppl.13934>
- 735 Egerton-Warburton LM, Querejeta JJ, Allen MF (2007) Common mycorrhizal networks provide a  
736 potential pathway for the transfer of hydraulically lifted water between plants. *J Exp Bot*  
737 58:1473–1483. <https://doi.org/10.1093/jxb/erm009>
- 738 Fitter AH (1987) An architectural approach to the comparative ecology of plant root systems. *New*  
739 *Phytol* 106:61–77. <https://doi.org/10.1111/j.1469-8137.1987.tb04683.x>
- 740 Fitzpatrick CR, Copeland J, Wang PW, et al (2018) Assembly and ecological function of the root  
741 microbiome across angiosperm plant species. *Proc Natl Acad Sci U S A* 115:E1157–E1165.  
742 <https://doi.org/10.1073/pnas.1717617115>
- 743 Frei ER, Gossner MM, Vitasse Y, et al (2022) European beech dieback after premature leaf senescence  
744 during the 2018 drought in northern Switzerland. *Plant Biol* 24:1132–1145.  
745 <https://doi.org/10.1111/plb.13467>
- 746 Frey B, Walthert L, Perez-Mon C, et al (2021) Deep Soil Layers of Drought-Exposed Forests Harbor Poorly  
747 Known Bacterial and Fungal Communities. *Front Microbiol* 12:.  
748 <https://doi.org/10.3389/fmicb.2021.674160>
- 749 Fu W, Chen B, Jansa J, et al (2022) Contrasting community responses of root and soil dwelling fungi to  
750 extreme drought in a temperate grassland. *Soil Biol Biochem* 169:108670.  
751 <https://doi.org/10.1016/j.soilbio.2022.108670>
- 752 Galvez DA, Landhäusser SM, Tyree MT (2011) Root carbon reserve dynamics in aspen seedlings: Does  
753 simulated drought induce reserve limitation? *Tree Physiol* 31:250–257.  
754 <https://doi.org/10.1093/treephys/tpq012>
- 755 Galvez DA, Landhäusser SM, Tyree MT (2013) Low root reserve accumulation during drought may lead  
756 to winter mortality in poplar seedlings. *New Phytol* 198:139–148.  
757 <https://doi.org/10.1111/nph.12129>
- 758 Gebauer R, Plichta R, Urban J, et al (2020) The resistance and resilience of European beech seedlings to  
759 drought stress during the period of leaf development. *Tree Physiol* 40:1147–1164.  
760 <https://doi.org/10.1093/treephys/tpaa066>
- 761 Germon A, Laclau JP, Robin A, Jourdan C (2020) Tamm Review: Deep fine roots in forest ecosystems:  
762 Why dig deeper? *For Ecol Manag* 466:.  
<https://doi.org/10.1016/j.foreco.2020.118135>
- 763 Geßler A, Keitel C, Kreuzwieser J, et al (2007) Potential risks for European beech (*Fagus sylvatica* L.) in a  
764 changing climate. *Trees - Struct Funct* 21:1–11. <https://doi.org/10.1007/s00468-006-0107-x>
- 765 Gundale MJ, Kardol P, Nilsson MC, et al (2014) Interactions with soil biota shift from negative to positive  
766 when a tree species is moved outside its native range. *New Phytol* 202:415–421.  
767 <https://doi.org/10.1111/nph.12699>

768 Gweon HS, Oliver A, Taylor J, et al (2015) PIPITS: An automated pipeline for analyses of fungal internal  
769 transcribed spacer sequences from the Illumina sequencing platform. *Methods Ecol Evol* 6:973–  
770 980. <https://doi.org/10.1111/2041-210X.12399>

771 Hartmann H, Adams HD, Hammond WM, et al (2018) Identifying differences in carbohydrate dynamics  
772 of seedlings and mature trees to improve carbon allocation in models for trees and forests.  
773 *Environ Exp Bot* 152:7–18. <https://doi.org/10.1016/j.envexpbot.2018.03.011>

774 Hesse BD, Goisser M, Hartmann H, Grams TEE (2018) Repeated summer drought delays sugar export  
775 from the leaf and impairs phloem transport in mature beech. *Tree Physiol* 39:192–200.  
776 <https://doi.org/10.1093/treephys/tpy122>

777 Hetrick BAD (1991) Mycorrhizas and root architecture. *Experientia* 47:355–362.  
778 <https://doi.org/10.1007/BF01972077>

779 Hikino K, Danzberger J, Riedel VP, et al (2022) Dynamics of initial C allocation after drought release in  
780 mature Norway spruce - Increased belowground allocation of current photoassimilates covers  
781 only half of the C used for fine-root growth. *Glob Change Biol* 1–17.  
782 <https://doi.org/10.1111/gcb.16388>

783 Hodge A (2004) The plastic plant: Root responses to heterogeneous supplies of nutrients. *New Phytol*  
784 162:9–24. <https://doi.org/10.1111/j.1469-8137.2004.01015.x>

785 Hommel R, Siegwolf R, Zavadlav S, et al (2016) Impact of interspecific competition and drought on the  
786 allocation of new assimilates in trees. *Plant Biol Stuttg Ger* 18:785–796.  
787 <https://doi.org/10.1111/plb.12461>

788 Izzo AD, Meyer M, Trappe JM, et al (2005) Hypogeous Ectomycorrhizal Fungal Species on Roots and in  
789 Small Mammal Diet in a Mixed-Conifer Forest. *For Sci* 51:243–254

790 Kahmen A, Basler D, Hoch G, et al (2022) Root water uptake depth determines the hydraulic  
791 vulnerability of temperate European tree species during the extreme 2018 drought. *Plant Biol*  
792 24:1224–1239. <https://doi.org/10.1111/plb.13476>

793 Karst J, Gaster J, Wiley E, Landhäuser SM (2017) Stress differentially causes roots of tree seedlings to  
794 exude carbon. *Tree Physiol* 37:154–164. <https://doi.org/10.1093/treephys/tpw090>

795 Kipfer T, Wohlgemuth T, Heijden MGA van der, et al (2012) Growth Response of Drought-Stressed *Pinus*  
796 *sylvestris* Seedlings to Single- and Multi-Species Inoculation with Ectomycorrhizal Fungi. *PLOS*  
797 *ONE* 7:e35275. <https://doi.org/10.1371/journal.pone.0035275>

798 Kivlin SN, Emery SM, Rudgers JA (2013) Fungal symbionts alter plant responses to global change. *Am J*  
799 *Bot* 100:1445–1457. <https://doi.org/10.3732/ajb.1200558>

800 Kõljalg U, Nilsson RH, Abarenkov K, et al (2013) Towards a unified paradigm for sequence-based  
801 identification of fungi. *Mol Ecol* 22:5271–5277. <https://doi.org/10.1111/mec.12481>

802 Körner C (2011) The Grand Challenges in Functional Plant Ecology. *Front Plant Sci* 2:.  
803 <https://doi.org/10.3389/fpls.2011.00001>

- 804 Landhäuser SM, Chow PS, Dickman LT, et al (2018) Standardized protocols and procedures can precisely  
805 and accurately quantify non-structural carbohydrates. *Tree Physiol* 38:1764–1778.  
806 <https://doi.org/10.1093/treephys/tpy118>
- 807 Lata R, Chowdhury S, Gond SK, White JF (2018) Induction of abiotic stress tolerance in plants by  
808 endophytic microbes. *Lett Appl Microbiol* 66:268–276. <https://doi.org/10.1111/lam.12855>
- 809 Lehto T, Zwiazek JJ (2011) Ectomycorrhizas and water relations of trees: a review. *Mycorrhiza* 21:71–90.  
810 <https://doi.org/10.1007/s00572-010-0348-9>
- 811 Lenzion J, Leuschner C (2008) Growth of European beech (*Fagus sylvatica* L.) saplings is limited by  
812 elevated atmospheric vapour pressure deficits. *For Ecol Manag* 256:648–655.  
813 <https://doi.org/10.1016/j.foreco.2008.05.008>
- 814 Leuschner C (2020) Drought response of European beech (*Fagus sylvatica* L.)—A review. *Perspect Plant  
815 Ecol Evol Syst* 47:125576. <https://doi.org/10.1016/j.ppees.2020.125576>
- 816 Leuschner C, Wedde P, Lübke T (2019) The relation between pressure–volume curve traits and stomatal  
817 regulation of water potential in five temperate broadleaf tree species. *Ann For Sci* 76:.  
818 <https://doi.org/10.1007/s13595-019-0838-7>
- 819 Liu JF, Arend M, Yang WJ, et al (2017) Effects of drought on leaf carbon source and growth of European  
820 beech are modulated by soil type. *Sci Rep* 7:1–9. <https://doi.org/10.1038/srep42462>
- 821 Liu Y, Li X, Kou Y (2020) Ectomycorrhizal fungi: Participation in nutrient turnover and community  
822 assembly pattern in forest ecosystems. *Forests* 11:.  
<https://doi.org/10.3390/F11040453>
- 823 Lozano YM, Aguilar-Trigueros CA, Roy J, Rillig MC (2021) Drought induces shifts in soil fungal  
824 communities that can be linked to root traits across 24 plant species. *New Phytol* 232:1917–  
825 1929. <https://doi.org/10.1111/nph.17707>
- 826 Marjanović Ž, Nehls U, Hampp R (2005a) Mycorrhiza Formation Enhances Adaptive Response of Hybrid  
827 Poplar to Drought. *Ann N Y Acad Sci* 1048:496–499. <https://doi.org/10.1196/annals.1342.080>
- 828 Marjanović Ž, Uehlein N, Kaldenhoff R, et al (2005b) Aquaporins in poplar: What a difference a symbiont  
829 makes! *Planta* 222:258–268. <https://doi.org/10.1007/s00425-005-1539-z>
- 830 Martinez Arbizu P (2020) pairwiseAdonis: Pairwise multilevel comparison using adonis
- 831 McCormack ML, Dickie IA, Eissenstat DM, et al (2015) Redefining fine roots improves understanding of  
832 below-ground contributions to terrestrial biosphere processes. *New Phytol* 207:505–518.  
833 <https://doi.org/10.1111/nph.13363>
- 834 Meier CE, Newton RJ, Puryear JD, Sen S (1992) Physiological Responses of Loblolly Pine (*Pinus taeda* L.)  
835 Seedlings to Drought Stress: Osmotic Adjustment and Tissue Elasticity. *J Plant Physiol* 140:754–  
836 760. [https://doi.org/10.1016/S0176-1617\(11\)81034-5](https://doi.org/10.1016/S0176-1617(11)81034-5)

- 837 Meier IC, Leuschner C (2008) Belowground drought response of European beech: Fine root biomass and  
838 carbon partitioning in 14 mature stands across a precipitation gradient. *Glob Change Biol*  
839 14:2081–2095. <https://doi.org/10.1111/j.1365-2486.2008.01634.x>
- 840 Meijer SS, Holmgren M, Van Der Putten WH (2011) Effects of plant-soil feedback on tree seedling  
841 growth under arid conditions. *J Plant Ecol* 4:193–200. <https://doi.org/10.1093/jpe/rtr011>
- 842 Meisner A, Jacquiod S, Snoek BL, et al (2018) Drought legacy effects on the composition of soil fungal  
843 and prokaryote communities. *Front Microbiol* 9:294. <https://doi.org/10.3389/fmicb.2018.00294>
- 844 Mohan JE, Cowden CC, Baas P, et al (2014) Mycorrhizal fungi mediation of terrestrial ecosystem  
845 responses to global change: Mini-review. *Fungal Ecol* 10:3–19.  
846 <https://doi.org/10.1016/j.funeco.2014.01.005>
- 847 Montague MS, Landhäuser SM, McNickle GG, Jacobs DF (2022) Preferential allocation of carbohydrate  
848 reserves belowground supports disturbance-based management of American chestnut  
849 (*Castanea dentata*). *For Ecol Manag* 509:. <https://doi.org/10.1016/j.foreco.2022.120078>
- 850 Moser B, Kipfer T, Richter S, et al (2015) Drought resistance of *Pinus sylvestris* seedlings conferred by  
851 plastic root architecture rather than ectomycorrhizal colonisation. *Ann For Sci* 72:303–309.  
852 <https://doi.org/10.1007/s13595-014-0380-6>
- 853 Muffler L, Schmeddes J, Weigel R, et al (2021) High plasticity in germination and establishment success  
854 in the dominant forest tree *Fagus sylvatica* across Europe. *Glob Ecol Biogeogr* 30:1583–1596.  
855 <https://doi.org/10.1111/geb.13320>
- 856 Nahm M, Matzarakis A, Rennenberg H, Geßler A (2007) Seasonal courses of key parameters of nitrogen,  
857 carbon and water balance in European beech (*Fagus sylvatica* L.) grown on four different study  
858 sites along a European North-South climate gradient during the 2003 drought. *Trees - Struct*  
859 *Funct* 21:79–92. <https://doi.org/10.1007/s00468-006-0098-7>
- 860 Navarro-Ródenas A, Bárzana G, Nicolás E, et al (2013) Expression analysis of aquaporins from desert  
861 truffle mycorrhizal symbiosis reveals a fine-tuned regulation under drought. *Mol Plant Microbe*  
862 *Interact* 26:1068–1078. <https://doi.org/10.1094/MPMI-07-12-0178-R>
- 863 Nguyen NH, Song Z, Bates ST, et al (2016a) FUNGuild: An open annotation tool for parsing fungal  
864 community datasets by ecological guild. *Fungal Ecol* 20:241–248.  
865 <https://doi.org/10.1016/j.funeco.2015.06.006>
- 866 Nguyen NH, Williams LJ, Vincent JB, et al (2016b) Ectomycorrhizal fungal diversity and saprotrophic  
867 fungal diversity are linked to different tree community attributes in a field-based tree  
868 experiment. *Mol Ecol* 25:4032–4046. <https://doi.org/10.1111/mec.13719>
- 869 Nickel UT, Weigl F, Kerner R, et al (2018) Quantitative losses vs. qualitative stability of ectomycorrhizal  
870 community responses to 3 years of experimental summer drought in a beech–spruce forest.  
871 *Glob Change Biol* 24:e560–e576. <https://doi.org/10.1111/gcb.13957>

- 872 Nikolova PS, Bauerle TL, Häberle KH, et al (2020) Fine-Root Traits Reveal Contrasting Ecological  
873 Strategies in European Beech and Norway Spruce During Extreme Drought. *Front Plant Sci* 11:.  
874 <https://doi.org/10.3389/fpls.2020.01211>
- 875 Nilsson RH, Tedersoo L, Ryberg M, et al (2015) A comprehensive, automatically updated fungal ITS  
876 sequence dataset for reference-based chimera control in environmental sequencing efforts.  
877 *Microbes Environ* 30:145–150. <https://doi.org/10.1264/jsme2.ME14121>
- 878 Oksanen AJ, Blanchet FG, Friendly M, et al (2019) Vegan. In: *Encyclopedia of Food and Agricultural*  
879 *Ethics*. Springer Netherlands, pp 2395–2396
- 880 Petrik P, Petek-Petrik A, Kurjak D, et al (2022) Interannual adjustments in stomatal and leaf  
881 morphological traits of European beech (*Fagus sylvatica* L.) demonstrate its climate change  
882 acclimation potential. *Plant Biol* 24:1287–1296. <https://doi.org/10.1111/plb.13401>
- 883 Pflug EE, Buchmann N, Siegwolf RTW, et al (2018) Resilient Leaf Physiological Response of European  
884 Beech (*Fagus sylvatica* L.) to Summer Drought and Drought Release. *Front Plant Sci* 9:
- 885 Pölme S, Abarenkov K, Henrik Nilsson R, et al (2020) FungalTraits: a user-friendly traits database of fungi  
886 and fungus-like stramenopiles. *Fungal Divers* 105:.. <https://doi.org/10.1007/s13225-020-00466-2>
- 887 Poorter H, Niklas KJ, Reich PB, et al (2012) Biomass allocation to leaves, stems and roots: Meta-analyses  
888 of interspecific variation and environmental control. *New Phytol* 193:30–50.  
889 <https://doi.org/10.1111/j.1469-8137.2011.03952.x>
- 890 Porter SS, Bantay R, Friel CA, et al (2020) Beneficial microbes ameliorate abiotic and biotic sources of  
891 stress on plants. *Funct Ecol* 34:2075–2086. <https://doi.org/10.1111/1365-2435.13499>
- 892 Pretzsch H, Rötzer T, Matyssek R, et al (2014) Mixed Norway spruce (*Picea abies* [L.] Karst) and European  
893 beech (*Fagus sylvatica* [L.] stands under drought: from reaction pattern to mechanism. *Trees -*  
894 *Struct Funct* 28:1305–1321. <https://doi.org/10.1007/s00468-014-1035-9>
- 895 Querejeta JL, Egerton-Warburton LM, Allen MF (2003) Direct nocturnal water transfer from oaks to their  
896 mycorrhizal symbionts during severe soil drying. *Oecologia* 134:55–64.  
897 <https://doi.org/10.1007/s00442-002-1078-2>
- 898 Rennenberg H, Seiler W, Matyssek R, et al (2004) Die Buche (*Fagus sylvatica* L.) – ein Waldbaum ohne  
899 Zukunft im südlichen Mitteleuropa? In: *Allgemeine Forst und Jagdzeitung*. pp 210–224
- 900 Richard F, Roy M, Shahin O, et al (2011) Ectomycorrhizal communities in a Mediterranean forest  
901 ecosystem dominated by *Quercus ilex*: Seasonal dynamics and response to drought in the  
902 surface organic horizon. *Ann For Sci* 68:57–68. <https://doi.org/10.1007/s13595-010-0007-5>
- 903 Richards L (1941) A pressure-membrane extraction apparatus for soil solution. *Soil Sci* 51(5):377e:
- 904 Ridout M, Houbraken J, Newcombe G (2017) Xerotolerance of *Penicillium* and *Phialocephala* fungi,  
905 dominant taxa of fine lateral roots of woody plants in the intermountain Pacific Northwest, USA.  
906 *Rhizosphere* 4:94–103. <https://doi.org/10.1016/j.rhisph.2017.09.004>

- 907 Rognes T, Flouri T, Nichols B, et al (2016) VSEARCH: A versatile open source tool for metagenomics.  
908 PeerJ 2016:1–22. <https://doi.org/10.7717/peerj.2584>
- 909 Ruehr NK, Offermann CA, Gessler A, et al (2009) Drought effects on allocation of recent carbon: From  
910 beech leaves to soil CO<sub>2</sub> efflux. *New Phytol* 184:950–961. <https://doi.org/10.1111/j.1469-8137.2009.03044.x>  
911
- 912 Sala A, Woodruff DR, Meinzer FC (2012) Carbon dynamics in trees: Feast or famine? *Tree Physiol*  
913 32:764–775. <https://doi.org/10.1093/treephys/tptr143>
- 914 Schmied G, Hilmers T, Mellert KH, et al (2023) Nutrient regime modulates drought response patterns of  
915 three temperate tree species. *Sci Total Environ* 868:161601.  
916 <https://doi.org/10.1016/j.scitotenv.2023.161601>
- 917 Selosse MA, Schneider-Maunoury L, Martos F (2018) Time to re-think fungal ecology? Fungal ecological  
918 niches are often prejudged. *New Phytol* 217:968–972. <https://doi.org/10.1111/nph.14983>
- 919 Shi L, Guttenberger M, Kottke I, Hampp R (2002) The effect of drought on mycorrhizas of beech (*Fagus*  
920 *sylvatica* L.): Changes in community structure, and the content of carbohydrates and nitrogen  
921 storage bodies of the fungi. *Mycorrhiza* 12:303–311. <https://doi.org/10.1007/s00572-002-0197-2>  
922
- 923 Smith GR, Finlay RD, Stenlid J, et al (2017) Growing evidence for facultative biotrophy in saprotrophic  
924 fungi: data from microcosm tests with 201 species of wood-decay basidiomycetes. *New Phytol*  
925 215:747–755. <https://doi.org/10.1111/nph.14551>
- 926 Steudle E, Heydt H (1997) Water transport across tree roots. In: *Trees—Contributions to Modern Tree*  
927 *Physiology*. Backhuys Publishers
- 928 Sun YP, Fries N (1992) The effect of tree-root exudates on the growth rate of ectomycorrhizal and  
929 saprotrophic fungi. *Mycorrhiza* 1:63–69. <https://doi.org/10.1007/BF00206138>
- 930 Swaty RL, Deckert RJ, Whitham TG, Gehring CA (2004) Ectomycorrhizal abundance and community  
931 composition shifts with drought: Predictions from tree rings. *Ecology* 85:1072–1084.  
932 <https://doi.org/10.1890/03-0224>
- 933 Talbot JM, Bruns TD, Smith DP, et al (2013) Independent roles of ectomycorrhizal and saprotrophic  
934 communities in soil organic matter decomposition. *Soil Biol Biochem* 57:282–291.  
935 <https://doi.org/10.1016/j.soilbio.2012.10.004>
- 936 Talbot JM, Martin F, Kohler A, et al (2015) Functional guild classification predicts the enzymatic role of  
937 fungi in litter and soil biogeochemistry. *Soil Biol Biochem* 88:441–456.  
938 <https://doi.org/10.1016/j.soilbio.2015.05.006>
- 939 Tang Y, Schiestl-Aalto P, Saurer M, et al (2022) Tree organ growth and carbon allocation dynamics  
940 impact the magnitude and  $\delta^{13}\text{C}$  signal of stem and soil CO<sub>2</sub> fluxes. *Tree Physiol* 42:2404–2418.  
941 <https://doi.org/10.1093/treephys/tpac079>

- 942 Tedersoo L, Anslan S, Bahram M, et al (2015) Shotgun metagenomes and multiple primer pair-barcode  
 943 combinations of amplicons reveal biases in metabarcoding analyses of fungi. *MycoKeys* 10:1–43.  
 944 <https://doi.org/10.3897/mycokeys.10.4852>
- 945 Tedersoo L, Smith ME (2013) Lineages of ectomycorrhizal fungi revisited: Foraging strategies and novel  
 946 lineages revealed by sequences from belowground. *Fungal Biol Rev* 27:83–99.  
 947 <https://doi.org/10.1016/j.fbr.2013.09.001>
- 948 Thiel D, Kreyling J, Backhaus S, et al (2014) Different reactions of central and marginal provenances of  
 949 *Fagus sylvatica* to experimental drought. *Eur J For Res* 133:247–260.  
 950 <https://doi.org/10.1007/s10342-013-0750-x>
- 951 Tomasella M, Beikircher B, Häberle KH, et al (2018) Acclimation of branch and leaf hydraulics in adult  
 952 *Fagus sylvatica* and *Picea abies* in a forest through-fall exclusion experiment. *Tree Physiol*  
 953 38:198–211. <https://doi.org/10.1093/treephys/tpx140>
- 954 Tomasella M, Nardini A, Hesse BD, et al (2019) Close to the edge: effects of repeated severe drought on  
 955 stem hydraulics and non-structural carbohydrates in European beech saplings. *Tree Physiol*  
 956 39:717–728. <https://doi.org/10.1093/treephys/tpy142>
- 957 Tumber-Dávila SJ, Schenk HJ, Du E, Jackson RB (2022) Plant sizes and shapes above and belowground  
 958 and their interactions with climate. *New Phytol* 235:1032–1056.  
 959 <https://doi.org/10.1111/nph.18031>
- 960 Unuk T, Martinović T, Finžgar D, et al (2019) Root-Associated Fungal Communities From Two  
 961 Phenologically Contrasting Silver Fir (*Abies alba* Mill.) Groups of Trees. *Front Plant Sci* 10:214.  
 962 <https://doi.org/10.3389/fpls.2019.00214>
- 963 Wambsganss J, Beyer F, Freschet GT, et al (2021) Tree species mixing reduces biomass but increases  
 964 length of absorptive fine roots in European forests. *J Ecol* 109:2678–2691.  
 965 <https://doi.org/10.1111/1365-2745.13675>
- 966 Wang C, Chen Z, Yin H, et al (2018) The Responses of Forest Fine Root Biomass/Necromass Ratio to  
 967 Environmental Factors Depend on Mycorrhizal Type and Latitudinal Region. *J Geophys Res*  
 968 *Biogeosciences* 123:1769–1788. <https://doi.org/10.1029/2017JG004308>
- 969 Wang J, Zhang H, Gao J, et al (2021) Effects of ectomycorrhizal fungi (*Suillus variegatus*) on the growth,  
 970 hydraulic function, and non-structural carbohydrates of *Pinus tabulaeformis* under drought  
 971 stress. *BMC Plant Biol* 21:1–13. <https://doi.org/10.1186/s12870-021-02945-3>
- 972 Wang M, Kong L, Zang M (2015) Effects of sample dimensions and shapes on measuring soil-water  
 973 characteristic curves using pressure plate. *J Rock Mech Geotech Eng* 7:463–468.  
 974 <https://doi.org/10.1016/j.jrmge.2015.01.002>
- 975 Wang Q, Garrity GM, Tiedje JM, Cole JR (2007) Naïve Bayesian classifier for rapid assignment of rRNA  
 976 sequences into the new bacterial taxonomy. *Appl Environ Microbiol* 73:5261–5267.  
 977 <https://doi.org/10.1128/AEM.00062-07>

- 978 Weemstra M, Sterck FJ, Visser EJW, et al (2017) Fine-root trait plasticity of beech (*Fagus sylvatica*) and  
979 spruce (*Picea abies*) forests on two contrasting soils. *Plant Soil* 415:175–188.  
980 <https://doi.org/10.1007/s11104-016-3148-y>
- 981 Weigt RB, Raidl S, Verma R, Agerer R (2012) Exploration type-specific standard values of extramatrical  
982 mycelium - a step towards quantifying ectomycorrhizal space occupation and biomass in natural  
983 soil. *Mycol Prog* 11:287–297. <https://doi.org/10.1007/s11557-011-0750-5>
- 984 Wiley E, King CM, Landhäusser SM (2019) Identifying the relevant carbohydrate storage pools available  
985 for remobilization in aspen roots. *Tree Physiol* 39:1109–1120.  
986 <https://doi.org/10.1093/treephys/tpz051>
- 987 Wilhelm RC, Munoz-Ucros J, Weigl F, et al (2022) The effects of mixed-species root zones on the  
988 resistance of soil bacteria and fungi to experimental and natural reductions in soil moisture. *J*  
989 *Ecol* 873:162266. <https://doi.org/10.1016/j.scitotenv.2023.162266>
- 990 Williams A, de Vries FT (2020) Plant root exudation under drought: implications for ecosystem  
991 functioning. *New Phytol* 225:1899–1905. <https://doi.org/10.1111/nph.16223>
- 992 Zang U, Goisser M, Grams TEE, et al (2014) Fate of recently fixed carbon in European beech (*Fagus*  
993 *sylvatica*) saplings during drought and subsequent recovery. *Tree Physiol* 34:29–38.  
994 <https://doi.org/10.1093/treephys/tpt110>
- 995



## Supplements

### Acclimation in root architecture rather than long-term adaptation of fungal symbiosis mitigates drought effect on European beech seedlings

Jasmin Danzberger, Kyohsuke Hikino, Simon M. Landhüsser, Benjamin D. Hesse, Sophie Meyer, Franz Buegger, Fabian Weikl, Thorsten E.E. Grams, Karin Pritsch

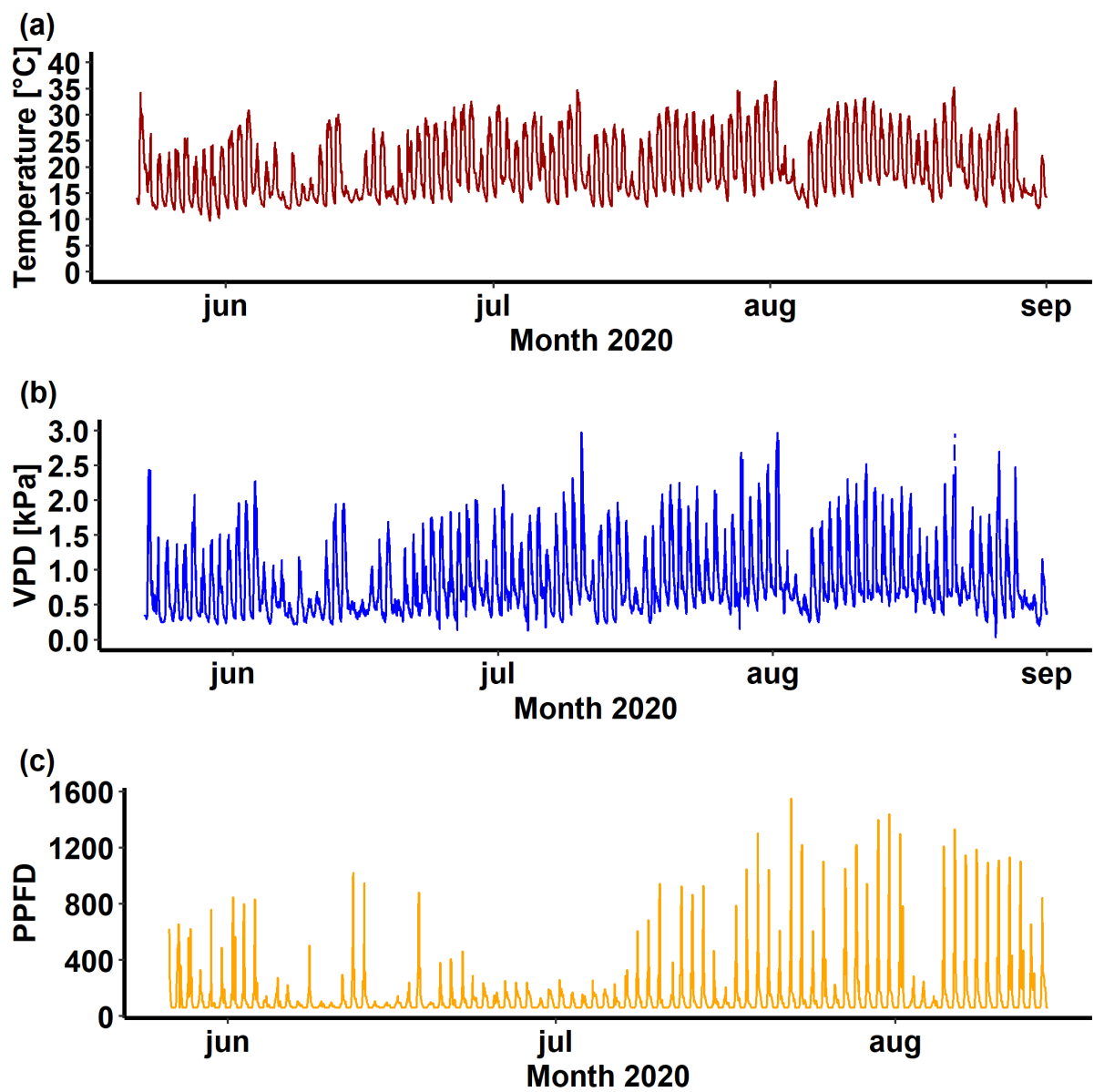
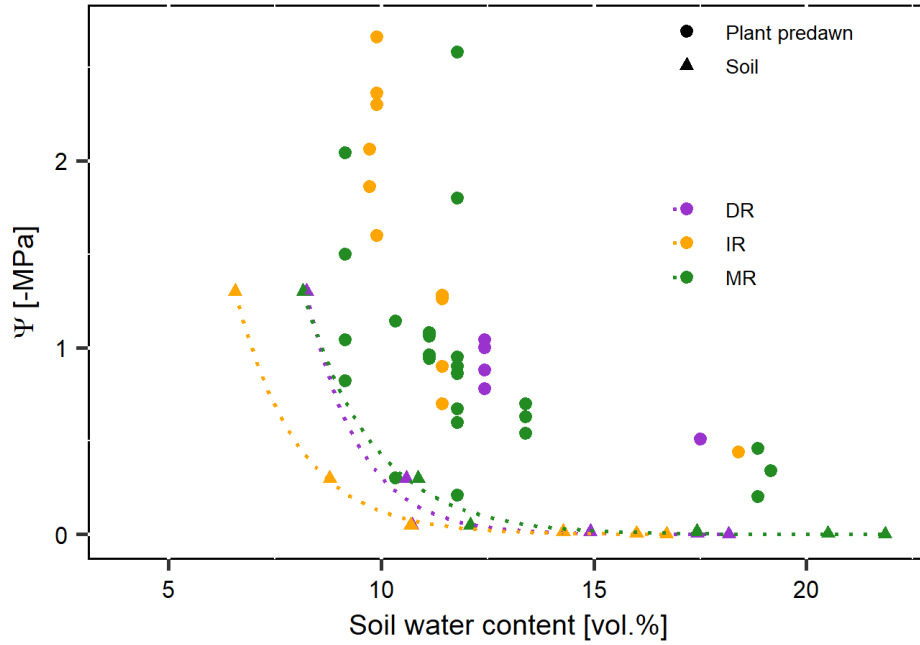
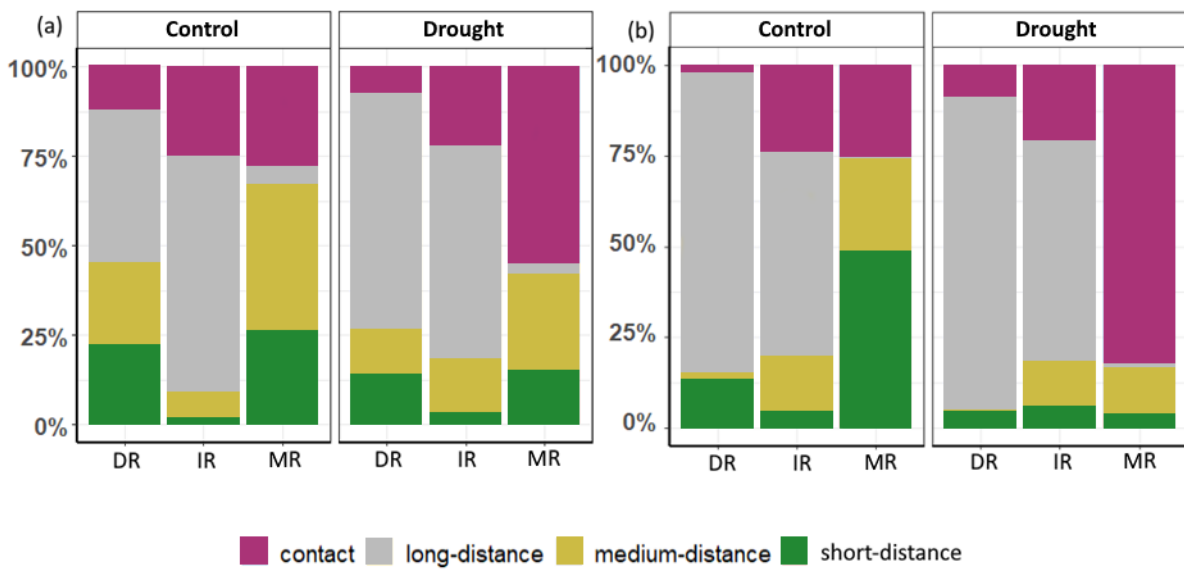


Fig. S1 a) Temperature, b) Vapour Pressure Deficit (VPD), and c) Photosynthetic photon flux density (PPFD) in the greenhouse.



**Fig. S2** Relationship between soil water potential ( $\Psi$ ) and soil water content (dotted lines and triangles) of the three different region soils; dry region (DR, purple), intermediate region (IR, yellow) and moist region (MR, green) soil. Circles represent the plant predawn water potential in the respective region soils at different soil water contents.



**Fig. S3** Summed up relative abundance of fungal exploration types, whereby contact types are represented in pink, long-distance types in grey, medium-distance types in gold and short-distance types in green in soil (a) and roots (b). Controls and drought treated samples are separated by different region soils (dry region = DR, intermediate region = IR, moist region = MR).

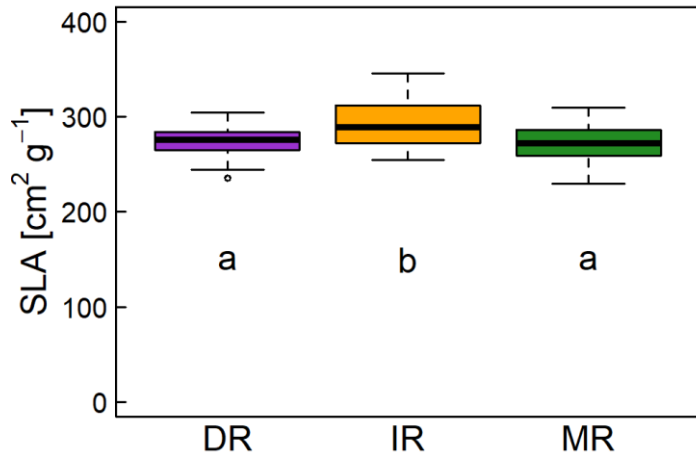


**Fig. S4** Specific leaf area (SLA) at the harvest in dry region (DR, purple), intermediate region (IR, yellow) and moist region (MR, green) soil. Lowercase letters indicate significant differences among the groups according to post-hoc test.

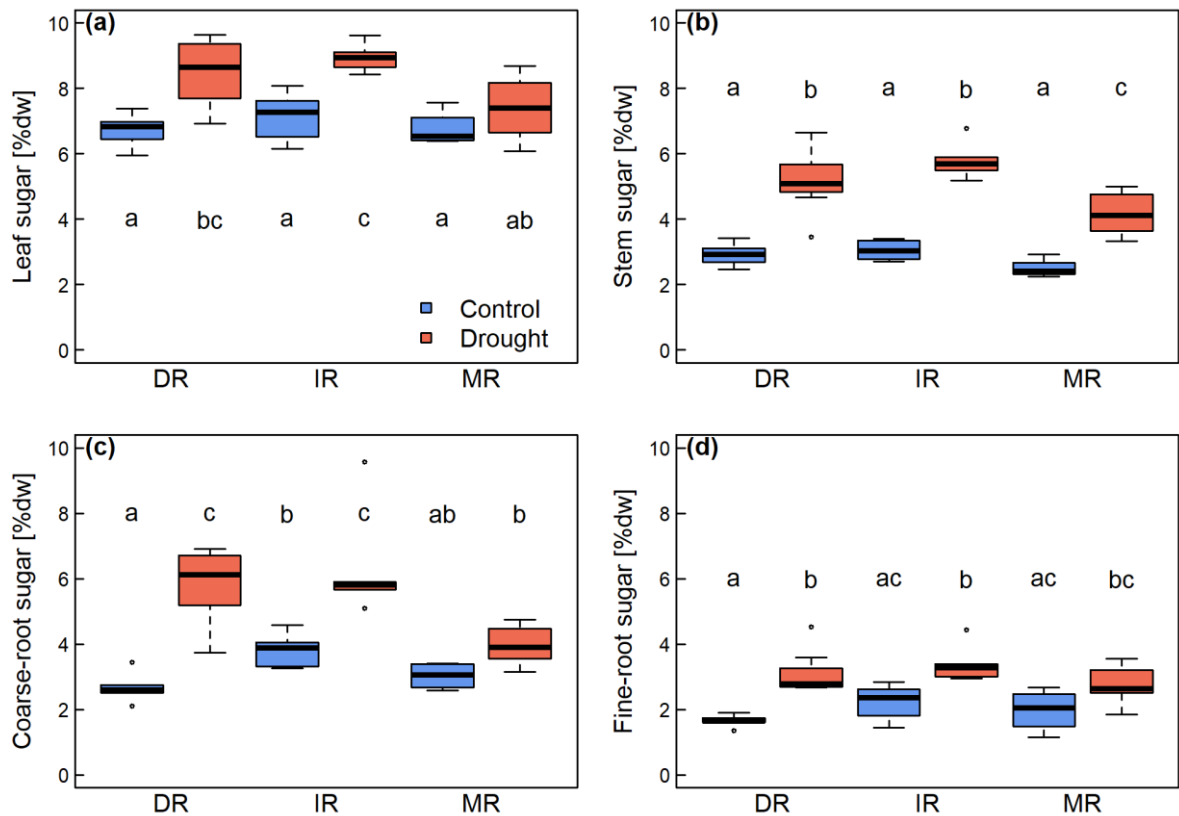


**Fig. S5** Sugar concentration in a) leaf, b) stem, c) coarse root, and d) fine root under control and drought treatments. Dry region (DR), intermediate region (IR) and moist region (MR) soil. Lowercase letters indicate significant differences among the groups according to post-hoc test.

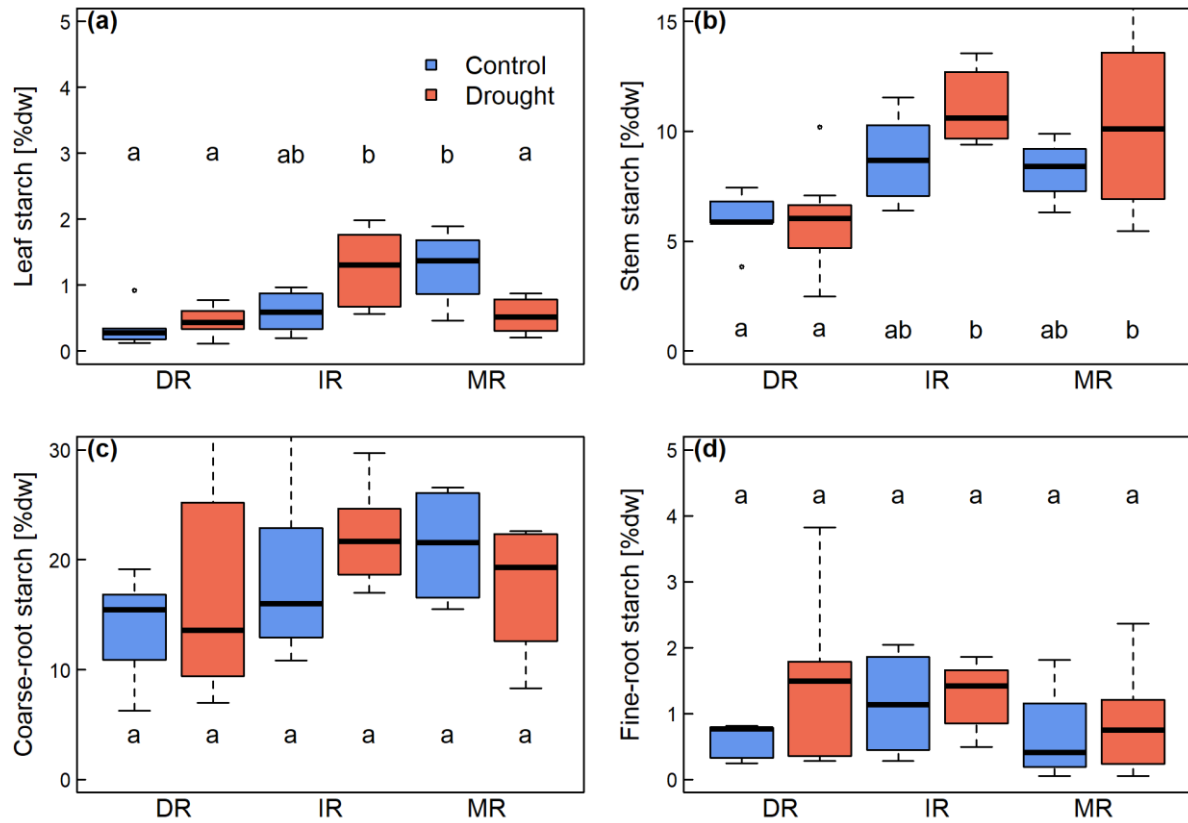


**Fig. S6** Starch concentration in a) leaf, b) stem, c) coarse root, and d) fine root under control and drought treatments. Dry region (DR), intermediate region (IR) and moist region (MR) soil. Lowercase letters indicate significant differences among the groups according to post-hoc test.

**Table S1** Soil characteristics at the three sites from Pretzsch et al. 2014.

	Arnstein (DR)	Kranzberg (IR)	Wasserburg (MR)
Parent material	Valley sediments	Loess over tertiary sediments	Morains from Würm glaciation
Soil quality	good	good	good
Cationexchange capacity	High	High	Medium
Waterholding capacity	High	High	High
P [mg/g]	0.04	0.04	0.05
C [%]	3.59	3.44	5.61
N [%]	0.20	0.20	0.27

**Table S2** Composition and nutrient content of the experimental soils from the dry, intermediate and moist regions (after mixing with 30 vol% quartzite sand).

	Dry region (DR)	Intermediate region (IR)	Moist region (MR)
C [%]	2.40	1.84	5.00
N [%]	0.16	0.12	0.23

C/N	15.50	15.20	21.49
Al [ $\mu\text{mol/g}$ ]	3.85	35.34	44.74
Ca [ $\mu\text{mol/g}$ ]	88.52	29.51	30.06
Fe [ $\mu\text{mol/g}$ ]	0.05	0.33	3.09
K [ $\mu\text{mol/g}$ ]	2.09	1.40	0.82
Mg [ $\mu\text{mol/g}$ ]	13.93	12.80	11.46
Mn [ $\mu\text{mol/g}$ ]	1.51	1.03	0.18
Na [ $\mu\text{mol/g}$ ]	4.06	3.10	4.17
P [ $\mu\text{mol/g}$ ]	0.02	0.03	0.03
Soil organic matter [%]	5.20 $\pm$ 0.29	5.80 $\pm$ 2.25	7.08 $\pm$ 1.35
pH(CaCl <sub>2</sub> )	4.98	4.15	3.89
pH(H <sub>2</sub> O)	5.27	4.64	4.30
pH(KCl)	4.31	3.69	3.54
Coarse sand [%]	28.60	33.40	49.90
Coarse silt [%]	21.20	22.70	10.90
Medium sand [%]	1.50	4.00	7.60
Medium silt [%]	18.60	15.00	8.20
Fine sand [%]	1.80	4.50	9.40
Fine silt [%]	5.60	4.20	4.10
Clay [%]	22.70	16.20	10.00

**Table S3** Stable C isotopic composition of leaves for the pre-labelling background, collected before the <sup>13</sup>C labelling.

	DR	IR	MR
Control	-28.03 $\pm$ 0.44	-28.45 $\pm$ 0.17	-28.16 $\pm$ 0.01
Drought	-28.22 $\pm$ 0.25	-29.02 $\pm$ 0.42	-28.19 $\pm$ 0.40

**Table S4** Climate conditions in the <sup>13</sup>C labelling tent during the labeling hours with the LED light on (6 am – 4 pm). Values are given as mean  $\pm$  SD. VPD: vapour pressure deficit, PPFD: photosynthetic photon flux density.

	1st labeling	2nd labeling	3rd labeling
atom%	18.9 $\pm$ 1.7	19.0 $\pm$ 0.1	19.0 $\pm$ 0.1
CO <sub>2</sub> concentration (ppm)	403 $\pm$ 25	397 $\pm$ 9	400 $\pm$ 10
Temperature ( $^{\circ}\text{C}$ )	30.2 $\pm$ 3.1	22.7 $\pm$ 2.8	31.2 $\pm$ 3.3
VPD (kPa)	1.3 $\pm$ 0.2	0.7 $\pm$ 0.2	1.4 $\pm$ 0.2
PPFD ( $\mu\text{mol m}^{-2} \text{s}^{-1}$ )	350 $\pm$ 20	363 $\pm$ 19	n.a.

**Table S5** Sequences of the individual primer for the amplification of ITS2 rDNA, according to Nickel et al. (2018) and Tedersoo et al. (2015). The DNA strand orientation is given as forward (fw) and reverse (rv), black nucleobases in the sequence refer to the ITS primer, blue nucleobases to the Illumina overhang.

Primer name	Orientation	Sequence	Target
ITS3-Mix1	fw	TCGTCGGCAGCGTCAGATGTGTATAAGAGACAG CATCGATGAAGAACGCAG	Fungi
ITS3-Mix2	fw	TCGTCGGCAGCGTCAGATGTGTATAAGAGACAG CAACGATGAAGAACGCAG	Chytridiomycota
ITS3-Mix3	fw	TCGTCGGCAGCGTCAGATGTGTATAAGAGACAG CACCGATGAAGAACGCAG	Sebacinales
ITS3-Mix4	fw	TCGTCGGCAGCGTCAGATGTGTATAAGAGACAG CATCGATGAAGAACGTAG	Glomeromycota
ITS3-Mix5	fw	TCGTCGGCAGCGTCAGATGTGTATAAGAGACAG CATCGATGAAGAACGTGG	Sordariales
ITS4-Mix1	rv	GTCTCGTGGGCTCGGAGATGTGTATAAGAGACAG TCCTCCGCTTATTGATATGC	Fungi
ITS4-Mix2	rv	GTCTCGTGGGCTCGGAGATGTGTATAAGAGACAG TCCTGCGCTTATTGATATGC	Chaetothyriales
ITS4-Mix3	rv	GTCTCGTGGGCTCGGAGATGTGTATAAGAGACAG TCCTCGCCTTATTGATATGC	Archaeorhizomycota
ITS4-Mix4	rv	GTCTCGTGGGCTCGGAGATGTGTATAAGAGACAG TCCTCCGCTGAWTAATATGC	Tulasnellaceae

**Table S6** The effects of treatment and region soil on different measured parameter. Significance was tested by a linear-mixed-model.

	Treatment	Region soil	Treatment x Region soil
	<i>F</i> -value ( <i>p</i> -value)	<i>F</i> -value ( <i>p</i> -value)	<i>F</i> -value ( <i>p</i> -value)
SWC at harvest	<b>554.786 (&lt;0.001)</b>	1.792 (0.177)	2.832 (0.069)
$\Psi_{PD}$ at harvest	<b>104.831 (&lt;0.001)</b>	<b>8.310 (&lt;0.001)</b>	<b>11.726 (&lt;0.001)</b>
Net carbon assimilation rates	<b>42.626 (&lt;0.001)</b>	<b>3.391 (&lt;0.05)</b>	<b>8.886 (&lt;0.001)</b>
Stomatal conductance	<b>109.275 (&lt;0.001)</b>	1.102 (0.341)	<b>8.952 (&lt;0.001)</b>
Initial biomass	0.027 (0.870)	<b>56.909 (&lt;0.001)</b>	0.291 (0.749)
Biomass at harvest	<b>11.873 (&lt;0.01)</b>	<b>11.023 (&lt;0.001)</b>	0.126 (0.882)
Relative stem growth	<b>7.036 (&lt;0.05)</b>	<b>3.422 (&lt;0.05)</b>	1.423 (0.252)
Root to shoot ratio	<b>11.538 (&lt;0.01)</b>	<b>6.960 (&lt;0.01)</b>	1.223 (0.303)
SLA (specific leaf area)	2.217 (0.143)	<b>4.294 (&lt;0.05)</b>	2.643 (0.083)
Taproot length	<b>42.64 (&lt; 0.001)</b>	<b>21.98 (&lt; 0.001)</b>	2.18 (0.12)
Branching intensity	<b>41.64 (&lt; 0.001)</b>	<b>6.72 (0.003)</b>	2.32 (0.11)
Vital tips	<b>6.00 (0.02)</b>	1.31 (0.28)	<b>3.24 (0.05)</b>
Degree of mycorrhization	<b>16.74 (&lt; 0.001)</b>	<b>8.92 (&lt; 0.001)</b>	1.69 (0.19)
Ratio belowground to total newly assimilated C	<b>18.661 (&lt;0.001)</b>	<b>5.309 (&lt;0.01)</b>	<b>4.728 (&lt;0.05)</b>
Leaf sugar concentration	<b>24.226 (&lt;0.001)</b>	<b>6.081 (&lt;0.01)</b>	2.741 (0.082)

Stem sugar concentration	<b>131.056 (&lt;0.001)</b>	<b>12.414 (&lt;0.001)</b>	0.950 (0.399)
Coarse root sugar concentration	<b>78.370 (&lt;0.001)</b>	<b>18.698 (&lt;0.001)</b>	<b>10.865 (&lt;0.001)</b>
Fine root sugar concentration	<b>37.191 (&lt;0.001)</b>	2.858 (0.074)	1.089 (0.351)
Leaf starch concentration	0.293 (0.592)	<b>5.798 (&lt;0.01)</b>	<b>3.808 (&lt;0.05)</b>
Stem starch concentration	1.159 (0.291)	<b>11.963 (&lt;0.001)</b>	0.879 (0.426)
Coarse root starch concentration	0.037 (0.849)	<b>4.339 (&lt;0.05)</b>	0.232 (0.794)
Fine root starch concentration	0.705 (0.408)	2.473 (0.103)	0.091 (0.914)
Ratio belowground to total sugar pool	0.006 (0.940)	1.318 (0.284)	0.323 (0.727)
Ratio belowground to total starch pool	0.159 (0.694)	<b>3.450 (&lt;0.05)</b>	0.797 (0.464)

**Table S7** Fungal alpha-diversity based on rDNA displayed by Shannon Index, Simpson Index, Pielou's Evenness and Species richness summarised by treatment and region soil (RS; DR = dry region, IR = intermediate region, MR = moist region). Values are displayed as means  $\pm$  standard error. The influence of treat and RS on fungal diversity was tested using either Kruskal-Wallis test ( $\chi^2$ ) or ANOVA ( $F$ ). Bold numbers indicate significances and df degrees of freedom.

Soil fungi									
Treat	RS	Shannon	Simpson	Species Richness	Evenness				
Control	DR	4.8 $\pm$ 0.1	1.0 $\pm$ 0.0	574.3 $\pm$ 27.1	0.8 $\pm$ 0.0				
Control	IR	4.4 $\pm$ 0.1	1.0 $\pm$ 0.0	419.2 $\pm$ 18.1	0.7 $\pm$ 0.0				
Control	MR	4.4 $\pm$ 0.0	1.0 $\pm$ 0.0	433.5 $\pm$ 8.4	0.7 $\pm$ 0.0				
Drought	DR	4.7 $\pm$ 0.1	1.0 $\pm$ 0.0	542.6 $\pm$ 22.4	0.7 $\pm$ 0.0				
Drought	IR	4.4 $\pm$ 0.0	1.0 $\pm$ 0.0	419.7 $\pm$ 6.2	0.7 $\pm$ 0.0				
Drought	MR	4.5 $\pm$ 0.0	1.0 $\pm$ 0.0	448.2 $\pm$ 10.6	0.7 $\pm$ 0.0				
	df	$\chi^2$	$p$	$\chi^2$	$p$	$\chi^2$	$p$	$\chi^2$	$p$
Treat	1	2.1	0.1	3.0	0.1	1.5	0.2	2.1	0.1
RS	2	<b>14.8</b>	<b>&lt; 0.001</b>	1.9	0.4	<b>31.0</b>	<b>&lt; 0.001</b>	6.1	0.05

Root-associated fungi									
Treat	RS	Shannon	Simpson	Species Richness	Evenness				
Control	DR	3.6 $\pm$ 0.1	0.9 $\pm$ 0.0	317.9 $\pm$ 9.2	0.6 $\pm$ 0.0				
Control	IR	3.3 $\pm$ 0.1	0.9 $\pm$ 0.0	246.9 $\pm$ 9.9	0.6 $\pm$ 0.0				
Control	MR	3.7 $\pm$ 0.0	0.9 $\pm$ 0.0	291 $\pm$ 0.0	0.6 $\pm$ 0.0				
Drought	DR	3.5 $\pm$ 0.1	0.9 $\pm$ 0.0	301.5 $\pm$ 27.0	0.6 $\pm$ 0.0				
Drought	IR	3.5 $\pm$ 0.2	0.9 $\pm$ 0.0	288.7 $\pm$ 26.9	0.6 $\pm$ 0.0				
Drought	MR	3.8 $\pm$ 0.1	0.9 $\pm$ 0.0	301.8 $\pm$ 21.7	0.7 $\pm$ 0.0				
	df	$F$	$p$	$F$	$p$	$F$	$p$	$F$	$p$
Treat	1	1.3	0.3	0.1	0.8	1.0	0.3	1.0	0.3
RS	2	<b>5.1</b>	<b>0.01</b>	2.3	0.1	<b>6.5</b>	<b>&lt; 0.005</b>	<b>3.9</b>	<b>0.03</b>

**Table S8** Ten most abundant soil saprotrophic fungal species divided by soil (DR = dry region, IR = intermediate region, MR = moist region) and control and drought treated. % displays the species abundance in percent. Sec. Life. gives information

about a facultative secondary lifestyle according to Pölme et al., (2020), whereby r.-endo. = root-endophyte, r.-assoc. = root-associated, lit.-sap. = litter-saprotroph, p.-path. = plant pathogen and epi. = epiphyte.

	Control			Drought		
	Species	%	Sec. Life.	Species	%	Sec. Life.
DR	<i>Penicillium</i> sp.	21,4	-	<i>Penicillium</i> sp.	20,1	-
	<i>Mortierella</i> sp.	12,4	r.-assoc.	<i>Mortierella</i> sp.	14,9	r.-assoc.
	<i>Cladosporium</i> sp.	5,6	p.-path.	<i>Absidia cylindrospora</i>	4,8	-
	<i>Oidiodendron chlamydosporicum</i>	4,0	r.-endo.	<i>Oidiodendron chlamydosporicum</i>	3,9	r.-endo.
	<i>Absidia cylindrospora</i>	3,9	-	<i>Solicoccozyma terricola</i>	3,6	epi.
	<i>Geomyces auratus</i>	3,1	-	<i>Mortierella</i> sp.	3,0	r.-assoc.
	<i>Apiotrichum</i> sp.	3,1	-	<i>Geomyces auratus</i>	3	-
	<i>Solicoccozyma terricola</i>	2,8	epi.	<i>Cladosporium</i> sp.	2,6	p.-path.
	<i>Cephalotrichum stemonitis</i>	2,7	-	<i>Clonostachys divergens</i>	2,3	p.-path.
	<i>Clonostachys</i> sp.	2,4	p.-path.	<i>Mortierella</i> sp.	2,1	r.-assoc.
IR	<i>Solicoccozyma terricola</i>	18,6	epi.	<i>Solicoccozyma terricola</i>	18,2	epi.
	<i>Mortierella</i> sp.	10,9	r.-assoc.	<i>Mortierella</i> sp.	12,4	r.-assoc.
	<i>Penicillium</i> sp.	5,4	-	<i>Penicillium</i> sp.	7,2	-
	<i>Apiotrichum</i> sp.	5,2	-	<i>Apiotrichum</i> sp.	5,0	-
	<i>Archaeorhizomyces</i> sp.	4,0	r.-assoc.	<i>Oidiodendron</i> sp.	3,8	r.-endo.
	<i>Oidiodendron</i> sp.	4,0	r.-endo.	<i>Mortierella pseudozygospora</i>	3,6	r.-assoc.
	<i>Mortierella</i> sp.	3,6	r.-assoc.	<i>Archaeorhizomyces</i> sp.	3,5	r.-assoc.
	<i>Apiotrichum wieringae</i>	3,6	-	<i>Apiotrichum wieringae</i>	3,4	-
	<i>Geomyces auratus</i>	3,2	-	<i>Geomyces auratus</i>	3,1	-
	<i>Mortierella pseudozygospora</i>	2,5	r.-assoc.	<i>Mortierella</i> sp.	2,8	r.-assoc.
MR	<i>Solicoccozyma terricola</i>	15	epi.	<i>Solicoccozyma terricola</i>	14,5	epi.
	<i>Oidiodendron chlamydosporicum</i>	13,5	r.-endo.	<i>Oidiodendron chlamydosporicum</i>	12,2	r.-endo.
	<i>Mortierella longigemmata</i>	8,3	r.-assoc.	<i>Mortierella longigemmata</i>	8,8	r.-assoc.
	<i>Mortierella</i> sp.	7,1	r.-assoc.	<i>Mortierella</i> sp.	7,8	r.-assoc.
	<i>Umbelopsis</i> sp.	6,8	r.-assoc.	<i>Oidiodendron</i> sp.	6,7	r.-endo.
	<i>Umbelopsis</i> sp.	6,4	r.-assoc.	<i>Umbelopsis</i> sp.	6,5	r.-assoc.
	<i>Oidiodendron</i> sp.	6,2	r.-endo.	<i>Umbelopsis</i> sp.	6,4	r.-assoc.
	<i>Oidiodendron</i> sp.	3,9	r.-endo.	<i>Oidiodendron</i> sp.	3,2	r.-endo.
	<i>Penicillium</i> sp.	3,6	-	<i>Penicillium</i> sp.	2,8	-
	<i>Archaeorhizomyces</i> sp,	2,9	r.-assoc.	<i>Cladophialophora</i> sp.	2,3	r.-endo.

**Table S9** Ten most abundant soil ECM fungal species divided by soil (DR = dry region, IR = intermediate region, MR = moist region) and control and drought treated. % displays the species abundance in percent. ET stands for exploration type assigned by Agerer (2001) (C = contact, SD = short-distance, MD = medium-distance, LD = long-distance and UK = unknown) and DT for drought tolerating. A + hereby indicates a drought-tolerating species. Lit. gives the respective literature to fungal drought tolerance.

	Control				Drought			
	Species	%	ET & DT	Lit.	Species	%	ET & DT	Lit.
DR	<i>Melanogaster</i> sp.	36,5	LD; +	7, 8	<i>Melanogaster</i> sp.	62,1	LD; +	7, 8
	<i>Piloderma</i> sp.	17,1	MD		<i>Piloderma</i> sp.	8,1	MD	
	<i>Tuber puberulum</i>	12,2	SD		<i>Inocybe asterospora</i>	7,8	SD; +	5



	<i>Clavulina</i> sp.	7,2	C		<i>Clavulina</i> sp.	4,3	C	
	<i>Melanogaster broomeanus</i>	5,6	LD; +	7, 8	<i>Melanogaster broomeanus</i>	3,1	LD; +	7, 8
	<i>Cenococcum</i> sp.	2,8	SD; +		<i>Cenococcum</i> sp.	2,5	SD; +	
	<i>Inocybe asterospora</i>	2,6	SD; +	5	<i>Hydnotrya</i> sp.	1,6	C	
	<i>Hydnotrya</i> sp.	1,9	C		<i>Rhodoscypha</i> sp.	1,3	UK	
	<i>Rhodoscypha</i> sp.	1,7	UK		<i>Sebacina incrustans</i>	1,1	SD	
	<i>Sebacina</i> sp.	1,5	SD		<i>Inocybe cincinnata</i>	1,0	SD; +	6
IR	<i>Melanogaster</i> sp.	63,8	LD; +	7, 8	<i>Melanogaster</i> sp.	57,6	LD; +	7, 8
	<i>Clavulina</i> sp.	24,1	C		<i>Clavulina</i> sp.	21,1	C	
	<i>Tomentella</i> sp.	3,5	MD		<i>Lactarius subdulcis</i>	10,5	MD	
	<i>Cortinarius</i> sp.	2,6	MD; +	2,3,4	<i>Cortinarius</i> sp.	3,4	MD; +	2,3,4
	<i>Cenococcum</i> sp.	1,5	SD; +		<i>Cenococcum</i> sp.	2,2	SD; +	
	<i>Rhizopogon</i> sp.	1,5	LD; +	9	<i>Rhizopogon</i> sp.	1,8	LD; +	9
	<i>Russula foetens</i>	0,8	C		<i>Thelephora</i> sp.	1,0	MD; +	1
	<i>Pseudotomentella mucidula</i>	0,7	MD		<i>Russula foetens</i>	0,7	C	
	<i>Thelephora</i> sp.	0,3	MD; +	1	<i>Pseudotomentella mucidula</i>	0,3	MD	
	<i>Tuber</i> sp.	0,2	SD		<i>Hymenogaster rehsteineri</i>	0,3	SD	
MR	<i>Lactarius</i> sp.	24,2	MD		<i>Amanita</i> sp.	30,4	C; +	1
	<i>Amanita</i> sp.	23,9	C; +	1	<i>Hydnotrya tulasnei</i>	20,5	C	
	<i>Hebeloma radicosum</i>	23,8	SD		<i>Piloderma sphaerosporum</i>	8,6	MD	
	<i>Pseudotomentella mucidula</i>	4,4	MD		<i>Phaeocollybia</i> sp.	6,9	UK	
	<i>Gautieria morchelliformis</i>	3,7	MD		<i>Inocybe</i> sp.	4,9	SD; +	6
	<i>Thelephora</i> sp.	2,2	MD; +	1	<i>Pseudotomentella mucidula</i>	4,6	MD	
	<i>Inocybe</i> sp.	2,1	SD; +	6	<i>Lactarius</i> sp.	4,0	MD	
	<i>Pseudotomentella mucidula</i>	2,0	MD		<i>Elaphomyces granulatus</i>	2,9	SD	
	<i>Cortinarius</i> sp.	2,0	MD; +	2,3,4	<i>Hebeloma radicosum</i>	2,8	SD	
	<i>Hydnotrya tulasnei</i>	2,0	C		<i>Tylospora asterophora</i>	2,8	SD	

1: Querejeta *et al.* (2003); 2: Boczoń *et al.* (2021); 3: de Jalón *et al.* (2020); 4: Bödeker *et al.* (2014); 5: Maghnia *et al.* (2017); 6: Long *et al.* (2016); 7: Izzo *et al.* (2005); 8: Frey *et al.* (2021); 9: Steinfeld *et al.* (2003)

**Table S10** Ten most abundant root-associated saprotrophic fungal species divided by soil (DR = dry region, IR = intermediate region, MR = moist region) and control and drought treated. % displays the species abundance in percent. Sec. Life. gives information about a facultative secondary lifestyle according to Pölme *et al.*, (2020), whereby r.-endo. = root-endophyte, r.-assoc. = root-associated, lit.-sap. = litter-saprotroph, p.-path. = plant pathogen and epi. = epiphyte.

	Control			Drought		
	Species	%	Sec. Life.	Species	%	Sec. Life.
DR	<i>Oidiodendron</i> sp.	21,5	r.-endo.	<i>Penicillium</i> sp.	34	-
	<i>Penicillium</i> sp.	19,9	-	<i>Oidiodendron</i> sp.	26,6	r.-endo.
	<i>Mycena olivaceomarginata</i>	13,3	r.-assoc.	<i>Mycena olivaceomarginata</i>	10,8	r.-assoc.
	<i>Oidiodendron echinulatum</i>	12,1	r.-endo.	<i>Oidiodendron echinulatum</i>	6,8	r.-endo.
	<i>Geomyces auratus</i>	7,0	-	<i>Geomyces auratus</i>	5,4	-
	<i>Oidiodendron rhodogenum</i>	4,0	r.-endo.	<i>Mortierella</i> sp.	2,4	r.-assoc.
	<i>Mycena sanguinolenta</i>	3,1	r.-assoc.	<i>Flagelloscypha</i> sp.	1,5	-
	<i>Mortierella</i> sp.	1,9	r.-assoc.	<i>Hyaloscypha finlandica</i>	1,1	-

	<i>Oidiodendron</i> sp.	1,6	r.-endo.	<i>Oidiodendron chlamyosporicum</i>	0,9	r.-endo.
	<i>Cephalotrichum stemonitis</i>	1,2	-	<i>Oidiodendron</i> sp.	0,8	r.-endo.
IR	<i>Oidiodendron</i> sp.	24,3	r.-endo.	<i>Oidiodendron</i> sp.	33,2	r.-endo.
	<i>Oidiodendron</i> sp.	19,3	r.-endo.	<i>Penicillium</i> sp.	15,1	-
	<i>Oidiodendron echinulatum</i>	10,7	r.-endo.	<i>Oidiodendron echinulatum</i>	13,1	r.-endo.
	<i>Galerina</i> sp.	8,2	Lit.-sap.	<i>Oidiodendron</i> sp.	8,1	r.-endo.
	<i>Phialocephala</i> sp.	7,4	r.-endo.	<i>Phialocephala</i> sp.	6,7	r.-endo.
	<i>Phialocephala</i> sp.	6,9	r.-endo.	<i>Phialocephala</i> sp.	4,9	r.-endo.
	<i>Penicillium</i> sp.	5,3	-	<i>Mortierella</i> sp.	2,0	r.-assoc.
	<i>Cladophialophora</i> sp.	2,2	r.-endo.	<i>Mortierella</i> sp.	1,5	r.-assoc.
	<i>Archaeorhizomyces</i> sp.	1,5	r.-assoc.	<i>Clonostachys</i> sp.	1,5	p.-path.
	<i>Mortierella</i> sp.	1,3	r.-assoc.	<i>Geomyces auratus</i>	1,1	-
MR	<i>Oidiodendron</i> sp.	32,9	r.-endo.	<i>Oidiodendron rhodogenum</i>	43,8	r.-endo.
	<i>Galerina</i> sp.	10,4	Lit.-sap.	<i>Oidiodendron</i> sp.	17,6	r.-endo.
	<i>Oidiodendron rhodogenum</i>	9,5	r.-endo.	<i>Oidiodendron echinulatum</i>	5,7	r.-endo.
	<i>Phialocephala</i> sp.	9,4	r.-endo.	<i>Phialocephala</i> sp.	3,9	r.-endo.
	<i>Cladophialophora</i> sp.	5,4	r.-endo.	<i>Penicillium</i> sp.	3,2	-
	<i>Clonostachys divergens</i>	3,8	p.-path.	<i>Oidiodendron</i> sp.	2,6	r.-endo.
	<i>Oidiodendron echinulatum</i>	3,8	r.-endo.	<i>Athelopsis lembospora</i>	1,7	-
	<i>Penicillium</i> sp.	2,9	-	<i>Galerina</i> sp.	1,6	Lit.-sap.
	<i>Oidiodendron</i> sp.	2,4	r.-endo.	<i>Cladosporium</i> sp.	1,5	p.-path.
	<i>Hyaloscypha finlandica</i>	1,7	-	<i>Oidiodendron chlamyosporicum</i>	1,5	r.-endo.

**Table S11** Ten most abundant root-associated ECM fungal species divided by soil (DR = dry region, IR = intermediate region, MR = moist region) and control and drought treated. % displays the species abundance in percent. ET stands for exploration type assigned by Agerer (2001) (C = contact, SD = short-distance, MD = medium-distance and LD = long-distance) and DT for drought tolerating. A + hereby indicates a drought-tolerating species. Lit. gives the respective literature to fungal drought tolerance.

	Control	%	ET & DT	Lit.	Drought	%	ET & DT	Lit.
	Species				Species			
DR	<i>Melanogaster</i> sp.	83,0	LD; +	7, 8	<i>Melanogaster</i> sp.	95,2	LD; +	7, 8
	<i>Tuber puberulum</i>	9,0	SD		<i>Cenococcum</i> sp.	3,7	SD; +	
	<i>Cenococcum</i> sp.	3,7	SD; +		<i>Sebacina</i> sp.	0,4	SD	
	<i>Clavulina</i> sp.	1,6	C		<i>Piloderma</i> sp.	0,1	MD	
	<i>Tomentella</i> sp.	0,7	MD		<i>Piloderma</i> sp.	0,1	MD	
	<i>Amphinema byssoides</i>	0,3	MD		<i>Tylospora asterophora</i>	0,1	SD	
	<i>Inocybe asterospora</i>	0,3	SD; +	5	<i>Clavulina</i> sp.	0,1	C	
	<i>Piloderma</i> sp.	0,2	MD		<i>Sebacina</i> sp.	0,0	SD	
	<i>Melanogaster broomeanus</i>	0,2	LD; +	7, 8	<i>Melanogaster broomeanus</i>	0,0	LD; +	7, 8
	<i>Piloderma</i> sp.	0,1	MD		<i>Piloderma</i> sp.	0,0	MD	
IR	<i>Melanogaster</i> sp.	56,4	LD; +	7, 8	<i>Melanogaster</i> sp.	60,8	LD; +	7, 8
	<i>Clavulina</i> sp.	23	C		<i>Clavulina</i> sp.	20,0	C	
	<i>Tomentella</i> sp.	10,2	MD		<i>Lactarius subdulcis</i>	12,8	MD	
	<i>Lactarius subdulcis</i>	4,5	MD		<i>Cenococcum</i> sp.	5,7	SD; +	
	<i>Cenococcum</i> sp.	3,1	SD; +		<i>Russula</i> sp.	0,2	C	

	<i>Hymenogaster huthii</i>	1,0	SD		<i>Amanita</i> sp.	0,1	C; +	1
	<i>Cortinarius obtusus</i>	0,7	MD; +	2,3,4	<i>Russula foetens</i>	0,1	C	
	<i>Russula</i> sp.	0,5	C		<i>Cortinarius</i> sp.	0,1	MD; +	2,3,4
	<i>Hymenogaster rehsteineri</i>	0,3	SD		<i>Hymenogaster rehsteineri</i>	0,0	SD	
	<i>Hydnотrya tulasnei</i>	0,1	C		<i>Rhizopogon</i> sp.	0,0	LD; +	9
MR	<i>Sebacina</i> sp.	96,0	SD		<i>Amanita</i> sp.	77,8	C; +	1
	<i>Hydnотrya tulasnei</i>	1,7	C		<i>Thelephora terrestris</i>	14,7	MD; +	1
	<i>Cenococcum</i> sp.	1,2	SD; +		<i>Cenococcum</i> sp.	4,4	SD; +	
	<i>Amanita</i> sp.	0,4	C; +	1	<i>Hydnотrya tulasnei</i>	0,9	C	
	<i>Piloderma sphaerosporum</i>	0,3	MD		<i>Piloderma sphaerosporum</i>	0,9	MD	
	<i>Clavulina</i> sp.	0,2	C		<i>Melanogaster</i> sp.	0,8	LD; +	7, 8
	<i>Gautieria morchelliformis</i>	0,1	MD		<i>Sebacina</i> sp.	0,1	SD	
	<i>Hysterangium nephriticum</i>	0,1	MD		<i>Russula</i> sp.	0,1	C	
	<i>Tuber</i> sp.	0,1	SD		<i>Octaviania asterosperma</i>	0,0	LD	
	<i>Amphinema</i> sp.	0,0	MD		<i>Pseudotomentella mucidula</i>	0,0	MD	

1: Querejeta *et al.* (2003); 2: Boczoń *et al.* (2021); 3: de Jalón *et al.* (2020); 4: Bödeker *et al.* (2014); 5: Maghnia *et al.* (2017); 6: Long *et al.* (2016); 7: Izzo *et al.* (2005); 8: Frey *et al.* (2021); 9: Steinfeld *et al.* (2003)

#### Method S1 DNA library preparation

Per sample, one reaction mix contained: 10 µl NEBNext High-Fidelity 2X PCR MasterMix (New England Biolabs, Frankfurt, Germany), 0.5 µl 10 pmol ITS3 tagmix forward primer, 0.5 µl 10 pmol ITS4 tagmix reverse primer, 8 µl ultra-pure H<sub>2</sub>O and 1 µl (c)DNA. PCR conditions were 5 min at 95°C, 28 cycles [30 s at 95°C, 30 s at 55°C, 60 s at 72°C] and 10 min at 72°C. When the success of the PCRs was confirmed on a 2 % agarose gel, the triplicates were pooled, purified and cleared from primer dimers via Agencourt AMPure XP DNA purification (Beckman Coulter, Krefeld, Germany) (bead:sample ratio 1:1). If no primer dimers were detected on a subsequent 2 % agarose gel, the DNA concentration was determined using the AccuClear Ultra High Sensitivity dsDNA Quantification (Biotium, Fremont, CA, USA), a microplate reader Infinite M1000 Pro and accompanying software i-control (Tecan, Männedorf, Switzerland) and then diluted to 5 ng. Thereafter, individual combinations of Illumina primers (Nextera XT Index Kit v2 Sets A-D) were attached to the amplicons via indexing PCR for future sample identification, with the PCR-mix containing per sample: 1 µl (c)DNA (5 ng), 2.5 µl Nexera i7 primer, 2.5 µl Nexera i5 primer, 12.5 µl NEBNext High-Fidelity 2X PCR MasterMix and 6.5 µl ultra-pure H<sub>2</sub>O. Conditions were 3 min at 95°C, 8 cycles [30 s at 95°C, 30 s at 55°C, 30 s at 72°C] and 10 min at 72°C. As before, the products were purified and the fragment length checked. In addition, samples were randomly tested with a Fragment Analyzer (Advanced Analytical, Heidelberg, Germany) (protocol DNF-473 Standard Sensitivity NGS-Fragment Analysis Kit 1 bp – 6000 bp) before and after indexing. If the fragment lengths were correct and no primer dimers were present, the samples were diluted to 10 nM, pooled and the amount determined using a Qubit 3 (Invitrogen, Carlsbad, CA, USA). The library was finally diluted to 4 nM and further steps were carried out according to Illumina protocol for 16S Metagenomic Sequencing Library Preparation (protocol Part # 15044223 Rev. B) and sequenced on a Miseq v3chemistry, 600 cycles flow cell (Illumina, San Diego, CA, USA).

## References

- Agerer, R. (2001) 'Exploration types of ectomycorrhizae', *Mycorrhiza*, 11(2), pp. 107–114. doi: 10.1007/s005720100108.
- Boczoń, A. *et al.* (2021) 'Drought in the forest breaks plant–fungi interactions', *European Journal of Forest Research*, 140(6), pp. 1301–1321. doi: 10.1007/s10342-021-01409-5.
- Bödeker, I. T. M. *et al.* (2014) 'Ectomycorrhizal Cortinarius species participate in enzymatic oxidation of humus in northern forest ecosystems', *New Phytologist*, 203(1), pp. 245–256. doi: 10.1111/nph.12791.
- Frey, B. *et al.* (2021) 'Deep Soil Layers of Drought-Exposed Forests Harbor Poorly Known Bacterial and Fungal Communities', *Frontiers in Microbiology*, 12(May). doi: 10.3389/fmicb.2021.674160.
- Izzo, A. D. *et al.* (2005) 'Hypogeous Ectomycorrhizal Fungal Species on Roots and in Small Mammal Diet in a Mixed-Conifer Forest', *Forest Science*, 51(3), pp. 243–254. Available at: <https://doi.org/10.1093/forestscience/51.3.243>.
- de Jalón, L. G. *et al.* (2020) 'Microhabitat and ectomycorrhizal effects on the establishment, growth and survival of *Quercus ilex* L. Seedlings under drought', *PLoS ONE*, 15(6). doi: 10.1371/journal.pone.0229807.
- Long, D. *et al.* (2016) 'Ectomycorrhizal fungal communities associated with *Populus simonii* and *Pinus tabuliformis* in the hilly-gully region of the Loess Plateau, China', *Scientific Reports*, 6(April), pp. 1–10. doi: 10.1038/srep24336.
- Maghnia, F. Z. *et al.* (2017) 'Habitat- and soil-related drivers of the root-associated fungal community of *Quercus suber* in the Northern Moroccan forest', *PLoS ONE*, 12(11), pp. 1–17. doi: 10.1371/journal.pone.0187758.
- Pölme, S. *et al.* (2020) 'FungalTraits: a user-friendly traits database of fungi and fungus-like stramenopiles', *Fungal Diversity*, 105(1). doi: 10.1007/s13225-020-00466-2.
- Querejeta, J. I., Egerton-Warburton, L. M. and Allen, M. F. (2003) 'Direct nocturnal water transfer from oaks to their mycorrhizal symbionts during severe soil drying', *Oecologia*, 134(1), pp. 55–64. doi: 10.1007/s00442-002-1078-2.
- Steinfeld, D., Amaranths, M. P. and Cazares, E. (2003) 'Survival of ponderosa pine (*Pinus ponderosa* dougl. ex laws.) seedlings outplanted with *Rhizopogon mycorrhizae* inoculated with spores at the nursery', *Journal of Arboriculture*, 29(4), pp. 197–203. doi: 10.48044/jauf.2003.023.

# Article I: High resilience of carbon transport in long-term drought-stressed mature Norway spruce trees within 2 weeks after drought release

Hikino, K., Danzberger, J., Riedel, V. P., Rehschuh, R., Ruehr, N. K., Hesse, B. D., Lehmann, M. M., Buegger, F., Weikl, F., Pritsch, K., & Grams, T. E. E. (2021). *Global Change Biology*.

## Open Access Publication



### High resilience of carbon transport in long-term drought-stressed mature Norway spruce trees within 2 weeks after drought release

**Author:** Thorsten E. E. Grams, Karin Pritsch, Fabian Weikl, et al

**Publication:** *Global Change Biology*

**Publisher:** John Wiley and Sons

**Date:** Dec 29, 2021

© 2021 The Authors. *Global Change Biology* published by John Wiley & Sons Ltd.

#### Open Access Article

This is an open access article distributed under the terms of the [Creative Commons CC BY](#) license, which permits unrestricted use, distribution, and reproduction in any medium, provided the original work is properly cited.

You are not required to obtain permission to reuse this article.

For an understanding of what is meant by the terms of the Creative Commons License, please refer to [Wiley's Open Access Terms and Conditions](#).

Permission is not required for this type of reuse.











Wiley offers a professional reprint service for high quality reproduction of articles from over 1400 scientific and medical journals. Wiley's reprint service offers:

- Peer reviewed research or reviews
- Tailored collections of articles
- A professional high quality finish
- Glossy journal style color covers
- Company or brand customisation
- Language translations
- Prompt turnaround times and delivery directly to your office, warehouse or congress.

Please contact our Reprints department for a quotation. Email [corporatesales@wiley.com](mailto:corporatesales@wiley.com) or [corporatesalesusa@wiley.com](mailto:corporatesalesusa@wiley.com) or [corporatesalesDE@wiley.com](mailto:corporatesalesDE@wiley.com).

## RESEARCH ARTICLE

# High resilience of carbon transport in long-term drought-stressed mature Norway spruce trees within 2 weeks after drought release

Kyohsuke Hikino<sup>1</sup>  | Jasmin Danzberger<sup>2</sup> | Vincent P. Riedel<sup>1</sup>  | Romy Rehschuh<sup>3</sup>  | Nadine K. Ruehr<sup>3</sup>  | Benjamin D. Hesse<sup>1</sup>  | Marco M. Lehmann<sup>4</sup>  | Franz Buegger<sup>2</sup>  | Fabian Weikl<sup>1,2</sup>  | Karin Pritsch<sup>2</sup>  | Thorsten E. E. Grams<sup>1</sup> 

<sup>1</sup>Technical University of Munich (TUM), TUM School of Life Sciences, Land Surface-Atmosphere Interactions, Ecophysiology of Plants, Freising, Germany

<sup>2</sup>Helmholtz Zentrum München – German Research Center for Environmental Health (GmbH), Institute of Biochemical Plant Pathology, Neuherberg, Germany

<sup>3</sup>Karlsruhe Institute of Technology, Institute of Meteorology and Climate Research—Atmospheric Environmental Research (KIT/IMK-IFU), Garmisch-Partenkirchen, Germany

<sup>4</sup>Swiss Federal Institute for Forest, Snow and Landscape Research (WSL), Forest Dynamics, Birmensdorf, Switzerland

## Correspondence

Kyohsuke Hikino, Technical University of Munich (TUM), TUM School of Life Sciences, Professorship for Land Surface-Atmosphere Interactions, Ecophysiology of Plants, Hans-Carl-von-Carlowitz Platz 2, 85354 Freising, Germany.  
Email: kyohsuke.hikino@tum.de

## Present address

Vincent P. Riedel, University of Würzburg, Julius-von-Sachs-Institute of Biological Sciences, Ecophysiology and Vegetation Ecology, Würzburg, Germany

## Funding information

Deutsche Forschungsgemeinschaft, Grant/Award Number: GR 1881/5-1, MA1763/10-1, PR292/22-1, PR555/2-1 and RU 1657/2-1; Deutsche Bundesstiftung Umwelt, Grant/Award Number: AZ 20018/535; Schweizerischer Nationalfonds zur Förderung der Wissenschaftlichen Forschung, Grant/Award Number: 179978; Bavarian State Ministries of the Environment and Consumer Protection as well as Food, Agriculture and Forestry, Grant/Award Number: W047/Kroof II

## Abstract

Under ongoing global climate change, drought periods are predicted to increase in frequency and intensity in the future. Under these circumstances, it is crucial for tree's survival to recover their restricted functionalities quickly after drought release. To elucidate the recovery of carbon (C) transport rates in c. 70-year-old Norway spruce (*Picea abies* [L.] KARST.) after 5 years of recurrent summer droughts, we conducted a continuous whole-tree <sup>13</sup>C labeling experiment in parallel with watering. We determined the arrival time of current photoassimilates in major C sinks by tracing the <sup>13</sup>C label in stem and soil CO<sub>2</sub> efflux, and tips of living fine roots. In the first week after watering, aboveground C transport rates (CTR) from crown to trunk base were still 50% lower in previously drought-stressed trees (0.16 ± 0.01 m h<sup>-1</sup>) compared to controls (0.30 ± 0.06 m h<sup>-1</sup>). Conversely, CTR below ground, that is, from the trunk base to soil CO<sub>2</sub> efflux were already similar between treatments (c. 0.03 m h<sup>-1</sup>). Two weeks after watering, aboveground C transport of previously drought-stressed trees recovered to the level of the controls. Furthermore, regrowth of water-absorbing fine roots upon watering was supported by faster incorporation of <sup>13</sup>C label in previously drought-stressed (within 12 ± 10 h upon arrival at trunk base) compared to control trees (73 ± 10 h). Thus, the whole-tree C transport system from the crown to soil CO<sub>2</sub> efflux fully recovered within 2 weeks after drought release, and hence showed high resilience to recurrent summer droughts in mature Norway spruce forests. This high resilience of the C transport system is an important prerequisite for the recovery of other tree functionalities and productivity.

This is an open access article under the terms of the Creative Commons Attribution License, which permits use, distribution and reproduction in any medium, provided the original work is properly cited.

© 2021 The Authors. *Global Change Biology* published by John Wiley & Sons Ltd.

## KEYWORDS

$^{13}\text{C}$  labeling, climate change, forest ecosystem, phloem, photosynthesis, *Picea abies*, recovery, soil  $\text{CO}_2$  efflux, stem  $\text{CO}_2$  efflux, watering

## 1 | INTRODUCTION

Global climate change has been causing significant and mostly negative impacts on forest ecosystem carbon (C) cycling such as reduced productivity (Ciais et al., 2005; Collins et al., 2013). Drought is one of the most influential drivers of tree mortality (Allen et al., 2010; 2015; McDowell et al., 2008; van Mantgem et al., 2009) and it is predicted to occur more frequently and for longer durations in the future (IPCC, 2007, 2014). Under these circumstances, tree survival primarily depends on the extent to which tree functionality is impaired by drought (i.e., resistance, Lloret et al., 2011). After drought release, it is then crucial that surviving trees recover their limited functionality back to pre-drought levels (i.e., resilience, Lloret et al., 2011). Since drought release typically causes a high C demand for repair and growth particularly in belowground sinks (Gao et al., 2021; Hagedorn et al., 2016; Joseph et al., 2020), C transport from leaves to sink organs is an important process for tree recovery (Ruehr et al., 2019). C assimilates are transported from the crown via the phloem to various above- and belowground C sinks (Lemoine et al., 2013; Salmon et al., 2019). Recent studies revealed that saplings (Barthel et al., 2011; Ruehr et al., 2009; Zang et al., 2014), young trees (Dannoura et al., 2019; Epron et al., 2016), and mature trees (Gao et al., 2021; Hesse et al., 2019; Wang et al., 2021) restricted transport of current photoassimilates under drought, thereby reducing the C supply to sinks. Upon drought release, C limitation in sink tissues can occur if the C transport would not recover fast enough to meet the sink demands (Hartmann et al., 2013; Hartmann et al., 2013; Sevanto, 2014; Winkler & Oberhuber, 2017), but knowledge on mature trees is scarce (Gao et al., 2021).

There are two main causes restricting transport of current photoassimilates from the crown along the stem to belowground C sinks under drought (Salmon et al., 2019). First, water limitation delays the export of sugars from leaves, increasing the mean residence time (MRT) of photoassimilates in leaves (Dannoura et al., 2019; Epron et al., 2012; Hesse et al., 2019; Ruehr et al., 2009). This is caused by accumulation of osmolytes, and/or production of secondary metabolites and volatile compounds (Epron & Dreyer, 1996; Ruehr et al., 2009; Salmon et al., 2019). Second, the phloem transport velocity can be reduced through increased phloem viscosity (Epron et al., 2016; Hesse et al., 2019; Sevanto, 2014, 2018; Woodruff, 2014), lower C source/sink strength (Lemoine et al., 2013; Ryan & Asao, 2014; Sevanto, 2014), and smaller phloem conduit diameter (Dannoura et al., 2019; Woodruff, 2014). Increased phloem viscosity is a result of water limitation in the xylem, as the xylem supplies the nearby phloem with water (Hölttä et al., 2006, 2009). Lower C source/sink strength (e.g., photosynthesis rates and stem/soil  $\text{CO}_2$  efflux rates) limits sugar loading/unloading processes between C source/sink and phloem. This hinders the osmotic regulation in

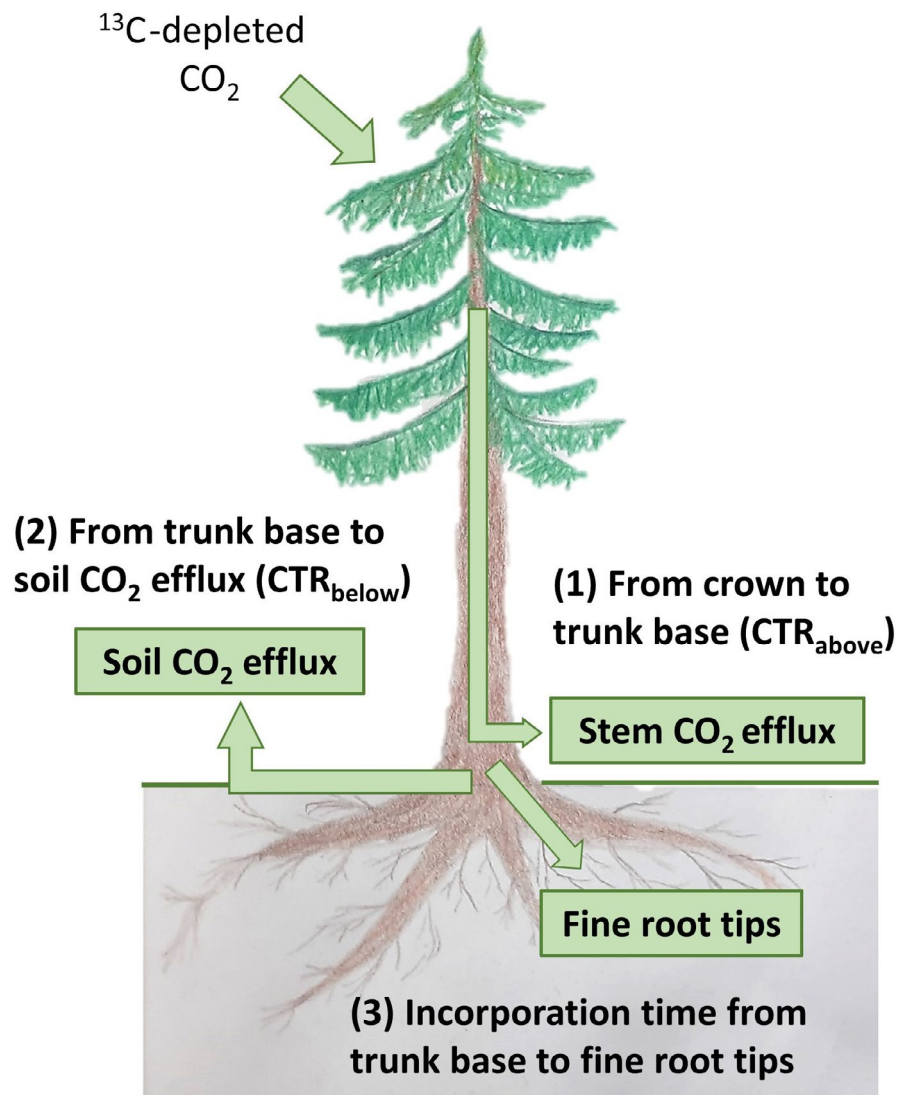
phloem and thus limits water exchange between phloem and xylem. Smaller phloem conduit diameter is caused by restricted cell expansion due to turgor reduction usually under severe drought (Hsiao, 1973), thereby reducing phloem conductivity.

Recovery of C transport depends on the restricting mechanisms. MRT of leaf sugars decreases after drought release within days (Zang et al., 2014). Drought release increases plant water potential and water availability in the xylem, typically followed by increased C source and sink strength (Gao et al., 2021; Hagedorn et al., 2016). Previous studies using young eucalypt trees (Epron et al., 2016) and a rainfall event in a naturally dry pine forest (Gao et al., 2021) reported that C transport velocity from crown to trunk base or soil was related to C source or sink strength, which typically decreases under drought and increases after drought release (Hagedorn et al., 2016; Joseph et al., 2020; Nikolova et al., 2009; Zang et al., 2014). Furthermore, there is increasing evidence that C source strength and C supply may be “sink controlled” (Fatichi et al., 2014; Gavito et al., 2019; Hagedorn et al., 2016; Körner, 2015). Conversely, drought-related reductions of phloem conduit diameter are expected to further restrict the phloem transport during the first weeks after stress release even if the phloem sap viscosity and C source/sink strength recover.

This present study was performed in the framework of the Kranzberg roof (KROOF) project, which was initiated to elucidate the drought responses of mature European beech (*Fagus sylvatica* L.) and Norway spruce (*Picea abies* [L.] KARST.; see details in Grams et al., 2021). Both tree species were exposed to recurrent summer droughts from 2014 to 2018 and leaf water potential reached values as low as  $-1.8$  MPa, causing distinct drought effects such as reduced stem and fine root growth (Grams et al., 2021; Pretzsch et al., 2020; Zwetsloot & Bauerle, 2021) and acclimation in tree hydraulics (Tomasella et al., 2018). To predict the trajectories of forests under future climates, it is important to understand, to what extent tree functionality recovers after drought release and how fast. To answer this question, former drought plots were watered in early summer 2019 (Grams et al., 2021). In parallel with watering, we performed a whole-tree  $^{13}\text{C}$  labeling experiment on mature spruce trees to assess the resilience of their C transport processes, that is, the ability to recover to the level of control trees (Lloret et al., 2011).

We divided the C transport path from the crown to the soil  $\text{CO}_2$  efflux into two parts (Figure 1), as drought release may affect them differently. (1) Aboveground transport from the crown (leaves) to the trunk base (aboveground transport hereafter), and (2) belowground transport from the trunk base to the soil  $\text{CO}_2$  efflux (belowground transport hereafter). In addition, we also investigated a third process, (3) incorporation of current photoassimilates in living fine roots (Figure 1). The aboveground transport comprises sugar export from leaves and transport along the woody structures in the

**FIGURE 1** Overview of the carbon transport paths assessed in this study. (1) Aboveground carbon transport rates ( $CTR_{above}$ , in  $m\ h^{-1}$ ) from crown to trunk base (assessed as stem  $CO_2$  efflux), (2) Belowground carbon transport rates ( $CTR_{below}$ , in  $m\ h^{-1}$ ) from trunk base to soil  $CO_2$  efflux, and (3) Incorporation time (in h) of current photoassimilates from trunk base to fine root tips



phloem. The aboveground C transport rates ( $CTR_{above}$  in  $m\ h^{-1}$ ) indicate how fast newly assimilated C can be supplied to belowground sinks. The belowground transport includes the phloem transport along roots and the  $CO_2$  diffusion in the soil. The belowground C transport rates ( $CTR_{below}$ ) indicate the rates of C flux from belowground plant tissues to the atmosphere, which is an important flux in analyzing forest C cycling. Based on the “sink-control” mechanism, we hypothesize that both  $CTR_{above}$  [H1] and  $CTR_{below}$  [H2] recover within 2 weeks in parallel to C sink and/or C source strength. The timing of the incorporation of current photoassimilates in fine roots indicates how fast trees use the available C to grow and restore the belowground tissues. Since a high C demand is expected in fine root growth of recovering trees upon drought release, the incorporation time can be even shorter in recovering trees compared to control trees. Therefore, our third hypothesis is that upon drought release, incorporation of current photoassimilates is faster in fine roots of trees recovering from drought than in control trees [H3].

In a similar experiment by Gao et al. (2021) conducted in a naturally dry pine forest after a rainfall event is the only study to date investigating CTR of mature trees after drought release. We still lack

knowledge on the recovery of highly productive forests under ongoing climate change. Furthermore, there is no study considering the effect of water availability on the above- and belowground transport individually. We show for the first time the resilience of the whole-tree C transport after repeated summer droughts in a highly productive Norway spruce forest stand of great ecological and economic relevance in central Europe (Caudullo et al., 2016).

## 2 | MATERIALS AND METHODS

### 2.1 | Experimental site

This study was conducted in a mixed forest with c. 90-year-old European beech and c. 70-year-old Norway spruce trees in Kranzberg Forest, located in southern Germany/Bavaria ( $11^{\circ}39'42''E$ ,  $48^{\circ}25'12''N$ ; 490 m a.s.l.). The experimental site consists of 12 plots with three to seven beech and spruce trees each. At this site, a long-term throughfall exclusion (TE) and subsequent watering experiment was conducted as described in detail



in Grams et al. (2021). Briefly, six plots were assigned to TE plots equipped with roofs and the other six plots without roofs to control plots (CO). All plots were trenched to 1 m of soil depth 4 years before the experiments started (Pretzsch et al., 2014). The mature beech and spruce trees in TE plots were then exposed to summer drought for five consecutive growing seasons (2014–2018). To investigate trees' recovery processes, in early summer 2019, all TE plots were watered with c. 90 mm over 36 h and the soil water content increased to the level of the CO plots within 1 week (for further details see Grams et al., 2021). In parallel with the watering, we conducted a  $^{13}\text{C}$  labeling experiment on four CO and three TE spruce trees on neighboring plots (Figure 2a, for details see Table S1). In addition to the two labeled plots, we assessed three spruce trees each on additional CO and TE plots as non-labeled controls (Table S2). A canopy crane located next to these plots enabled the measurements of leaf photosynthesis, leaf water potential, and leaf osmotic potential in sun-lit canopy.

## 2.2 | Weather data

The mean photosynthetic photon flux density during the labeling period accounted to  $788 \pm 534$  (SD)  $\mu\text{mol m}^{-2} \text{s}^{-1}$  (Figure 3a). During the daytime (from 5 am to 7 pm, CET) on the labeling days, mean temperature was  $18.8 \pm 4.3$  (SD)°C (Figure 3b) and mean vapor pressure deficit was  $0.6 \pm 0.4$  (SD) kPa. There were several rain periods during labeling on day 3, 7, and 9. Only on day 9, however, weak but continuous rainfall event with a high wind speed occurred throughout the daytime, accumulating to 7.8 mm (Figure 3b). Due to this weather conditions, a smaller  $\delta^{13}\text{C}$  shift in canopy air was achieved on day 9 (see below).

## 2.3 | $\text{CO}_2$ exposure and assessment of canopy air

The whole crowns of all spruce trees on the CO and TE plot, that is, four and three trees, respectively, were fumigated with  $^{13}\text{C}$ -depleted

tank  $\text{CO}_2$  ( $\delta^{13}\text{C}$  of  $-44.3 \pm 0.2\text{‰}$ ) using the isoFACE system described earlier (Grams et al., 2011; Kuptz et al., 2011). Depending on its crown size, each tree crown was equipped with 9–17 micro-perforated PVC tubes hanging vertically from a carrier structure (Figure 2b). These fumigation tubes were then connected to the  $\text{CO}_2$  tank and the  $^{13}\text{C}$ -depleted  $\text{CO}_2$  was released directly within the seven tree crowns.

The atmospheric  $\text{CO}_2$  concentration and  $\delta^{13}\text{C}$  in tree canopy ( $\delta^{13}\text{C}_a$ ) were continuously monitored during the labeling using a cavity ring-down spectroscopy (CRDS, ESP-1000; PICARRO). Two air measurement points were installed per tree c. 2 m inside the sun-lit crowns at 1 m distance from the stem (east and west orientation, one CO tree had only one measurement point, Figure 2a and Table S2). We took care that these sampling points had enough distances from the fumigation tubes (c. 1 m). A sample point above the canopy was used as a reference. The sample air was continuously transported to the CRDS by membrane pumps via PVC tubes. A computer-automated multiplexer system switched every 5 min between measurement positions and averages of the last 3 min were recorded by the CRDS. According to the mean  $\text{CO}_2$  concentration of all 13 measurement points in canopy, which was measured continuously by an infra-red gas analyzer (BINOS 100 4P; Rosemount-Emerson Electric Co.), a mass flow controller regulated the amount of the  $\text{CO}_2$  exposure through fumigation tubes. To calibrate the CRDS, two commercially available calibration gases were used (Ref.1:  $-9.7 \pm 0.3\text{‰}$  and Ref.2:  $-27.8 \pm 0.3\text{‰}$ ; Thermo Fisher Scientific). All  $\delta^{13}\text{C}$  values in this study were referenced to international standards (Vienna Pee Dee Belemnite).

The  $^{13}\text{C}$  labeling started in parallel with the watering and continued for 14 days, that is, from July 4, 2019 (day 0) to July 17, 2019 (day 13), from 5 am to 7 pm (CET). We targeted the mean  $\text{CO}_2$  concentration in canopy air at +130 ppm relative to the ambient air above the canopy to create a shift of  $-8.3\text{‰}$ . Due to variable wind exposition, however, each tree received different amounts of added  $\text{CO}_2$ . In CO trees, the mean canopy  $\text{CO}_2$  concentration increased to  $541 \pm 16$  ppm during labeling (Figure 3c, see values for individual trees in Table S1), shifting the  $\delta^{13}\text{C}_a$  by

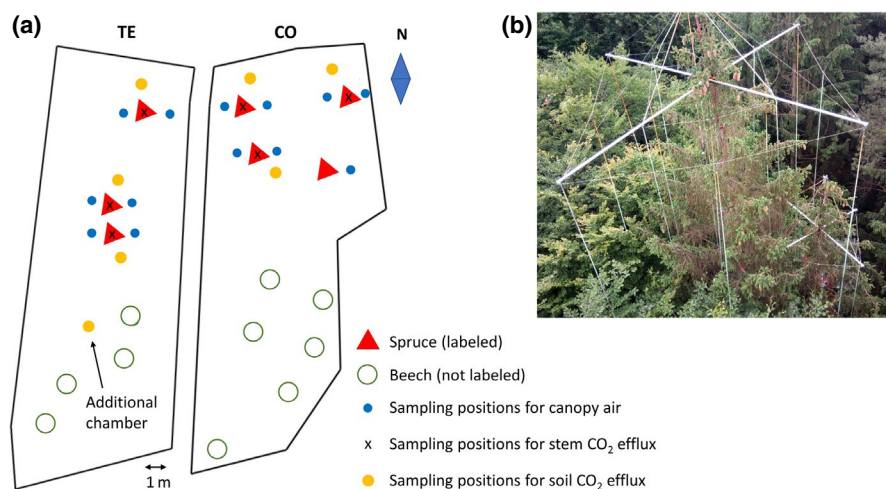


**FIGURE 2** (a) Overview of the two  $^{13}\text{C}$ -labeled plots (CO = control, TE = throughfall exclusion), giving positions of trees (red triangles = labeled spruce trees, green open circles = beech), sampling positions of canopy air (blue circles), stem  $\text{CO}_2$  efflux (x), and soil  $\text{CO}_2$  efflux (yellow circles). (b) Picture of the structure for the  $^{13}\text{C}$  labeling with PVC tubes hanging vertically through the spruce crowns

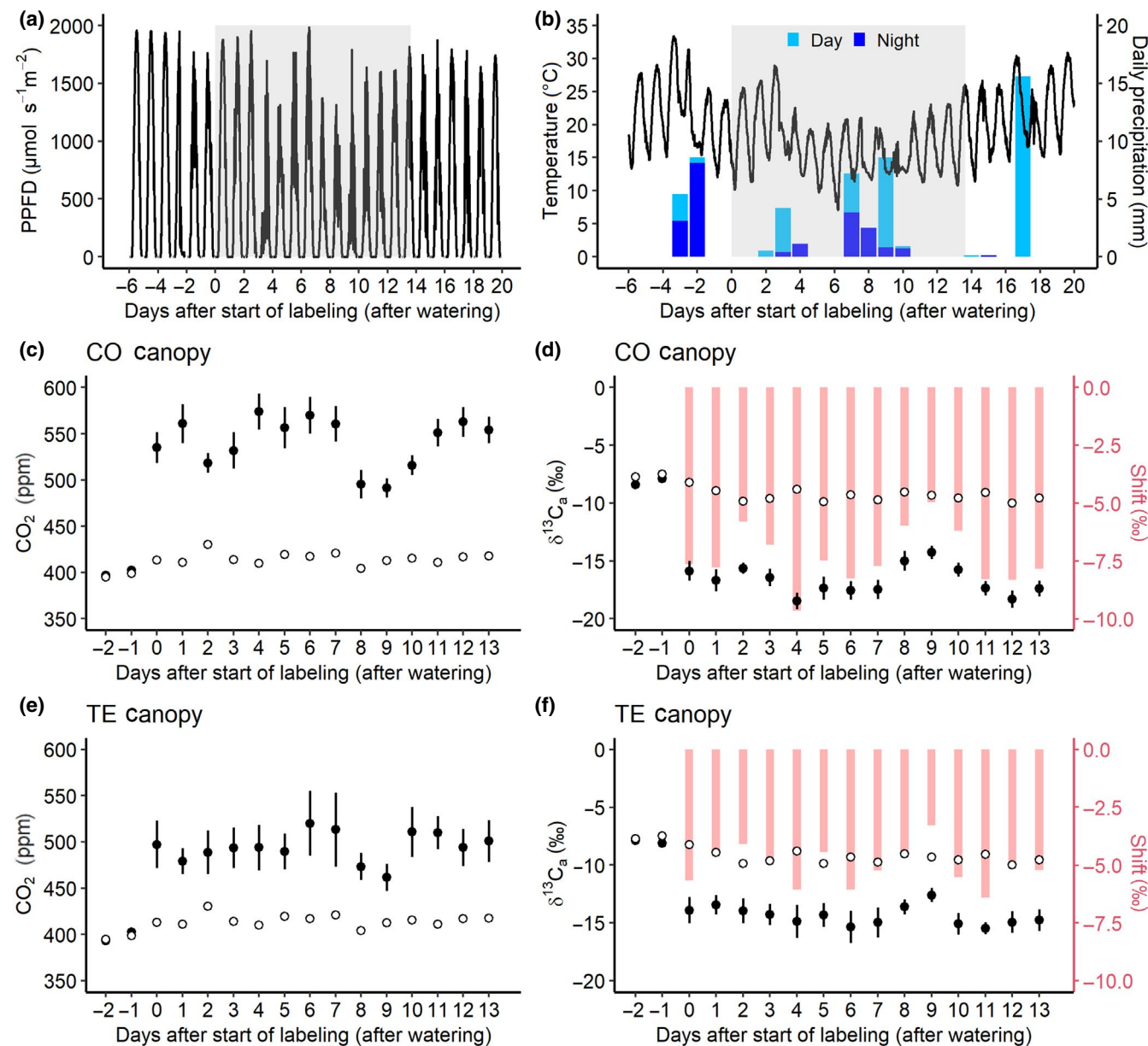


**FIGURE 3** (a) Photosynthetic photon flux density (PPFD) before, during, and after labeling. (b) Temperature (lines) and precipitation (bars) before, during, and after labeling. Precipitation is given as daytime (5 am–7 pm CET, fumigation hours, light blue), and nighttime (7 pm–5 am, dark blue). The ticks on the x-axis indicate 0 am of each day. The labeling started in parallel with the watering on day 0 and continued during daytime until day 13 (marked with gray areas). (c, e) Daily mean CO<sub>2</sub> concentration and (d, f) δ<sup>13</sup>C of canopy air (δ<sup>13</sup>C<sub>a</sub>) of control (CO) and previously drought-stressed (throughfall exclusion, TE) trees during labeling hours (5 am–7 pm), respectively. The closed circles are the averages of the canopy air and the open circles are the non-labeled reference air measured above the canopy. The mean daily shift in δ<sup>13</sup>C<sub>a</sub> was expressed with red bars. Error bars give SE. Error bars of the reference air (open circles) are removed, as they are much shorter than the size of the circles due to the large amount of measurement points

–7.3 ± 0.5‰ on average (Figure 3d). In contrast, TE trees received less <sup>13</sup>C-depleted CO<sub>2</sub> with an increase in the mean canopy CO<sub>2</sub> concentration to 495 ± 23 ppm (Figure 3e), causing smaller mean shift of δ<sup>13</sup>C<sub>a</sub> by –5.1 ± 1.3‰ (Figure 3f) compared to CO trees. Furthermore, during the weak but longer rainfall event associated with a high wind speed on day 9, a smaller mean shift in δ<sup>13</sup>C<sub>a</sub> was achieved in both CO and TE trees. Mean CO<sub>2</sub> concentration and δ<sup>13</sup>C of the ambient air above the canopy were 413 ppm and –9.2‰ during labeling hours.

To track the current photoassimilates through the tree/soil system, we used the two experimentally induced changes in δ<sup>13</sup>C<sub>a</sub>: (1) Turn-on of CO<sub>2</sub> exposure with <sup>13</sup>C-depleted tank CO<sub>2</sub> on day 0 of watering. This part of the experiment was used to calculate the arrival time of the <sup>13</sup>C-depleted tracer in the observed C sinks in the first week after watering. (2) Turn-off of the CO<sub>2</sub> exposure system and subsequent increase in δ<sup>13</sup>C in the canopy air back to the initial, ambient level on day 13 of watering. In this part of the experiment, the arrival of unlabeled tracer (C with ambient δ<sup>13</sup>C)

in the studied C sinks was used to calculate CTR 2 weeks after watering.

## 2.4 | Measurement of phloem sugar

On day -1, 7, 13, and 21 around midday, phloem tissue samples were collected at the breast height of four labeled CO and three labeled TE trees using a cork borer (two disks with diameter of 5 mm for each tree, Tables S2 and S3). The dead bark was removed and the remaining phloem samples were immediately frozen on dry ice and subsequently freeze-dried. The dried material was milled to fine powder using a steel ball-mill (Retsch) and about 70 mg per sample were transferred into a 2 ml reaction vial and mixed with 1.5 ml deionized water. The fractions of water-soluble compounds were then extracted in a water bath at 85°C for 30 min and further purified to neutral sugars using commercial available ion-exchange cartridges (OnGuard II H, A, & P; Dionex) as described in detail by Lehmann et al. (2020). An aliquot of 1 mg of the neutral sugar fraction was then transferred to 5 × 9 mm silver capsules (Saentis Analytical AG), frozen at -20°C, freeze-dried, and the capsules were closed before isotopic analysis. The C isotopic composition of phloem sugars ( $\delta^{13}\text{C}_{\text{phloem}}$ ) was analyzed with a thermal conversion elemental analyzer (PYRO cube; Elementar) that was coupled via a ConFlo III reference system to an isotope-ratio mass spectrometer (Finnigan Delta Plus XP, all supplied by Thermo Fisher Scientific). The typical measurement precision for in-house sugar standards was 0.3‰ (SD).

## 2.5 | Measurement of stem CO<sub>2</sub> efflux

Rates of stem CO<sub>2</sub> efflux and its stable C isotope composition ( $\delta^{13}\text{C}_{\text{stem}}$ ) before and after watering were recorded using an isotope ratio infrared spectrometer (IRIS, DeltaRay, Thermo Fisher Scientific; Braden-Behrens et al., 2017). A total of 12 spruce trees were measured, three <sup>13</sup>C-labeled and three non-labeled trees in each treatment, that is, CO and TE ( $n = 3$ ; Figure 2a; Tables S2 and S3). The non-labeled trees were used to correct for changes in <sup>13</sup>C discrimination caused by the watering and weather fluctuations. Plexiglas (Röhm GmbH) chambers (61–204 cm<sup>2</sup>) were attached at ca. 1 m height on each stem after removing mosses, lichens, and algae. After a leak test using a slight overpressure (c. 2000 Pa), each chamber was supplied with reference air of a constant CO<sub>2</sub> concentration of c. 413 ppm. Excess air was exhausted before entering the chamber to avoid an overpressure. The mixture of reference air plus stem-derived CO<sub>2</sub> of each chamber was continuously pumped through PVC tubes to a computer-automated manifold with 16 channels, which changed the channel flowing to IRIS every 5 min. The CO<sub>2</sub> concentration and the stable C isotope composition of the reference air were determined between measurement cycles (c. every 80 min). The same reference gases as for the CRDS system were used for calibration of the IRIS system (see above).

The rate of stem-derived CO<sub>2</sub> efflux was calculated according to mass balance equation as described by Gamnitzer et al. (2009), using the mean values of the closest two measurements of the reference air.

$$\text{Stem CO}_2 \text{ efflux} (\mu\text{mol m}^{-2} \text{ s}^{-1}) = \frac{F_{\text{air}}}{V_{\text{mol}} A_{\text{chamber}}} ([\text{CO}_2]_{\text{sample}} - [\text{CO}_2]_{\text{reference}}),$$

where  $F_{\text{air}}$  gives the air flow through the chamber (L s<sup>-1</sup>);  $V_{\text{mol}}$ , the molar volume of gases (22.4 L mol<sup>-1</sup>);  $A_{\text{chamber}}$ , the chamber base area (m<sup>2</sup>);  $[\text{CO}_2]_{\text{sample}}$  and  $[\text{CO}_2]_{\text{reference}}$ , the CO<sub>2</sub> concentration (ppm) of sample air from stem chambers and reference air, respectively.

$\delta^{13}\text{C}_{\text{stem}}$  was calculated by the following equation using a two end-member mixing model (Dawson et al., 2002),

$$\delta^{13}\text{C}_{\text{stem}} (\text{‰}) = \frac{([\text{CO}_2]_{\text{sample}} \times \delta^{13}\text{C}_{\text{sample}}) - ([\text{CO}_2]_{\text{reference}} \times \delta^{13}\text{C}_{\text{reference}})}{[\text{CO}_2]_{\text{sample}} - [\text{CO}_2]_{\text{reference}}},$$

where  $\delta^{13}\text{C}_{\text{sample}}$  and  $\delta^{13}\text{C}_{\text{reference}}$  give the  $\delta^{13}\text{C}$  signature of sample air from stem chambers and that of reference air, respectively.

$\delta^{13}\text{C}_{\text{stem}}$  can be affected by CO<sub>2</sub> transported from belowground in xylem sap (Teskey et al., 2008). However, Kuptz et al. (2011) observed a positive correlation in  $\delta^{13}\text{C}$  between stem phloem and stem CO<sub>2</sub> efflux in spruce trees at the same experimental site. In this study, we also found a positive linear correlation between  $\delta^{13}\text{C}_{\text{stem}}$  and  $\delta^{13}\text{C}_{\text{phloem}}$  (slope = 0.94,  $R^2 = .30$ ,  $p < .01$ ; Figure S1). Likewise,  $\delta^{13}\text{C}_{\text{stem}}$  showed no significant difference between daytime and nighttime (data not shown). Therefore, as reported in previous studies (Kodama et al., 2008; Kuptz et al., 2011; Ubierna et al., 2009), we concluded that CO<sub>2</sub> in xylem sap had negligible effect on  $\delta^{13}\text{C}_{\text{stem}}$ . Thus, we assessed the  $\delta^{13}\text{C}_{\text{stem}}$  as a surrogate of  $\delta^{13}\text{C}_{\text{phloem}}$ .

## 2.6 | Measurement of soil CO<sub>2</sub> efflux

Soil CO<sub>2</sub> efflux rates and its isotopic C composition ( $\delta^{13}\text{C}_{\text{soil}}$ ) were measured using a Li-8100 automated soil CO<sub>2</sub> flux system with a Li-8150 multiplexer (Li-Cor Inc.), connected to an IRIS. The air stream leaving the Li-8100 was sampled by the IRIS at a flow rate of 80 ml min<sup>-1</sup> and added back to the chamber air stream. Three automatically operating soil chambers (8100-104) per treatment, that is, CO and TE, were installed with 1 m distance from the spruce trees (Figure 2a; Table S2). Additionally, one chamber was installed close to the non-labeled beech trees in the TE plot (Figure 2a), which was used to correct for effects of physical CO<sub>2</sub> diffusion due to watering (see the last paragraph of this section). Each chamber enclosed a permanently installed soil collar, which was inserted 2–3 cm into the soil 3 days before the measurements started. All chambers were measured at a frequency of c. 30 min (Table S3). Measurement time per chamber was adapted based on the CO<sub>2</sub> efflux rate: 5 min in the TE plot and 2:30 min in the CO plot.  $\delta^{13}\text{C}_{\text{soil}}$  was calculated using the Keeling plot approach (Keeling, 1958, 1961). Each single measurement was quality controlled based on the fit of the linear regressions. For soil CO<sub>2</sub> efflux values were kept if  $R^2 \geq .8$  and for

$\delta^{13}\text{C}_{\text{soil}}$  based on the Keeling plot approach if  $R^2 \geq .9$ . To calibrate the IRIS, two commercially available calibration gases were used (Ref.1:  $-9.9 \pm 0.3\text{‰}$  and Ref.2:  $-27.8 \pm 0.3\text{‰}$ , Thermo Fisher Scientific).

During watering of the TE plots, the soil pores fill with water and the lighter  $^{13}\text{C}$ -depleted  $\text{CO}_2$  gets pushed-out (Andersen et al., 2010; Subke et al., 2009; Unger et al., 2010). This interfered with our labeling experiment. Hence, we corrected for the  $\delta^{13}\text{C}_{\text{soil}}$  of the TE plot based on measurements of the additional chamber close to the non-labeled beech trees (see details in Figures S2 and S3). Due to a limitation in the number of soil chambers, a non-labeled chamber was not available for the CO plot. For purposes not related to this study, the CO plot was slightly watered (c. 12 mm over 12 h) in parallel to the TE plots. As we did not observe any significant effect of the watering on the  $\delta^{13}\text{C}_{\text{soil}}$  of the wet CO plot (Figure 4c), there was no need to apply this correction here.

## 2.7 | Measurement of root tips

Fine roots were collected on day -7 and repeatedly after the watering with an interval of 1–2 days until day 25 (Table S3), from random sampling positions (17–18 samples per treatment and day, Table S2). The collected samples were carefully washed in petri dishes, and representative living root tips were cut off under a stereomicroscope. Individual root tips were placed in pre-weighed tin capsules and dried at  $60^\circ\text{C}$ . Their stable C isotope composition ( $\delta^{13}\text{C}_{\text{root}}$ ) was determined with an isotope-ratio mass spectrometer (delta V Advantage; Thermo Fisher Scientific) coupled to an Elemental Analyzer (Euro EA; Eurovector). Due to the very small sample quantities (the smallest samples with c.  $3 \mu\text{g C}$ ), the C-blank (c.  $0.6 \mu\text{g C}$ ) of the tin capsules and their  $\delta^{13}\text{C}$  were taken into account in the evaluation. As with  $\delta^{13}\text{C}_{\text{stem}}$ ,  $\delta^{13}\text{C}_{\text{root}}$  of non-labeled plots was assessed to correct for the effect of watering and weather fluctuations.

## 2.8 | Calculation of arrival time and CTR

To determine the arrival time of the two tracers ( $^{13}\text{C}$ -depleted tracer after the start of labeling, and unlabeled tracer after the end of labeling) in stem/soil  $\text{CO}_2$  efflux and living root tips, the courses of  $\delta^{13}\text{C}$  were fitted by piecewise function (Figure 4). Since  $^{13}\text{C}$ -depleted  $\text{CO}_2$  decreases  $\delta^{13}\text{C}$ , the arrival time of the  $^{13}\text{C}$ -depleted tracer was defined as the point when  $\delta^{13}\text{C}$  started to decrease. First,  $\delta^{13}\text{C}$  data of each C sink were cut to contain only two linear segments before and after the arrival of the tracers. Then, we performed a linear regression for the  $\delta^{13}\text{C}$  data ("lm" function, R package "stats," version: 3.6.1). Finally, the intersection of two linear fits was determined using "segmented" function (R package "segmented," version: 1.3-0, red lines fitted to the  $\delta^{13}\text{C}$  data). This function calculated a new regression model and automatically estimated the break point (intersection) of two lines including standard errors, where the linear relationship changed. This intersection was then defined as the arrival time of the  $^{13}\text{C}$ -depleted tracer (red vertical lines in Figure 4a–f). In the case of soil  $\text{CO}_2$  efflux,

the first line before arrival was fitted as a horizontal line (Figure 4c,d). After the end of labeling,  $\delta^{13}\text{C}$  of each C sink started to increase again, as the unlabeled tracer (with ambient  $\delta^{13}\text{C}$  values) arrived. This point of increasing  $\delta^{13}\text{C}$  was calculated with the same method described above (blue lines fitted to the  $\delta^{13}\text{C}$  data) and was then defined as the arrival time of unlabeled C (blue vertical lines in Figure 4a–f). In the case of root tips, it was not possible to assign each root to the belonging tree. Therefore, all values were pooled for each treatment (Figure 4e,f), providing only one arrival time for each treatment.

Using the arrival time in stem and soil  $\text{CO}_2$  efflux, the  $\text{CTR}_{\text{above}}$  (aboveground C transport rates from crown to trunk base in  $\text{m h}^{-1}$ , Figure 1) and  $\text{CTR}_{\text{below}}$  (belowground C transport rates from trunk base to soil  $\text{CO}_2$  efflux in  $\text{m h}^{-1}$ , Figure 1) were calculated by:

$$\text{CTR}(\text{m h}^{-1}) = \frac{d}{t_l}$$

For  $\text{CTR}_{\text{above}}$ ,  $t_l$  (in h) gives the time lag between the start respectively end of labeling and the arrival time of the tracers at trunk base (stem  $\text{CO}_2$  efflux).  $d$  (in m) represents the distance between the mean crown height (the middle of the crown, Table S1) of the tree and the height of the stem chamber. For  $\text{CTR}_{\text{below}}$ ,  $t_l$  (in h) gives the time lag between the arrival time of the tracers at trunk base and the arrival time at soil  $\text{CO}_2$  efflux, with  $d$  (in m) representing the height of the stem chamber plus 1 m, since each soil chamber was placed at 1 m distance from each trunk. The real transport distance from trunk base to soil chamber can vary depending on the structure of roots. We assumed that there is no time lag between arrival of current photoassimilates at trunk base/roots and the use of them in stem/root  $\text{CO}_2$  efflux. We did not calculate CTR to living root tips, since the transport distance was unknown due to random sampling positions. Therefore, for the incorporation time of current photoassimilates in fine roots, the time lags between the arrival time of the tracers at trunk base and the arrival time at root tips were compared between CO and TE trees instead (Figure 1).

The additional soil chamber in the TE plot enabled to correct for the effects of watering on  $\delta^{13}\text{C}_{\text{soil}}$  (see details in Figures S2 and S3). Due to stable weather conditions in the first week of the labeling with only few short and weak rain events, we were able to calculate the arrival time of  $^{13}\text{C}$ -depleted tracer in soil  $\text{CO}_2$  efflux. However, unstable weather conditions during the second part of the experiment (day 7–13) did not allow to calculate the arrival time of unlabeled tracer in soil  $\text{CO}_2$  efflux (they caused negative time lags). Reduced C gain on day 9 increased the  $\delta^{13}\text{C}_{\text{soil}}$  already before the unlabeled tracer arrived in soil  $\text{CO}_2$  efflux, likely as more  $^{13}\text{C}$ -enriched old C was used (Steinmann et al., 2004; Wingate et al., 2010). Thus, we excluded the  $\text{CTR}_{\text{below}}$  calculated using unlabeled tracer 2 weeks after watering.

## 2.9 | Measurement of light-saturated $\text{CO}_2$ assimilation rates ( $A_{\text{sat}}$ ), predawn leaf water potential ( $\Psi_{\text{PD}}$ ), and leaf osmotic potential ( $\pi_{\text{O}}$ )

The light-saturated  $\text{CO}_2$  assimilation rates at  $\text{CO}_2$  concentration of 400 ppm ( $A_{\text{sat}}$ , expressed on the basis of total needle surface area)

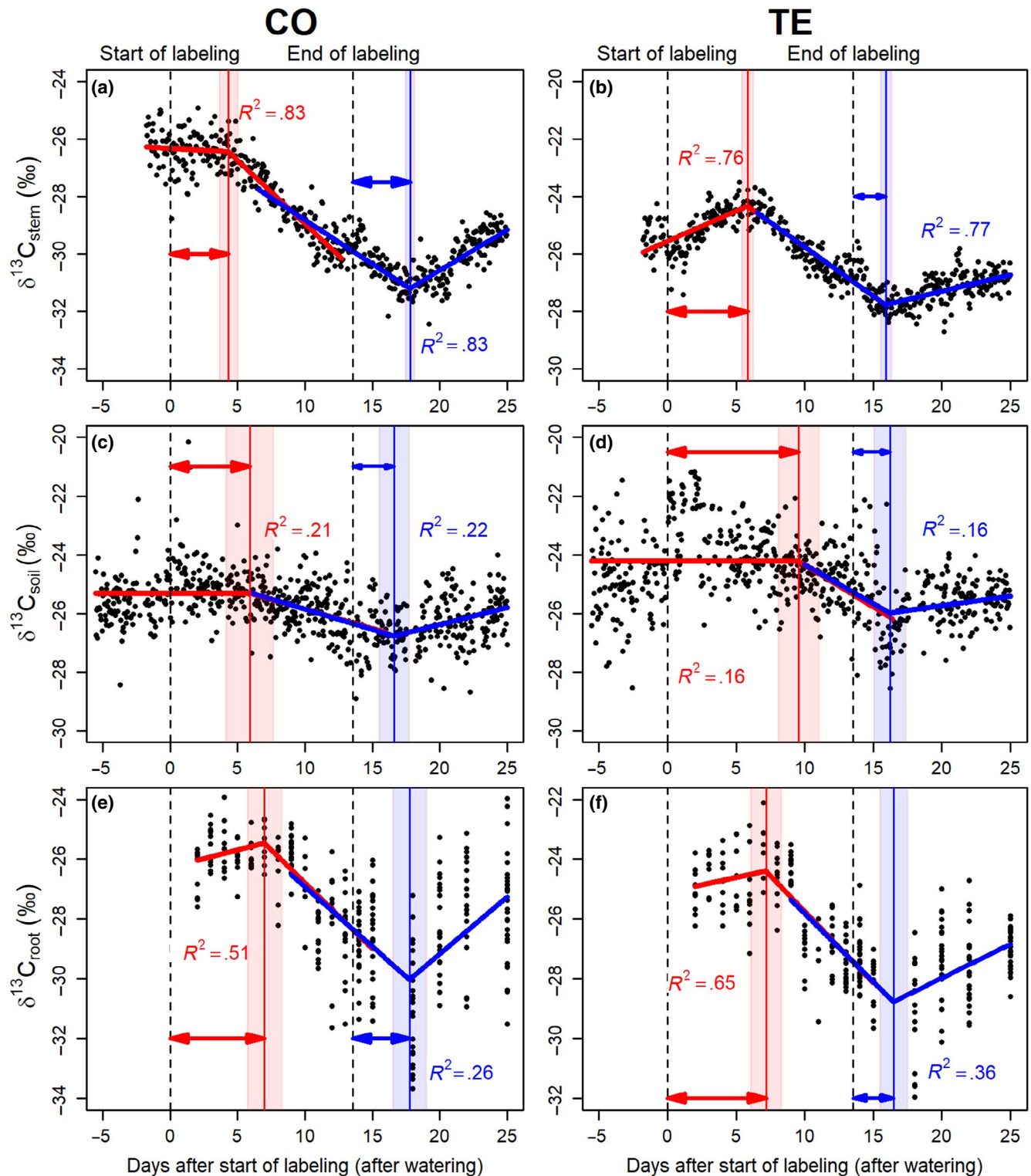


**FIGURE 4** Examples for the calculation of the arrival time of the <sup>13</sup>C-tracers, using: (a, b) δ<sup>13</sup>C of stem CO<sub>2</sub> efflux (δ<sup>13</sup>C<sub>stem</sub>) of one control (CO) and one previously drought-stressed (throughfall exclusion, TE) tree, (c, d) δ<sup>13</sup>C of soil CO<sub>2</sub> efflux (δ<sup>13</sup>C<sub>soil</sub>) of one CO and one TE soil chamber, and (e, f) δ<sup>13</sup>C of living root tips (δ<sup>13</sup>C<sub>root</sub>) of CO and TE trees. Dashed vertical lines are the start and the end of labeling. The red and blue lines fitted to the data show the results of the piecewise functions to estimate the arrival time of <sup>13</sup>C-depleted and unlabeled tracer, respectively (see Section 2). The intersections of two lines, marked with solid red and blue vertical lines are the calculated arrival times in the first week and 2 weeks after the watering, respectively. These arrival times (displayed here with arrows) were then used to calculate the above- and belowground carbon transport rates (CTR<sub>above</sub>, CTR<sub>below</sub>) and the incorporation time in fine roots (see Section 2). The red and blue shaded area give the 95% confidence interval of the intersections. The data of the other trees are displayed in Figure S4 (stem CO<sub>2</sub> efflux) and in Figures S3 and S5 (soil CO<sub>2</sub> efflux). All the root samples were pooled for each plot (CO and TE)

were measured on fully sun-exposed 1-year-old needles using a LI-6800 gas exchange system (Li-Cor Inc.) between 8 am and 3 pm (CET), before (around day -14) and after watering on days 4 and 14 (Table S3). In TE trees, when annual branch growth was not sufficiently long to cover the measurement chamber, needles from the previous year(s) were also included. Because of the small number of replicates in the present labeling plots (access by the canopy crane was limited by the labeling infrastructure), we additionally measured four spruce trees of each treatment in other plots (in total  $n = 6$ ; Table S2). During the measurements, we set the light intensity to  $1500 \mu\text{mol m}^{-2} \text{s}^{-1}$  and kept the leaf temperature at  $25^\circ\text{C}$ . The relative humidity was set to 60–65%. After the measurements, the needles were harvested and scanned (Epson Perfection 4990 Photo; Epson Deutschland GmbH). The projected needle surface area was multiplied by the factor 3.2 to determine the total needle surface area (Goisser et al., 2016).

Pre-dawn leaf water potential ( $\Psi_{\text{PD}}$ ) and leaf osmotic potential ( $\pi_{\text{O}}$ ) on fully sun-exposed twigs were determined on day -6, 2, 7, and 22 ( $n = 6$ , same trees used for  $A_{\text{sat}}$ , Tables S2 and S3).  $\Psi_{\text{PD}}$  was measured using a Scholander pressure bomb (mod. 1505D; PMS Instrument Co.) before sunrise (3 am–5 am CET).  $\pi_{\text{O}}$  was determined with pressure volume curves (PV curves), following Tomasella et al. (2018). Collected twigs (two needle age classes) were rehydrated, and subsequently, their weight and water potential were repeatedly measured.

## 2.10 | Statistical analysis

We analyzed all data using R (version 4.0.3) in R studio (version 1.3.1093). The treatment effect on the CTR and the time lags were tested using a  $t$  test. Beforehand, we tested the homogeneity of variances ( $F$ -test) and the normality of the data (Shapiro test). Since the homogeneity of variances between  $\text{CTR}_{\text{above}}$  and  $\text{CTR}_{\text{below}}$  was violated, we tested their difference with `wilcox.test` (package: stats, version: 3.6.1). The differences in  $A_{\text{sat}}$ , rates of stem/soil  $\text{CO}_2$  efflux,  $\Psi_{\text{PD}}$ , and  $\pi_{\text{O}}$  were tested using a linear-mixed model (package: nlme, version: 3.1-151). We defined the treatment and day as fixed, and tree/chamber as random effects. Since  $A_{\text{sat}}$ ,  $\Psi_{\text{PD}}$ , and  $\pi_{\text{O}}$  were also measured in other plots, the plot was defined as a random effect. For every model, we tested the homogeneity of variances (Levene test) and the normality of the residuals (Shapiro test). If any fixed factor was significant, we performed a post-hoc test with Tukey correction (package: lsmeans, version: 2.30-0). The correlation between  $\pi_{\text{O}}$  and  $\Psi_{\text{PD}}$  was fitted with the following sigmoid curve.

$$\pi_{\text{O}} = d + \frac{a - d}{1 + e^{\frac{\Psi_{\text{PD}} - c}{b}}}$$

where  $a$  represents the start value of  $\pi_{\text{O}}$  before watering,  $b$  the slope coefficient of the regression,  $c$  the instant of the regression inflection point, and  $d$  the end value of  $\pi_{\text{O}}$ .

## 3 | RESULTS

### 3.1 | Aboveground transport rates ( $\text{CTR}_{\text{above}}$ ) from crown to trunk base

The  $^{13}\text{C}$ -depleted  $\text{CO}_2$  was successfully taken up by tree crowns and transported downwards along the stem after the start of labeling. For example,  $\delta^{13}\text{C}_{\text{stem}}$  of one CO tree in Figure 4a was  $-26.1 \pm 0.1\%$  before the start of labeling and remained almost constant for 4 days after the start of labeling. Then,  $\delta^{13}\text{C}_{\text{stem}}$  suddenly decreased after the  $^{13}\text{C}$ -depleted tracer arrived. Similar courses of  $\delta^{13}\text{C}_{\text{stem}}$  were observed in all six labeled trees assessed in this study (Figure 4b; Figure S4). Despite similar transport distance of  $28.4 \pm 0.3$  and  $27.0 \pm 0.9$  m in CO and TE trees, respectively (Table S1), the arrival of the  $^{13}\text{C}$ -depleted tracer in stem  $\text{CO}_2$  efflux was significantly delayed in TE trees compared to CO trees ( $p < .05$ ). The  $^{13}\text{C}$ -depleted tracer was found in stem  $\text{CO}_2$  efflux of CO trees  $95 \pm 10$  h after the start of labeling and watering, whereas in TE trees the tracer arrived after  $163 \pm 12$  h.  $\text{CTR}_{\text{above}}$ , calculated from these arrival times, was  $0.16 \pm 0.01 \text{ m h}^{-1}$  and thus about half in TE spruce compared to CO spruce with  $0.30 \pm 0.06 \text{ m h}^{-1}$  (Figure 5a;  $p = .06$ ). Already 2 weeks after watering,  $\text{CTR}_{\text{above}}$  determined with the arrival of unlabeled tracer did not differ between treatments anymore, because of a significant increase in  $\text{CTR}_{\text{above}}$  of TE trees to  $0.39 \pm 0.13 \text{ m h}^{-1}$  (Figure 5b).  $\text{CTR}_{\text{above}}$  of CO trees remained almost constant during the study period ( $0.32 \pm 0.05 \text{ m h}^{-1}$  2 weeks after watering).

### 3.2 | Leaf osmotic potential ( $\pi_{\text{O}}$ ) and predawn water potential ( $\Psi_{\text{PD}}$ )

$\pi_{\text{O}}$  increased with  $\Psi_{\text{PD}}$  following a sigmoidal fit (Figure 6;  $p < .001$ ). Before watering,  $\Psi_{\text{PD}}$  of the TE trees was on average  $-0.93 \pm 0.03 \text{ MPa}$ , which was significantly lower than that of CO trees with  $-0.59 \pm 0.02 \text{ MPa}$  ( $p < .05$ ). On day 7,  $\Psi_{\text{PD}}$  was then similar between treatments with  $-0.61 \pm 0.02$  and  $-0.69 \pm 0.05 \text{ MPa}$  in CO and TE trees, respectively ( $p > .6$ ). The lowest  $\pi_{\text{O}}$  of  $-2.44 \pm 0.05 \text{ MPa}$  was observed for TE trees before watering, which was significantly lower than in CO trees with  $-1.67 \pm 0.04 \text{ MPa}$  ( $p < .01$ ). Correlated with  $\Psi_{\text{PD}}$ ,  $\pi_{\text{O}}$  of TE trees increased by  $0.5 \text{ MPa}$  until day 22 to  $-2.00 \pm 0.04 \text{ MPa}$ . Nevertheless, on day 22,  $\pi_{\text{O}}$  of TE trees was still somewhat lower than in CO trees ( $p < .1$ ) that stayed around  $-1.6 \text{ MPa}$  throughout the study.

### 3.3 | Belowground transport rates ( $\text{CTR}_{\text{below}}$ ) from trunk base to soil $\text{CO}_2$ efflux

The labeling with  $^{13}\text{C}$ -depleted  $\text{CO}_2$  also caused a sudden decrease in  $\delta^{13}\text{C}_{\text{soil}}$ , but with a smaller shift compared to  $\delta^{13}\text{C}_{\text{stem}}$  (Figure 4c,d). In the first week after watering, the  $^{13}\text{C}$ -depleted tracer was detected in soil  $\text{CO}_2$  efflux under CO trees  $73 \pm 22$  h

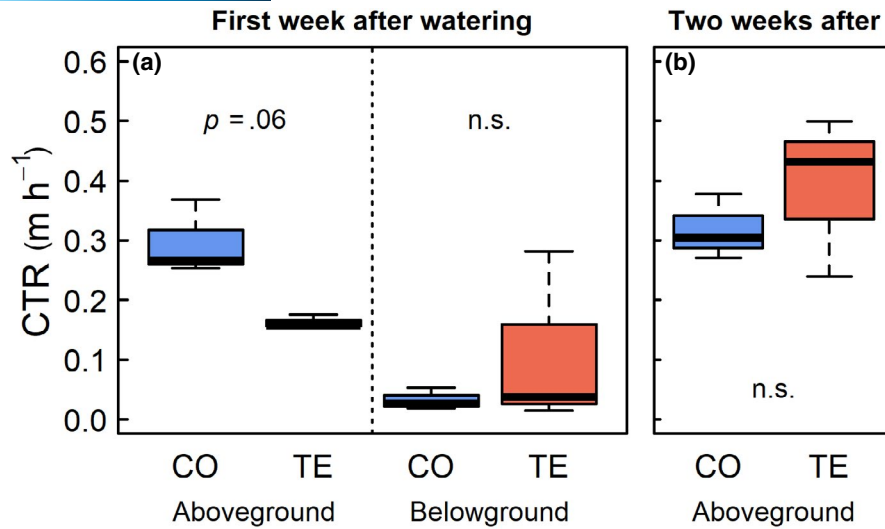


**FIGURE 5** (a) Aboveground and belowground carbon transport rates (CTR) in the first week after watering determined by the arrival time of the  $^{13}\text{C}$ -depleted tracer after the start of labeling; Aboveground CTR ( $\text{CTR}_{\text{above}}$  in text), from crown to trunk base (detected as stem  $\text{CO}_2$  efflux); belowground CTR ( $\text{CTR}_{\text{below}}$  in text), from trunk base to soil  $\text{CO}_2$  efflux. (b)  $\text{CTR}_{\text{above}}$  2 weeks after watering, determined by the arrival time of the unlabeled tracer in stem  $\text{CO}_2$  efflux after the end of labeling.  $p$ -value and n.s. (no significance) give the results of  $t$  tests comparing CO (control) and TE (previously drought-stressed, throughfall exclusion) trees

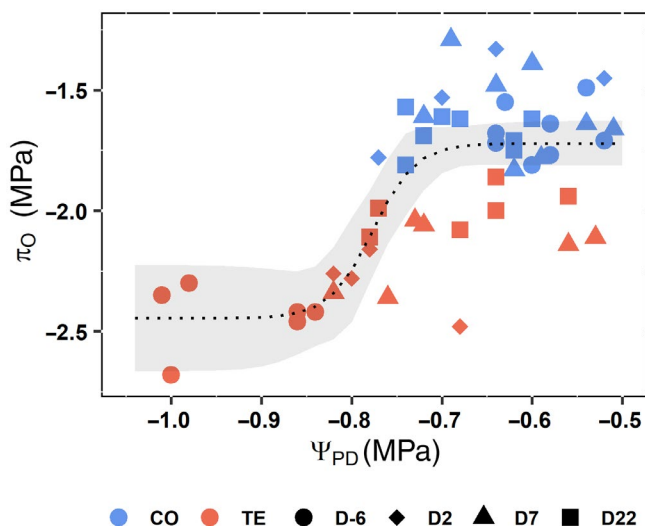


**FIGURE 6** Correlation between leaf osmotic potential ( $\pi_{\text{O}}$ ) and predawn leaf water potential ( $\Psi_{\text{PD}}$ ) of control (CO, blue) and previously drought-stressed trees (throughfall exclusion, TE, red). Circles show the measurements 6 days before watering, diamonds on day 2 (2 days after watering), triangles on day 7, and rectangles on day 22. The dotted curve displays the prediction of the sigmoid curve (all points were fitted together). The gray area gives the 95% confidence interval

after the detection in the stem  $\text{CO}_2$  efflux. The time lag was similar in TE trees with  $62 \pm 37$  h ( $p > .8$ ).  $\text{CTR}_{\text{below}}$  calculated from these time lags, was not significantly different between CO and TE trees with  $0.03 \pm 0.01$  and  $0.11 \pm 0.08$   $\text{m h}^{-1}$ , respectively (Figure 5a,  $p > .7$ ). The large variance of TE trees was caused by one tree with a high  $\text{CTR}_{\text{below}}$  ( $0.28$   $\text{m h}^{-1}$ ).  $\text{CTR}_{\text{below}}$  was significantly lower than  $\text{CTR}_{\text{above}}$  ( $p < .05$ ).

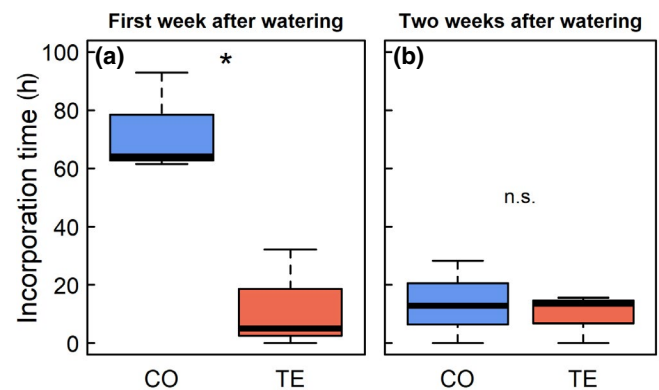


**FIGURE 7** Incorporation time of current photoassimilates in living root tips (time lag between the arrival time at trunk base and arrival time in living root tips), (a) in the first week after watering, determined with the  $^{13}\text{C}$ -depleted tracer after the start of labeling, and (b) 2 weeks after watering, determined with the unlabeled tracer after the end of labeling. Asterisk ( $p < .05$ ) and n.s. (no significance) give the results of  $t$  tests comparing CO (control) and TE (previously drought-stressed, throughfall exclusion) trees

### 3.4 | Incorporation of current photoassimilates in living fine roots

In the first week after watering, the  $^{13}\text{C}$ -depleted tracer was detected in the living root tips of TE trees within  $12 \pm 10$  h after the detection in the stem  $\text{CO}_2$  efflux, whereas CO trees incorporated the current photoassimilates much later, that is, within  $73 \pm 10$  h ( $p < .05$ ; Figure 7a). Two weeks after watering, the incorporation time of the unlabeled tracer significantly decreased in CO trees to  $14 \pm 8$  h after the detection at the trunk base ( $p < .05$ ), which was similar to that of TE trees ( $10 \pm 5$  h,  $p > .7$ ; Figure 7b).

**TABLE 1** Light-saturated CO<sub>2</sub> assimilation rates ( $A_{\text{sat}}$ ) before (around day -14) and after (day 4 and 14) the watering (means  $\pm$  SE,  $n = 6$ , expressed on the basis of total needle area), and rates of stem and soil CO<sub>2</sub> efflux before (day -1) and after (day 4 and 14/15) watering (means  $\pm$  SE,  $n = 3$ ) in CO (control) and TE (previously drought-stressed, throughfall exclusion) trees. The lowercase letters indicate the significant differences among treatments and days, determined by a post-hoc test after applying a linear-mixed model.  $A_{\text{sat}}$ , stem CO<sub>2</sub> efflux, and soil CO<sub>2</sub> efflux were tested separately

	Before	Day 4	Day 14/15
$A_{\text{sat}}$ ( $\mu\text{mol CO}_2 \text{ m}^{-2} \text{ s}^{-1}$ )			
CO	2.7 $\pm$ 0.2 <sup>a</sup>	2.6 $\pm$ 0.3 <sup>a</sup>	2.3 $\pm$ 0.3 <sup>a</sup>
TE	2.1 $\pm$ 0.3 <sup>a</sup>	2.4 $\pm$ 0.3 <sup>a</sup>	2.1 $\pm$ 0.2 <sup>a</sup>
Stem CO <sub>2</sub> efflux ( $\mu\text{mol CO}_2 \text{ m}^{-2} \text{ s}^{-1}$ )			
CO	2.8 $\pm$ 0.8 <sup>a</sup>	2.9 $\pm$ 0.7 <sup>a</sup>	3.3 $\pm$ 0.8 <sup>a</sup>
TE	3.3 $\pm$ 0.7 <sup>a</sup>	2.8 $\pm$ 0.2 <sup>a</sup>	3.3 $\pm$ 0.6 <sup>a</sup>
Soil CO <sub>2</sub> efflux ( $\mu\text{mol CO}_2 \text{ m}^{-2} \text{ s}^{-1}$ )			
CO	6.7 $\pm$ 0.4 <sup>a</sup>	5.4 $\pm$ 0.3 <sup>b</sup>	6.6 $\pm$ 0.4 <sup>a</sup>
TE	1.7 $\pm$ 0.1 <sup>c</sup>	1.8 $\pm$ 0.1 <sup>c</sup>	2.1 $\pm$ 0.2 <sup>c</sup>

### 3.5 | Changes in C source/sink relations upon watering

Before watering, light-saturated CO<sub>2</sub> assimilation rates ( $A_{\text{sat}}$ ) were  $2.7 \pm 0.2 \mu\text{mol m}^{-2} \text{ s}^{-1}$  and thus hardly higher in CO compared to TE spruce with  $2.1 \pm 0.3 \mu\text{mol m}^{-2} \text{ s}^{-1}$  (Table 1;  $p > .6$ ). Watering did not significantly affect the  $A_{\text{sat}}$  of TE spruce, which remained almost constant under both treatments until day 14 (on day 4: CO,  $2.6 \pm 0.3$ ; TE,  $2.4 \pm 0.3$ ; on day 14: CO,  $2.3 \pm 0.3$ ; TE,  $2.1 \pm 0.2 \mu\text{mol m}^{-2} \text{ s}^{-1}$ ).

Similarly, the rates of stem CO<sub>2</sub> efflux did not significantly differ between treatments before watering (Table 1;  $p > .9$ ), although the CO<sub>2</sub> efflux was slightly higher in TE with  $3.3 \pm 0.7 \mu\text{mol m}^{-2} \text{ s}^{-1}$  compared to CO spruce with  $2.8 \pm 0.8 \mu\text{mol m}^{-2} \text{ s}^{-1}$ . Upon watering, the stem CO<sub>2</sub> efflux rates remained almost constant with  $2.9 \pm 0.7$  and  $3.3 \pm 0.8$  in CO, and  $2.8 \pm 0.2$  and  $3.3 \pm 0.6 \mu\text{mol m}^{-2} \text{ s}^{-1}$  in TE trees on days 4 and 14.

Before watering, rates of soil CO<sub>2</sub> efflux were  $1.7 \pm 0.1 \mu\text{mol m}^{-2} \text{ s}^{-1}$  under TE trees, which were much lower than under CO trees with  $6.7 \pm 0.4 \mu\text{mol m}^{-2} \text{ s}^{-1}$  ( $p < .01$ ; Table 1). Soil CO<sub>2</sub> efflux rates under TE trees around  $2.0 \mu\text{mol m}^{-2} \text{ s}^{-1}$  hardly increased after watering and remained significantly lower than those under CO trees with  $5.4 \pm 0.3$  and  $6.6 \pm 0.4 \mu\text{mol m}^{-2} \text{ s}^{-1}$  on days 4 and 15, respectively.

## 4 | DISCUSSION

This study aims to elucidate the whole-tree C transport in highly productive Norway spruce forests upon watering in a long-term climate-change experiment with repeated experimental summer droughts. In the last decades, Norway spruce forests have been

showing immense dieback through severe drought (Arend et al., 2021; Boczoń et al., 2018; Hentschel et al., 2014; Rosner et al., 2016; Solberg, 2004). Also in our experimental site, we lost a couple of TE spruce trees during the drought period (Grams et al., 2021). In the present study, we ask whether surviving trees recover both the aboveground C transport, that is, from the crown to the trunk base, and the belowground C transport, that is, from the trunk base to the soil CO<sub>2</sub> efflux after drought release. As the third transport process, we show how fast the current photoassimilates are incorporated in fine roots after drought release.

### 4.1 | Aboveground transport from crown to trunk base recovered within 2 weeks after drought release

The observed  $\text{CTR}_{\text{above}}$  of CO spruce (c.  $0.30 \text{ m h}^{-1}$ ) is somewhat higher than the average of gymnosperm trees calculated in a meta-analysis ( $0.22 \text{ m h}^{-1}$ , Liesche et al., 2015), and corresponds to the values observed at the same site 10 years before (Kuptz et al., 2011). The repeated summer droughts restricted the  $\text{CTR}_{\text{above}}$  of mature spruce. In the first week after drought release, the arrival of <sup>13</sup>C-depleted tracer was still delayed by 2–3 days in TE trees, indicating a 46% reduction in  $\text{CTR}_{\text{above}}$  compared to CO spruce (Figure 5a). In a counterpart experiment with pine trees growing on a naturally dry site (Gao et al., 2021),  $\text{CTR}$  from crown to rhizosphere doubled upon watering, similar to findings on mature spruce trees in the present study. This delay was likely to be caused by longer MRT of sugars in leaves (Dannoura et al., 2019; Epron et al., 2012; Hesse et al., 2019; Ruehr et al., 2009; Zang et al., 2014) and/or slower phloem transport (Hesse et al., 2019; Sevanto, 2014).

About 2 weeks after watering,  $\text{CTR}_{\text{above}}$  of TE trees significantly increased to the level of CO trees, while  $\text{CTR}_{\text{above}}$  of CO trees remained constant (Figure 5b). However, neither C source strength, that is, photosynthesis rates nor sink strength, assessed here as stem and soil CO<sub>2</sub> efflux, significantly increased within the first 2 weeks after watering (Table 1). Likewise, unaffected soil CO<sub>2</sub> efflux rates during 2 weeks after drought release were also observed in other Norway spruce forests, likely due to slow recovery of microbial activity (Muhr & Borken, 2009; Schindlbacher et al., 2012). Considering that ratio of autotrophic (root-derived) to heterotrophic (microbial) soil respiration under the present spruce trees is known to decrease during drought (Nikolova et al., 2009), autotrophic respiration also likely remained low after drought release. Thus, changes of C source/sink relations are unlikely to be a major cause for the impaired  $\text{CTR}_{\text{above}}$ . This led to the rejection of H1 that  $\text{CTR}_{\text{above}}$  would recover with C source and/or sink strength, which is different from the study of Gao et al. (2021) on pine trees.

Although still not fully recovered to the rather constant level of CO trees,  $\pi_{\text{O}}$  of TE trees increased until day 22 after watering in parallel with  $\Psi_{\text{PD}}$  (Figure 6). This indicates a declined C demand for osmotic adjustments, implying a decrease in leaf sugar concentration and MRT after drought release. Therefore, the delayed



sugar export from leaves under drought was likely a component of slower C translocation from the crown to the trunk base. A quick recovery of MRT of sugars in leaves was also observed in beech saplings after drought release (Zang et al., 2014). In addition, since  $\Psi_{PD}$  of TE trees was significantly lower than that of CO trees before watering and increased to the control level by day 7 (Figure 6), increased phloem viscosity due to water limitation in the xylem might be another cause for the slower phloem transport under drought (Epron et al., 2016; Woodruff, 2014). In principle, CTR may be reduced by intensified leakage–retrieval of transported sugars in the phloem (van Bel, 2003; De Schepper et al., 2013; Epron et al., 2016), however, there is no evidence to date that this mechanism is enhanced under drought (Salmon et al., 2019). Considering the rapid increase in  $CTR_{above}$  within 2 weeks, reduction in phloem conduit diameter is unlikely to have occurred, which is in line with unaffected branch phloem lumen area of the same TE spruce trees (Giai Petit, University of Padova, in preparation). Miller et al. (2020) also reported an unaffected sieve cell production of mature spruce under summer drought. Furthermore, phloem production of the present spruce likely peaked before watering under moderate water stress (c.  $-0.9$  MPa), since it has been found to peak before mid-June in spruce trees (Gričar et al., 2014; Jyske et al., 2015; Miller et al., 2020). This explains the different results on other tree species including conifers, which decreased phloem growth and diameter under more severe water stress (Dannoura et al., 2019; Woodruff, 2014).

It is important to note that the xylem water potential and to some extent also  $\pi_o$  were continuously increasing after watering until the  $^{13}C$ -depleted tracer arrived in stem  $CO_2$  efflux around day 7 in TE trees. Therefore, the drought-induced reduction in  $CTR_{above}$  might have been even more pronounced before the watering. Most importantly, the aboveground CTR from crown to trunk base of mature spruce fully recovered within 2 weeks after watering, hence showing high resilience to long-term and recurrent summer droughts.

#### 4.2 | Belowground transport from trunk base to soil $CO_2$ efflux was similar between treatments already in the first week after watering

The observed  $CTR_{below}$  of CO trees (c.  $0.03$   $m\ h^{-1}$ ) was about 10 times lower than  $CTR_{above}$  (Figure 5a), which is in line with the study of Mencuccini and Hölttä (2010) reporting on a slower belowground transport compared to transport along the stem phloem. The variance of  $CTR_{below}$  in TE trees was high, likely due to the soil heterogeneities and unknown root structures from the trunk base to the spot of soil  $CO_2$  efflux assessments. Already in the first week after watering,  $CTR_{below}$  was similar between CO and TE trees. However, conversely to our expectation, rates of soil  $CO_2$  efflux did not increase after watering (as discussed above), which led to the rejection of H2 that  $CTR_{below}$  would recover in parallel with increasing C sink or source strength. Upon watering, water potential in leaves fully recovered within 1 week (Figure 6) and can be expected to have

increased faster in roots in parallel with increasing soil water potential (Fiscus, 1972; Gleason et al., 2017; McCully, 1999). Therefore, we suggest a fast and full recovery of root phloem transport within few days, that is, even before the  $^{13}C$ -depleted tracer arrived at the trunk base (i.e., around day 7). Moreover, speed of soil  $CO_2$  diffusion was likely similar in soils of both treatments, as gas diffusion in soils is negatively correlated with soil water content (Kuzakov & Gavrichkova, 2010) that was very similar in TE and CO plots within few days after watering (Grams et al., 2021).

Since the distance of the aboveground transport is much longer than belowground in tall mature trees, particularly in shallow rooting spruce trees, the drought-reduced transport rates from crown to soil  $CO_2$  efflux are mainly caused by the restricted aboveground C transport from crown to trunk base. However, short young trees or deep rooting mature trees have higher ratio of belowground to total transport distance. Thus, the belowground C transport from trunk base to soil  $CO_2$  efflux might play a significant role for the whole-tree transport processes and forest C cycling (Gao et al., 2021), since  $CTR_{below}$  is much lower than  $CTR_{above}$ . Most importantly, not only aboveground but the whole-tree CTR from crown to soil  $CO_2$  efflux showed a full recovery within 2 weeks after watering, hence indicating high resilience to long-term and recurrent summer droughts.

#### 4.3 | Incorporation of current photoassimilates in fine roots was faster in trees recovering from drought than in control trees

The  $^{13}C$ -depleted tracer was detected in living root tips of TE trees within 12 h after the arrival at the trunk base, but only 60 h later in CO trees (Figure 7a), confirming H3 that incorporation of current photoassimilates is faster in trees recovering from drought. The faster use of the tracers in living root tips of TE trees compared to controls coincided with the growth of new roots that started within few days after watering (personal observations on site), suggesting a higher C demand in fine roots of TE trees. However, the enhanced fine root growth upon watering in TE plots was not reflected in soil  $CO_2$  efflux, likely due to a small contribution of respiration of fine roots grown after watering to total soil  $CO_2$  efflux: that is, small biomass share of growing fine roots to total roots. Furthermore, Nikolova et al. (2020) found on the same spruce trees that respiration rates of fine roots and proportion of absorptive fine roots to the total root biomass were both small. A preferential investment of current photoassimilates following high C sink strength of growing fine roots has also been observed in young beech trees upon drought release (Hagedorn et al., 2016) and in naturally drought-stressed mature pine trees after a rainfall event (Gao et al., 2021; Joseph et al., 2020).

Not only previously drought-stressed spruce but also control trees responded with fast C incorporation in living fine roots after increase in soil water availability. During an intensive rain event on day 17 (following a short dry spell), fine root growth was likely induced in the shallow soil layers (Joseph et al., 2020; Meier & Leuschner, 2008). This may explain the fast arrival of unlabeled tracer in root

tips in both treatments 2 weeks after drought release (Figure 7b). Our results suggest, therefore, that the speed of incorporation of current photoassimilates in living root tips of mature spruce trees is strongly dependent on the C demand for root production, that is, “sink controlled” as suggested earlier (Faticchi et al., 2014; Gavito et al., 2019; Hagedorn et al., 2016; Körner, 2015). In contrast to previous studies (Gao et al., 2021; Hagedorn et al., 2016), the increased “sink demand” by stimulated fine root growth in mature spruce did not significantly affect the whole-tree CTR from crown to soil, since they were still reduced in the first week after drought release (Figure 5a). Above all, mature drought-stressed spruce trees respond to drought release by quickly supplying the growing root tips with current photoassimilates. In addition to the high resilience in whole-tree C transport, this response is essential to regenerate the water-absorbing root system.

## 5 | CONCLUSION

The present study reveals high resilience of the whole-tree C transport system in Norway spruce forests even after recurrent summer droughts. Once spruce trees manage to survive drought periods, their whole-tree C transport system may be expected to recover quickly after drought release. This ensures high resilience of C supply with current photoassimilates, in particular to belowground sinks such as growing fine roots. Once the water-absorbing root system is restored, long-term recovery of C uptake and supply to further sinks can be expected. However, recovery of the C transport is only one of the many important prerequisites for the recovery of tree productivity. Thus, long-term observations of C source and sink activities upon drought release are necessary to elucidate the recovery potential of productivity in central European forests dominated by Norway spruce stands.

## ACKNOWLEDGMENTS

We thank Thomas Feuerbach (TUM) for technical support and maintenance of the measurement equipment. We also thank Timo Gebhardt, Karl-Heinz Häberle, Josef Heckmair, Peter Kuba, bachelor/master students (TUM), Laura Pohlenz, Ramona Werner, and ecology volunteers (Helmholtz Zentrum München) for support during the fieldwork, Phillip Papastefanou (TUM) for support with the calculation of CTR, Timo Knüver (KIT) for his support with the soil respiration unit, and Manuela Laski and Manuela Oettli for laboratory support (both WSL). This study was funded by the German Research Foundation (DFG) through grants GR 1881/5-1, MA1763/10-1, PR555/2-1, PR292/22-1 and by the Bavarian State Ministries of the Environment and Consumer Protection as well as Food, Agriculture and Forestry (W047/Kroof II). RR and NKR were supported by the German Research Foundation through its Emmy Noether Program (RU 1657/2-1). MML was supported by the Ambizione grant (179978) from the Swiss National Science Foundation (SNSF). BDH was funded by a doctoral scholarship from the German Federal Environmental Foundation (DBU, AZ 20018/535). Open Access funding enabled and organized by Projekt DEAL.

## CONFLICT OF INTEREST

The authors declare that there is no conflict of interest.





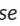





## AUTHOR CONTRIBUTIONS

TEEG and KP designed the experiment. KH, VR, and TEEG prepared and conducted the <sup>13</sup>C labeling experiment. All authors contributed to the data collection. KH analyzed and interpreted the data with supports from TEEG, JD, and VR. KH wrote the manuscript with contributions of all authors.

## DATA AVAILABILITY STATEMENT

The data that support the findings of this study are openly available in mediaTUM at <https://doi.org/10.14459/2021mp1637391>.

## ORCID

Kyohsuke Hikino  <https://orcid.org/0000-0002-6981-3988>  
 Vincent P. Riedel  <https://orcid.org/0000-0003-1685-8135>  
 Romy Rehschuh  <https://orcid.org/0000-0001-9140-0306>  
 Nadine K. Ruehr  <https://orcid.org/0000-0001-5989-7463>  
 Benjamin D. Hesse  <https://orcid.org/0000-0003-1113-9801>  
 Marco M. Lehmann  <https://orcid.org/0000-0003-2962-3351>  
 Franz Buegger  <https://orcid.org/0000-0003-3526-4711>  
 Fabian Weigl  <https://orcid.org/0000-0003-3973-6341>  
 Karin Pritsch  <https://orcid.org/0000-0001-6384-2473>  
 Thorsten E. E. Grams  <https://orcid.org/0000-0002-4355-8827>

## REFERENCES

- Allen, C. D., Breshears, D. D., & McDowell, N. G. (2015). On underestimation of global vulnerability to tree mortality and forest die-off from hotter drought in the Anthropocene. *Ecosphere*, 6(8), art129. <https://doi.org/10.1890/ES15-00203.1>
- Allen, C. D., Macalady, A. K., Chenchouni, H., Bachelet, D., McDowell, N., Vennetier, M., Kitzberger, T., Rigling, A., Breshears, D. D., Hogg, E. H., Gonzalez, P., Fensham, R., Zhang, Z., Castro, J., Demidova, N., Lim, J.-H., Allard, G., Running, S. W., Semerci, A., & Cobb, N. (2010). A global overview of drought and heat-induced tree mortality reveals emerging climate change risks for forests. *Forest Ecology and Management*, 259(4), 660–684. <https://doi.org/10.1016/j.foreco.2009.09.001>
- Andersen, C. P., Ritter, W., Gregg, J., Matyssek, R., & Grams, T. E. E. (2010). Below-ground carbon allocation in mature beech and spruce trees following long-term, experimentally enhanced O<sub>3</sub> exposure in Southern Germany. *Environmental Pollution*, 158(8), 2604–2609. <https://doi.org/10.1016/j.envpol.2010.05.008>
- Arend, M., Link, R. M., Patthey, R., Hoch, G., Schuldt, B., & Kahmen, A. (2021). Rapid hydraulic collapse as cause of drought-induced mortality in conifers. *Proceedings of the National Academy of Sciences of the United States of America*, 118(16), e2025251118. <https://doi.org/10.1073/pnas.2025251118>
- Barthel, M., Hammerle, A., Sturm, P., Baur, T., Gentsch, L., & Knohl, A. (2011). The diel imprint of leaf metabolism on the δ<sup>13</sup>C signal of soil respiration under control and drought conditions. *The New Phytologist*, 192(4), 925–938. <https://doi.org/10.1111/j.1469-8137.2011.03848.x>
- Boczoń, A., Kowalska, A., Ksepko, M., & Sokotowski, K. (2018). Climate warming and drought in the Białowieża Forest from 1950–2015 and their impact on the dieback of Norway spruce stands. *Water*, 10(11), 1950–2015. <https://doi.org/10.3390/w10111502>

- Braden-Behrens, J., Yan, Y., & Knohl, A. (2017). A new instrument for stable isotope measurements of  $^{13}\text{C}$  and  $^{18}\text{O}$  in  $\text{CO}_2$  – Instrument performance and ecological application of the Delta Ray IRIS analyzer. *Atmospheric Measurement Techniques*, 10(11), 4537–4560. <https://doi.org/10.5194/amt-10-4537-2017>
- Caudullo, G., Tinner, W., & De Rigo, D. (2016). *Picea abies* in Europe: Distribution, habitat, usage and threats. In J. San-Miguel-Ayanz, D. de Rigo, G. Caudullo, T. Houston Durrant, & A. Mauri (Eds.), *European atlas of forest tree species* (pp. 114–116). Publications Office of the EU, e012300+ pp.
- Ciais, P. H., Reichstein, M., Viovy, N., Granier, A., Ogée, J., Allard, V., Aubinet, M., Buchmann, N., Bernhofer, C., Carrara, A., Chevallier, F., De Noblet, N., Friend, A. D., Friedlingstein, P., Grünwald, T., Heinesch, B., Keronen, P., Knohl, A., Krinner, G., ... Valentini, R. (2005). Europe-wide reduction in primary productivity caused by the heat and drought in 2003. *Nature*, 437(7058), 529–533. <https://doi.org/10.1038/nature03972>
- Collins, M., Knutti, R., Arblaster, J., Dufresne, J.-L., Fichetef, T., Friedlingstein, P., Gao, X., Gutowski, W. J., Johns, T., Krinner, G., Shongwe, M., Tebaldi, C., Weaver, A. J., & Wehner, M. (2013). Long-term climate change: Projections, commitments and irreversibility. In T. F. Stocker, D. Qin, G.-K. Plattner, M. Tignor, S. K. Allen, J. Boschung, A. Nauels, Y. Xia, V. Bex, & P. M. Midgley (Eds.), *Climate change 2013: The physical science basis. Contribution of working group I to the fifth assessment report of the Intergovernmental Panel on Climate Change* (pp. 1029–1136). Cambridge University Press.
- Dannoura, M., Epron, D., Desalme, D., Massonnet, C., Tsuji, S., Plain, C., Priault, P., & Gérard, D. (2019). The impact of prolonged drought on phloem anatomy and phloem transport in young beech trees. *Tree Physiology*, 39(2), 201–210. <https://doi.org/10.1093/treephys/tpy070>
- Dawson, T. E., Mambelli, S., Plamboeck, A. H., Templer, P. H., & Tu, K. P. (2002). Stable isotopes in plant ecology. *Annual Review of Ecology and Systematics*, 33(1), 507–559. <https://doi.org/10.1146/annurev.ecolsys.33.020602.095451>
- De Schepper, V., De Swaef, T., Bauweraerts, I., & Steppe, K. (2013). Phloem transport: A review of mechanisms and controls. *Journal of Experimental Botany*, 64(16), 4839–4850. <https://doi.org/10.1093/jxb/ert302>
- Epron, D., Bahn, M., Derrien, D., Lattanzi, F. A., Pumpanen, J., Gessler, A., Högberg, P., Maillard, P., Dannoura, M., Gérard, D., & Buchmann, N. (2012). Pulse-labelling trees to study carbon allocation dynamics: A review of methods, current knowledge and future prospects. *Tree Physiology*, 32(6), 776–798. <https://doi.org/10.1093/treephys/tps057>
- Epron, D., Cabral, O. M. R., Laclau, J.-P., Dannoura, M., Packer, A. P., Plain, C., Battie-Laclau, P., Moreira, M. Z., Trivelin, P. C. O., Bouillet, J.-P., Gérard, D., & Nouvellon, Y. (2016). In situ  $^{13}\text{C}$  pulse labelling of field-grown eucalypt trees revealed the effects of potassium nutrition and throughfall exclusion on phloem transport of photosynthetic carbon. *Tree Physiology*, 36(1), 6–21. <https://doi.org/10.1093/treephys/tpv090>
- Epron, D., & Dreyer, E. (1996). Starch and soluble carbohydrates in leaves of water-stressed oak saplings. *Annales Des Sciences Forestières*, 53(2–3), 263–268. <https://doi.org/10.1051/forest:19960209>
- Fatichi, S., Leuzinger, S., & Körner, C. (2014). Moving beyond photosynthesis: From carbon source to sink-driven vegetation modeling. *The New Phytologist*, 201(4), 1086–1095. <https://doi.org/10.1111/nph.12614>
- Fiscus, E. L. (1972). In situ measurement of root-water potential. *Plant Physiology*, 50(1), 191–193. <https://doi.org/10.1104/pp.50.1.191>
- Gammitzer, U., Schäufele, R., & Schnyder, H. (2009). Observing  $^{13}\text{C}$  labelling kinetics in  $\text{CO}_2$  respired by a temperate grassland ecosystem. *The New Phytologist*, 184(2), 376–386. <https://doi.org/10.1111/j.1469-8137.2009.02963.x>
- Gao, D., Joseph, J., Werner, R. A., Brunner, I., Zürcher, A., Hug, C., Wang, A., Zhao, C., Bai, E., Meusburger, K., Gessler, A., & Hagedorn, F. (2021). Drought alters the carbon footprint of trees in soils-tracking the spatio-temporal fate of  $^{13}\text{C}$ -labelled assimilates in the soil of an old-growth pine forest. *Global Change Biology*. <https://doi.org/10.1111/gcb.15557>
- Gavito, M. E., Jakobsen, I., Mikkelsen, T. N., & Mora, F. (2019). Direct evidence for modulation of photosynthesis by an arbuscular mycorrhiza-induced carbon sink strength. *The New Phytologist*, 223(2), 896–907. <https://doi.org/10.1111/nph.15806>
- Gleason, S. M., Wiggins, D. R., Bliss, C. A., Young, J. S., Cooper, M., Willi, K. R., & Comas, L. H. (2017). Embolized stems recover overnight in *Zea mays*: The role of soil water, root pressure, and nighttime transpiration. *Frontiers in Plant Science*, 8, 662. <https://doi.org/10.3389/fpls.2017.00662>
- Goisser, M., Geppert, U., Rötzer, T., Paya, A., Huber, A., Kerner, R., Bauerle, T., Pretsch, H., Pritsch, K., Häberle, K. H., Matyssek, R., & Grams, T. (2016). Does belowground interaction with *Fagus sylvatica* increase drought susceptibility of photosynthesis and stem growth in *Picea abies*? *Forest Ecology and Management*, 375, 268–278. <https://doi.org/10.1016/j.foreco.2016.05.032>
- Grams, T. E. E., Hesse, B. D., Gebhardt, T., Weigl, F., Rötzer, T., Kovacs, B., Hikino, K., Hafner, B. D., Brunn, M., Bauerle, T. L., Häberle, K.-H., Pretsch, H., & Pritsch, K. (2021). The Kroof experiment: Realization and efficacy of a recurrent drought experiment plus recovery in a beech/spruce forest. *Ecosphere*, 12(3). <https://doi.org/10.1002/ecs2.3399>
- Grams, T. E. E., Werner, H., Kuptz, D., Ritter, W., Fleischmann, F., Andersen, C. P., & Matyssek, R. (2011). A free-air system for long-term stable carbon isotope labeling of adult forest trees. *Trees*, 25(2), 187–198. <https://doi.org/10.1007/s00468-010-0497-7>
- Gričar, J., Prislán, P., Gryc, V., Vavrčik, H., de Luis, M., & Cufar, K. (2014). Plastic and locally adapted phenology in cambial seasonality and production of xylem and phloem cells in *Picea abies* from temperate environments. *Tree Physiology*, 34(8), 869–881. <https://doi.org/10.1093/treephys/tpu026>
- Hagedorn, F., Joseph, J., Peter, M., Luster, J., Pritsch, K., Geppert, U., Kerner, R., Molinier, V., Egli, S., Schaub, M., Liu, J.-F., Li, M., Sever, K., Weiler, M., Siegwolf, R. T. W., Gessler, A., & Arend, M. (2016). Recovery of trees from drought depends on belowground sink control. *Nature Plants*, 2, 16111. <https://doi.org/10.1038/NPLAN.TS.2016.111>
- Hartmann, H., Ziegler, W., Kolle, O., & Trumbore, S. (2013). Thirst beats hunger – Declining hydration during drought prevents carbon starvation in Norway spruce saplings. *The New Phytologist*, 200(2), 340–349. <https://doi.org/10.1111/nph.12331>
- Hartmann, H., Ziegler, W., & Trumbore, S. (2013). Lethal drought leads to reduction in nonstructural carbohydrates in Norway spruce tree roots but not in the canopy. *Functional Ecology*, 27(2), 413–427. <https://doi.org/10.1111/1365-2435.12046>
- Hentschel, R., Rosner, S., Kayler, Z. E., Andreassen, K., Børja, I., Solberg, S., Tveito, O. E., Priesack, E., & Gessler, A. (2014). Norway spruce physiological and anatomical predisposition to dieback. *Forest Ecology and Management*, 322, 27–36. <https://doi.org/10.1016/j.foreco.2014.03.007>
- Hesse, B. D., Goisser, M., Hartmann, H., & Grams, T. E. E. (2019). Repeated summer drought delays sugar export from the leaf and impairs phloem transport in mature beech. *Tree Physiology*, 39(2), 192–200. <https://doi.org/10.1093/treephys/tpy122>
- Hölttä, T., Mencuccini, M., & Nikinmaa, E. (2009). Linking phloem function to structure: Analysis with a coupled xylem-phloem transport model. *Journal of Theoretical Biology*, 259(2), 325–337. <https://doi.org/10.1016/j.jtbi.2009.03.039>
- Hölttä, T., Vesala, T., Sevanto, S., Perämäki, M., & Nikinmaa, E. (2006). Modeling xylem and phloem water flows in trees according to

- cohesion theory and Münch hypothesis. *Trees*, 20(1), 67–78. <https://doi.org/10.1007/s00468-005-0014-6>
- Hsiao, T. C. (1973). Plant responses to water stress. *Annual Review of Plant Physiology*, 24(1), 519–570. <https://doi.org/10.1146/annurev.ev.pp.24.060173.002511>
- IPCC. (2007). Summary for policymakers. In M. L. Parry, O. F. Canziani, J. P. Palutikof, P. J. van der Linden, & C. E. Hanson (Eds.), *Climate change 2007: Impacts, adaptation and vulnerability. Contribution of working group II to the fourth assessment report of the intergovernmental panel on climate change* (pp. 7–22). Cambridge University Press.
- IPCC. (2014). *Climate change 2014: Synthesis report. Contribution of working groups I, II and III to the fifth assessment report of the intergovernmental panel on climate change* [Core Writing Team, R. K. Pachauri, & L. A. Meyer (Eds.)]. IPCC, 151 pp.
- Joseph, J., Gao, D., Backes, B., Bloch, C., Brunner, I., Gleixner, G., Haeni, M., Hartmann, H., Hoch, G., Hug, C., Kahmen, A., Lehmann, M. M., Li, M.-H., Luster, J., Peter, M., Poll, C., Rigling, A., Rissanen, K. A., Ruehr, N. K., ... Gessler, A. (2020). Rhizosphere activity in an old-growth forest reacts rapidly to changes in soil moisture and shapes whole-tree carbon allocation. *Proceedings of the National Academy of Sciences of the United States of America*, 117(40), 24885–24892. <https://doi.org/10.1073/pnas.2014084117>
- Jyske, T. M., Suuronen, J.-P., Pranovich, A. V., Laakso, T., Watanabe, U., Kuroda, K., & Abe, H. (2015). Seasonal variation in formation, structure, and chemical properties of phloem in *Picea abies* as studied by novel microtechniques. *Planta*, 242(3), 613–629. <https://doi.org/10.1007/s00425-015-2347-8>
- Keeling, C. D. (1958). The concentration and isotopic abundances of atmospheric carbon dioxide in rural areas. *Geochimica Et Cosmochimica Acta*, 13(4), 322–334. [https://doi.org/10.1016/0016-7037\(58\)90033-4](https://doi.org/10.1016/0016-7037(58)90033-4)
- Keeling, C. D. (1961). The concentration and isotopic abundances of carbon dioxide in rural and marine air. *Geochimica Et Cosmochimica Acta*, 24(3–4), 277–298. [https://doi.org/10.1016/0016-7037\(61\)90023-0](https://doi.org/10.1016/0016-7037(61)90023-0)
- Kodama, N., Barnard, R. L., Salmon, Y., Weston, C., Ferrio, J. P., Holst, J., Werner, R. A., Saurer, M., Rennenberg, H., Buchmann, N., & Gessler, A. (2008). Temporal dynamics of the carbon isotope composition in a *Pinus sylvestris* stand: From newly assimilated organic carbon to respired carbon dioxide. *Oecologia*, 156(4), 737–750. <https://doi.org/10.1007/s00442-008-1030-1>
- Körner, C. (2015). Paradigm shift in plant growth control. *Current Opinion in Plant Biology*, 25, 107–114. <https://doi.org/10.1016/j.pbi.2015.05.003>
- Kuptz, D., Fleischmann, F., Matyssek, R., & Grams, T. E. E. (2011). Seasonal patterns of carbon allocation to respiratory pools in 60-yr-old deciduous (*Fagus sylvatica*) and evergreen (*Picea abies*) trees assessed via whole-tree stable carbon isotope labeling. *The New Phytologist*, 191(1), 160–172. <https://doi.org/10.1111/j.1469-8137.2011.03676.x>
- Kuzyakov, Y., & Gavrichkova, O. (2010). REVIEW: Time lag between photosynthesis and carbon dioxide efflux from soil: A review of mechanisms and controls. *Global Change Biology*, 16(12), 3386–3406. <https://doi.org/10.1111/j.1365-2486.2010.02179.x>
- Lehmann, M. M., Egli, M., Brinkmann, N., Werner, R. A., Saurer, M., & Kahmen, A. (2020). Improving the extraction and purification of leaf and phloem sugars for oxygen isotope analyses. *Rapid Communications in Mass Spectrometry*, 34(19), e8854. <https://doi.org/10.1002/rcm.8854>
- Lemoine, R., La Camera, S., Atanassova, R., Dédaldéchamp, F., Allario, T., Pourtau, N., Bonnemain, J.-L., Laloi, M., Coutos-Thévenot, P., Maurousset, L., Faucher, M., Girousse, C., Lemonnier, P., Parrilla, J., & Durand, M. (2013). Source-to-sink transport of sugar and regulation by environmental factors. *Frontiers in Plant Science*, 4, 272. <https://doi.org/10.3389/fpls.2013.00272>
- Liesche, J., Windt, C., Bohr, T., Schulz, A., & Jensen, K. H. (2015). Slower phloem transport in gymnosperm trees can be attributed to higher sieve element resistance. *Tree Physiology*, 35(4), 376–386. <https://doi.org/10.1093/treephys/tpv020>
- Lloret, F., Keeling, E. G., & Sala, A. (2011). Components of tree resilience: Effects of successive low-growth episodes in old ponderosa pine forests. *Oikos*, 120(12), 1909–1920. <https://doi.org/10.1111/j.1600-0706.2011.19372.x>
- McCully (1999). Root xylem embolisms and refilling. Relation To water potentials of soil, roots, and leaves, and osmotic potentials of root xylem Sap. *Plant Physiology*, 119(3), 1001–1008. <https://doi.org/10.1104/pp.119.3.1001>
- McDowell, N., Pockman, W. T., Allen, C. D., Breshears, D. D., Cobb, N., Kolb, T., Plaut, J., Sperry, J., West, A., Williams, D. G., & Yepez, E. A. (2008). Mechanisms of plant survival and mortality during drought: Why do some plants survive while others succumb to drought? *The New Phytologist*, 178(4), 719–739. <https://doi.org/10.1111/j.1469-8137.2008.02436.x>
- Meier, I. C., & Leuschner, C. (2008). Belowground drought response of European beech: Fine root biomass and carbon partitioning in 14 mature stands across a precipitation gradient. *Global Change Biology*, 14(9), 2081–2095. <https://doi.org/10.1111/j.1365-2486.2008.01634.x>
- Mencuccini, M., & Hölttä, T. (2010). The significance of phloem transport for the speed with which canopy photosynthesis and below-ground respiration are linked. *The New Phytologist*, 185(1), 189–203. <https://doi.org/10.1111/j.1469-8137.2009.03050.x>
- Miller, T. W., Stangler, D. F., Larysch, E., Seifert, T., Spiecker, H., & Kahle, H.-P. (2020). Plasticity of seasonal xylem and phloem production of Norway spruce along an elevational gradient. *Trees*, 34(5), 1281–1297. <https://doi.org/10.1007/s00468-020-01997-6>
- Muhr, J., & Borken, W. (2009). Delayed recovery of soil respiration after wetting of dry soil further reduces C losses from a Norway spruce forest soil. *Journal of Geophysical Research*, 114(G4). <https://doi.org/10.1029/2009JG000998>
- Nikolova, P. S., Bauerle, T. L., Häberle, K.-H., Blaschke, H., Brunner, I., & Matyssek, R. (2020). Fine-root traits reveal contrasting ecological strategies in European beech and Norway spruce during extreme drought. *Frontiers in Plant Science*, 11, 1211. <https://doi.org/10.3389/fpls.2020.01211>
- Nikolova, P. S., Raspe, S., Andersen, C. P., Mainiero, R., Blaschke, H., Matyssek, R., & Häberle, K.-H. (2009). Effects of the extreme drought in 2003 on soil respiration in a mixed forest. *European Journal of Forest Research*, 128(2), 87–98. <https://doi.org/10.1007/s10342-008-0218-6>
- Pretzsch, H., Grams, T. E. E., Häberle, K.-H., Pritsch, K., Bauerle, T. L., & Rötzer, T. (2020). Growth and mortality of Norway spruce and European beech in monospecific and mixed-species stands under natural episodic and experimentally extended drought. Results of the KROOF throughfall exclusion experiment. *Trees*, 34(4), 957–970. <https://doi.org/10.1007/s00468-020-01973-0>
- Pretzsch, H., Rötzer, T., Matyssek, R., Grams, T. E. E., Häberle, K.-H., Pritsch, K., Kerner, R., & Munch, J.-C. (2014). Mixed Norway spruce (*Picea abies* [L.] Karst) and European beech (*Fagus sylvatica* [L.] stands under drought: From reaction pattern to mechanism. *Trees*, 28(5), 1305–1321. <https://doi.org/10.1007/s00468-014-1035-9>
- Rosner, S., Světlík, J., Andreassen, K., Børja, I., Dalsgaard, L., Evans, R., Luss, S., Tveito, O. E., & Solberg, S. (2016). Novel hydraulic vulnerability proxies for a boreal conifer species reveal that opportunists may have lower survival prospects under extreme climatic events. *Frontiers in Plant Science*, 7, 831. <https://doi.org/10.3389/fpls.2016.00831>
- Ruehr, N. K., Grote, R., Mayr, S., & Arneth, A. (2019). Beyond the extreme: Recovery of carbon and water relations in woody plants following heat and drought stress. *Tree Physiology*, 39(8), 1285–1299. <https://doi.org/10.1093/treephys/tpz032>

- Ruehr, N. K., Offermann, C. A., Gessler, A., Winkler, J. B., Ferrio, J. P., Buchmann, N., & Barnard, R. L. (2009). Drought effects on allocation of recent carbon: From beech leaves to soil CO<sub>2</sub> efflux. *The New Phytologist*, 184(4), 950–961. <https://doi.org/10.1111/j.1469-8137.2009.03044.x>
- Ryan, M. G., & Asao, S. (2014). Phloem transport in trees. *Tree Physiology*, 34(1), 1–4. <https://doi.org/10.1093/treephys/tpt123>
- Salmon, Y., Dietrich, L., Sevanto, S., Hölttä, T., Dannoura, M., & Epron, D. (2019). Drought impacts on tree phloem: From cell-level responses to ecological significance. *Tree Physiology*, 39(2), 173–191. <https://doi.org/10.1093/treephys/tpy153>
- Schindlbacher, A., Wunderlich, S., Borken, W., Kitzler, B., Zechmeister-Boltenstern, S., & Jandl, R. (2012). Soil respiration under climate change: Prolonged summer drought offsets soil warming effects. *Global Change Biology*, 18(7), 2270–2279. <https://doi.org/10.1111/j.1365-2486.2012.02696.x>
- Sevanto, S. (2014). Phloem transport and drought. *Journal of Experimental Botany*, 65(7), 1751–1759. <https://doi.org/10.1093/jxb/ert467>
- Sevanto, S. (2018). Drought impacts on phloem transport. *Current Opinion in Plant Biology*, 43, 76–81. <https://doi.org/10.1016/j.pbi.2018.01.002>
- Solberg, S. (2004). Summer drought: A driver for crown condition and mortality of Norway spruce in Norway. *Forest Pathology*, 34(2), 93–104. <https://doi.org/10.1111/j.1439-0329.2004.00351.x>
- Steinmann, K., Siegwolf, R. T. W., Saurer, M., & Körner, C. (2004). Carbon fluxes to the soil in a mature temperate forest assessed by <sup>13</sup>C isotope tracing. *Oecologia*, 141(3), 489–501. <https://doi.org/10.1007/s00442-004-1674-4>
- Subke, J.-A., Vallack, H. W., Magnusson, T., Keel, S. G., Metcalfe, D. B., Högberg, P., & Ineson, P. (2009). Short-term dynamics of abiotic and biotic soil <sup>13</sup>CO<sub>2</sub> effluxes after in situ <sup>13</sup>CO<sub>2</sub> pulse labelling of a boreal pine forest. *The New Phytologist*, 183(2), 349–357. <https://doi.org/10.1111/j.1469-8137.2009.02883.x>
- Teskey, R. O., Saveyn, A. N., Steppe, K., & McGuire, M. A. (2008). Origin, fate and significance of CO<sub>2</sub> in tree stems. *The New Phytologist*, 177(1), 17–32. <https://doi.org/10.1111/j.1469-8137.2007.02286.x>
- Tomasella, M., Beikircher, B., Häberle, K.-H., Hesse, B., Kallenbach, C., Matyssek, R., & Mayr, S. (2018). Acclimation of branch and leaf hydraulics in adult *Fagus sylvatica* and *Picea abies* in a forest through-fall exclusion experiment. *Tree Physiology*, 38(2), 198–211. <https://doi.org/10.1093/treephys/tpx140>
- Ubierna, N., Marshall, J. D., & Cernusak, L. A. (2009). A new method to measure carbon isotope composition of CO<sub>2</sub> respired by trees: Stem CO<sub>2</sub> equilibration. *Functional Ecology*, 23(6), 1050–1058. <https://doi.org/10.1111/j.1365-2435.2009.01593.x>
- Unger, S., Máguas, C., Pereira, J. S., David, T. S., & Werner, C. (2010). The influence of precipitation pulses on soil respiration – Assessing the “Birch effect” by stable carbon isotopes. *Soil Biology and Biochemistry*, 42(10), 1800–1810. <https://doi.org/10.1016/j.soilbio.2010.06.019>
- van Bel, A. J. E. (2003). The phloem, a miracle of ingenuity. *Plant, Cell & Environment*, 26(1), 125–149. <https://doi.org/10.1046/j.1365-3040.2003.00963.x>
- van Mantgem, P. J., Stephenson, N. L., Byrne, J. C., Daniels, L. D., Franklin, J. F., Fulé, P. Z., Harmon, M. E., Larson, A. J., Smith, J. M., Taylor, A. H., & Veblen, T. T. (2009). Widespread increase of tree mortality rates in the western United States. *Science*, 323(5913), 521–524. <https://doi.org/10.1126/science.1165000>
- Wang, A., Siegwolf, R. T. W., Joseph, J., Thomas, F. M., Werner, W., Gessler, A., Rigling, A., Schaub, M., Saurer, M., Li, M.-H., & Lehmann, M. M. (2021). Effects of soil moisture, needle age and leaf morphology on carbon and oxygen uptake, incorporation and allocation: A dual labeling approach with <sup>13</sup>CO<sub>2</sub> and H<sub>2</sub><sup>18</sup>O in foliage of a coniferous forest. *Tree Physiology*, 41(1), 50–62. <https://doi.org/10.1093/treephys/tpaa114>
- Wingate, L., Ogée, J., Burrell, R., Bosc, A., Devaux, M., Grace, J., Loustau, D., & Gessler, A. (2010). Photosynthetic carbon isotope discrimination and its relationship to the carbon isotope signals of stem, soil and ecosystem respiration. *The New Phytologist*, 188(2), 576–589. <https://doi.org/10.1111/j.1469-8137.2010.03384.x>
- Winkler, A., & Oberhuber, W. (2017). Cambial response of Norway spruce to modified carbon availability by phloem girdling. *Tree Physiology*, 37(11), 1527–1535. <https://doi.org/10.1093/treephys/tpx077>
- Woodruff, D. R. (2014). The impacts of water stress on phloem transport in Douglas-fir trees. *Tree Physiology*, 34(1), 5–14. <https://doi.org/10.1093/treephys/tpt106>
- Zang, U., Goisser, M., Grams, T. E. E., Häberle, K.-H., Matyssek, R., Matzner, E., & Borken, W. (2014). Fate of recently fixed carbon in European beech (*Fagus sylvatica*) saplings during drought and subsequent recovery. *Tree Physiology*, 34(1), 29–38. <https://doi.org/10.1093/treephys/tpx110>
- Zwetsloot, M. J., & Bauerle, T. L. (2021). Repetitive seasonal drought causes substantial species-specific shifts in fine-root longevity and spatio-temporal production patterns in mature temperate forest trees. *The New Phytologist*, 231(3), 974–986. <https://doi.org/10.1111/nph.17432>

## SUPPORTING INFORMATION

Additional supporting information may be found in the online version of the article at the publisher's website.

**How to cite this article:** Hikino, K., Danzberger, J., Riedel, V. P., Rehschuh, R., Ruehr, N. K., Hesse, B. D., Lehmann, M. M., Buegger, F., Weikl, F., Pritsch, K., & Grams, T. E. E. (2022). High resilience of carbon transport in long-term drought-stressed mature Norway spruce trees within 2 weeks after drought release. *Global Change Biology*, 28, 2095–2110. <https://doi.org/10.1111/gcb.16051>

## Supplementary figures and tables

### High resilience of carbon transport in long-term drought stressed mature Norway spruce trees within two weeks after drought release

Kyohsuke Hikino, Jasmin Danzberger, Vincent P. Riedel, Romy Rehschuh, Nadine K. Ruehr, Benjamin D. Hesse, Marco M. Lehmann, Franz Buegger, Fabian Weikl, Karin Pritsch, Thorsten E. E. Grams

## Supplementary figures

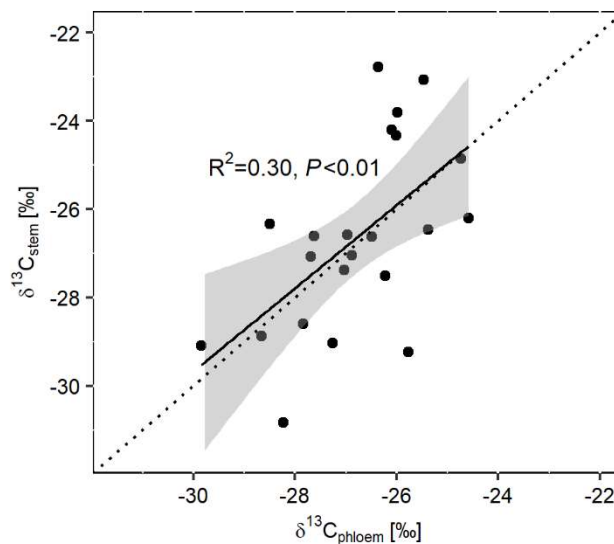


Figure S 1: Correlation between  $\delta^{13}\text{C}$  of stem  $\text{CO}_2$  efflux ( $\delta^{13}\text{C}_{\text{stem}}$ ) and  $\delta^{13}\text{C}$  of stem phloem sugar ( $\delta^{13}\text{C}_{\text{phloem}}$ ). The dashed line is 1:1 line and the solid line is the calculated regression line (slope = 0.94). The gray area displays the 95% confidence interval.

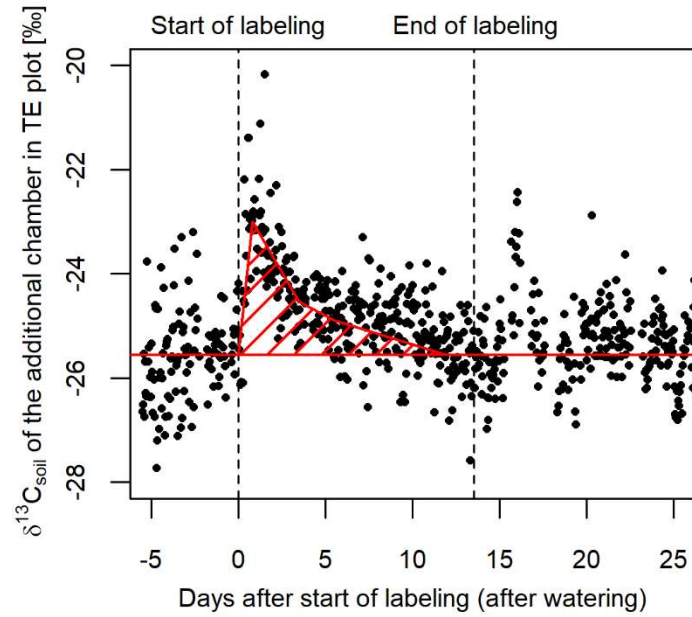


Figure S 2:  $\delta^{13}\text{C}$  of the additional soil chamber ( $\delta^{13}\text{C}_{\text{soil}}$ ) close to the non-labeled beech trees in the TE (previously drought-stressed, throughfall exclusion) plot (see Figure 2a). Dashed lines indicate start and end of labeling. The red horizontal line displays the mean  $\delta^{13}\text{C}_{\text{soil}}$  before the start of labeling. The shift of  $\delta^{13}\text{C}_{\text{soil}}$  after watering/start of labeling (roughly marked with red striped area for the first 12 days) was subtracted from the  $\delta^{13}\text{C}_{\text{soil}}$  of the soil chambers under labeled trees in the TE plot (for details see Figure S3).

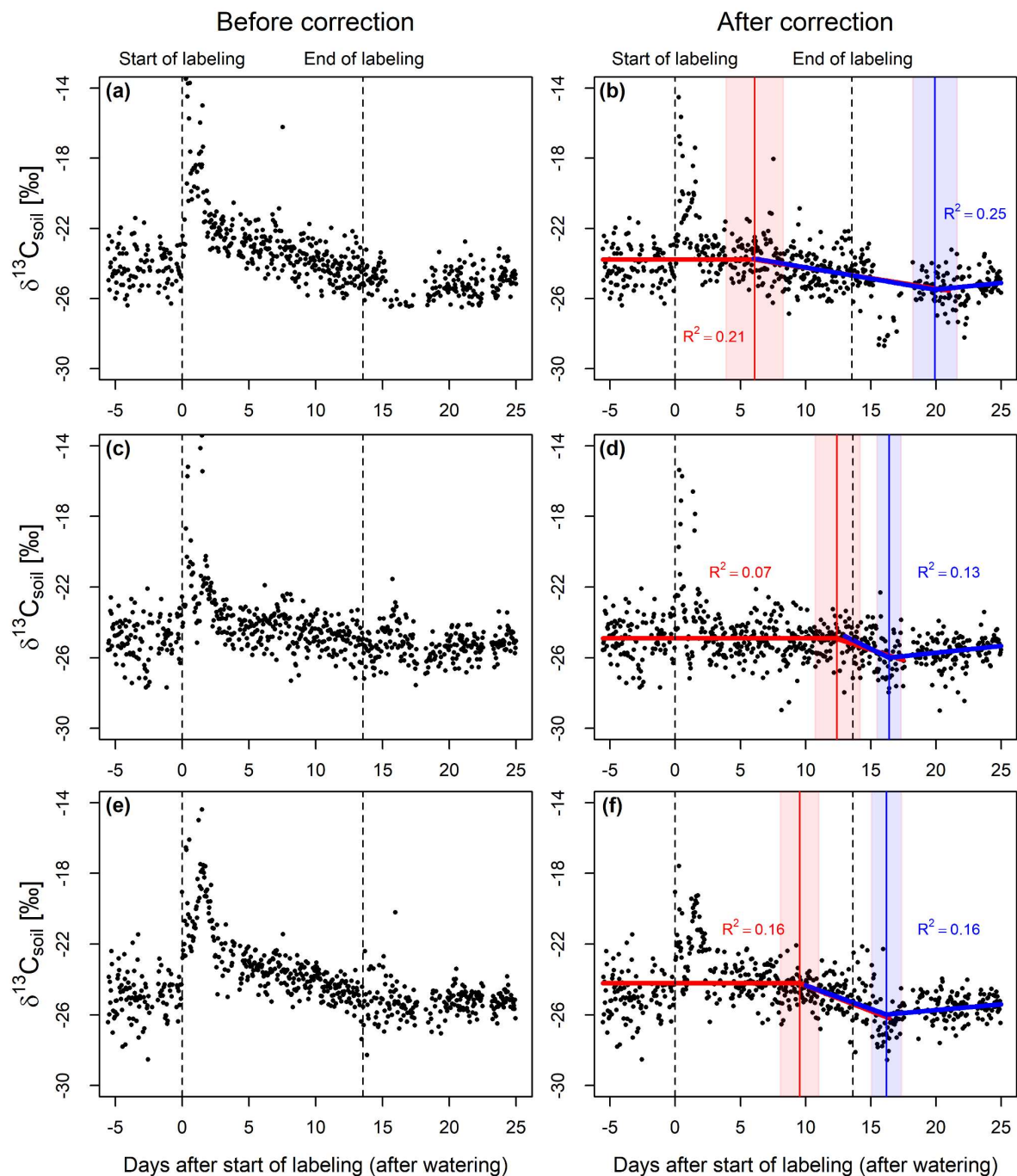


Figure S 3: The correction of  $\delta^{13}\text{C}$  of soil  $\text{CO}_2$  efflux ( $\delta^{13}\text{C}_{\text{soil}}$ ) under labeled, previously drought-stressed trees (TE, throughfall exclusion,  $n = 3$ ) using the additional soil chamber (see Figure S2):  $\delta^{13}\text{C}_{\text{soil}}$  of three TE soil chamber before (a, c, e) and after the correction (b, d, f), respectively. The gap between the values before and after the watering (start of labeling) was properly corrected, enabling to calculate the arrival time of the tracers with piecewise functions. Dashed lines indicate the start and the end of the labeling period. The red and blue lines fitted to the data show the results of the piecewise functions (see Materials and Methods in the main document). The red and blue vertical lines give the calculated arrival time of  $^{13}\text{C}$ -depleted (after turn-on of the  $\text{CO}_2$  exposure) and unlabeled tracer (after turn-off of the  $\text{CO}_2$  exposure), respectively. The red and blue shaded area show the 95% confidence interval of the intersections.



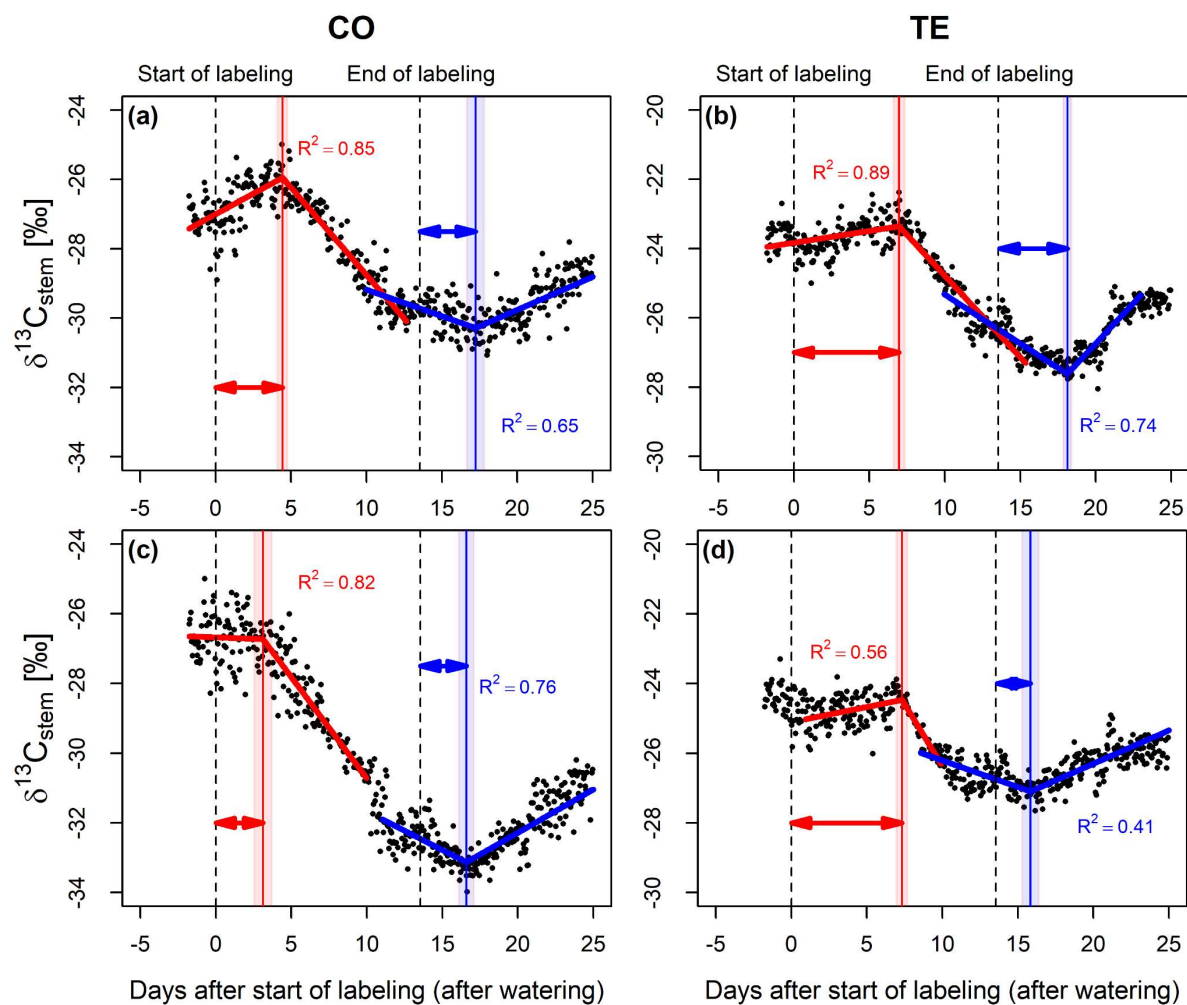


Figure S 4: The other data of  $\delta^{13}\text{C}$  of stem  $\text{CO}_2$  efflux ( $\delta^{13}\text{C}_{\text{stem}}$ ) in CO (control, a, c) and TE (previously drought-stressed, throughfall exclusion, b,d) plots, used for the calculation of the arrival time of the  $^{13}\text{C}$ -tracers (see Materials and Methods in the main document, Figure 4). Dashed vertical lines are the start and the end of labeling. The red and blue lines fitted to the data show the results of the piecewise functions to estimate the arrival time of  $^{13}\text{C}$ -depleted and unlabeled tracer, respectively. The intersections of two lines, marked with solid red and blue vertical lines are the calculated arrival times in the first week and two weeks after the watering, respectively. These arrival times (displayed here with arrows) were then used to calculate the aboveground carbon transport rates ( $\text{CTR}_{\text{above}}$ ). The red and blue shaded area give the 95% confidence interval of the intersections.

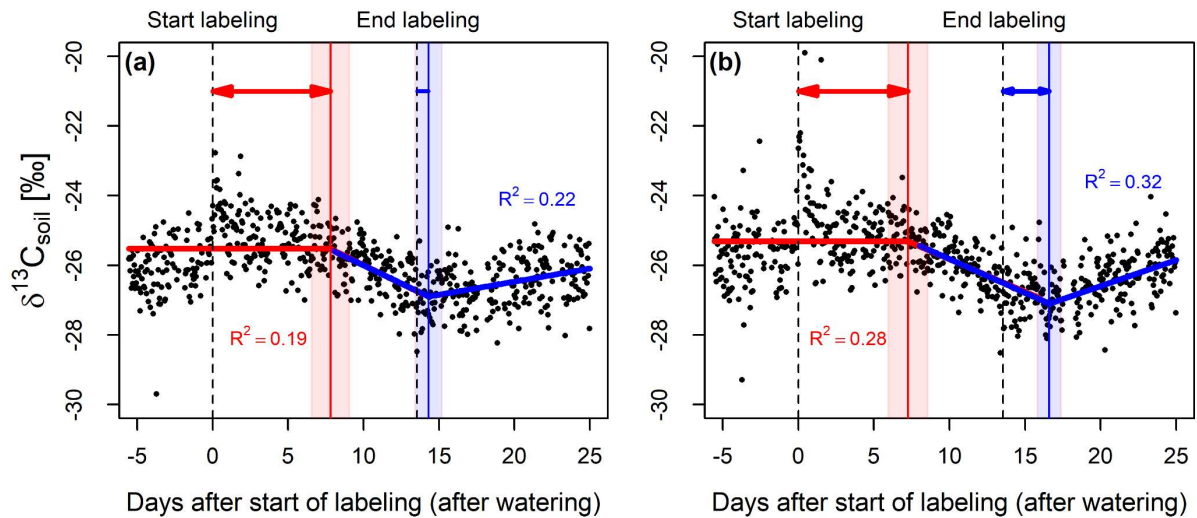


Figure S 5: The other data of  $\delta^{13}\text{C}$  of soil  $\text{CO}_2$  efflux ( $\delta^{13}\text{C}_{\text{soil}}$ ) in CO (control) plot, used for the calculation of the arrival time of the  $^{13}\text{C}$ -tracers (see Materials and Methods in the main document, Figure 4). Dashed vertical lines are the start and the end of labeling. The red and blue lines fitted to the data show the results of the piecewise functions to estimate the arrival time of  $^{13}\text{C}$ -depleted and unlabeled tracer, respectively. The intersections of two lines, marked with solid red and blue vertical lines are the calculated arrival times in the first week and two weeks after the watering, respectively. These arrival times (displayed here with arrows) were then used to calculate the belowground carbon transport rates ( $\text{CTR}_{\text{below}}$ ). The red and blue shaded area give the 95% confidence interval of the intersections.

## Supplementary tables

Table S 1: Diameter at breast height (DBH), mean crown height (middle of the crown), and daily mean shift of CO<sub>2</sub> concentration and stable carbon isotope composition ( $\delta^{13}\text{C}_a$ ) of canopy air during labeling hours (5 am – 7 pm CET) of four labeled control (CO) and three labeled throughfall exclusion (TE, previously drought stressed) trees. Shifts are given in means  $\pm$  SE. The fourth tree on the CO plot was not the object of the calculation of arrival time and C transport rates (CTR), therefore, its mean crown height was not measured.

	DBH [cm]	Mean crown height [m]	Shift of CO <sub>2</sub> concentration [ppm]	Shift of $\delta^{13}\text{C}_a$ [‰]
CO_1	30.5	28.6	111 $\pm$ 8	-6.7 $\pm$ 0.4
CO_2	34.9	27.9	112 $\pm$ 8	-6.7 $\pm$ 0.4
CO_3	46.3	28.7	119 $\pm$ 8	-7.2 $\pm$ 0.4
CO_4	37.7	-	162 $\pm$ 10	-8.8 $\pm$ 0.4
TE_1	45.1	27.3	72 $\pm$ 5	-5.0 $\pm$ 0.3
TE_2	27.3	25.4	132 $\pm$ 8	-7.3 $\pm$ 0.4
TE_3	38.3	28.4	35 $\pm$ 5	-2.9 $\pm$ 0.3

Table S 2: Number of trees and sampling positions assessed for this study in labeled and non-labeled plots in each treatment: i.e. control (CO) and throughfall exclusion (TE, previously drought stressed). n.a.= not assessed.  $A_{\text{sat}}$  (light-saturated CO<sub>2</sub> assimilation rates),  $\Psi_{\text{PD}}$  (Pre-dawn leaf water potential),  $\pi_{\text{O}}$  (leaf osmotic potential).

Number of trees/ sampling positions	Labeled		Non-labeled	
	CO	TE	CO	TE
Spruce tree	4	3	3	3
Canopy air	7	6	1	1
Stem CO <sub>2</sub> efflux	3	3	3	3
Soil CO <sub>2</sub> efflux	3	3	n.a.	1
Root tips	18	17	11	5
Stem phloem	4	3	n.a.	n.a.
$A_{\text{sat}}$ , $\Psi_{\text{PD}}$ , $\pi_{\text{O}}$	2	2	4	4




## Article II: Dynamics of initial C allocation after drought release in mature Norway spruce - Increased belowground allocation of current photoassimilates covers only half of the C used for fine-root growth


Hikino, K. \*, Danzberger, J. \*, Riedel, V. P., Hesse, B. D., Hafner, B. D., Gebhardt, T., Rehschuh, R., Ruehr, N. K., Brunn, M., Bauerle, T. L., Landhäusser, S. M., Lehmann, M. M., Rötzer, T., Pretzsch, H., Buegger, F., Weigl, F., Pritsch, K., & Grams, T. E. E. (2022). *Global Change Biology*.

\* Kyohsuke Hikino and Jasmin Danzberger contributed equally to this work and share the first authorship.

### Open Access Publication

 ? Help Live Chat

---



**Dynamics of initial carbon allocation after drought release in mature Norway spruce—Increased belowground allocation of current photoassimilates covers only half of the carbon used for fine-root growth**

**Author:** Thorsten E. E. Grams, Karin Pritsch, Fabian Weigl, et al  
**Publication:** *Global Change Biology*  
**Publisher:** John Wiley and Sons  
**Date:** Aug 30, 2022

© 2022 The Authors. *Global Change Biology* published by John Wiley & Sons Ltd.

---

**Open Access Article**

This is an open access article distributed under the terms of the [Creative Commons CC BY](#) license, which permits unrestricted use, distribution, and reproduction in any medium, provided the original work is properly cited.

You are not required to obtain permission to reuse this article.

For an understanding of what is meant by the terms of the Creative Commons License, please refer to [Wiley's Open Access Terms and Conditions](#).

Permission is not required for this type of reuse.

Wiley offers a professional reprint service for high quality reproduction of articles from over 1400 scientific and medical journals. Wiley's reprint service offers:

- Peer reviewed research or reviews
- Tailored collections of articles
- A professional high quality finish
- Glossy journal style color covers
- Company or brand customisation
- Language translations
- Prompt turnaround times and delivery directly to your office, warehouse or congress.

Please contact our Reprints department for a quotation. Email [corporatesales@wiley.com](mailto:corporatesales@wiley.com) or [corporatesalesusa@wiley.com](mailto:corporatesalesusa@wiley.com) or [corporatesalesDE@wiley.com](mailto:corporatesalesDE@wiley.com).

## RESEARCH ARTICLE

# Dynamics of initial carbon allocation after drought release in mature Norway spruce—Increased belowground allocation of current photoassimilates covers only half of the carbon used for fine-root growth

Kyohsuke Hikino<sup>1</sup>  | Jasmin Danzberger<sup>2</sup>  | Vincent P. Riedel<sup>1</sup>  | Benjamin D. Hesse<sup>1</sup>  | Benjamin D. Hafner<sup>3</sup>  | Timo Gebhardt<sup>1</sup> | Romy Rehschuh<sup>4</sup>  | Nadine K. Ruehr<sup>4</sup>  | Melanie Brunn<sup>5</sup>  | Taryn L. Bauerle<sup>3</sup>  | Simon M. Landhäusser<sup>6</sup>  | Marco M. Lehmann<sup>7</sup>  | Thomas Rötzer<sup>8</sup>  | Hans Pretzsch<sup>8</sup>  | Franz Buegger<sup>2</sup>  | Fabian Weigl<sup>1,2</sup>  | Karin Pritsch<sup>2</sup>  | Thorsten E. E. Grams<sup>1</sup> 

<sup>1</sup>Professorship for Land Surface-Atmosphere Interactions, Ecophysiology of Plants, TUM School of Life Sciences, Technical University of Munich, Freising, Germany

<sup>2</sup>Institute of Biochemical Plant Pathology, Helmholtz Zentrum München – German Research Center for Environmental Health (GmbH), Neuherberg, Germany

<sup>3</sup>School of Integrative Plant Science, Cornell University, Ithaca, New York, USA

<sup>4</sup>Karlsruhe Institute of Technology, Institute of Meteorology and Climate Research—Atmospheric Environmental Research (KIT/IMK-IFU), Garmisch-Partenkirchen, Germany

<sup>5</sup>Institute for Environmental Sciences, University Koblenz-Landau, Landau, Germany

<sup>6</sup>Department of Renewable Resources, University of Alberta, Edmonton, Alberta, Canada

<sup>7</sup>Swiss Federal Institute for Forest, Snow and Landscape Research (WSL), Forest Dynamics, Birmensdorf, Switzerland

<sup>8</sup>Forest Growth and Yield Science, TUM School of Life Sciences, Technical University of Munich, Freising, Germany

## Correspondence

Kyohsuke Hikino, Professorship for Land Surface-Atmosphere Interactions, Ecophysiology of Plants, TUM School of Life Sciences, Technical University of Munich, Hans-Carl-von-Carlowitz Platz 2, 85354 Freising, Germany.  
Email: [kyohsuke.hikino@tum.de](mailto:kyohsuke.hikino@tum.de)

Jasmin Danzberger, Institute of Biochemical Plant Pathology, Helmholtz Zentrum München – German Research Center for Environmental Health (GmbH), Ingolstaedter Landstr. 1, 85764 Neuherberg, Germany.  
Email: [jasmin.danzberger@helmholtz-muenchen.de](mailto:jasmin.danzberger@helmholtz-muenchen.de)

## Abstract

After drought events, tree recovery depends on sufficient carbon (C) allocation to the sink organs. The present study aimed to elucidate dynamics of tree-level C sink activity and allocation of recent photoassimilates ( $C_{\text{new}}$ ) and stored C in c. 70-year-old Norway spruce (*Picea abies*) trees during a 4-week period after drought release. We conducted a continuous, whole-tree  $^{13}\text{C}$  labeling in parallel with controlled watering after 5 years of experimental summer drought. The fate of  $C_{\text{new}}$  to growth and  $\text{CO}_2$  efflux was tracked along branches, stems, coarse- and fine roots, ectomycorrhizae and root exudates to soil  $\text{CO}_2$  efflux after drought release. Compared with control trees, drought recovering trees showed an overall 6% lower C sink activity and 19% less allocation of  $C_{\text{new}}$  to aboveground sinks, indicating a low priority for aboveground sinks during recovery. In contrast, fine-root growth in recovering trees was seven times greater than that of controls. However, only half of the C used for new fine-root

Kyohsuke Hikino and Jasmin Danzberger contributed equally to this work and share the first authorship.

This is an open access article under the terms of the [Creative Commons Attribution](https://creativecommons.org/licenses/by/4.0/) License, which permits use, distribution and reproduction in any medium, provided the original work is properly cited.

© 2022 The Authors. *Global Change Biology* published by John Wiley & Sons Ltd.

**Present address**

Vincent P. Riedel, Julius-von-Sachs-Institute of Biological Sciences, Ecophysiology and Vegetation Ecology, University of Würzburg, Julius-von-Sachs-Platz 3, Würzburg, 97082, Germany

Romy Rehschuh, Institute of General Ecology and Environmental Protection, Technische Universität Dresden, Piennner Str. 7, Tharandt, 01737, Germany

**Funding information**

Deutsche Bundesstiftung Umwelt, Grant/Award Number: AZ 20018/535; Deutsche Forschungsgemeinschaft, Grant/Award Number: GR 1881/5-1, MA1763/10-1, PR292/22-1, PR555/2-1 and RU1657/2-1; Schweizerischer Nationalfonds zur Förderung der Wissenschaftlichen Forschung, Grant/Award Number: 179978; Technische Universität München

growth was comprised of  $C_{\text{new}}$  while the other half was supplied by stored C. For drought recovery of mature spruce trees, in addition to  $C_{\text{new}}$ , stored C appears to be critical for the regeneration of the fine-root system and the associated water uptake capacity.

**KEYWORDS**

$^{13}\text{C}$  labeling, belowground carbon allocation, carbon partitioning, climate change, drought recovery, forest ecosystems, *Picea abies*, watering

## 1 | INTRODUCTION

Forests store ~45% of terrestrial carbon (C), which is in form of carbon dioxide ( $\text{CO}_2$ ) a rapidly increasing greenhouse gas (IPCC, 2021). Thus, conditions and C sequestration capacity of forests have a large impact on the global C cycle (Bonan, 2008; Lal et al., 2018). As a consequence of climate change, forests are globally facing repeated droughts leading to immense tree dieback (Allen et al., 2010; Hartmann et al., 2018; Schuldt et al., 2020). Under these circumstances, tree survival depends not only on water availability, but also on C supply to each above- and belowground tree organs (Hartmann et al., 2020; Ruehr et al., 2019; Sala et al., 2010). Previous studies revealed that allocation of both, structural (i.e., growth) and non-structural (i.e., maintenance and storage) C, was altered to increase tree survival: for example, enhanced C allocation to root growth (Gaul et al., 2008; Hommel et al., 2016; Meier & Leuschner, 2008; Poorter et al., 2012) and C storage (Blessing et al., 2015; Chuste et al., 2020; Hart et al., 2021).

Because the frequency of drought events is predicted to increase in the future (IPCC, 2021), recovery from these events is an important aspect of tree survival, which has attracted less attention compared with direct drought effects (Ruehr et al., 2019). On the one hand, drought release can increase aboveground C sink activity for repair processes such as growth of new xylem and embolism refilling (Brodersen & McElrone, 2013; Ruehr et al., 2019; Zang et al., 2014) or C storage to prepare for future droughts (Galiano et al., 2017; Rehschuh et al., 2021). On the other hand, drought release can stimulate belowground C sinks such as root production, mycorrhizal and microbial activity, and associated soil respiration (Brunner et al., 2019; Gao et al., 2021; Hagedorn et al., 2016; Joseph et al., 2020; Werner et al., 2021). Fine-root growth dynamics are especially challenging to assess

(Ruehr et al., 2019), are typically tree species-specific, and therefore difficult to generalize (Nikolova et al., 2020; Zwetsloot & Bauerle, 2021).

To improve our understanding of the tree recovery processes from drought, it is crucial to analyze the whole-tree C allocation including belowground sinks, which has been often restricted to young trees (Brüggemann et al., 2011; Hartmann et al., 2018). Recovery of tree function can be expected only if the increased C sink activity after drought release can be met by available C that is newly assimilated C ( $C_{\text{new}}$ , see Table 1 for terms and abbreviations) and stored C. A previous study using young European beech trees directly related allocation of  $C_{\text{new}}$  belowground to the capacity of trees to recover from drought (Hagedorn et al., 2016). However, for mature trees, recovery from repeated drought events is critically understudied and experimental evidence on the allocation of both  $C_{\text{new}}$  and stored C for tree recovery processes is still scarce (Gao et al., 2021; Joseph et al., 2020; Werner et al., 2021).

The present study was conducted as part of the Kranzberg forest roof (KROOF) project, which was established to investigate mature Norway spruce (*Picea abies* [L.] Karst.) trees exposed to 5 years of experimental summer droughts (Grams et al., 2021). This long-term repetitive drought treatment significantly reduced leaf and twig growth (Tomasella et al., 2018), stem growth (Pretzsch et al., 2020), fine-root growth (Nickel et al., 2018; Zwetsloot & Bauerle, 2021), total C uptake (Brunn et al., 2022), and C storage pools (Hesse et al., 2021) in Norway spruce. To gain insight into the recovery processes, the drought-stressed trees were watered in early summer of the sixth year (Grams et al., 2021). In parallel with the watering, we performed a continuous  $^{13}\text{C}$  labeling and assessed the use of both  $C_{\text{new}}$  and stored C at the whole-tree level for tree recovery from drought.

In this study, leaves were considered C sources, and we focused on the allocation of newly assimilated C ( $C_{\text{new}}$ ) exported

TABLE 1 Terms and abbreviations used in this study

Terms	Unit	Abbreviations	Explanation
Newly assimilated C	gC	$C_{\text{new}}$	Labeled, newly assimilated C
Stored C	gC	-	C originating from C reserves within a tree
C sink activity	$\text{gC tree}^{-1} 28 \text{ days}^{-1}$	-	Total C that was used for growth and respiratory sinks (cumulative sum during 28 days after drought release)
Amount of $C_{\text{new}}$	$\text{gC tree}^{-1} 28 \text{ days}^{-1}$	-	Total amount of $C_{\text{new}}$ allocated to each C sink (cumulative sum during 28 days after drought release)
Proportional allocation of $C_{\text{new}}$	%	-	Proportion of $C_{\text{new}}$ in each C sink to the total $C_{\text{new}}$ detected in the whole tree
Fraction of labeled C	%	$f_{\text{Label}}$	Proportion of $C_{\text{new}}$ to the C sink activity at each measurement point
Contribution of $C_{\text{new}}$ to each C sink activity	%	$\text{cont}C_{\text{new}}$	Proportion of $C_{\text{new}}$ to the C sink activity at the new isotopic equilibrium (asymptote of Equation 11)

from leaves to the different above- and belowground sinks. We examined the following three aspects: (i) whole-tree C sink activity (in g C used for growth and respiration, see Table 1), (ii) allocation of  $C_{\text{new}}$ , and (iii) contribution of  $C_{\text{new}}$  to each C sink activity ( $\text{cont}C_{\text{new}}$ ). We expected the regeneration of the water-absorbing fine roots to be a high priority for drought-recovering spruce trees and thus we hypothesized a higher C sink activity belowground and correspondingly a lower C sink activity aboveground compared with control trees [H1] and that the high belowground C sink activity of recovering trees would be supported by preferential allocation of  $C_{\text{new}}$  into belowground sinks at the expense of aboveground sinks [H2]. Due to reduced leaf and twig growth under drought, the total C uptake per tree can be expected to be much lower in recovering trees even after drought release compared with controls. Thus, we further hypothesized that for recovering trees, the relative contribution of  $C_{\text{new}}$  to the different sinks (i.e.,  $\text{cont}C_{\text{new}}$ ) would be lower compared with control trees, particularly when sink activity is increased [H3].

## 2 | MATERIALS AND METHODS

### 2.1 | Experimental site and $^{13}\text{C}$ labeling

The present study was conducted at the Kranzberg Forest experimental site, a mixed forest in southern Germany (11°39'42" E, 48°25'12" N; 490 m a.s.l.). A long-term drought experiment was established in 2014, which is described in detail by Grams et al. (2021). In brief, this experimental site consists of 12 plots with c. 70-year-old Norway spruce (*P. abies* [L.] Karst.) trees. The plots were trenched 4 years before the start of the drought treatment and separated by buried plastic tarps from the surrounding soil (Pretzsch et al., 2014). Half of the plots were equipped with under-canopy roofs, thereby excluding precipitation throughfall throughout the entire growing season (from April to November) between 2014 and 2018 and leading to recurrent summer droughts; remaining control plots were exposed to natural rainfall events. Accordingly,  $459 \pm 21$  mm ( $69 \pm 7\%$  of the

annual precipitation) was excluded during the growing seasons and predawn leaf water potential of drought-stressed trees significantly decreased to as low as  $-1.8$  MPa (Grams et al., 2021). In early summer of 2019, all drought plots were watered to initiate the recovery processes (Grams et al., 2021) by supplying c. 90 mm water over 40 h to increase the soil water content to the control level (around 20%–30%, Grams et al., 2021). Accordingly, the predawn leaf water potential of previously drought-stressed trees fully recovered from  $-0.93 \pm 0.03$  MPa to  $-0.69 \pm 0.05$  MPa within 7 days after watering, while that of control trees remained constant at  $-0.61 \pm 0.02$  MPa (Grams et al., 2021; Hikino et al., 2022). In parallel with the watering, we conducted a continuous  $^{13}\text{C}$  labeling experiment in four control and three recovering spruce trees on two neighboring plots (Figure 1a, for details see Hikino et al., 2022). In brief, each tree (average height of  $32.3 \pm 0.7$  m, Table S1) was equipped with perforated PVC tubes, which continuously released  $^{13}\text{C}$ -depleted  $\text{CO}_2$  ( $\delta^{13}\text{C}$  of  $-44.3 \pm 0.2\%$ ) into the entire crowns from 5 a.m. to 7 p.m. (CET). The  $\text{CO}_2$  exposure started at the same time as watering on July, 4th 2019 (day 0), lasted until July, 17th 2019 (day 13) and  $\text{CO}_2$  concentration and its stable C isotopic signature ( $\delta^{13}\text{C}$ ) were monitored by means of a cavity ring-down spectroscopy (CRDS, ESP-1000; PICARRO). The change of the  $\text{CO}_2$  concentration and  $\delta^{13}\text{C}$  of individual crown air during labeling were on average  $+126$  ppm and  $-7.3\%$  for control trees,  $+80$  ppm and  $-5.1\%$  for recovering trees, due to different wind exposure of each tree. The individual shift in crown air (Table S1) was considered in the tree-specific analyses. To assess the whole-tree C allocation, we investigated the following C sinks (Figure 2): Growth and/or  $\text{CO}_2$  efflux of branch, upper and lower stem, coarse-root, fine-root, ectomycorrhizae (ECM), fine-root exudates, and soil. Because the  $^{13}\text{C}$  label in soil  $\text{CO}_2$  efflux showed a peak 14–20 days after the start of labeling/watering and a rapid decrease until day 28 (Hikino et al., 2022), C allocation during the first 4 weeks (28 days) of drought release was considered. In addition to the seven labeled trees, three control and three recovering spruce trees on non-labeled plots were assessed to correct for the effect of watering and weather influences on  $\delta^{13}\text{C}$  of studied parameters.



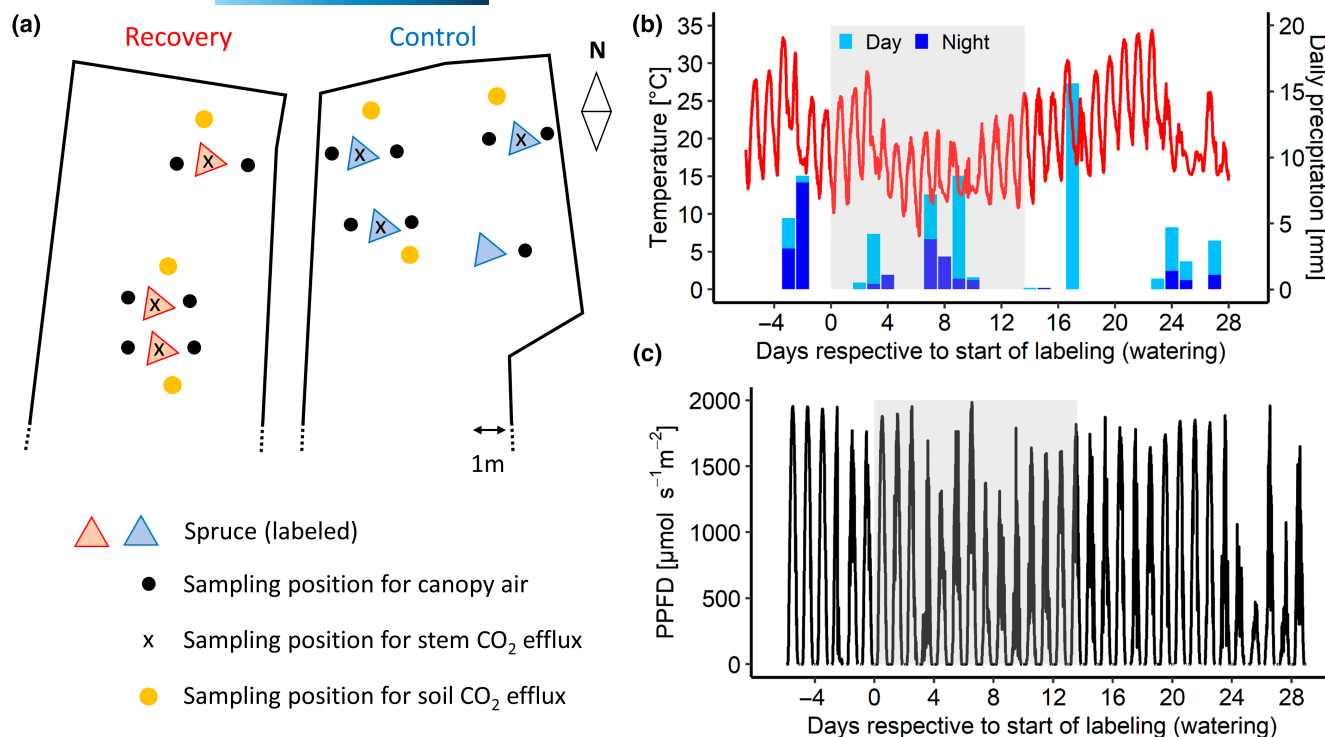


**FIGURE 1** (a) Overview of the two  $^{13}\text{C}$ -labeled plots: Control and recovery (previously drought-stressed), giving positions of trees (red and blue triangles = labeled spruce trees), sampling points of canopy air (black circles), stem  $\text{CO}_2$  efflux (x), and soil  $\text{CO}_2$  efflux (yellow circles). Modified from Hikino et al. (2022). (b) Temperature (red lines), daily precipitation (blue bars), and (c) photosynthetic photon flux density (PPFD) before and after the watering until day 28. Precipitation amount is split into day (5 a.m.–7 p.m. CET, fumigation hours, light blue), and night (7 p.m.–5 a.m., dark blue). Day 0 is the day of the watering. The gray areas show the labeling days (day 0–13).  $^{13}\text{C}$  labeling started in parallel with the watering on day 0.

## 2.2 | Weather data

Daytime (from 5 a.m. to 7 p.m., CET), mean temperature during the experiment (i.e., 0–28 days after watering) was  $21.4 \pm 5.4$  (1SD) °C (Figure 1b) with a mean vapor pressure deficit of  $0.6 \pm 0.4$  (1SD) kPa. There were prolonged periods with minor daytime precipitation on days 9 (7.8 mm) and 17 (15.6 mm). The mean daytime photosynthetically active photon flux density was  $772 \pm 545$  (1SD)  $\mu\text{mol m}^{-2} \text{s}^{-1}$  ( $38 \pm 14$  [1SD]  $\text{mol m}^{-2} \text{day}^{-1}$ , Figure 1c).

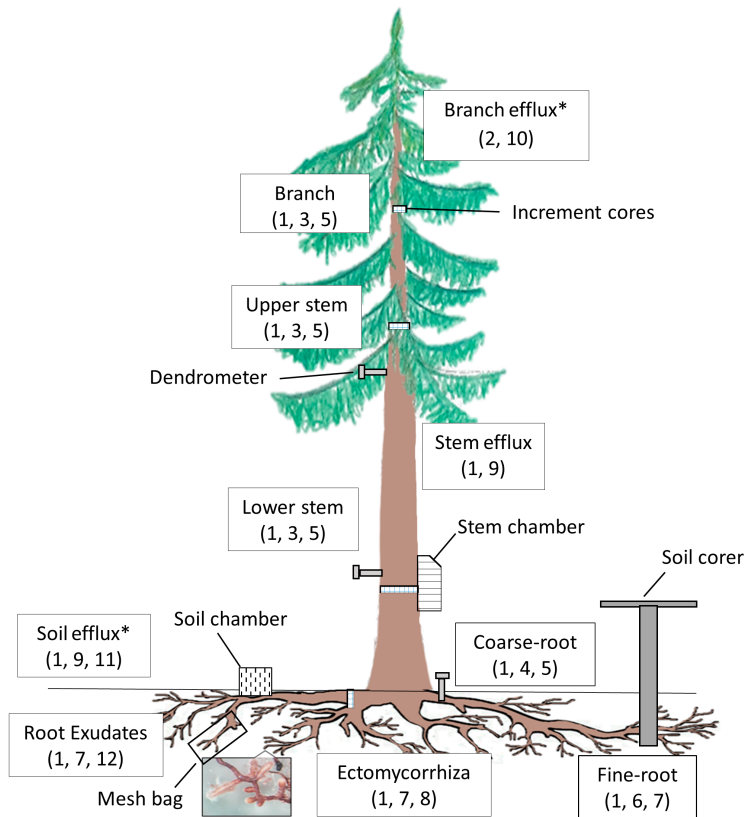
## 2.3 | Sample collection

After the 2019 growing season, increment cores (diameter 0.5 cm) were collected at three different stem heights (breast height, crown base, mid-crown), and from coarse-roots (Figure 2) and immediately dried at 64°C for 72 h. Tree rings from 2019 were separated with a razor blade and subsequently thin-sectioned (c. 5  $\mu\text{m}$ ) in radial direction, using a microtome (Sledge Microtome G.S.L.1; Schenkung Dapples).

To record the isotopic signature of fine-root tips and mycorrhizae and trace fine-root growth, vital fine-roots (diameter  $\leq 2$  mm) were selected based on their turgid appearance and active meristems, and placed in mesh bags as follows. In April 2019, eight fine-roots for each sampling day and treatment were excavated

within the first 10 cm of the soil, photographed, placed in 1/3 soil filled nylon mesh bags (12.5  $\times$  6.5 cm, mesh width 80  $\mu\text{m}$ , open area of 29%), sprayed with water to enhance root soil contact, and covered with soil. Seven days before and weekly after the watering, roots were harvested from the mesh bags and photographed. Additional fine roots from 0 to 10 cm depth were also randomly sampled within the plots daily to gain a more detailed time resolution of the change in C isotope signature (Table S2). Thus, a total of 1166 root tips were sampled. After sampling, vital ECM and non-mycorrhizal root tips were distinguished by the presence/absence of a hyphal mantle using a stereomicroscope (M125; Leica), and dried for 1 h at 60°C.

Root exudates were collected according to the method described by Phillips et al. (2008) and Brunn et al. (2022). Excavated root branches were rinsed with a nutrient solution (0.5 mM  $\text{NH}_4\text{NO}_3$ , 0.1 mM  $\text{KH}_2\text{PO}_4$ , 0.2 mM  $\text{K}_2\text{SO}_4$ , 0.15 mM  $\text{MgSO}_4$ , 0.3 mM  $\text{CaCl}_2$ ) after attached soil was gently removed with tweezers. Roots were then left to recover in a 1:1 mixture of native soil from the site and sand for 48 h, cleaned, and placed into 30 ml glass syringes with sterile glass beads. Syringes were flushed three times with the nutrient solution, equilibrated for 48 h, flushed again, and left shielded with aluminum foil and leaf litter. Between days –5 and 7, and 20 and 24 (Table S2), exudates trapped in the syringes were collected from the same root branches every 48 h by adding 30 ml of nutrient solution, extracted using a membrane pump, filtered through sterile



Parameters	Methods used for measurement
Fraction of labeled C ( $f_{\text{Label}}$ )	1) Stable C isotope measurements (IRMS, IRIS, or isoTOC cube)
	2) Values adopted from stem efflux
Growth	3) Allometry (DBH)
	4) Excavation
	5) Dendrometer
	6) Picture analysis (Mesh bag)
Fine-root and ectomycorrhizal biomass	7) Soil cores
	8) Picture analysis & projection (Mesh bag)
Efflux rates	9) Measuring chambers (IRMS)
	10) Calculation based on literature values
	11) Auto- and heterotrophic ratio taken from literatures
Exudation rates	12) isoTOC cube

\* Calculation (partly) based on literatures

**FIGURE 2** Overview of C sinks and sampling/calculation methods used for this study. In few cases, data from literature were adopted for calculations (i.e., branch  $\text{CO}_2$  efflux and autotrophic soil  $\text{CO}_2$  efflux).

syringe filters (0.22  $\mu\text{m}$ , ROTILABO® MCE; Carl Roth GmbH + Co. KG), and stored at  $-20^\circ\text{C}$ . A blank syringe without roots served as a reference. Root branches were harvested after exudate collection, dried, and total dry biomass recorded to normalize exudation rates to root mass.

## 2.4 | Analysis of stable C isotopic composition ( $\delta^{13}\text{C}$ ), rates of $\text{CO}_2$ efflux, and root exudates

$\delta^{13}\text{C}$  of tree ring slices (stem and coarse-roots) and vital root tips (ECM and non-mycorrhizal) were determined with an isotope ratio mass spectrometer (IRMS, delta V Advantage; Thermo Fisher Scientific) coupled to an Elemental Analyzer (Euro EA; Eurovector).

Rates and  $\delta^{13}\text{C}$  of stem  $\text{CO}_2$  efflux were assessed approx. every 80 min at c. 1 m height on stems of six labeled ( $n = 3$  per treatment, Figures 1a and 2) and six non-labeled trees as controls with custom-built stem chambers connected to an isotope ratio infrared spectrometer (IRIS, DeltaRay; Thermo Fisher Scientific), as described in detail by Hikino et al. (2022). Soil  $\text{CO}_2$  efflux chambers (Li-8100; Li-Cor, Inc.) were installed at a 1 m distance from each measured tree ( $n = 3$ , Figures 1a and 2), connected to a Li-8150 (Li-Cor, Inc.) multiplexer and a second IRIS. Rates and  $\delta^{13}\text{C}$  of soil  $\text{CO}_2$  efflux were then recorded every 30 min (Table S2).  $\delta^{13}\text{C}$  of the three soil chambers in the recovering plot was corrected for the physical back-diffusion of

soil air during watering (Andersen et al., 2010; Subke et al., 2009; Unger et al., 2010), using an additional chamber installed next to non-labeled trees in the same plot.

$\delta^{13}\text{C}$  and total organic C concentration of root exudate samples were analyzed with an isoTOC cube (Elementar).

## 2.5 | Calculation of total C sink activity

Below, cumulative sum of C sink activity during 28 days (in  $\text{gC}_{\text{tree}}^{-1} 28\text{days}^{-1}$ ) after drought release was calculated for each C sink (Figure 2).

### 2.5.1 | Stem and branch growth

The total growth during the 2019 growing season ( $Y$  in  $\text{kg tree}^{-1}$ ) was determined with an allometric function provided for Norway spruce by Forrester et al. (2017), using the diameter at breast height (DBH,  $d$  in cm, Table S1) as input parameter:

$$\text{For stem } \ln(Y) = -2.5027 + 2.3404 \cdot \ln(d) \quad (1)$$

$$\text{For branch } \ln(Y) = -3.3163 + 2.1983 \cdot \ln(d) \quad (2)$$

Because crown length was c. 1/3 of the total tree height (Table S1), 1/9 of the total stem growth was assigned to the upper

stem (from top to crown base) and the remaining 8/9 to the lower stem (from crown base to trunk base), assuming a conical shape of the stems.

The total annual growth in 2019 was then multiplied by the proportional growth (in %) during the 28 days after watering (ratio of the radial growth during 28 days to the total annual growth), determined by automatic point dendrometers (DR-type; Ecomatik) installed at 50% tree height (used for branch and upper stem) and breast height (used for lower stem, Figure 2; see Methods S1). The % C of samples was ascertained by IRMS measurement (same for coarse-root growth, fine-root growth, and ECM).

## 2.5.2 | Branch CO<sub>2</sub> efflux

Total branch and twig surface area was estimated for each tree (Table S3) using field data including length, number, and mean diameter of branches and twigs, separated into each needle class and sun/shade crowns. Based on earlier studies on spruce trees at the same site using a infrared gas analyser (Binos 4b; Emerson Process Management; Kuptz et al., 2011; Reiter, 2004), maintenance respiration rates ( $R_M$ ), growth respiration rates ( $R_G$ ), and total CO<sub>2</sub> efflux of branch CO<sub>2</sub> efflux ( $R_{\text{branch}}$ ) were calculated as follows:

$$R_{\text{branch}} = R_M + R_G \quad (3)$$

$$R_M = R_{M10} \cdot Q_{10}^{\frac{T-10}{10}} \quad (4)$$

$$R_G = \frac{330 - \text{DOY}}{330 - 130} \cdot R_{G10\text{max}} \cdot Q_{10}^{\frac{T-10}{10}} \quad (5)$$

where  $R_{M10}$  represents the maintenance respiration rates at 10°C ( $0.13 \mu\text{mol m}^{-2} \text{s}^{-1}$  for sun branch, and  $0.048 \mu\text{mol m}^{-2} \text{s}^{-1}$  for shade branch),  $R_{G10\text{max}}$  the maximum growth respiration at 10°C ( $0.23 \mu\text{mol m}^{-2} \text{s}^{-1}$  for sun branch, and  $0.12 \mu\text{mol m}^{-2} \text{s}^{-1}$  for shade branch),  $Q_{10}$  the temperature sensitivity (2.45 for both sun and shade branches), and  $T$  the temperature. Since rates of stem CO<sub>2</sub> efflux did not significantly differ between control and recovering trees, rates of branch CO<sub>2</sub> efflux were also assumed to be similar.

## 2.5.3 | Stem CO<sub>2</sub> efflux

Stem efflux rates of each tree (Figure S1a,b) were multiplied by the stem surface area (Table S3), which was calculated using DBH and tree height, assuming a conical shape of the stems. For stems above 6.5 m, efflux rates at the breast height were multiplied by 1.4 as previously assessed on spruce trees from the same site (Kuptz et al., 2011). The mean rates of stem CO<sub>2</sub> efflux of three measured control trees were used for the fourth control tree, which was not assessed in this study (Figure 1a).

## 2.5.4 | Coarse-root growth

Coarse roots were counted, and the length of one coarse root (root diameter  $\geq 2\text{mm}$ ) per tree was measured on site after excavating. Using root wood density of  $0.416 \text{g cm}^{-3}$  (Pretzsch et al., 2018), mean diameter, length, and ring width from 2019 based on coring, the total coarse-root growth in 2019 was determined, and subsequently multiplied by the proportional growth during the 28 days after watering, according to automatic dendrometers installed at one coarse root (diameter of  $9.4 \pm 1.1 \text{cm}$ ) on each tree (Ecomatik, Figure 2) as described above for stem and branch growth.

## 2.5.5 | Fine-root growth and ECM

To avoid massive soil disturbance in the long-term plots, not more than one coarse-root per tree was excavated. Thus it was not possible to assign the ECM samples, non-mycorrhizal root tips, or root exudates unequivocally to a specific tree. Special care was taken to gain representative samples by avoiding clustered sampling spots and covering the whole area underneath the labeled spruce each sampling day. For this reason, the total C sink activity of fine-root growth, ECM, and root exudates was first extrapolated to the area occupied by spruce trees (Figure 1a). From coring within the plot, we knew that fine-roots of spruce were evenly spread in the spruce area. The total spruce tree C sink activity belowground was then assigned to individual trees according to the area occupied by each tree using a positive exponential relationship between DBH and root biomass (Table S1, spatial contribution belowground and area; Häberle et al., 2012).

The initial fine-root biomass ( $\text{mg cm}^{-3}$ ) was determined with fine roots taken from 10 soil cores (diameter of 1.4 cm) within the first 10 cm of the uppermost soil layers on day -7. Because the biomass values of the two labeled plots differed from all other sampled plots and the previous years, the average initial biomass of all control and recovery plots of the experimental site, which agrees to fine-root area values of Brunn et al. (2022) on the same site and year, was accounted for further calculations. To calculate the fine-root biomass at 10–30 cm depth and thus the total initial fine-root biomass from 0 to 30 cm soil depth ( $M_{\text{FR30}}$ ), a root biomass ratio between upper (0–10 cm) and lower (10–30 cm) soil layer was used, measured in summer 2018 on the same plots (Table 2). The total fine-root gain in the spruce area (Table 2) was calculated:

$$\text{Fine root length growth rate} = \frac{\text{Root length growth}}{\text{Initial root length in mesh bag}} \quad (6)$$

where the initial root length on day -7 and root length growth was determined by image analysis of respective pre- and post-harvest mesh bag root pictures via ImageJ (version 1.53a; National Institute of Health). The biomass gain per soil volume ( $\text{mg cm}^{-3}$ ) was then calculated (Equation 7), assuming a constant fine-root diameter, corrected

**TABLE 2** Fine-root (FR) biomass (BM) and its ratio between upper (0–10 cm depth, U) and lower (10–30 cm depth, L) soil layer in summer 2018 to calculate the initial BM and root growth in the lower layer in 2019: In control and recovery (previously drought-stressed) plots

	FR BM summer 2018 (mg cm <sup>-3</sup> )	FR BM ratio U/L	M <sub>FR</sub> (mg cm <sup>-3</sup> )	M <sub>ECM</sub> (mg cm <sup>-3</sup> )	FR BM gain (g)	FR length growth rate
Control	1.1 (U)	2.0	1.0 (U)	0.3 (U)	1113	0.1 ± 0.0
	0.6 (L)		0.5 (L)	0.1 (L)		
Recovery	0.6 (U)	1.3	0.9 (U)	0.1 (U)	5905	0.3 ± 0.2
	0.5 (L)		0.7 (L)	0.1 (L)		

Note: Initial FR BM ( $M_{FR}$ ) and ECM BM ( $M_{ECM}$ ) display the BM before the watering. FR BM gain reflects the cumulative sum of growth within the plot of each treatment during 28 days after watering (total g biomass per treatment, i.e., sum of four trees for control and three trees for recovery plot). FR length growth rate represents the mean ratio of fine-root growth to initial length during 28 days after watering (calculated by Equation 6, given with SE).

by the average biomass gain on day -7 to exclude root growth between mesh bag placement and first harvest, and extrapolated to the soil volume of the plot at 0–30 cm depth.

$$\text{fine root biomass gain} = \text{fine root length growth rate} \times \text{dry mass per soil volume} \quad (7)$$

Helmisaari et al. (2009) found the most spruce fine roots in the upper soil layer and Zwetsloot and Bauerle (2021) reported no changes in vertical root distribution of the present spruce during drought compared with controls which support a sufficient coverage of our calculated fine-root biomass. For determination of fine-root biomass, we manually selected vital fine-roots based on the same morphologic criteria as for the fine-roots included in mesh bags, which was used to calculate root growth. Within the mesh bag roots, we found that 96% of the sampled fine-roots in control and 57% in recovering trees were colonized by ectomycorrhizal fungi. Assuming no significant change in ECM biomass on root tips during our 28 day study period, since full formation of ECM takes longer (Ineichen & Wiemken, 1992), the biomass of mycorrhized fine-roots ( $M_{FR-ECM}$ ) at 0–30 cm depth was calculated based on the initial fine-root biomass at 0–30 cm ( $M_{FR30}$ , Table 2):

$$M_{FR-ECM} = \frac{M_{FR30}}{100} \times 96 \text{ (or 57)} \quad (8)$$

ECM biomass ( $M_{ECM}$ ) was calculated based on the finding by Helmisaari et al. (2007, 2009), that ECM make up 28% of one spruce fine-root's biomass, determined under the same terms as in our study (mature spruce trees, root diameter <2 mm, most fine-roots found within 0–10 cm depth):

$$M_{ECM} = \frac{M_{FR-ECM}}{100} \times 28 \quad (9)$$

## 2.5.6 | Root exudates

The total root exudates C contribution was calculated for the soil at 0–30 cm depth using the organic C concentration in root exudates and the total fine-root biomass determined by soil cores.

## 2.5.7 | Soil CO<sub>2</sub> efflux

Soil efflux rates of each tree (Figure S1c,d) were multiplied by the area belowground occupied by each tree (Table S1). The mean rates of soil CO<sub>2</sub> efflux close to the three measured control trees were used for the fourth control tree, which was not assessed (Figure 1a). For the contribution of autotrophic respiration (root-derived including rhizosphere) to total soil respiration (autotrophic + heterotrophic), we used as value 51% in control and 38% in recovering trees based on previous measurements on spruce trees at the same site in July during 1 year with drought and 1 year without drought (Nikolova et al., 2009). We assumed that the contribution of autotrophic respiration did not significantly change after drought release, as soil CO<sub>2</sub> efflux rates under recovering trees remained unaffected by the drought release (Hikino et al., 2022).

## 2.6 | Calculation of fraction of labeled C ( $f_{Label}$ ) and contribution of C<sub>new</sub> to each C sink activity (contC<sub>new</sub>)

Fraction of labeled C ( $f_{Label}$ ) was calculated at each measurement point using the following equation (Kuptz et al., 2011):

$$f_{Label} = \frac{\delta^{13}C_{old} - \delta^{13}C_{sample}}{\delta^{13}C_{old} - \delta^{13}C_{new}} \quad (10)$$

where  $\delta^{13}C_{old}$  gives the mean  $\delta^{13}C$  before the start of labeling,  $\delta^{13}C_{sample}$  is the  $\delta^{13}C$  of each measurement, and  $\delta^{13}C_{new}$  represents  $\delta^{13}C$  at the new isotopic equilibrium (Figure S2, for the calculation of  $\delta^{13}C_{new}$  see Methods S2). Rarely occurring negative  $f_{Label}$  values were set to zero.  $f_{Label}$  of stem CO<sub>2</sub> efflux was used for branch CO<sub>2</sub> efflux, which was not assessed in this study.

contC<sub>new</sub>, representing  $f_{Label}$  at the new isotopic equilibrium, was determined by fitting the course of  $f_{Label}$  with the following sigmoid curve (Figures S3 and S4).

$$f_{Label} = \frac{\text{cont C}_{new}}{1 + e^{-\frac{t-t_0}{b}}} \quad (11)$$

where  $t$  is the time of measurement,  $t_0$  the inflection point of the curve, and  $b$  the slope coefficient of the regression.  $\text{contC}_{\text{new}}$  would be one (100%) if C sink was supplied solely with  $\text{C}_{\text{new}}$  and zero (0%) if supplied exclusively by stored C. Since  $f_{\text{Label}}$  decreased again after the end of labeling, only  $f_{\text{Label}}$  before reaching the maximum were used for the fitting.

Similar to C sink activity, we pooled all samples of ECM, non-mycorrhizal root tips, and root exudates for the calculation of  $\text{contC}_{\text{new}}$  for control and recovering trees. Thus, only one value was available for each treatment, so that a statistical test between treatments was not possible for these three C sinks.  $\text{contC}_{\text{new}}$  to soil  $\text{CO}_2$  efflux was divided by the contribution of autotrophic part to calculate the  $\text{contC}_{\text{new}}$  to autotrophic soil  $\text{CO}_2$  efflux.

### 2.6.1 | Methods used for branch, stem, and coarse-root growth

For branch, stem, and coarse-root growth,  $\delta^{13}\text{C}_{\text{old}}$  and  $\delta^{13}\text{C}_{\text{sample}}$  (for Equation 10) were determined by fitting the  $\delta^{13}\text{C}$  of tree ring slices with a piecewise function (R package "segmented", version: 1.3-0) as described by Hikino et al. (2022; for details see Methods S3; Figure S5). The applied labeling with  $^{13}\text{C}$ -depleted  $\text{CO}_2$  caused a sudden and steep decrease of  $\delta^{13}\text{C}$ , after the  $^{13}\text{C}$ -depleted tracer was incorporated into the tree ring. The  $\delta^{13}\text{C}$  value at this point was determined with a piecewise function (marked by the green horizontal dashed lines in Figure S5a,b) and then defined as  $\delta^{13}\text{C}_{\text{old}}$ . After the steep decrease,  $\delta^{13}\text{C}$  increased again as unlabeled C arrived after the end of labeling. The minimum  $\delta^{13}\text{C}$  value at this point was determined with the same method (purple horizontal dashed lines) and defined as  $\delta^{13}\text{C}_{\text{sample}}$ . In addition to the labeled trees, we also determined the natural shifts of  $\delta^{13}\text{C}$  of non-labeled control trees for each treatment ( $n = 3$ ) to correct  $\delta^{13}\text{C}_{\text{sample}}$  for the effect of watering, weather fluctuation, and seasonal changes (Helle & Schleser, 2004). Finally, using  $\delta^{13}\text{C}_{\text{old}}$ , corrected  $\delta^{13}\text{C}_{\text{sample}}$ , and Equation (10),  $f_{\text{Label}}$  was calculated.

For the course of  $f_{\text{Label}}$  (Figure S6), C transport rates determined by Hikino et al. (2022) were used to define the day on which the first  $^{13}\text{C}$ -depleted tracer arrived at each tree height (i.e., when  $f_{\text{Label}}$  started to increase). A linear increase of  $f_{\text{Label}}$  was assumed until the new isotopic equilibrium was reached, that is  $\text{contC}_{\text{new}}$ .  $\text{contC}_{\text{new}}$  calculated with the samples from the middle of the crown was used for branch and upper stem growth. For the lower stem growth, we used the mean  $\text{contC}_{\text{new}}$  calculated for the crown base and breast height.

### 2.7 | Calculation of allocation of newly assimilated C ( $\text{C}_{\text{new}}$ ) to each C sink

Total amount of  $\text{C}_{\text{new}}$  allocated to each C sink during 28 days after drought release was calculated as the cumulative sum of  $\text{C}_{\text{new}}$  after multiplying C sink activity and their respective  $f_{\text{Label}}$ .

As soon as  $f_{\text{Label}}$  started to decrease due to the end of labeling, sigmoid curves (Equation 11) or in the case of branch, stem, and coarse-root growth (Figure S6) a constant  $f_{\text{Label}}$  was used. For soil  $\text{CO}_2$  efflux, total C sink activity (autotrophic + heterotrophic) was multiplied with respective  $f_{\text{Label}}$ , since C isotopic signatures and  $f_{\text{Label}}$  comprise the mixed signal of both autotrophic and heterotrophic efflux. Using the amount of  $\text{C}_{\text{new}}$  (in g C), proportional allocation of  $\text{C}_{\text{new}}$  (in %) to each sink was calculated for each tree.

## 2.8 | Statistical analysis

All data were analyzed using R (version 4.0.3) in R studio (version 1.3.1093). For the non-linear regression (Equation 11), nls function (package: stats, version: 4.0.3) was applied. The differences in C sink activity,  $\text{contC}_{\text{new}}$ , and allocation of  $\text{C}_{\text{new}}$  between control and recovering trees were tested with a  $t$ -test for each C sink. Beforehand, we tested the homogeneity of variances ( $F$ -test) and the normality of the data (Shapiro test). If these prerequisites were violated, data were either transformed (logarithms, square root, multiplicative inverse), or wilcox.test (package: stats, version: 4.0.3) was used. Proportional allocation of  $\text{C}_{\text{new}}$  was tested using a linear-mixed model (package: nlme, version: 3.1-151). We defined the treatment and above- and belowground sinks as fixed, and tree as a random effect. Beforehand, we tested the homogeneity of variances (Levene test) and the normality of the residuals (Shapiro test). If the fixed factor was significant, a post-hoc test with Tukey correction (package: lsmeans, version: 2.30-0) was performed. All results are given in  $\text{mean} \pm \text{SE}$ , unless otherwise noted.

## 3 | RESULTS

### 3.1 | Total C sink activity

We assessed the cumulative sum of C sink activity for each sink (in  $\text{g C tree}^{-1} 28 \text{ days}^{-1}$ , Figure 3) during the first 4 weeks after drought release. In aboveground sinks, the recovering trees had a significantly lower sink activity for branch  $\text{CO}_2$  efflux with  $558 \pm 86 \text{ g C}$  ( $p < .01$ , Figure 3) than control trees with  $1205 \pm 131 \text{ g C}$ . The activity of the other aboveground sinks was slightly but insignificantly lower in recovering trees compared with controls.

In belowground sinks of recovering trees, fine-root growth was the major C sink with  $965 \pm 136 \text{ g C}$ , which was seven times higher than that of control trees ( $136 \pm 12 \text{ g C}$ ,  $p < .001$ ). Sink activity of coarse roots and ECM was  $126 \pm 48 \text{ g C}$ , and  $302 \pm 43 \text{ g C}$  in recovering trees, respectively, which was similar to controls with  $98 \pm 43 \text{ g C}$  and  $306 \pm 27 \text{ g C}$ . Autotrophic soil  $\text{CO}_2$  efflux under recovering trees was significantly lower with  $649 \pm 123 \text{ g C}$  than under control trees with  $1643 \pm 220 \text{ g C}$  ( $p = .01$ ). Sink activity of root exudates tended to be higher under recovering trees than

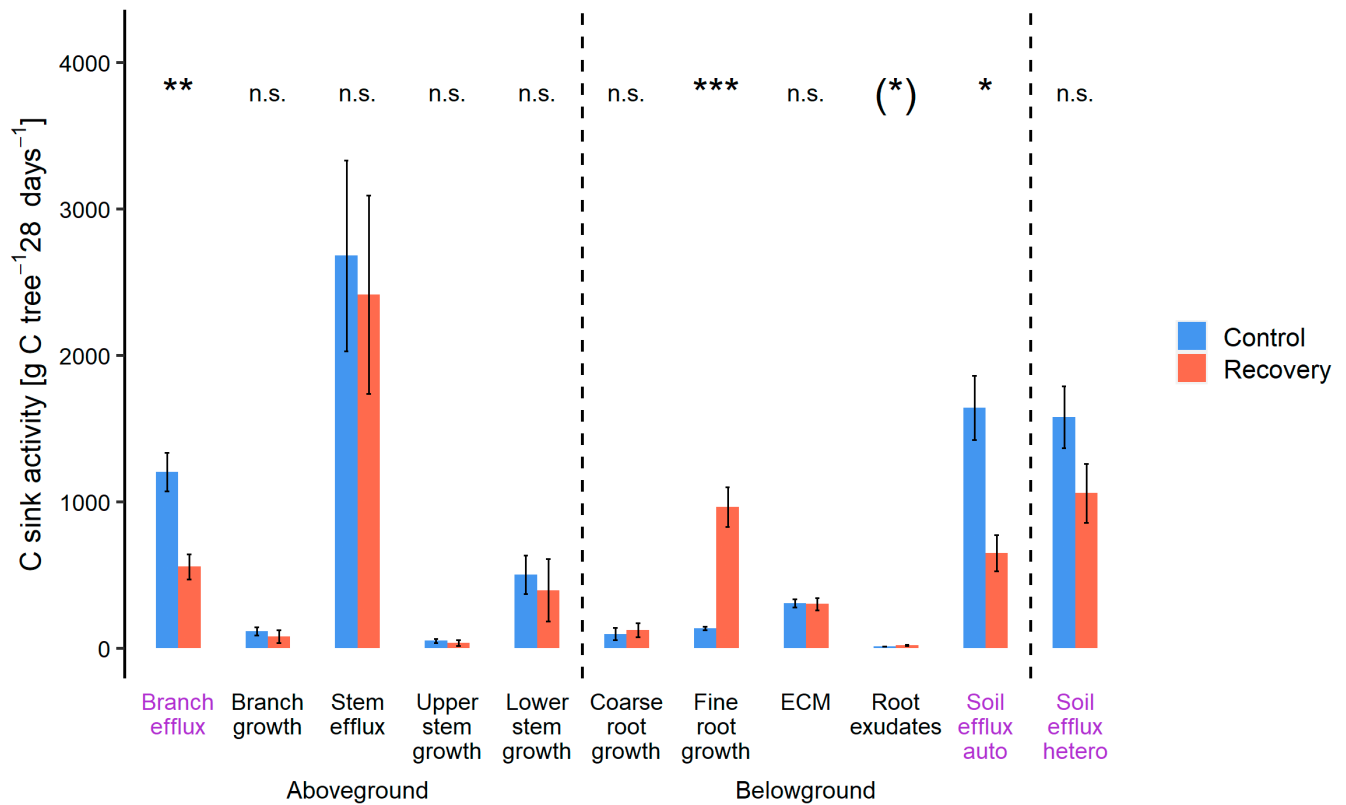


**FIGURE 3** Total C sink activity (cumulative sum during 28 days after watering in  $\text{g C tree}^{-1} 28 \text{ days}^{-1}$ ) in each above- and belowground sink in four control and three recovering (previously drought-stressed) trees (mean  $\pm$  SE): In branch  $\text{CO}_2$  efflux, branch growth, stem  $\text{CO}_2$  efflux, upper and lower stem growth, coarse-root growth, fine-root growth, ectomycorrhizae (ECM), root exudates, and soil  $\text{CO}_2$  efflux (autotrophic and heterotrophic). C sinks which were (partly) not directly measured are marked with purple color. Asterisks indicate significant results based on t-tests comparing control and recovering trees, \*\*\* $p < .001$ ; \*\* $p < .01$ ; \* $p < .05$ ; (\*),  $p < .1$ ; n.s., not significant.

controls ( $p < .1$ ) although it was very small with  $< 20 \text{ g C}$  in both treatments.

### 3.2 | Allocation of newly assimilated C ( $C_{\text{new}}$ )

We calculated the cumulative sum of  $C_{\text{new}}$  allocated to each sink (in  $\text{g C tree}^{-1} 28 \text{ days}^{-1}$ , Figure 4b) during the first 4 weeks after drought release, and the proportional allocation of  $C_{\text{new}}$  to the total  $C_{\text{new}}$  detected in the whole tree (in %, Figure 4a). At the whole-tree level, recovering trees tended to shift allocation towards belowground sinks (although not significant,  $p = .14$ , Figure 4a), that is,  $60 \pm 7\%$  to aboveground and  $40 \pm 7\%$  to belowground sinks, compared with control trees ( $79 \pm 3\%$  aboveground and  $21 \pm 3\%$  belowground).

Recovering trees tended to allocate less  $C_{\text{new}}$  to branch  $\text{CO}_2$  efflux with  $317 \pm 83 \text{ g}$  ( $p = .07$ ), to branch growth with  $19 \pm 13 \text{ g}$  ( $p = .15$ ), and to upper stem growth with  $8 \pm 6 \text{ g}$  ( $p = .17$ ), compared with control trees with  $766 \pm 145 \text{ g C}$ ,  $52 \pm 15 \text{ g C}$ , and  $23 \pm 7 \text{ g C}$ , respectively. Lower stem growth of recovering trees received  $76 \pm 44 \text{ g}$  of  $C_{\text{new}}$ , which was similar to that of control trees with  $66 \pm 6 \text{ g C}$ . Allocation to stem  $\text{CO}_2$  efflux in recovering trees ( $1209 \pm 439 \text{ g C}$ )

was slightly but insignificantly lower than that of control trees with  $1557 \pm 474 \text{ g C}$ . Looking at the proportional allocation (Figure 4a), branch efflux, branch growth, and upper stem growth of recovering trees received  $13 \pm 0\%$ ,  $< 1 \pm 0\%$ , and  $< 1 \pm 0\%$  of total  $C_{\text{new}}$  detected, which all tended to be lower than that of control trees with  $26 \pm 2\%$ ,  $2 \pm 0\%$ , and  $1 \pm 0\%$ , respectively ( $p < .1$ ). Proportional allocation to stem  $\text{CO}_2$  efflux was also slightly but insignificantly lower in recovering ( $44 \pm 6\%$ ) than in control trees ( $48 \pm 5\%$ ).

Belowground, the most prominent difference between control and recovering trees was the allocation of  $C_{\text{new}}$  to growing fine-roots with  $406 \pm 57 \text{ g C}$  in recovering and only  $38 \pm 3 \text{ g C}$  in control trees ( $p < .001$ ). This makes fine-root growth the major belowground sink for the allocation of  $C_{\text{new}}$  after drought release, representing  $18 \pm 4\%$  of the total  $C_{\text{new}}$  detected in recovering trees ( $1 \pm 0\%$  in control trees,  $p < .001$ ). In coarse-root growth, a strong tendency of a higher allocation ( $p < .1$ ) was detected in recovering trees ( $20 \pm 8 \text{ g C}$  and proportional allocation of  $1 \pm 0\%$ ) compared with controls ( $4 \pm 3 \text{ g C}$  representing  $< 1 \pm 0\%$ ). Allocation to root exudates was also significantly higher ( $p < .05$ ) in recovering trees with  $17 \pm 2 \text{ g C}$  than in control controls with  $7 \pm 1 \text{ g C}$  (but both  $< 1\%$ ). In contrast, there was no significant difference in ECM ( $171 \pm 24 \text{ g C}$  and  $8 \pm 2\%$  in recovering,  $174 \pm 16 \text{ g C}$  and  $6 \pm 1\%$  in control trees).

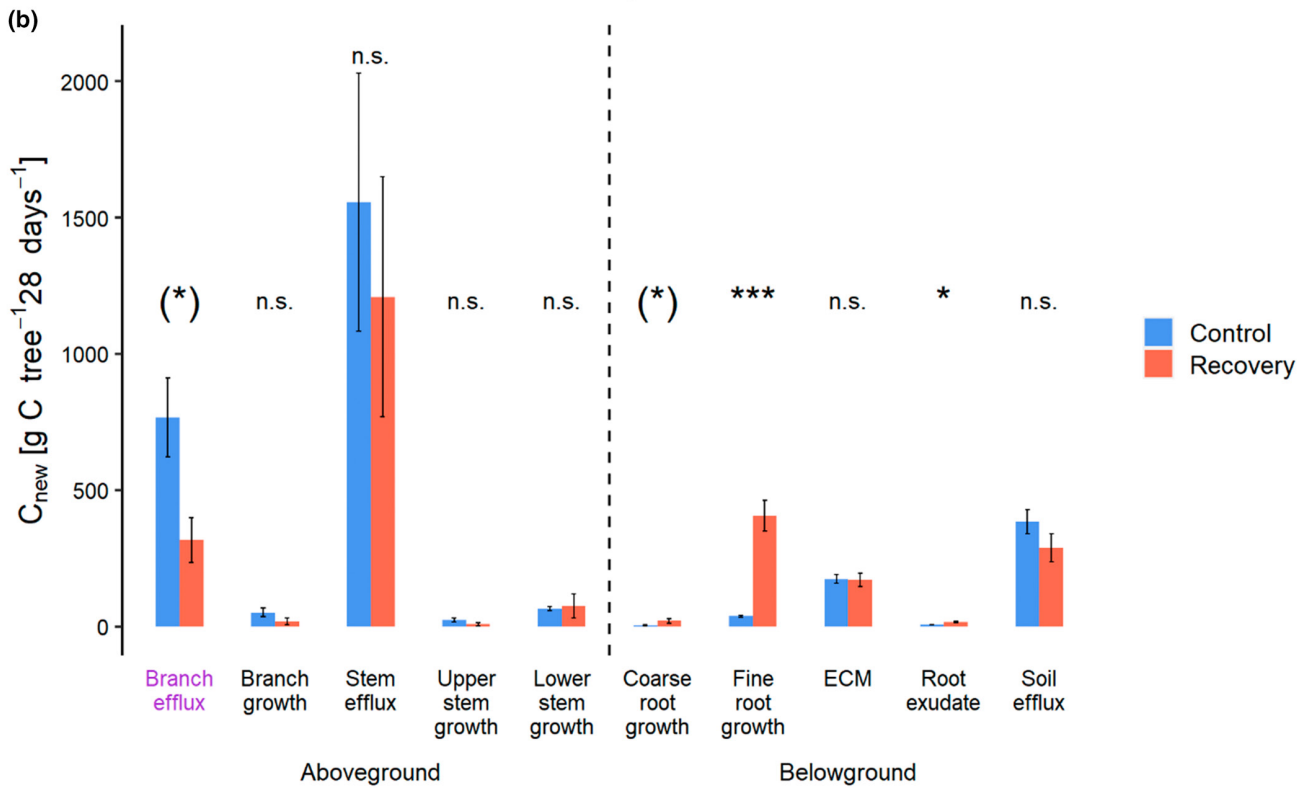
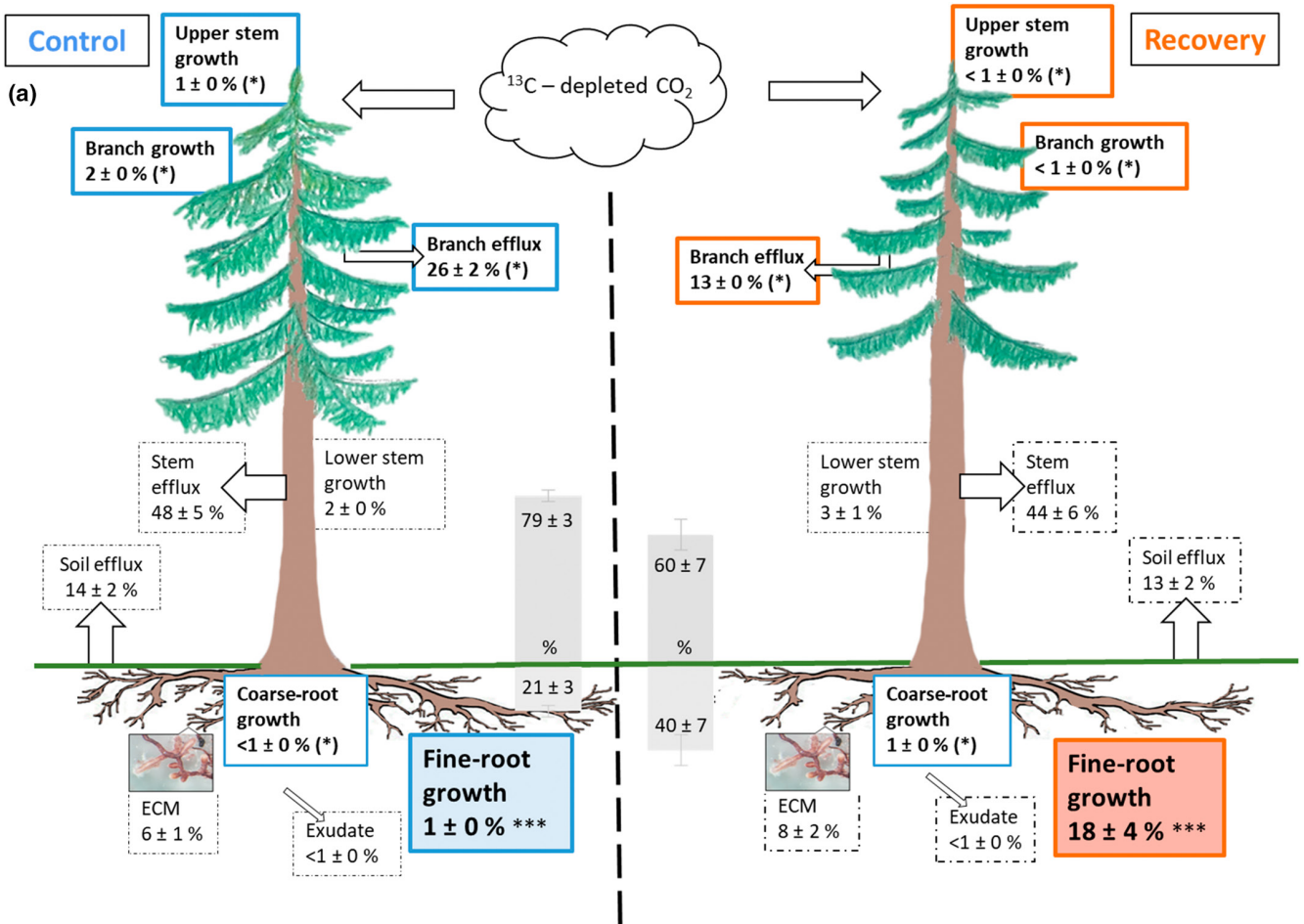
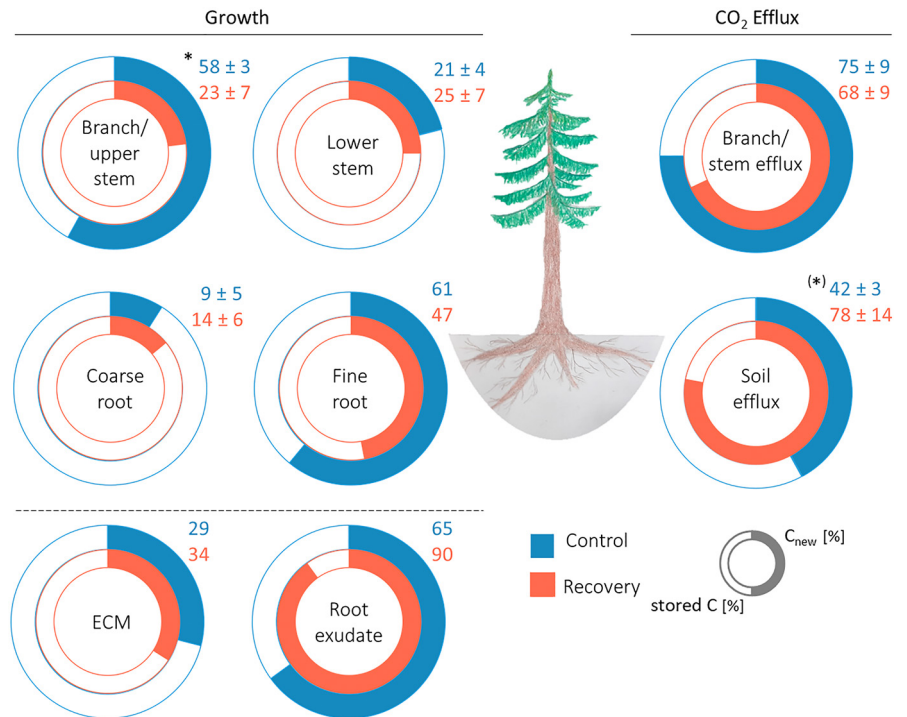


**FIGURE 4** (a) Proportional allocation of newly assimilated C ( $C_{new}$ ) to total  $C_{new}$  detected and (b) amount of  $C_{new}$  (cumulative sum during 28 days after watering in  $gC\ tree^{-1}\ 28\ days^{-1}$ ) allocated to each above- and belowground sink in four control and three recovering (previously drought-stressed) trees, that is, branch  $CO_2$  efflux, branch growth, stem  $CO_2$  efflux, upper and lower stem growth, coarse-root growth, fine-root growth, ectomycorrhizae (ECM), root exudates, and autotrophic soil  $CO_2$  efflux (mean  $\pm$  SE). C sinks which were not directly measured in this study are marked with purple color. Asterisks give the results of *t*-tests or linear-mixed model comparing control and recovering trees, \*\*\* $p < .001$ ; \* $p < .05$ ; (\*),  $p < .1$ ; n.s., not significant.

**FIGURE 5** Contribution of newly assimilated C ( $C_{new}$ ) to each C sink activity at the new isotopic equilibrium (cont $C_{new}$  in %) in each above- and belowground C sink, that is, stem and branch  $CO_2$  efflux, branch and upper stem growth, lower stem growth, coarse-root growth, fine-root growth, ectomycorrhizae (ECM), root exudates, and autotrophic soil  $CO_2$  efflux, in control and recovering (previously drought-stressed) trees. Numbers next to the charts give means  $\pm$  SE of each treatment. Asterisk indicates a significant difference between control and recovering trees, \* $p < .05$ ; (\*),  $p < .1$ . For fine-root, ECM, and root exudate, there are no SE, since we pooled all samples for the calculation of cont $C_{new}$ . Statistical tests for these three sinks were thus not possible.



Allocation to soil  $CO_2$  efflux was slightly but insignificantly lower in recovering trees ( $289 \pm 51\ gC$ ,  $13 \pm 2\%$ ) compared with controls ( $384 \pm 44\ g$ ,  $14 \pm 2\%$ ).

### 3.3 | Contribution of $C_{new}$ to each C sink activity (cont $C_{new}$ )

cont $C_{new}$  represents the contribution (in %) of  $C_{new}$  to meet the C sink activity (Figure 5). Belowground sinks with high C sink activity tended to show low contribution of  $C_{new}$ .

In aboveground sinks,  $C_{new}$  contributed to  $23 \pm 7\%$  of the C sink activity of upper stem and branch growth in recovering trees, which was significantly lower ( $p = .02$ ) compared with controls with  $58 \pm 3\%$ . In other aboveground sinks of recovering trees, cont $C_{new}$  was similar between control and recovering trees.

In belowground sinks of recovering trees,  $C_{new}$  contributed to 47% of the fine-root growth, which was lower compared with control trees with 61%. In root exudates and autotrophic soil  $CO_2$  efflux, cont $C_{new}$  tended to be higher in recovering trees with 90% and  $78 \pm 14\%$  ( $p = .08$ ), compared with controls with 65% and  $42 \pm 3\%$ . Remaining belowground sinks showed similar cont $C_{new}$  between control and recovering trees.

## 4 | DISCUSSION

The present study elucidates the C sink activity and the allocation of  $C_{new}$  and stored C in mature Norway spruce upon drought release after 5 years of experimental summer drought. The recovering trees increased C sink activity of fine-root growth upon drought release, while that of aboveground growth and  $CO_2$  efflux tended to be less (Figure 3), confirming H1 that belowground sink activity would increase with a parallel decrease aboveground. The high belowground C sink activity was supported by a preferential  $C_{new}$  allocation to the root system (Figure 4a,b), with a parallel decrease of  $C_{new}$  allocation aboveground, which is in line with H2: preferential allocation  $C_{new}$  belowground at the expense of aboveground sinks. cont $C_{new}$  to fine-root growth was lower in recovering trees compared with controls (Figure 5), which was driven by the high belowground C sink activity in recovering trees, confirming H3 that contribution of  $C_{new}$  would be lower under high sink activity. As a result, the preferential allocation of  $C_{new}$  to fine-roots was not sufficient to meet the increased C sink activity of these growing roots.

The broad measurement data set used here allowed for scaling from the organ to whole-tree level. Although a broad overview is gained, some uncertainties remain, in particular estimates of branch  $CO_2$  efflux and partitioning of soil  $CO_2$  efflux into autotrophic and



heterotrophic processes due to the lack of direct measurements. However, these uncertainties do not change the main conclusions of this study that enhanced fine-root growth was supported by both,  $C_{\text{new}}$  and stored C. For example for soil  $\text{CO}_2$  efflux, the contribution of autotrophic respiration in control trees may be significantly lower than assumed (e.g. as low as 5%, Muhr & Borken, 2009), which would even reinforce our conclusions that recovering trees increased belowground sink activity compared with controls. Moreover, the contribution of autotrophic respiration might have decreased after drought release (Schindlbacher et al., 2012), but overall it cannot be lower than  $\text{cont}C_{\text{new}}$  to total soil  $\text{CO}_2$  efflux, that is, around 20%–36%. Within these boundaries, significance of the results do not change.

#### 4.1 | Preferential allocation of $C_{\text{new}}$ to enhanced fine-root growth after drought release

In control trees, majority of the aboveground C demand was found in the respiratory sinks. Small C demand and allocation of  $C_{\text{new}}$  to the aboveground growth in the control trees might be explained by seasonal variations (Arneith et al., 1998; DeLucia et al., 2007), as only 15%–20% of the annual radial growth occurred during the study period (data not shown). Compared with control trees, Norway spruce recovering from drought tended to show lower aboveground C sink activity (Figure 3). Similarly, these recovering trees tended to allocate less  $C_{\text{new}}$  to aboveground growth and  $\text{CO}_2$  efflux (Figure 4b), and had a lower proportional allocation of  $C_{\text{new}}$  to aboveground (Figure 4a). A comparable decreased allocation of  $C_{\text{new}}$  to aboveground organs during drought recovery has also been observed in saplings of other tree species (Galiano et al., 2017; Hagedorn et al., 2016). The lower allocation of  $C_{\text{new}}$  to aboveground sinks likely resulted from reduced C sink activity aboveground as branch and stem growth had significantly decreased during drought (Pretzsch et al., 2020; Tomasella et al., 2018) and remained lower compared with controls 4 weeks after drought release (Figure 3). Before watering in early July, predawn leaf water potential of the recovering trees was c.  $-0.9$  MPa (Grams et al., 2021), which is much higher than the water potential of  $-4$  MPa that could cause a 50% loss of branch xylem conductivity determined for the same trees (Tomasella et al., 2018). Therefore, aboveground repair processes, which would increase the amount of C used for  $\text{CO}_2$  efflux (Bucci et al., 2003; Secchi & Zwieniecki, 2011; Trugman et al., 2018; Zang et al., 2014), were unlikely to have played a significant role in the recovery of these trees. This is further supported by rates of stem  $\text{CO}_2$  efflux of recovering trees after drought release (Hikino et al., 2022) which were unaffected. Accordingly, smaller growth and the lack of repair processes, both explain the lower C sink activity of aboveground respiratory sinks in recovering trees compared with controls (Figure 3).

Belowground, we observed a seven times greater C sink activity of fine-root growth in recovering trees after drought release compared with controls (Figure 3), which was supported by the preferential allocation of  $C_{\text{new}}$  to roots (Figure 4a,b). A strong reduction

of fine-root growth was observed throughout the drought period (Nickel et al., 2018; Zwetsloot & Bauerle, 2021), corroborating the need to restore the essential functions of fine-roots for resource uptake (Bardgett et al., 2014; Germon et al., 2020; Solly et al., 2018). Thus, the faster transport of  $C_{\text{new}}$  to fine-root tips (Hikino et al., 2022) and the increased allocation of  $C_{\text{new}}$  both facilitated the fine-root growth upon drought release. C sink activity and the allocation of  $C_{\text{new}}$  to coarse-root growth also increased in recovering trees compared with controls (Figure 4a,b), likely supporting the increased fine-root growth and water transport (Zhang & Wang, 2015). Our findings are in agreement with Joseph et al. (2020) who reported that naturally drought-stressed mature pine trees invested more  $C_{\text{new}}$  into root biomass after rainfall compared with long-term irrigated trees, while the allocation of  $C_{\text{new}}$  to aboveground sinks was slightly lower. These findings support the optimal partitioning theory by Bloom et al. (1985) stating that plants allocate C to the organ which is responsible for the uptake of the limiting resource—in our case water, most likely along with dissolved nutrients (Gessler et al., 2017).

Ectomycorrhizae of recovering spruce trees showed a similar C sink activity (Figure 3) and similar allocation of  $C_{\text{new}}$  as control trees (Figure 4a,b). This is in contrast to young beech trees, which preferentially allocated newly assimilated C to ECM during recovery from drought (Hagedorn et al., 2016). Species-specific root traits particularly under and following drought most likely explain these contrasting C allocation patterns. Beech forms fine-roots with a short lifespan and sustains fine-root formation under drought (Nikolova et al., 2020; Zwetsloot & Bauerle, 2021). Beech ECMs, thus, need to be continuously formed resulting in fast C turnover and a high C sink activity of ECMs immediately after drought release (Hagedorn et al., 2016). In contrast, spruce trees with long-lived fine-roots and slow C turnover, show a temporal dormancy during drought by suberization and reduced growth to prevent resource loss (Nikolova et al., 2020). Our findings on unaffected C allocation to vital ECM on trees that experienced long-term drought are in accordance with previous results on sustained functionality of the ectomycorrhizal symbiosis under drought (Fuchslueger et al., 2014; Nickel et al., 2018). In addition, the lack of an increased C allocation to ECM may reflect an asynchrony between fast fine-root growth after watering with the supply of  $C_{\text{new}}$  from day 7 on (Hikino et al., 2022) and slower ECM formation (duration around 4 weeks, Ineichen & Wiemken, 1992) on newly grown roots. Therefore, we suggest that C allocation in newly formed ECM peaked later in spruce and was not captured during this 4-week study period.

Root exudation was a negligible C sink with less than 1% of total C sink activity (Figure 3) and of  $C_{\text{new}}$  (Figure 4a), thus similar to Mediterranean conifer saplings (Rog et al., 2021), but somewhat lower than in other natural forest stands with 2%–6% of total  $C_{\text{new}}$  (Abramoff & Finzi, 2016; Gougherty et al., 2018) and saplings with up to 30% of total  $C_{\text{new}}$  (Liese et al., 2018). Allocation of  $C_{\text{new}}$  to root exudates, which was already small during the drought period (approx. 1%–2%, Brunn et al., 2022), remained small after drought release. Furthermore, allocation in the recovering trees tended to be

higher than in the controls, which is consistent with findings during the drought phase (Brunn et al., 2022).

The increased C sink activity and allocation of  $C_{\text{new}}$  to root growth in the recovering trees was not reflected in soil  $\text{CO}_2$  efflux, that is, lower soil  $\text{CO}_2$  efflux rates (Figure 3) and lower allocation of  $C_{\text{new}}$  to autotrophic soil  $\text{CO}_2$  efflux compared with control trees even after drought release (Figure 4a,b), despite the similar soil water content between treatments after drought release (Grams et al., 2021). Sun et al. (2020) state that maintenance respiration of spruce fine-roots accounts for 70% of the total respiration (maintenance and growth). Due to increased suberization during drought (Nikolova et al., 2020; Zwetsloot & Bauerle, 2021), root maintenance respiration was likely decreased (Barnard & Jorgensen, 1977). This reduction cannot be compensated by increased root-growth, which only accounts for 30% of the initial fine-root biomass (Table 2, fine-root length growth rate). This result also suggests that soil microbial activity, which was potentially reduced during drought (Nikolova et al., 2009), did not increase immediately after drought release as observed in other Norway spruce forests (Muhr & Borken, 2009; Schindlbacher et al., 2012). During repeated drought, the microbial communities might have adapted to drought conditions leading to a higher C use efficiency and thus reduces respiration with the number of repetitive droughts (Canarini et al., 2021; de Nijs et al., 2019; Evans & Wallenstein, 2012). Therefore, in contrast to previous studies on young beech and slow-growing, mature pine trees (Gao et al., 2021; Hagedorn et al., 2016; Joseph et al., 2020), we assume that microbial biomass did not receive an enhanced amount of  $C_{\text{new}}$  after drought release, which is supported by the low allocation of  $C_{\text{new}}$  to root exudates.

#### 4.2 | Use of the stored C is essential for fine-root growth during recovery

Despite the preferential allocation of  $C_{\text{new}}$  to fine-root recovery, less than half of the increased fine-root growth in recovering trees was supported by  $C_{\text{new}}$  (Figure 5), which was lower than in control trees (61%) and what had been reported for other species (c. 75%; Lynch et al., 2013; Matamala et al., 2003). This suggests that the relative contribution of  $C_{\text{new}}$  decreases with high C sink activity belowground, which was also observed in autotrophic soil  $\text{CO}_2$  efflux of controls (Figures 3 and 5). Likewise for coarse-root growth, around 86% of the present C was comprised of stored C (Figure 5), indicating the importance of stored C for root growth during drought recovery. Increased suberization and reduced respiration of fine-roots in recovery plots during drought (Nikolova et al., 2020; Zwetsloot & Bauerle, 2021) was accompanied by twice the starch concentration stored in these fine-roots before watering compared with the controls (data not shown). Reduction of these starch concentrations to the level of control trees within the first 7 days after watering indicates that they were most likely used for initial fine-root growth after drought release, which is similar to observations by Yang et al. (2016) in Chinese fir saplings.

Lack of complete depletion might indicate an existence of regulation mechanism through enzymes degrading starch (Tsamir-Rimon et al., 2021). Furthermore, in addition to the starch conversion, reversal of osmotic potential in leaves (Hikino et al., 2022) and also in other organs likely released large amounts of osmolytes during first 4 weeks after watering, which became available for other C sinks (Tsamir-Rimon et al., 2021). Indeed, a reduced  $C_{\text{new}}$  allocated to branches and upper stem growth in the recovering trees compared with controls might indicate a direct incorporation of C derived from the released osmolytes to sinks in the crowns, allowing  $C_{\text{new}}$  to bypass towards belowground sinks. C storage pools of the spruce trees (in leaves, branches, stem, and roots) had significantly decreased during the drought period (Hesse et al., 2021), and thus remobilized C from osmolytes also likely played a significant role as a C source.

## 5 | CONCLUSION

Restoring water uptake is crucial for long-term drought recovery of whole-tree functionality and preparation for upcoming drought periods. Following drought release, we found recovering spruce trees prioritized root growth by preferential allocation of new photoassimilates (i.e.,  $C_{\text{new}}$ ). The high belowground C sink activity was not entirely met by  $C_{\text{new}}$  and was largely subsidized by stored C. This highlights the role of both, the availability of C stores and the allocation of new photoassimilates to support repair and regrowth of functional tissues. It remains an open question whether (and how) the belowground C sink activity can be met over longer periods, even years, following drought release. Our findings also highlight the importance of belowground C sinks for analyses of post-drought growth increment and C stores of trees. If the altered C allocation towards belowground sinks persists in the following growing seasons, the drought effect on stem growth may remain for years. Thus, long-term observation of above- and belowground biomass partitioning is necessary to elucidate the longstanding consequences of altered C allocation upon drought release for forest productivity and C storage dynamics.

### AUTHOR CONTRIBUTIONS

Thorsten E. E. Grams and Karin Pritsch originally designed the experiment. Kyohsuke Hikino, Vincent P. Riedel, and Thorsten E. E. Grams prepared and performed the  $^{13}\text{C}$  labeling. Kyohsuke Hikino, Jasmin Danzberger, Vincent P. Riedel, Benjamin D. Hesse, Benjamin D. Hafner, Timo Gebhardt, Romy Rehschuh, Nadine K. Ruehr, Melanie Brunn, Simon M. Landhäusser, Marco M. Lehmann, Thomas Rötzer, Franz Buegger, Fabian Weikl, Karin Pritsch, and Thorsten E. E. Grams collected and processed the samples/data. Kyohsuke Hikino and Jasmin Danzberger finalized the experimental design, analyzed and interpreted the data with supports from Thorsten E. E. Grams, Karin Pritsch, Benjamin D. Hesse, Benjamin D. Hafner, Franz Buegger, Fabian Weikl, Romy Rehschuh, Nadine K. Ruehr, Simon M. Landhäusser, Marco M. Lehmann, Timo Gebhardt, Thomas Rötzer,







- forests. *Plant and Soil*, 446(1–2), 471–486. <https://doi.org/10.1007/s11104-019-04343-z>
- Tomasella, M., Beikircher, B., Häberle, K.-H., Hesse, B. D., Kallenbach, C., Matyssek, R., & Mayr, S. (2018). Acclimation of branch and leaf hydraulics in adult *Fagus sylvatica* and *Picea abies* in a forest through-fall exclusion experiment. *Tree Physiology*, 38(2), 198–211. <https://doi.org/10.1093/treephys/tpx140>
- Trugman, A. T., Detto, M., Bartlett, M. K., Medvigy, D., Anderegg, W. R. L., Schwalm, C., Schaffer, B., & Pacala, S. W. (2018). Tree carbon allocation explains forest drought-kill and recovery patterns. *Ecology Letters*, 21(10), 1552–1560. <https://doi.org/10.1111/ele.13136>
- Tsamir-Rimon, M., Ben-Dor, S., Feldmesser, E., Oppenhimer-Shaanan, Y., David-Schwartz, R., Samach, A., & Klein, T. (2021). Rapid starch degradation in the wood of olive trees under heat and drought is permitted by three stress-specific beta amylases. *New Phytologist*, 229(3), 1398–1414. <https://doi.org/10.1111/nph.16907>
- Unger, S., Máguas, C., Pereira, J. S., David, T. S., & Werner, C. (2010). The influence of precipitation pulses on soil respiration – Assessing the “Birch effect” by stable carbon isotopes. *Soil Biology and Biochemistry*, 42(10), 1800–1810. <https://doi.org/10.1016/j.soilbio.2010.06.019>
- Werner, C., Meredith, L. K., Ladd, S. N., Ingrisch, J., Kübert, A., van Haren, J., Bahn, M., Bailey, K., Bamberger, I., Beyer, M., Blomdahl, D., Byron, J., Daber, E., Deleeuw, J., Dippold, M. A., Fudyma, J., Gil-Loaiza, J., Honeker, L. K., Hu, J., ... Williams, J. (2021). Ecosystem fluxes during drought and recovery in an experimental forest. *Science (New York, N.Y.)*, 374(6574), 1514–1518. <https://doi.org/10.1126/science.abj6789>
- Yang, Q., Zhang, W., Li, R., Xu, M., & Wang, S. (2016). Different responses of non-structural carbohydrates in above-ground tissues/organs and root to extreme drought and re-watering in Chinese fir (*Cunninghamia lanceolata*) saplings. *Trees*, 30(5), 1863–1871. <https://doi.org/10.1007/s00468-016-1419-0>
- Zang, U., Goisser, M., Grams, T. E. E., Häberle, K.-H., Matyssek, R., Matzner, E., & Borken, W. (2014). Fate of recently fixed carbon in European beech (*Fagus sylvatica*) saplings during drought and subsequent recovery. *Tree Physiology*, 34(1), 29–38. <https://doi.org/10.1093/treephys/tpt110>
- Zhang, X., & Wang, W. (2015). The decomposition of fine and coarse roots: Their global patterns and controlling factors. *Scientific Reports*, 5, 9940. <https://doi.org/10.1038/srep09940>
- Zwetsloot, M. J., & Bauerle, T. L. (2021). Repetitive seasonal drought causes substantial species-specific shifts in fine-root longevity and spatio-temporal production patterns in mature temperate forest trees. *New Phytologist*, 231, 974–986. <https://doi.org/10.1111/nph.17432>

## SUPPORTING INFORMATION

Additional supporting information can be found online in the Supporting Information section at the end of this article.

**How to cite this article:** Hikino, K., Danzberger, J., Riedel, V. P., Hesse, B. D., Hafner, B. D., Gebhardt, T., Rehschuh, R., Ruehr, N. K., Brunn, M., Bauerle, T. L., Landhäusser, S. M., Lehmann, M. M., Rötzer, T., Pretzsch, H., Buegger, F., Weikl, F., Pritsch, K., & Grams, T. E. E. (2022). Dynamics of initial carbon allocation after drought release in mature Norway spruce—Increased belowground allocation of current photoassimilates covers only half of the carbon used for fine-root growth. *Global Change Biology*, 28, 6889–6905. <https://doi.org/10.1111/gcb.16388>

1 **Supporting information**

2 **Article title:** Dynamics of initial C allocation after drought release in mature Norway spruce -  
3 Increased belowground allocation of current photoassimilates covers only half of the C used for  
4 fine-root growth

5 **Authors:** Kyohsuke Hikino, Jasmin Danzberger, Vincent P. Riedel, Benjamin D. Hesse,  
6 Benjamin D. Hafner, Timo Gebhardt, Romy Rehschuh, Nadine K. Ruehr, Melanie Brunn,  
7 Taryn L. Bauerle, Simon M. Landhäusser, Marco M. Lehmann, Thomas Rötzer, Hans Pretzsch,  
8 Franz Buegger, Fabian Weikl, Karin Pritsch, Thorsten E. E. Grams

9

10

11

12

13

14

15

16 *Table S1: Detailed data of the labeled four control and three recovering (previously drought-stressed)*  
17 *trees: Diameter at breast height (DBH), tree height, height of the crown base, the daily mean change of*  
18 *stable carbon isotope composition ( $\delta^{13}\text{C}$ ) and  $\text{CO}_2$  concentration in crown air during labeling, spatial*  
19 *contribution and area of each tree for the calculation of belowground C sink activity and allocation of*  
20 *newly assimilated C ( $C_{\text{new}}$ ): in fine-root growth, ectomycorrhizae (ECM), root exudates, and soil  $\text{CO}_2$*   
21 *efflux (see Material and Methods). The changes are given in means  $\pm$  SE.*

<b>Tree</b>	<b>DBH [cm]</b>	<b>Tree height [m]</b>	<b>Height of the crown base [m]</b>	<b>Change in crown air <math>\delta^{13}\text{C}</math> [‰]</b>	<b>Change in <math>\text{CO}_2</math> concentration [ppm]</b>	<b>Spatial contribution belowground [%]</b>	<b>Area [m<sup>2</sup>]</b>
<b>Conrol_1</b>	30.5	33.7	23.6	$-6.7 \pm 0.4$	$111 \pm 8$	21	11
<b>Conrol_2</b>	34.9	32.6	23.1	$-6.7 \pm 0.4$	$112 \pm 8$	23	13
<b>Control_3</b>	46.3	34.3	23.1	$-7.2 \pm 0.4$	$119 \pm 8$	31	17
<b>Control_4</b>	37.7	32.5	21.0	$-8.8 \pm 0.4$	$162 \pm 10$	25	14
<b>Recovery_1</b>	45.1	32.0	22.7	$-5.0 \pm 0.3$	$72 \pm 5$	41	26
<b>Recovery_2</b>	27.3	28.3	22.5	$-7.3 \pm 0.4$	$132 \pm 8$	25	16
<b>Recovery_3</b>	38.3	33.6	23.3	$-2.9 \pm 0.3$	$35 \pm 5$	36	22

22

23 *Table S2: Days of samplings/assessments of each parameter (days marked in gray are the timing of*  
 24 *samplings/assessments) and number of samples per treatment (i.e. control and recovery) and day. n.a.,*  
 25 *not assessed.*

Days respective to watering/ start of labeling	-7	-6	-5	-4	-3	-2	-1	0	1	2	3	4	5	6	7	8	9	10	11	12	13	14	15	16	17	18	19	20	21	22	23	24	25	26	27	28	after growing season	samples treatment <sup>-1</sup> day <sup>-1</sup>	
Branch growth																																							3-4
Branch efflux																																							n.a.
Stem growth																																							4
Stem efflux																																							3
Coarse-root growth																																							3-4
Fine-roots in mesh bags																																							8
Additional fine-roots																																							6-13
Ectomycorrhizae																																							5-12
Root exudates																																							3-5
Soil efflux																																							3



27 *Table S3: Total length and surface area of branch/twig and stem estimated for each tree based on field*  
 28 *data. Data of branches and twigs are separated into sun and shade crowns.*

	<b>Sun branch/twig length [m]</b>	<b>Sun branch/twig area [m<sup>2</sup>]</b>	<b>Shade branch/twig length [m]</b>	<b>Shade branch/twig area [m<sup>2</sup>]</b>	<b>Stem area (&lt; 6.5 m) [m<sup>2</sup>]</b>	<b>Stem area (&gt; 6.5 m) [m<sup>2</sup>]</b>
Conrol_1	3359	40	1287	14	6	11
Conrol_2	3847	45	1474	18	7	12
Control_3	5103	60	1956	25	9	17
Control_4	4140	38	1590	21	7	12
Recovery_1	1883	21	1411	22	9	15
Recovery_2	1138	13	853	12	5	8
Recovery_3	1597	20	1198	14	7	14

29

30

31 **Methods S1: Determination of proportional growth using dendrometer**

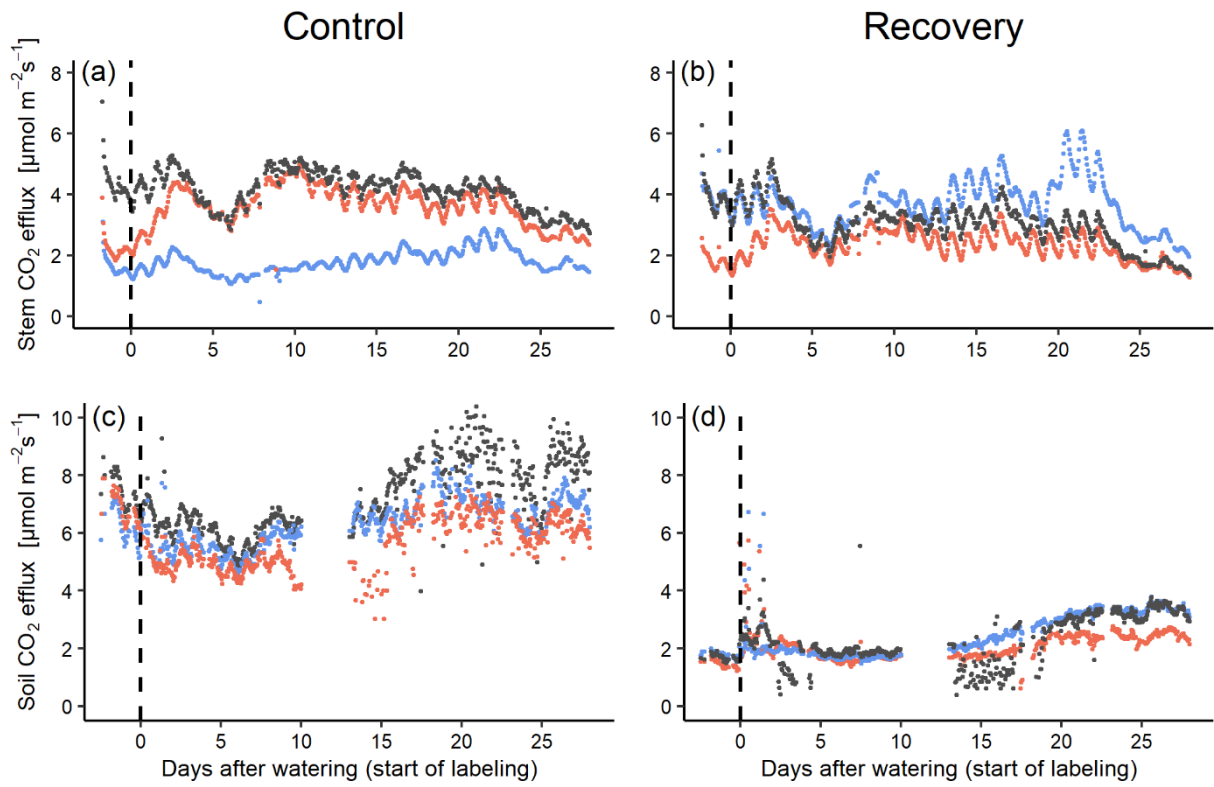
32 To determine the proportional growth (in %) during the 28 days after watering (ratio of the  
 33 radial growth during 28 days to the total annual growth), dendrometer data at 6 am was used  
 34 and fitted with the following sigmoid curve:

35 
$$X = d + \frac{a - d}{1 + e^{\frac{DOY - c}{b}}} \text{ (Eqn. S1),}$$

36 where X is the output voltage (in mV) corresponding to the radial growth, DOY is the day of  
 37 year, a is the starting value of X before the growing season, b the slope coefficient of the  
 38 regression, c the inflection point of the curve, and d the end value of X after the growing season.

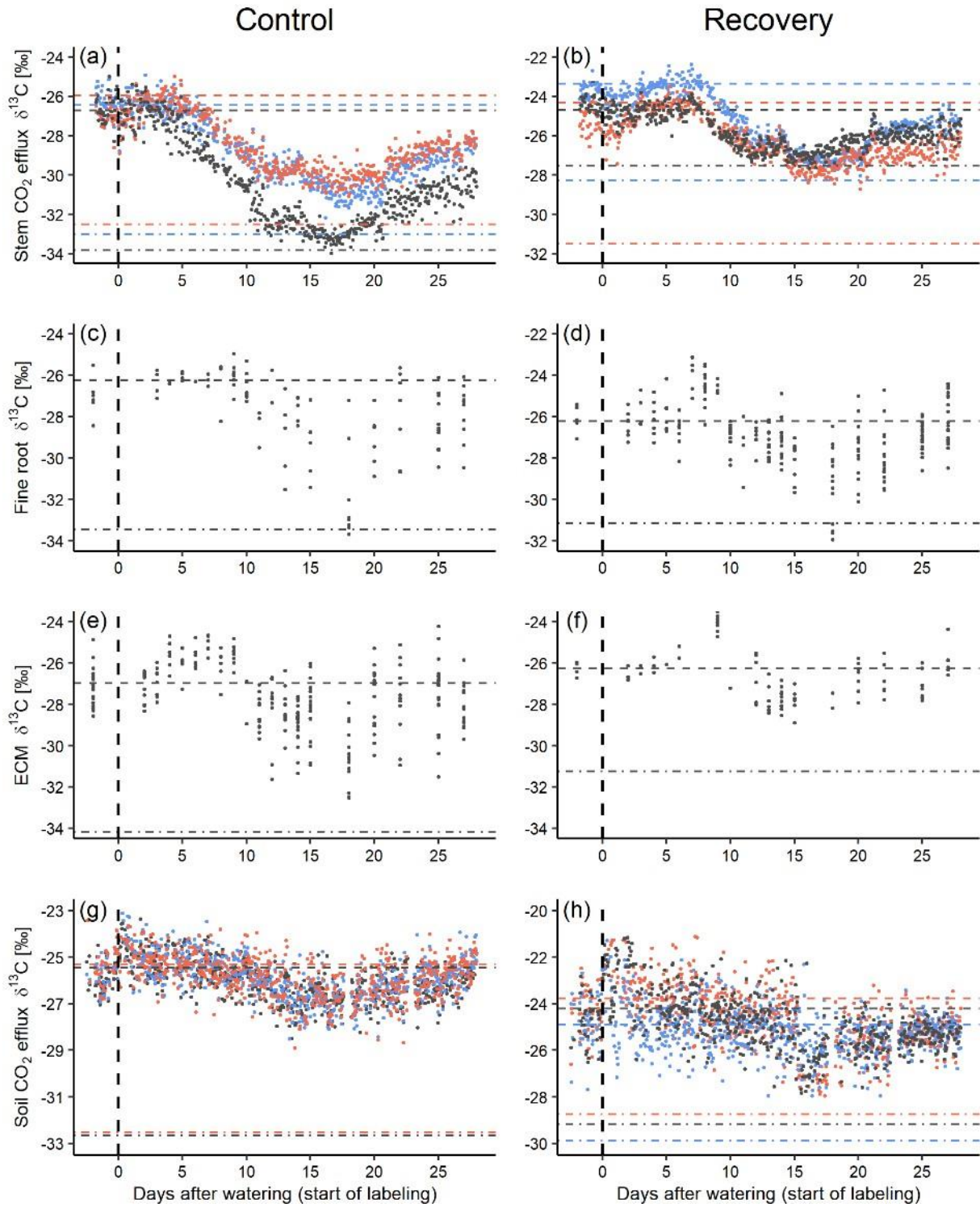
39 Using these curves, proportional growth was calculated by relating the growth during the 28  
 40 days to the total annual growth. Since only two labeled trees per treatment were assessed with  
 41 the dendrometers, additional spruce trees in neighboring plots were included in the evaluation  
 42 of the proportional growth (n = 9 for control and n = 6 for recovering trees).

43



44

45 *Fig. S1: Rates of stem (a, b) and soil CO<sub>2</sub> efflux (c, d) in control (left) and recovery (right) trees during*  
 46 *the study period. Each color represents each measurement tree (n = 3).*



47

48 *Fig. S2: Raw  $\delta^{13}\text{C}$  data ( $\delta^{13}\text{C}_{\text{sample}}$ ) used for Eqn. 10. (a,b) stem  $\text{CO}_2$  efflux, (c,d) non-mycorrhized fine-*  
 49 *root tips, (e, f) ectomycorrhizae (ECM), and (g,h) soil  $\text{CO}_2$  efflux, separated in control trees (left) and*  
 50 *recovering (previously drought-stressed, right) trees. Different colors represent each measurement tree*  
 51 *( $n = 3$ ) for stem  $\text{CO}_2$  efflux and soil  $\text{CO}_2$  efflux. All measurements were pooled for non-mycorrhizal root*  
 52 *tips and ECM. Horizontal dashed and dot-dash lines display  $\delta^{13}\text{C}_{\text{old}}$  and  $\delta^{13}\text{C}_{\text{new}}$  in Eqn. 10, respectively.*  
 53  *$\delta^{13}\text{C}_{\text{new}}$  was calculated with Eqn. S2,S3 using  $\delta^{13}\text{C}_{\text{old}}$  and the individual change in crown air  $\delta^{13}\text{C}$  (Table*  
 54 *S1).*

55

56

57 **Methods S2: Calculation of  $\delta^{13}\text{C}_{\text{new}}$  for Eqn. 10**

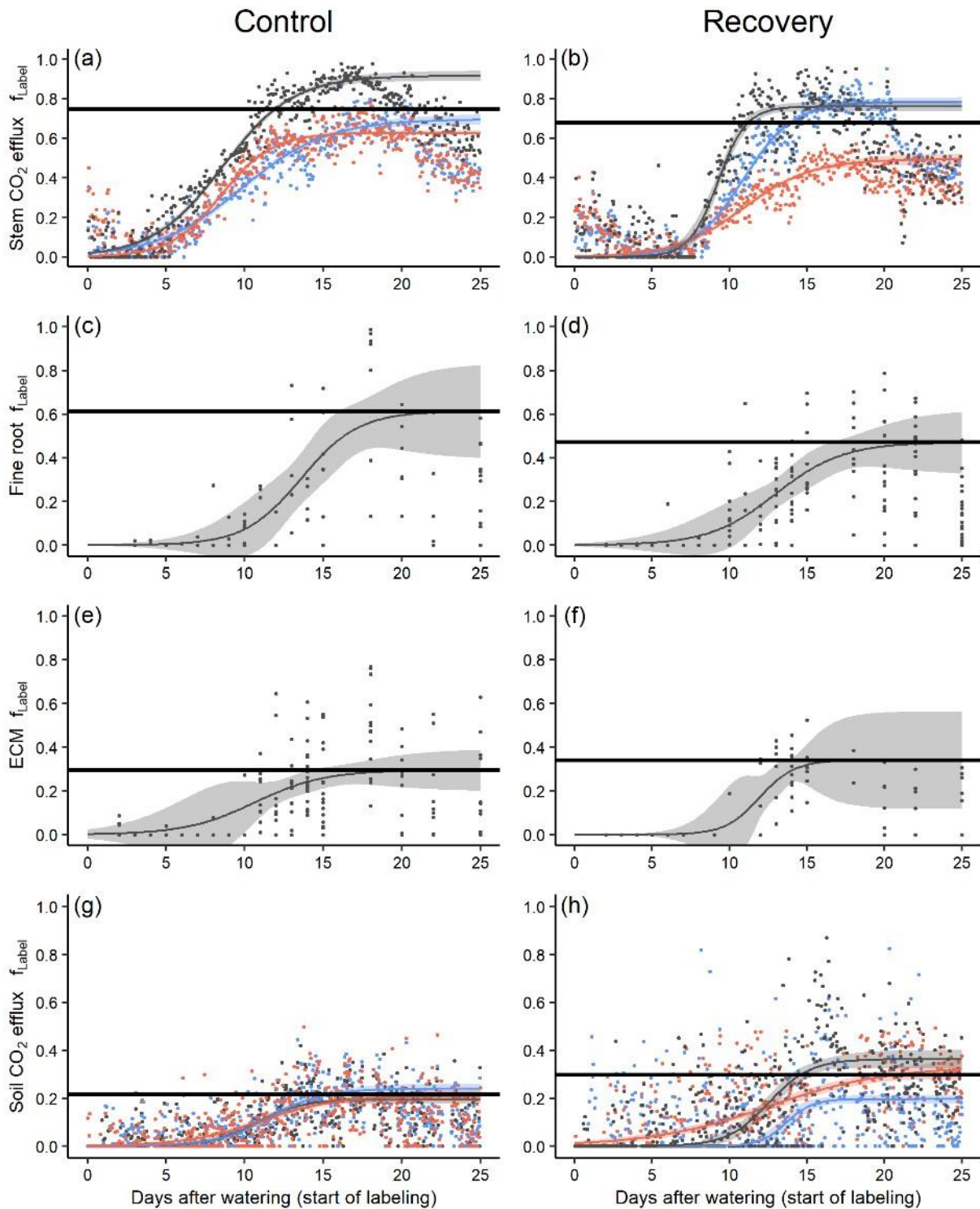
58  $\delta^{13}\text{C}_{\text{new}}$  for Eqn. 10 was calculated as described by Kuptz *et al.* (2011), following (Schnyder *et*  
59 *al.*, 2003):

60 
$$\delta^{13}\text{C}_{\text{A-O}} (\text{‰}) = \left( \frac{1000 + \delta^{13}\text{C}_{\text{Air-Unlabeled}}}{1000 + \delta^{13}\text{C}_{\text{old}}} - 1 \right) \times 1000 \text{ (Eqn. S2),}$$

61 which gives the mean apparent  $^{13}\text{C}$  discrimination ( $\delta^{13}\text{C}_{\text{A-O}}$ ) between unlabeled crown air  
62 (reference air above canopy,  $\delta^{13}\text{C}_{\text{Air-Unlabeled}}$ ) and  $\delta^{13}\text{C}_{\text{old}}$ .

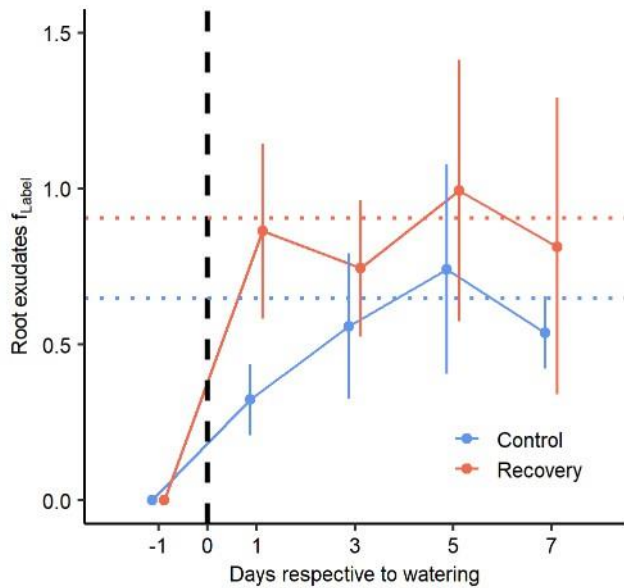
63 
$$\delta^{13}\text{C}_{\text{new}} (\text{‰}) = 1000 \times \frac{1000 + \delta^{13}\text{C}_{\text{Air-Labeled}}}{1000 + \delta^{13}\text{C}_{\text{A-O}}} - 1000 \text{ (Eqn. S3),}$$

64 where  $\delta^{13}\text{C}_{\text{Air-Labeled}}$  is the mean  $\delta^{13}\text{C}$  of crown air of each tree. For belowground sinks that were  
65 not assigned to specific trees, mean  $\delta^{13}\text{C}_{\text{Air-Labeled}}$  of four (control) or three (recovering) trees  
66 was used.



67

68 *Fig. S3:  $f_{Label}$  (fraction of labeled C) and sigmoid curves with 95% confidence intervals to calculate the*  
 69  *$contC_{new}$  (contribution of  $C_{new}$  to C sink activity) to stem  $CO_2$  efflux (a,b), non-mycorrhizal fine-root tips*  
 70 *(c,d), ectomycorrhizae (ECM, e,f), and soil  $CO_2$  efflux (g,h), separated in control trees (left) and*  
 71 *recovering (previously drought-stressed, right) trees. Different colors represent each measurement tree*  
 72 *( $n = 3$ ) for stem  $CO_2$  efflux and soil  $CO_2$  efflux. All measurements were pooled for non-mycorrhizal root*  
 73 *tips and ECM. Only  $f_{Label}$  before reaching the maximum were used for the fitting, since  $f_{Label}$  decreased*  
 74 *again after the end of labeling. Black horizontal lines display the mean  $contC_{new}$ .*



75

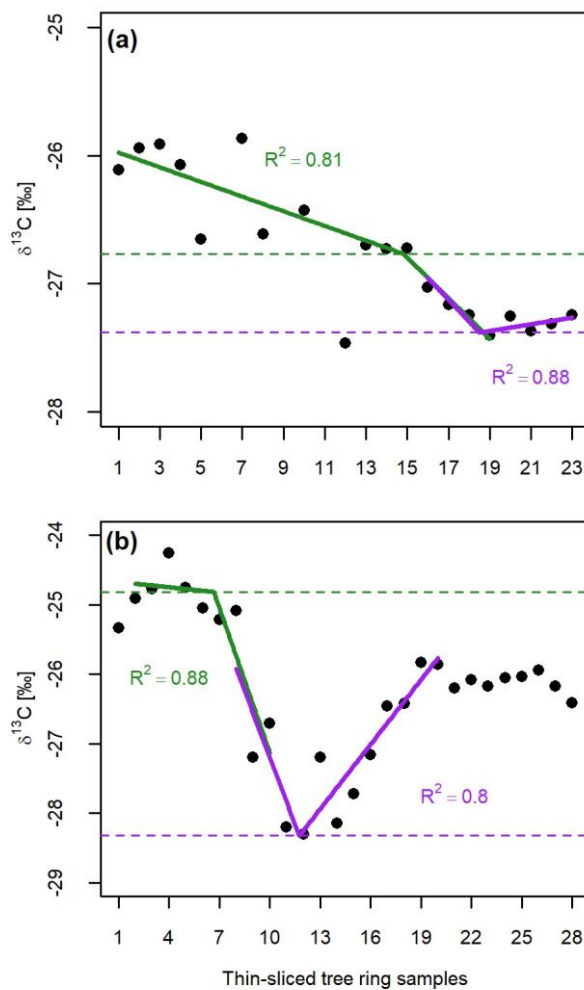
76 Fig. S4:  $f_{Label}$  (fraction of labeled C) and  $contC_{new}$  (contribution of  $C_{new}$  to C sink activity) to root exudates  
 77 in control (blue) and recovering trees (previously drought-stressed, red). The calculated  $contC_{new}$  is  
 78 shown in horizontal dotted lines for control (blue) and recovering trees (red), respectively. The data are  
 79 displayed in mean  $\pm$  SE.

80 **Methods S3: Detailed descriptions for the calculation of fraction of labeled C ( $f_{Label}$ ) and**  
 81 **contribution of  $C_{new}$  to each C sink activity ( $contC_{new}$ ) for branch, stem, and coarse-root**  
 82 **growth**

83 For branch, stem, and coarse-root growth,  $\delta^{13}C_{old}$  and  $\delta^{13}C_{sample}$  (for Eqn. 10) were determined  
 84 by fitting the  $\delta^{13}C$  of tree ring slices with a piecewise function (Hikino *et al.*, 2022). The applied  
 85 labeling with  $^{13}C$ -depleted  $CO_2$  caused a sudden and steep decrease of  $\delta^{13}C$ , after the  $^{13}C$ -  
 86 depleted tracer was incorporated in the tree ring and was thus defined as tracer arrival. To  
 87 determine this point, linear segments before and after the start of the steep decrease (e.g. slices  
 88 1 - 19 for the sample in Fig. S5a) were extracted from the course of the  $\delta^{13}C$  data. Then, these  
 89 linear segments were fitted by linear regression (“lm” function, R package “stats”, version:  
 90 3.6.1). Subsequently, the “segmented” function (R package “segmented”, version: 1.3-0) was  
 91 used to determine the point where the linear relationship (slope and intercept) changes, giving  
 92 the intersection between the two green lines as exemplified in Fig. S5. The  $\delta^{13}C$  value at this  
 93 point (marked by the green horizontal dashed lines in Fig. S5a,b) was then defined as  $\delta^{13}C_{old}$ .

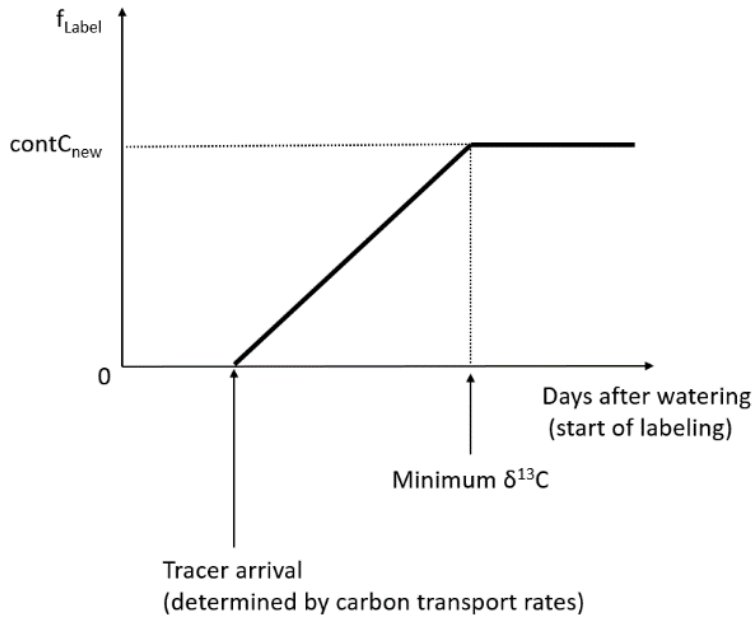
94 After the steep decrease,  $\delta^{13}C$  started to increase again as unlabeled C arrived after the end of  
 95 labeling. We determined this minimum value of  $\delta^{13}C$  by fitting with the piecewise function  
 96 using the same method (intersection between the purple linear segments fitted to the data in Fig.  
 97 S5). The  $\delta^{13}C$  value at this point (purple horizontal dashed lines) was then defined as  $\delta^{13}C_{sample}$ .  
 98 In addition to the labeled trees, we also determined the natural shifts of  $\delta^{13}C$  of non-labeled

99 control trees for each treatment ( $n = 3$ ). These shifts without the effect of the labeling were  
 100 subtracted from the  $\delta^{13}\text{C}_{\text{sample}}$  determined above to correct for the effect of watering, weather  
 101 fluctuation, and seasonal changes (Helle & Schleser, 2004). Finally, using  $\delta^{13}\text{C}_{\text{old}}$ , corrected  
 102  $\delta^{13}\text{C}_{\text{sample}}$ , and Eqn. 10,  $f_{\text{Label}}$  was calculated. Since we could not apply the sigmoid curve (Eqn.  
 103 11) to determine  $\text{cont}C_{\text{new}}$ , the calculated  $f_{\text{Label}}$  was defined as  $\text{cont}C_{\text{new}}$ . Thus, we could not  
 104 consider that the new isotopic equilibrium was not completely reached by the labeling. However,  
 105 since c. 98% of the calculated  $\text{cont}C_{\text{new}}$  to stem  $\text{CO}_2$  efflux was reached with the recorded  $f_{\text{Label}}$   
 106 data (Fig. S3a,b), the underestimation of  $\text{cont}C_{\text{new}}$  to the branch, stem, and the coarse-root  
 107 growth is likely negligible.



108

109 *Fig. S5: Two examples for the calculation of  $\text{cont}C_{\text{new}}$  (contribution of  $C_{\text{new}}$  to  $C$  sink activity) to stem*  
 110 *and coarse-root growth, using piecewise functions. X-axis is each tree ring sample thin-sectioned in*  
 111 *radial direction (c. 5  $\mu\text{m}$  thick). The green and purple line segments fitted to the data show the results*  
 112 *of the piecewise functions for the arrival of  $^{13}\text{C}$ -depleted tracer (green) and minimum  $\delta^{13}\text{C}$  (purple),*  
 113 *respectively.  $\delta^{13}\text{C}$  at the intersections of two line segments of the respective color, marked with*  
 114 *horizontal dashed lines, are the calculated  $\delta^{13}\text{C}_{\text{old}}$  and  $\delta^{13}\text{C}_{\text{sample}}$ , respectively. These values were then*  
 115 *used for the calculation of  $\text{cont}C_{\text{new}}$  (see main text and Methods S3).*



116

117 *Fig. S6: Estimation of the course of  $f_{Label}$  (fraction of labeled C) in branch, stem, and coarse-root growth,*  
 118 *using  $contC_{new}$  (contribution of  $C_{new}$  to C sink activity) and the arrival time of the  $^{13}C$ -depleted tracer.*  
 119  *$f_{Label}$  between tracer arrival and the minimum  $\delta^{13}C$  was assumed to increase linearly.*

120

121

## 122 References

123 **Helle G, Schleser GH. 2004.** Beyond CO<sub>2</sub>-fixation by Rubisco - an interpretation of <sup>13</sup>C/<sup>12</sup>C  
 124 variations in tree rings from novel intra-seasonal studies on broad-leaf trees. *Plant, cell &*  
 125 *environment* **27**: 367–380.

126 **Hikino K, Danzberger J, Riedel VP, Rehschuh R, Ruehr NK, Hesse BD, Lehmann MM,**  
 127 **Buegger F, Weigl F, Pritsch K et al. 2022.** High resilience of carbon transport in long-term  
 128 drought stressed mature Norway spruce trees within two weeks after drought release. *Global*  
 129 *Change Biology*. doi: 10.1111/gcb.16051.

130 **Kuptz D, Fleischmann F, Matyssek R, Grams TEE. 2011.** Seasonal patterns of carbon  
 131 allocation to respiratory pools in 60-yr-old deciduous (*Fagus sylvatica*) and evergreen (*Picea*  
 132 *abies*) trees assessed via whole-tree stable carbon isotope labeling. *The New phytologist* **191**:  
 133 160–172.

134 **Schnyder H, Schäufele R, Lötscher M, Gebbing T. 2003.** Disentangling CO<sub>2</sub> fluxes: direct  
 135 measurements of mesocosm-scale natural abundance <sup>13</sup>CO<sub>2</sub> / <sup>12</sup>CO<sub>2</sub> gas exchange, <sup>13</sup>C  
 136 discrimination, and labelling of CO<sub>2</sub> exchange flux components in controlled environments.  
 137 *Plant, cell & environment* **26**: 1863–1874.

138



## Article III: Drought legacy effects on fine-root-associated fungal communities are modulated by root interactions between tree species

Danzberger, J., Werner, R., Mucha, R., Pritsch, K., Weigl, F.. (2023). *Frontiers in Forests and Global Change*.

### Open Access Publication

**Keywords:** drought recovery, European beech, fine roots, Norway spruce, root-associated fungi, tree mixture

**Citation:** Danzberger J, Werner R, Mucha J, Pritsch K and Weigl F (2023) Drought legacy effects on fine-root-associated fungal communities are modulated by root interactions between tree species. *Front. For. Glob. Change* 6:1197791. doi: 10.3389/ffgc.2023.1197791

**Received:** 31 March 2023; **Accepted:** 19 July 2023;

**Published:** 03 August 2023.

**Edited by:**

Camille Emilie Defrenne, Michigan Technological University, United States

**Reviewed by:**

Marco Cosme, University of Antwerp, Belgium

Jose G. Maciá-Vicente, Wageningen University and Research, Netherlands

**Copyright** © 2023 Danzberger, Werner, Mucha, Pritsch and Weigl. This is an open-access article distributed under the terms of the [Creative Commons Attribution License \(CC BY\)](#). The use, distribution or reproduction in other forums is permitted, provided the original author(s) and the copyright owner(s) are credited and that the original publication in this journal is cited, in accordance with accepted academic practice. No use, distribution or reproduction is permitted which does not comply with these terms.

\*Correspondence: Jasmin Danzberger, [jasmin.danzberge@freenet.de](mailto:jasmin.danzberge@freenet.de)

†ORCID: Jasmin Danzberger, [orcid.org/0000-0002-1683-7345](https://orcid.org/0000-0002-1683-7345); Ramona Werner, [orcid.org/0000-0003-0075-1720](https://orcid.org/0000-0003-0075-1720); Joanna Mucha, [orcid.org/0000-0002-1290-9639](https://orcid.org/0000-0002-1290-9639); Karin Pritsch, [orcid.org/0000-0001-6384-2473](https://orcid.org/0000-0001-6384-2473); Fabian Weigl, [orcid.org/0000-0003-3973-6341](https://orcid.org/0000-0003-3973-6341)

**Disclaimer:** All claims expressed in this article are solely those of the authors and do not necessarily represent those of their affiliated organizations, or those of the publisher, the editors and the reviewers. Any product that may be evaluated in this article or claim that may be made by its manufacturer is not guaranteed or endorsed by the publisher.



## OPEN ACCESS

## EDITED BY

Camille Emilie Defrenne,  
Michigan Technological University,  
United States

## REVIEWED BY

Marco Cosme,  
University of Antwerp, Belgium  
Jose G. Maciá-Vicente,  
Wageningen University and Research,  
Netherlands

## \*CORRESPONDENCE

Jasmin Danzberger  
✉ [jasmin.danzberge@freenet.de](mailto:jasmin.danzberge@freenet.de)

RECEIVED 31 March 2023

ACCEPTED 19 July 2023

PUBLISHED 03 August 2023

## CITATION

Danzberger J, Werner R, Mucha J, Pritsch K  
and Weigl F (2023) Drought legacy effects on  
fine-root-associated fungal communities are  
modulated by root interactions between tree  
species.

*Front. For. Glob. Change* 6:1197791.  
doi: 10.3389/ffgc.2023.1197791

## COPYRIGHT

© 2023 Danzberger, Werner, Mucha, Pritsch  
and Weigl. This is an open-access article  
distributed under the terms of the [Creative Commons Attribution License \(CC BY\)](https://creativecommons.org/licenses/by/4.0/). The  
use, distribution or reproduction in other  
forums is permitted, provided the original  
author(s) and the copyright owner(s) are  
credited and that the original publication in this  
journal is cited, in accordance with accepted  
academic practice. No use, distribution or  
reproduction is permitted which does not  
comply with these terms.

# Drought legacy effects on fine-root-associated fungal communities are modulated by root interactions between tree species

Jasmin Danzberger <sup>1,2\*</sup>, Ramona Werner <sup>2,3</sup>,  
Joanna Mucha <sup>4</sup>, Karin Pritsch <sup>2</sup> and Fabian Weigl <sup>1,2</sup>

<sup>1</sup>Ecophysiology of Plants, Professorship for Land Surface-Atmosphere Interactions, Research Department Life Science Systems, TUM School of Life Sciences, Technical University of Munich, Freising, Germany, <sup>2</sup>Helmholtz Zentrum München—German Research Center for Environmental Health (GmbH), Research Unit Environmental Simulation, Neuherberg, Germany, <sup>3</sup>Institute of Forest Ecology, Department of Forest and Soil Sciences, University of Natural Resources and Life Sciences (BOKU), Vienna, Austria, <sup>4</sup>Department of Forest Entomology and Pathology, Faculty of Forestry and Wood Technology, Poznań University of Life Sciences, Poznań, Poland

With climate change, the frequency of severe droughts is predicted to increase globally, resulting in increased forest dieback. Although fine-root systems and their associated fungi are considered crucial for tree nutrient exchange after a drought period and consequently for tree recovery, post-drought dynamics remain poorly understood. We rewatered mature European beech and Norway spruce after a 5-year experimental summer drought to shed light on belowground recovery processes. Therefore, we tracked the fine-root parameters growth, vitality, and mycorrhization in monospecific rooting zones with intraspecific root contact and mixed rooting zones with interspecific root contact of both tree species during the first 3 months of recovery, and we analyzed compositions of their root-associated fungal communities by DNA- and RNA-ITS2 sequencing. During recovery, the fine-root parameters differed between both tree species, with only minor effects of the tree rooting zone. Root-associated fungal communities showed no significant response to irrigation within 3 months after drought release. The rooting zone was the dominating factor affecting the root-associated fungal diversity, the abundance of trophic modes, and the response of individual saprotrophic and ectomycorrhizal (ECM) species. Furthermore, an analysis of the most abundant fungal species revealed that for ECM fungi, drought tolerance was common and for saprotrophs, a facultative, root-associated lifestyle. These results suggest that tree species-specific fungal communities are stable despite previous long-term drought and are closely associated with tree species-specific response patterns related to root survival and recovery. Moreover, an association between saprotrophic fungi and roots might be a strategy to support fungal drought survival.

## KEYWORDS

drought recovery, European beech, fine roots, Norway spruce, root-associated fungi, tree mixture

## Introduction

Climate change is predicted to increase the frequency and duration of severe droughts worldwide (IPCC, 2021), causing an alarming expansion of forest dieback (Allen et al., 2010, 2015; Anderegg et al., 2013).

Some tree species such as Norway spruce [*Picea abies* (L.) Karst.] and European beech (*Fagus sylvatica* L.) often grow better in mixed stands compared to monospecific stands (Pretzsch et al., 2015; Pretzsch, 2022). Therefore, mixing tree species has been suggested as a strategy of forest management to counteract the damages of climate change (Zhang et al., 2012; Forrester, 2015; Pretzsch et al., 2015). Thus, beech trees growing in mixture with conifers have been shown to exploit water of deeper soil layers and to have an improved water use in dry stands (Grossiord et al., 2014; González de Andrés et al., 2018). Reciprocally, spruce growth may profit from being mixed with beech, particularly at dry sites (Rukh et al., 2020) due to hydraulic redistribution (Hafner et al., 2017).

While studies are adding increasingly more details on the drought reactions of aboveground tree organs (e.g., McDowell et al., 2008; Brunner et al., 2015), the belowground system is much less studied, despite access to soil water being crucial for tree survival (Körner, 2019). It is well established that European beech and Norway spruce react differently to drought at the fine-root level (Nikolova et al., 2020). While beech continuously produces fine roots with low biomass, high metabolic activity, and short life span under drought (e.g., Reich, 2014; Nikolova et al., 2020; Zwetsloot and Bauerle, 2021), spruce preserves its long-living fine roots of larger diameter by increased suberisation (e.g., Gaul et al., 2008; Nikolova et al., 2020; Zwetsloot and Bauerle, 2021). The longevity of beech fine roots with interspecific contact with spruce fine roots was increased under drought compared to fine roots with only intraspecific contact, while the survival of spruce fine roots was not related to inter- or intraspecific root contact (Zwetsloot and Bauerle, 2021). However, the interaction of fine roots with mycorrhizal fungi forms the interface for water and nutrients between a tree and the surrounding soil (Lehto and Zwiazek, 2011), with pioneer roots exploring the soil and short roots being colonized primarily by symbiotrophic ectomycorrhizal (ECM) fungi (Kottke and Oberwinkler, 1986; Zadworny and Eissenstat, 2011). Therefore, it is necessary to look at both the root system and the root-associated fungi together to better understand how they interact under changing soil water availability.

Root-associated fungal communities comprise fungi of different trophic modes [saprotrophic, pathotrophic, and symbiotrophic (*sensu* Nguyen et al., 2016)] and fungi with unknown ecological role (e.g., Tedersoo and Smith, 2013; Nguyen et al., 2016; Unuk et al., 2019). Some saprotrophic species were reported to be able to colonize fine roots and even form mantle and Hartig net-like structures (Smith et al., 2017). As dark septate endophytes, they can accumulate high concentrations of melanin in their hyphae within the roots, which is considered a response to environmental pressure such as drought (Berthelot et al., 2019). Nowadays, they are considered as an important evolutionary step between free-living saprotrophs and mycorrhizal fungi (Ruotsalainen et al., 2022). Furthermore, ECM fungi were shown to play a crucial role in the evolutionary adaptation of land plants to drought and thus can promote both the gain and loss of plant

drought resistance to the same extent (Cosme, 2023). Tree mixture increases the local heterogeneity in the soil, thus creating a diverse habitat for fungi (Conn and Dighton, 2000; Aponte et al., 2010). ECM fungi can buffer drought effects on trees (Mohan et al., 2014; Bennett and Classen, 2020) by, e.g., improved water uptake (Maurel et al., 2015; Bennett and Classen, 2020) and improved nutrient status (Köhler et al., 2018). A strong link between plant drought response and ECM fungi has been found, resulting in considerable changes of the root fungal community composition through drought and watering (Veach et al., 2020). Moreover, mycorrhizal fungi can be less affected by drought than free-living soil fungi (Castaño et al., 2018). The ECM community composition shifted during drought in most cases (Shi et al., 2002; Swaty et al., 2004; Richard et al., 2011; Nickel et al., 2018). The drought tolerance of ECM fungi differs between species (Lehto and Zwiazek, 2011), with drought-sensitive species such as *Hygrophorus* sp. declining (Taniguchi et al., 2018) and tolerant species such as *Cenococcum geophilum* being highly abundant during desiccation (Quejeto et al., 2009; Peter et al., 2016; Gehring et al., 2020).

After drought release, both beech and spruce prioritize resource allocation to the recovery of the fine roots (Hagedorn et al., 2016; Hikino et al., 2022). A study on black cottonwood seedlings suggested that after drought release, roots of smaller diameter were produced that had a better water uptake capacity than old roots but a lower total surface area (Dhiman et al., 2018). Nevertheless, it remains unclear how individual fine-root parameters such as vitality, growth, and mycorrhization of individual tree species as well as the composition of root-associated fungal communities change after rewatering and how they are influenced by tree species mixture. Furthermore, field studies that control soil moisture are rare in mature stands but necessary to understand changes in root-associated fungal communities and their interplay with roots in terms of drought tolerance and ability to recover in a natural environment. Therefore, we asked if previous droughts would affect the response patterns of fine-root-associated fungal communities upon rewatering.

The Kranzberg roof experiment (KROOF) was initiated in Southern Germany to study the effects of experimental drought by excluded precipitation (throughfall exclusion) during the vegetation period from April to November for five consecutive years on mature beech and spruce trees. The trees were growing in plots each with areas of interspecific and intraspecific fine-root contact (rooting zone, RZ) [details in Grams et al. (2021)]. To better assess the trajectories of forests under future climates, it is necessary to understand to what extent the forest can recover. Therefore, the experimental drought phase ended with controlled watering in 2019. In this study on belowground recovery, we focused on the fungal community composition of regenerating fine roots of mature beech and spruce trees within 3 months after drought release. To do this, we used DNA and RNA metabarcoding to analyze the root-associated fungal communities and examined the vitality, growth, and mycorrhization of the fine roots.

Based on the different drought reactions of both tree species on the fine-root level and an increased beech fine-root longevity in mixture during drought, we anticipate that after drought release, both species follow different fine-root regeneration patterns, with beech reacting faster than spruce while profiting more from the tree mixture. The close interaction between fungi and trees leads us to hypothesize that the root-associated fungal communities change

differently in the RZ, with ECM fungi being more abundant and less affected on beech roots after watering due to a continuous fine-root production during drought and a higher heterogeneity in the mixture having a positive effect on fungal diversity [H1]. Furthermore, we hypothesize that changes in soil moisture favor the abundance of fungal species tolerating high variations in soil moisture and saprotrophic fungal species with optional root-associated lifestyle [H2].

## Materials and methods

### Sampling site and experimental design

The KROOF experimental site is a 0.5 ha mature European beech and Norway spruce stand (c. 90 and 70 years old) located in Kranzberg Forest in Southern Germany (11° 39' 42" E, 48° 25' 12" N, 490 m a.s.l.) (Pretzsch et al., 2014; Goisser et al., 2016). From May to September, the mean rainfall in the 1971–2000 period was 460–500 mm, and the mean air temperature was 13.8°C (Pretzsch et al., 2020). The soil is a nutrient-rich Luvisol from Tertiary sediments and has good water supply (Pretzsch et al., 1998). In 2010, 12 experimental plots of 110–200 m<sup>2</sup> were trenched to a depth of 1 m to inhibit water transport from outside the plots, while a clay layer at approximately 1 m depth limited vertical water transport (Grams et al., 2021). Each plot depicts three RZs: beech neighboring beech (BB), spruce neighboring spruce (SS)—both with mainly intraspecific fine-root contact—and beech neighboring spruce (MIX) with interspecific fine-root contact (Figure 1A; Goisser et al., 2016; Nickel et al., 2018). Retractable roofs were installed on six throughfall exclusion (TE) plots in 2013, and the drought experiment started in 2014. Rain was excluded over five whole vegetation periods (March to November) from 2014 to 2018. In 2015, two TE plots and their corresponding control (CO) plots were excluded due to bark beetle infestation in order to keep a balanced experimental design of 4 CO and 4 TE plots (Figure 1A). In 2019, the drought was released by rewetting of the TE plots using controlled drop irrigation within 40 h (total water supply of 12,849 ± 2,802 l) to reach a similar soil water content to their corresponding CO plots, as described in detail by Grams et al. (2021). After watering, the soil water contents were 14 ± 1% in CO and 15 ± 2% in TE (9 ± 1% before watering). The watering took place in three campaigns over 3 weeks to allow for sampling, measurements, and sample preparation. Therefore, plots 7 and 8 were watered on 25th of June 2019, plots 3, 4, 11, and 12 on 4th of July 2019, and plots 5 and 6 on 10th of July 2019. To reduce the watering effects between the treatments regarding soil temperature or nutrient availability, a low amount of water was added to the CO plots in parallel (average 2,035 ± 537 l). From day 15 after watering, the roofs of the TE plots were kept open.

### Temperature, precipitation, and soil moisture

Temperature at 2 m height and precipitation (Figure 1B) were continuously measured every 10 min by a climate station on site, including the experimental period from June

to October 2019. Volumetric soil water contents at different depths (0–7 cm, 10–30 cm, 30–50 cm, and 50–70 cm) were assessed by time-domain reflectometers (TDR 100, Campbell Scientific Inc., Logan, Utah, USA) (Figure 1C). Within each treatment, the soil water contents did not significantly differ between the CO or TE plots of the different watering campaigns at each sampling day, thus justifying a combination of the data from the staggered watering campaigns (Supplementary Figure 1).

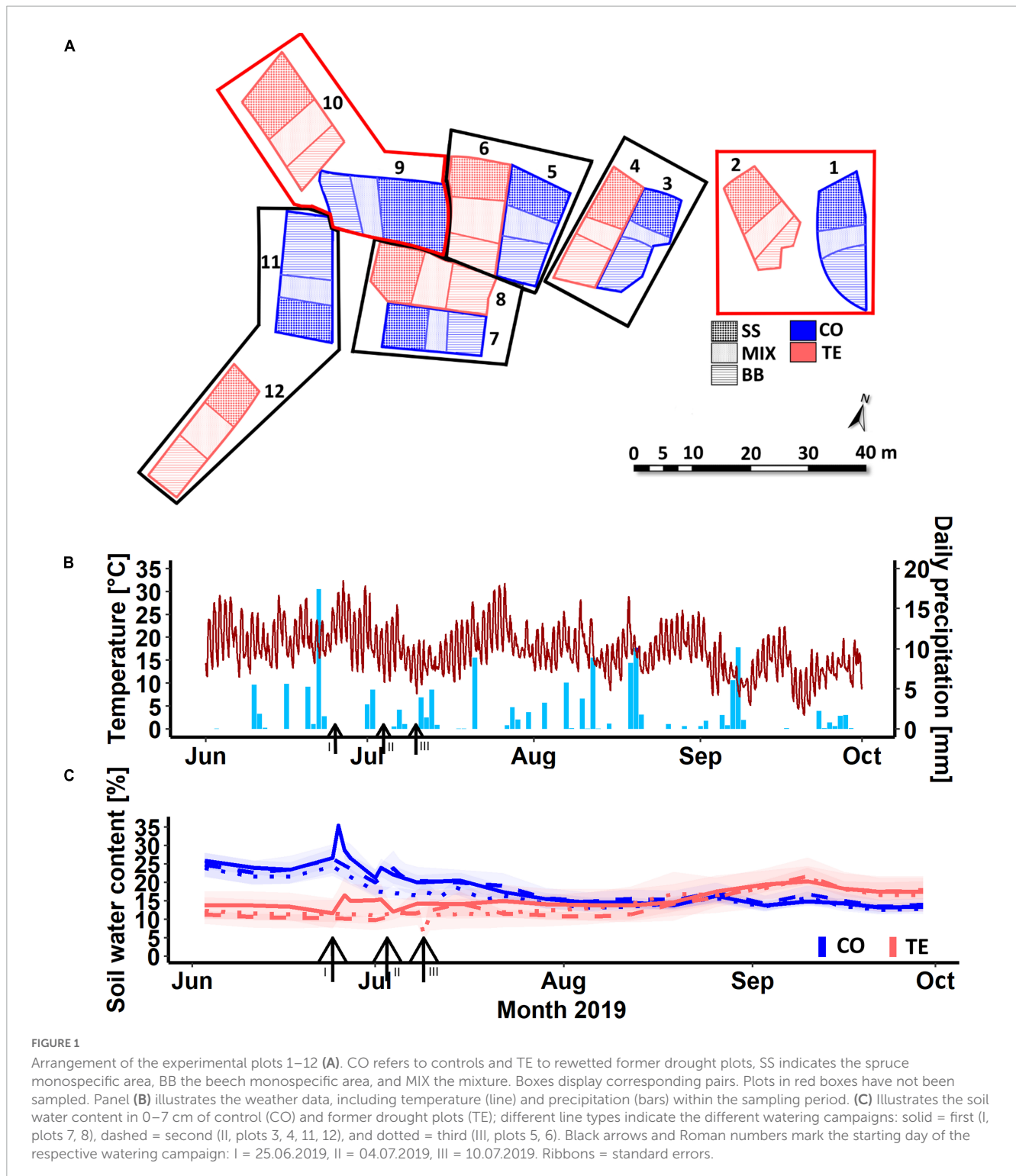
### Fine-root sampling

Soil samples were taken on days (d) –7, 6, 18, 41, and 84 with regard to the respective irrigation event on each of the eight plots from each RZ (Figure 2). During sampling, ten drill cores (diameter 1.4 cm each, 25 cm depth) were taken, which corresponded to a surface area of 15.4 cm<sup>2</sup>, and the dark-colored organic topsoil layer (2–12 cm, average 9.4 cm) of the ten soil cores was pooled, resulting in 120 samples for further processing (8 plots × 3 RZ × 5 sampling dates). Fine roots (diameter < 2 mm) were separated from the soil on site on the sampling day by careful manual sorting with sterile forceps, put on dry ice, and frozen at –80°C until nucleic acid extractions and biomass analysis.

In April 2019, individual, tree-connected fine roots from depths of 0–5 cm (CO) and 0–10 cm (TE) were photographed, put into 1/3 soil-filled mesh bags (mesh width 80 µm, open area 29%), moisturized to improve root–soil contact, and covered with soil. Roots growing in MIX were classified as beech in mixture (Bmix) and spruce in mixture (Smix). A total of 608 mesh bags (2 tree species × 2 RZ per species × 4 replicates × 38 samplings; Supplementary Table 1) were thus prepared. Mesh bag roots were harvested and photographed on graph paper 7 days before and 10, 17, 28, 35, 42, and 89 days after watering (Figure 2).

### Root vitality

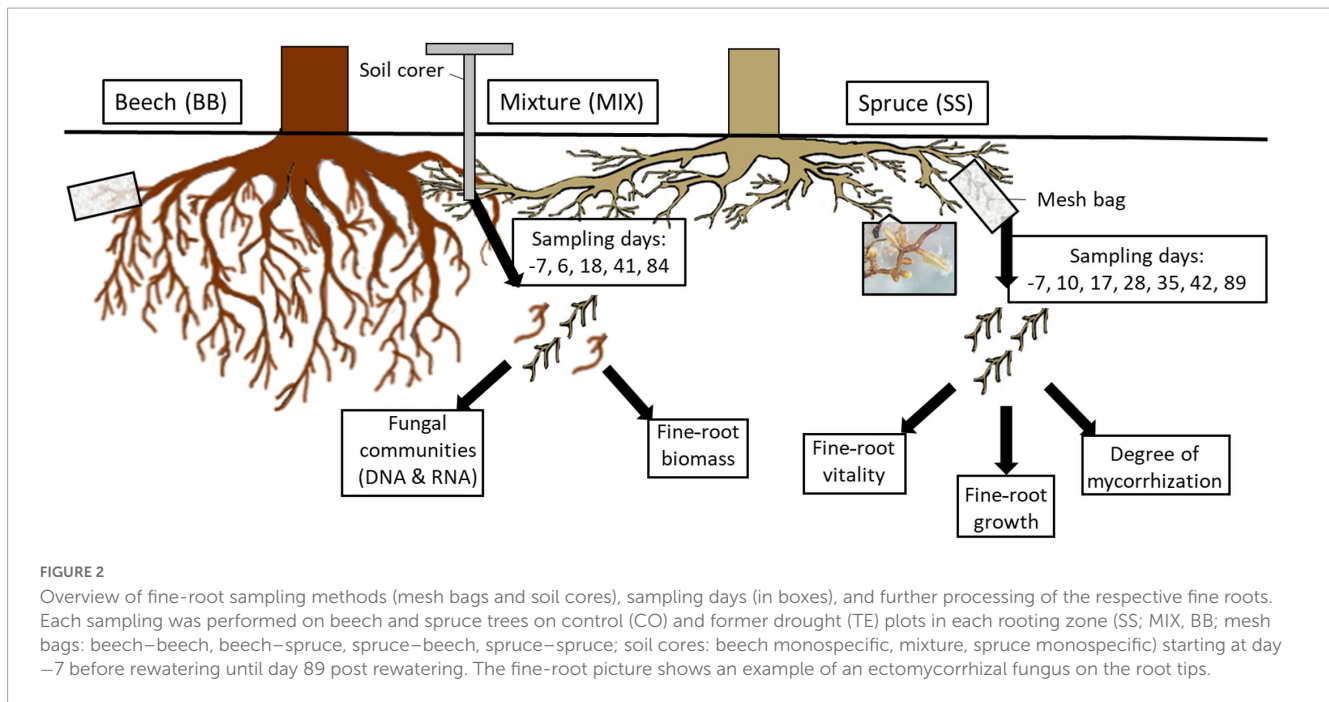
For vitality assays, the method of Qian et al. (1998) was used. In brief, a 10% (w/v) stock solution of fluorescein diacetate (FDA) in acetone was 1:10 diluted with Sørensen phosphate buffer KH<sub>2</sub>PO<sub>4</sub>/Na<sub>2</sub>HPO<sub>4</sub> pH 7.5 and used for staining fine-root sections. From each mesh bag, ten representative fine-root tips were cut longitudinally into three slices with a razor blade, whereby the middle slice was stained in FDA–phosphate buffer solution for 15 min in the dark, washed twice in phosphate buffer, and analyzed by fluorescent microscopy (Axioplan, Zeiss, Oberkochen, Germany). The fluorescence intensity of meristem, Hartig net (if mycorrhized) or root cortex, central cylinder, and hyphal mantle (if mycorrhized) was evaluated by eye and categorized in numbers from 0 (no fluorescence/dead) to 3 (bright green/very vital). Missing parts were excluded from the calculation. The vitality score per root tip is described by the mean of the root compartment's vitality scores, and the vitality of one fine-root sample is reflected by the mean of their 10 accompanying tips' vitality scores.



## Root growth and degree of mycorrhization

Root growth was calculated by measuring the total root length based on the root pictures taken on graph paper before enclosure into mesh bags and at harvest using ImageJ (version 1.53a, National Institute of Health, USA) by subtracting the initial length from the length at harvest. To exclude growth between the mesh bag

placement and first sampling day, the average growth at day  $-7$  (per RZ and treatment) was subtracted from the growth values of all the other days. Growth at day  $-7$  thus corresponded to 0. The degree of mycorrhization per root (given in % of ECM and non-ECM root tips relative to the total number of root tips) was determined by visual inspection of the root pictures and assignments based on growth form, tip shape, color, and presence of a hyphal mantle and external hyphae.



## Fine-root biomass

Fine-root dry weights were calculated from the fresh weight of each mixed fine-root sample from soil cores using a subsample of 30 mg fine-cut root material dried for 24 h at 75°C. The dry root mass per soil volume was then calculated, accounting for the soil volume of the respective cores from which the samples were taken.

## DNA/RNA extraction and high-throughput sequencing

The analysis of rapidly degrading fungal RNA allows to trace sudden changes in the community composition of metabolically active fungi, while DNA analysis can include residual DNA of dead fungi. To validate if the DNA-based data captures the dynamics of root-associated fungal communities in a changing environment correctly, we analyzed RNA-based data in parallel.

Frozen roots were ground in liquid nitrogen with sterile instruments and treated with RNase AWAY (Sigma-Aldrich, St. Louis, MO, USA). In all, 100–250 mg of root powder from each root was collected in 2 ml screw cap vials for DNA and RNA analysis. DNA of 120 root samples (and 5 negative extraction controls without root powder) was extracted using the DNeasy Power soil Kit (Qiagen, Hilden, Germany) with modifications, as described in Nickel et al. (2018). Due to the limited sample material, only 87 samples and 3 negative controls were processed for RNA extraction using the ZymoBIOMICS DNA/RNA Miniprep Kit (Zymo Research, Irvine, CA, USA) following the manufacturer's protocol. RNA was transcribed to cDNA by applying the High-Capacity cDNA Reverse Transcription Kit (Applied Biosystems, Waltham, MA, USA). DNA and cDNA were treated equally during the library preparation. For high-throughput sequencing, the fungal ITS2 rDNA was amplified by PCR using primer mixes,

as described in Tedersoo et al. (2015), which held overhangs with Illumina adapter sequences (Supplementary Table 2) for Miseq sequencing (protocol Part # 15044223; Illumina, San Diego, CA, USA). The reaction mix per sample included 10 µl NEBNext High-Fidelity 2X PCR MasterMix (New England Biolabs, Frankfurt, Germany), 0.5 µl 10 pmol ITS3 tagmix forward primer (equally mixed ITS3-Mix1 – 5), 0.5 µl 10 pmol ITS4 tagmix reverse primer (equally mixed ITS4-Mix 1–4), 8 µl ultra-pure H<sub>2</sub>O, and 1 µl (c)DNA (5 ng DNA, 10 ng cDNA). The PCR conditions were 5 min at 95°C, 28 cycles (30 s 95°C, 30 s 55°C, 60 s 72°C), and 10 min at 72°C. PCRs were performed in triplicates, which were pooled after quality verification on a 2% agarose gel. The samples were cleaned with the Agencourt AMPure XP DNA purification kit (Beckman Coulter, Krefeld, Germany) using a bead:sample ratio of 1:1. Success was tested on agarose gels. (c)DNA concentration was determined using AccuClear Ultra High Sensitivity dsDNA Quantification (Biotium, Fremont, CA, USA). Individual combinations of Illumina indexing primers (Nextera XT Index Kit v2 Sets A–D) were attached to each sample by indexing the PCR containing 1 µl (c)DNA (5 ng), 2.5 µl Nextera i7 primer, 2.5 µl Nextera i5 primer, 12.5 µl NEBNext High-Fidelity 2X PCR MasterMix, and 6.5 µl ultra-pure H<sub>2</sub>O. Conditions were 3 min at 95°C, 8 cycles (30 s 95°C, 30 s 55°C, 30 s 72°C), and 10 min at 72°C. Indexing products were purified and size- and quantity-checked as before, and additionally, a Fragment Analyzer (Advanced Analytical, Heidelberg, Germany) (protocol DNF-473 Standard Sensitivity NGS-Fragment Analysis Kit 1–6,000 bp) was used with randomly picked sample pairs before and after indexing. Diluted amplicons (10 nM) were pooled, quantity checked using Qubit 3 (Invitrogen, Carlsbad, CA, USA), and diluted to 4 nM. The final library preparation was handled following the Illumina protocol for the 16S Metagenomic Sequencing Library Preparation (protocol Part # 15044223 Rev. B) and sequenced on Miseq v3chemistry, 600 cycles flow cell (Illumina, San Diego, CA, USA).

## Bioinformatics

Output FASTQ files from the Illumina Miseq system were prepared for analysis using the fungal analysis pipeline PIPITS v2.7 (Gweon et al., 2015). Briefly, in the first step, read pairs were joined and sequences filtered by quality corresponding to the pipeline's default settings. In the second step, the fungal ITS2 was extracted with ITSx (Bengtsson-Palme et al., 2013). In the last step, small sequences (<100 bp) were erased, remaining sequences assigned to operational taxonomic units (OTUs) with a sequence identity of 97 % using VSEARCH (Rognes et al., 2016), and chimeras removed using the UNITE v8.2 (Abarenkov et al., 2020) UCHIME database. The taxonomic classification was achieved with RDP Classifier (Wang et al., 2007), comparing the sequences against the UNITE fungal ITS database (Kõljalg et al., 2013). The database FungalTraits (Pöhlme et al., 2020) was used to assign the functional traits "fungal trophic mode," ECM "exploration types" (Agerer, 2001), and saprotrophic "primary" and "secondary" lifestyle to the fungi by combining the taxonomic output file with correlating information on the genus level.

## Statistical analysis

Data were analyzed using R (version 4.0.2, R Core Team, 2021) and RStudio (version 1.4.1717, RStudio Inc.), with significances being defined as  $p < 0.05$ . Sequencing data were rarefied with 1,000 repetitions using the "rarefy" function in GNuniFrac (Chen et al., 2012) to a depth of 10,000 sequences per sample. Taxa that occurred less than 10 times in the whole experiment were removed. To investigate the dissimilarity of the individual samples, the Bray–Curtis dissimilarity was calculated ("vegdist" function in R package *vegan*). The Shannon–Wiener Diversity Index ("Shannon Index") and Simpson's Index of Diversity ("Simpson Index") were determined using the function "diversity" in *vegan* (version 2.5-7; Oksanen et al., 2019) and species richness by using the function "specnumber" in the same package. Evenness was then assessed with the Shannon Index/log (species count). To analyze both the diversity parameters described above and the fine-root parameters "vitality," "growth," and "mycorrhization," normal distribution was tested by the Shapiro–Wilk test ("shapiro.test" in package *stats*). Subsequently, normally distributed data were examined using an analysis of variance (ANOVA) ("aov" in package *stats*) and non-normally distributed data using a Kruskal–Wallis test ("kruskal.test" in package *stats*). Significant differences between levels of one factor were assessed using appropriate *post-hoc* tests with Bonferroni  $p$ -value correction. In the case of an ANOVA, a Tukey's honest significance test ("TukeyHSD" in package *stats*) was subsequently used, and in the case of a Kruskal–Wallis test, a Dunn's test for multiple comparisons ("dunn.test" in package *dunn.test*). After dispersion heterogeneity was tested using the function "betadisper" in *vegan*, community data were analyzed comparatively with a permutational multivariate analysis of variance (PERMANOVA) ("adonis2" in *vegan*) to determine the effects of treatment, RZ, and time after watering, with nested plot location and time being a random effect after testing its significance as a factor. All models were run with 9,999 permutations. Significant differences between individual

levels of a factor were tested by multilevel pairwise comparisons of permutational multivariate analysis of variance (pairwise PERMANOVA) (*pairwise.adonis*; Martínez Arbizu, 2020) with Bonferroni  $p$ -value correction. The fungal community composition was represented by non-metric multi-dimensional scaling (NMDS) with Bray–Curtis dissimilarity using the "ordinate" function in *phyloseq*. Correlations between fine-root parameters and between ECM fungal community composition, represented by NMDS axis 1 (NMDS1), and fine-root growth, as well as vitality, were determined by Pearson correlation using the function "cor.test" (*stats*). Relative abundances of fungal trophic modes and exploration types were assessed using the *phyloseq* (version 1.36.0; McMurdie and Holmes, 2013) functions "prune\_taxa" for trimming and "transform\_sample\_counts" for sample-by-sample abundance data transformation. Graphs were created using *ggplot2* (Wickham, 2016). Relative proportions of fungal trophic modes on TE compared to CO (averaged "by day relative to watering"), as portrayed in Figure 5B, were created in *phyloseq*. The respective standard errors of the difference between the means ( $\sigma_{M_1-M_2}$ ) were calculated according to Foster et al. (2018):

$$\sigma_{M_1-M_2} = \sqrt{\frac{\sigma_1^2}{n_1} + \frac{\sigma_2^2}{n_2}}$$

where  $\sigma_1^2$  and  $\sigma_2^2$  describe the variances of the CO and TE samples and  $n_1$  and  $n_2$  the respective number of replicates.

## Results

### Recovery of the fine-root system

Fine-root vitality was significantly lower in TE than CO before watering in all RZs except for Bmix (Figure 3A). Neither beech nor spruce generally showed significant differences in time course or treatment between RZs. However, the dynamics in fine-root vitality after watering were species specific. Root vitality in BB and Bmix TE increased from low levels (0–0.2) until d 42 (0.6) to reach CO levels but, in contrast to CO, declined to zero on d 89. For spruce, fine-root vitality in TE increased after rewatering and resembled controls already on d 17 with a faster increase when growing in mixture (Smix).

Similarly, fine-root growth after rewatering followed different dynamics in the two tree species (Figure 3B). In beech, growth did not significantly differ between the CO and TE or RZ and remained around zero except in BB CO on d 35 and d 42. Growth of spruce roots was more dynamic, with significant differences between SS and Smix [CO:  $p = 0.02$ ,  $z = (-2.08)$ ; TE:  $p = 0.03$ ,  $z = (-1.82)$ ; Dunn-Test], and responded faster to watering in SS than in Smix. Growth in Smix CO was significantly higher than in TE on d 35 and d 89, while it did not significantly differ between treatments in SS.

The degree of mycorrhization (Figure 3C) was slightly below 25% in all TEs and RZs and significantly lower compared to CO until day 35. In beech, the degree of mycorrhization increased (earlier in BB than in Bmix), while it decreased in spruce RZ until d 17 and then reached the CO level from d 42.

The fine-root biomass was highly variable (Supplementary Figure 2), and thus the roughly two-fold increase of dry mass in all TEs and RZs between d -7 and d 7 was not significant.

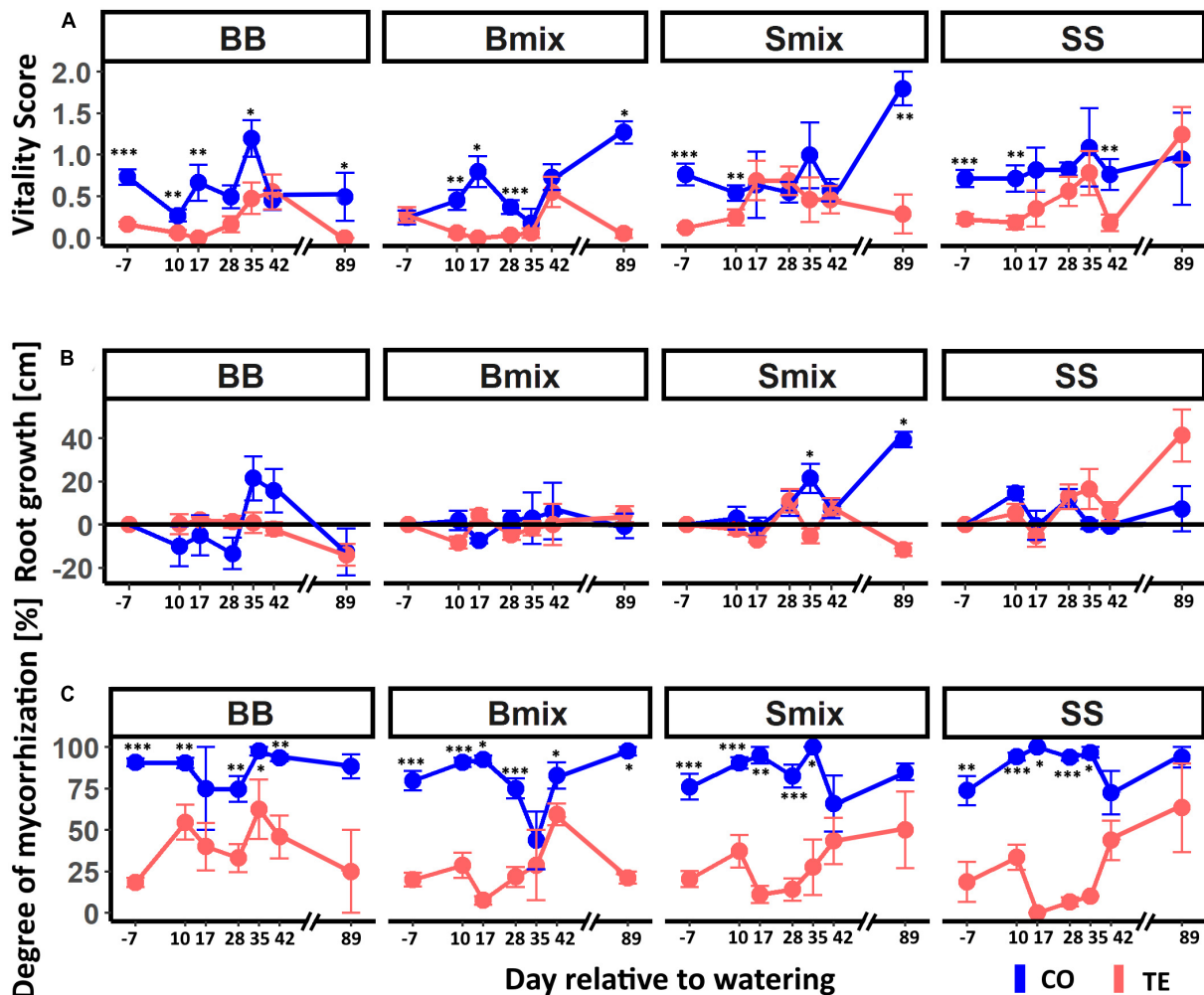


**FIGURE 3**  
 Vitality, growth, and mycorrhization of beech and spruce fine roots in different rooting zones after drought release. CO lines represent control roots and TE lines roots in recovering plots. (A) displays the dynamics in average fine-root vitality on a score from 0 (dead) to 3 (maximal vitality). Panel (B) shows the average root growth (cm) after watering in which the black horizontal line indicates equality between growth (positive) and degradation (negative). Panel (C) illustrates the average mycorrhization of the roots. All mean values are given with standard error. Asterisks indicate significances between the treatments with \* $p < 0.05$ , \*\* $p < 0.01$ , and \*\*\* $p < 0.001$ .

Fine-root vitality positively correlated with fine-root growth for both treatments and both tree species (Supplementary Table 3). Fine-root growth and degree of mycorrhization correlated in CO but not TE for both tree species, while vitality and degree of mycorrhization correlated in CO for both species and in TE only for beech.

Taken together, these results indicate differences in the recovery of the fine-root system between beech and spruce, with no clear effect of species mixture.

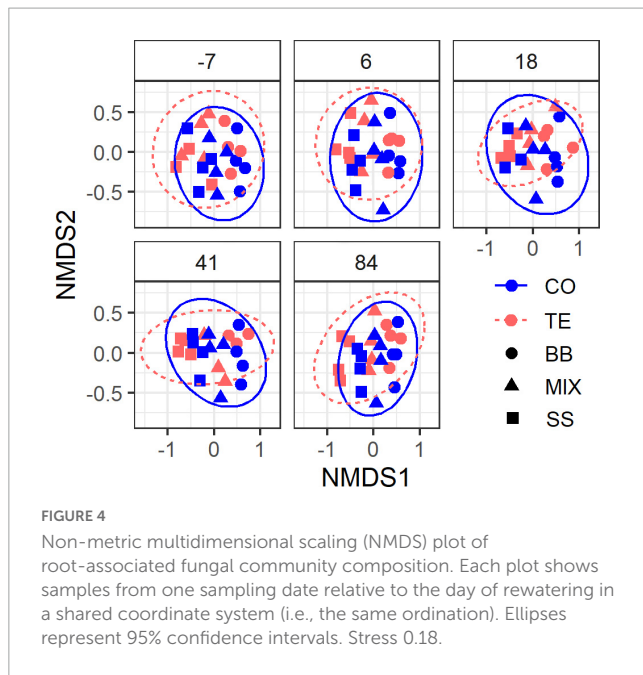
### Dynamics of root-associated fungal communities

Sequencing of 120 rDNA samples resulted in 3,028,498 quality-filtered ITS2 sequences, which could be assigned to 2,233 OTUs and 989 taxa, whereby the 100 most abundant OTUs represented 86% of all sequences. Four samples were excluded from analysis

due to their low sequencing depth (<10,000). For the 87 rRNA samples, we obtained 1,443,868 quality-filtered ITS2 sequences assigned to 2,303 OTUs and 1,002 taxa, whereby the top 100 OTUs made up 80% of all sequences. After excluding ten samples of low sequencing depth (<8,000), 77 samples remained for further analysis. Community compositions did not significantly change within 84 days after the watering event (Figure 4) (DNA:  $p = 0.87$ ,  $R^2 < 0.01$ ; RNA:  $p = 0.82$ ,  $R^2 = 0.01$ ; PERMANOVA). Significant differences in community composition were found between treatments (DNA:  $p < 0.001$ ,  $R^2 = 0.04$ ; RNA:  $p < 0.001$ ,  $R^2 = 0.03$ ; PERMANOVA), plots (DNA:  $p < 0.001$ ,  $R^2 = 0.19$ ; RNA:  $p < 0.001$ ,  $R^2 = 0.23$ ; PERMANOVA), and RZ (DNA:  $p < 0.001$ ,  $R^2 = 0.21$ ; RNA:  $p < 0.001$ ,  $R^2 = 0.13$ ; PERMANOVA).

The factor RZ had a highly significant effect on all alpha diversity metrics of root-associated fungi (Table 1). The factor treatment had significant effects on Shannon diversity and OTU richness. The factor time after watering did not significantly affect any diversity metric. Shannon diversity was generally higher in CO





than in TE without differences in evenness. Shannon diversity and evenness were higher in SS than in BB. OTU richness was highest in the mixture (Table 1). Fungal diversity (Shannon, Simpson) and evenness significantly differed between all three RZs, and OTU richness differed significantly between the beech monospecific and mixture zone (Supplementary Table 4).

Overall, there was no significant correlation between the growth and fine-root vitality or community composition of all the root-associated fungi or ECM fungi (Supplementary Table 5).

In summary, the fungal community composition did not significantly change after rewatering, and RZ formed fungal diversity the most.

## Dynamics of functional traits of root-associated fungi

In all,  $53 \pm 0.9\%$  (Supplementary Figures 3, 4) of the fungi were of unknown trophic mode irrespective of treatment and RZ and were excluded from further analysis on trophic modes. The fungal community composition according to trophic modes differed significantly between the treatments (Symbiotrophs:  $p < 0.001$ ,  $R^2 = 0.05$ , Saprotrophs:  $p < 0.001$ ,  $R^2 = 0.04$ , Pathotrophs:  $p < 0.001$ ,  $R^2 = 0.02$ ; PERMANOVA) and tree RZ for both treatments (Table 2). The factor day after watering only had a significant effect in TE on pathotrophic fungi, which accounted only for c. 1% of the fungal community (Supplementary Figure 3).

Within the tree RZ, relative abundances (Figure 5A) of symbiotrophic fungi were highest in BB with  $77 \pm 2.0\%$  in CO and  $72 \pm 5.2\%$  in TE, compared to SS with  $48 \pm 3.7\%$  and  $30 \pm 1.6\%$ , respectively (Figure 5A; Table 2). Accordingly, saprotrophs showed the opposite share, with lower abundances in BB and higher abundances in SS, while MIX was in between (Figure 5A; Table 2).

Temporal dynamics after rewatering showed a trend of decreasing saprotrophs in BB TE and increasing in SS CO, with

MIX RZ again in between BB and SS, with a tendency to decrease in TE after watering to CO levels (Figure 5B). A similar pattern was observed in the RNA-based data (Supplementary Figure 5).

The OTU richness of saprotrophic fungi ( $57.1 \pm 1.2$ ) did not significantly differ between treatments and RZ. OTU richness of ECM fungi differed significantly between the treatments ( $p < 0.001$ ,  $F = 31.7$ ; ANOVA) and RZ ( $p < 0.001$ ,  $F = 15.1$ ; ANOVA), with SS being different from the other RZs (SS–BB:  $p_{adj} = 0.002$ ; SS–MIX:  $p_{adj} < 0.001$ ; Tukey HSD). Thus, fewer ECM OTUs were found in TE than in CO in all RZs. The highest number of OTUs appeared in MIX (average richness CO:  $27.6 \pm 1.4$ , TE:  $23.2 \pm 1.0$ ), followed by BB (average richness CO:  $25.2 \pm 1.0$ , TE:  $20.8 \pm 0.7$ ) and SS (average richness CO:  $22.2 \pm 1.0$ , TE:  $15.5 \pm 0.8$ ).

The ten most abundant saprotrophic OTUs in BB were classified as litter saprotrophs and six with a facultative root-associated or root-endophytic lifestyle, while in SS, most saprotrophs were soil saprotrophs with facultative root-endophytic abilities (Table 3; Supplementary Table 6). Among the top 10 most abundant OTUs of saprotrophic fungi (Table 3; Supplementary Table 6), *Oidiiodendron* sp. was overall highly abundant. *Phialocephala* sp. was also present in all RZs and treatments, mostly reaching between 13 and 20% of the respective top 10 OTUs. In SS TE, *Acephala appianata* was the second most identified saprotrophic species.

Regarding pathotrophic fungi, *Trichoderma* sp. was by far the most abundant species in all RZs and treatments, accounting for, on average,  $68\% \pm 4\%$  of the top ten OTUs, mostly followed by *Ilyonectria* sp. (Table 4; Supplementary Table 7).

The top 10 ECM fungi (Table 5; Supplementary Table 8) varied more than saprotrophs between the RZs. While *Lactarius subdulcis* and *Russula fellea* were the most abundant species in both treatments of BB, they did not appear in SS, which was dominated by *Elaphomyces granulatus* and *Russula* sp. in both treatments. MIX contained species of BB and SS, but MIX TE was dominated by *Russula* sp. and *Lactarius subdulcis* (48%) within the top 10, whereas *Lactarius* sp., *Piloderma* sp. and *Tomentella botryoides* dominated MIX CO (21%, 12%, 11%).

Regarding ECM exploration types (Table 5; Supplementary Table 8; Supplementary Figure 6A), BB CO was dominated by medium-distance types at all time points (averaged over all sampling times:  $56.6 \pm 2.7\%$ ), while in TE, the abundance of both contact and medium-distance types was around 43% at all time points. In SS roots, differences between CO and TE were more distinct. While in CO the abundances of short-distance, medium-distance, and contact types were evenly distributed with minor changes over time, contact types were the most dominant exploration type in TE before and shortly after watering ( $53 \pm 0.6\%$ ) but tended to decrease after drought release ( $24 \pm 0.9\%$ ) in favor of short- and long-distance types, with the latter even exceeding CO levels at later sampling dates (Supplementary Figure 6A). In mixture, contact types were most abundant in TE at all time points ( $60 \pm 4.2\%$ ), while it was medium-distance types in CO. The abundance patterns of BB CO in RNA strongly resembled DNA communities, with medium-distance types being dominant in CO at all time points ( $\geq 50\%$ ), while contact types were more abundant ( $51 \pm 3\%$ ) in TE (Supplementary Figure 6B).

In summary, the abundance of fungal species with different fungal traits differed between the RZs, with drought-tolerating

**TABLE 1** Root-associated fungal alpha-diversity based on rDNA displayed by Shannon Index, Simpson Index, Pielou’s Evenness, and Species richness summarized by treatment (treat; CO = controls, TE = drought recovering) and tree rooting zones (RZ; BB = beech monospecific, SS = spruce monospecific, MIX = mixture).

Treat	RZ	Shannon Index		Simpson Index		Pielou’s Evenness		Species richness	
CO	BB	3.12 ± 0.12		0.90 ± 0.01		0.58 ± 0.02		205.95 ± 7.75	
CO	MIX	3.44 ± 0.06		0.93 ± 0.01		0.63 ± 0.01		234.85 ± 8.33	
CO	SS	3.57 ± 0.08		0.95 ± 0.01		0.67 ± 0.01		216.95 ± 10.12	
TE	BB	3.02 ± 0.06		0.89 ± 0.01		0.57 ± 0.01		195.89 ± 9.23	
TE	MIX	3.32 ± 0.08		0.93 ± 0.01		0.62 ± 0.01		209.47 ± 8.95	
TE	SS	3.43 ± 0.06		0.94 ± 0.00		0.65 ± 0.01		190.05 ± 5.31	
		Shannon Index <sup>+</sup>		Simpson Index <sup>+</sup>		Pielou’s Evenness <sup>+</sup>		Species richness <sup>*</sup>	
	df	χ <sup>2</sup>	p	χ <sup>2</sup>	p	χ <sup>2</sup>	p	F	p
Treat	1	<b>4.58</b>	<b>0.03</b>	3.18	0.07	2.22	0.13	<b>8.71</b>	<b>&lt;0.01</b>
RZ	2	<b>25.57</b>	<b>&lt;0.001</b>	<b>32.39</b>	<b>&lt;0.001</b>	<b>35.93</b>	<b>&lt;0.001</b>	<b>3.65</b>	<b>0.03</b>
DR	4	0.26	0.99	0.10	0.99	0.07	0.99	0.34	0.56

Values are displayed as means ± standard error. The influence of treat, RZ, and day after watering (DR) on fungal diversity was tested using either Kruskal–Wallis test (+) or ANOVA (\*). Bold numbers indicate significances and df degrees of freedom.

**TABLE 2** The effect of rooting zone (RZ) and day after watering (DR) on root-associated fungal community composition based on rDNA sequences.

CO:	df	Saprotrophs		Symbiotrophs		Pathotrophs	
		R <sup>2</sup>	p	R <sup>2</sup>	p	R <sup>2</sup>	p
Rooting zone (RZ) +	2	<b>0.20</b>	<b>&lt;0.001</b>	<b>0.21</b>	<b>&lt;0.001</b>	<b>0.11</b>	<b>&lt;0.001</b>
Day after watering (DR) +	4	<0.01	0.96	<0.01	1.00	0.02	0.90
RZ × DR +	8	0.02	0.98	0.01	1.00	0.02	0.83
SS vs. MIX*	1	<b>0.09</b>	<b>0.001</b>	<b>0.10</b>	<b>&lt;0.001</b>	<b>0.06</b>	<b>0.02</b>
SS vs. BB*	1	<b>0.23</b>	<b>&lt;0.001</b>	<b>0.25</b>	<b>&lt;0.001</b>	<b>0.12</b>	<b>&lt;0.001</b>
MIX vs. BB*	1	<b>0.14</b>	<b>&lt;0.001</b>	<b>0.14</b>	<b>&lt;0.001</b>	<b>0.07</b>	<b>0.001</b>
TE:							
Rooting zone (RZ) +	2	<b>0.18</b>	<b>&lt;0.001</b>	<b>0.22</b>	<b>&lt;0.001</b>	<b>0.08</b>	<b>&lt;0.001</b>
Day after watering (DR) +	4	0.02	0.21	0.01	0.46	<b>0.03</b>	<b>0.02</b>
RZ × DR +	8	0.03	0.37	0.02	0.90	0.04	0.15
SS vs. MIX *	1	<b>0.06</b>	<b>0.03</b>	<b>0.13</b>	<b>&lt;0.001</b>	0.03	0.49
SS vs. BB*	1	<b>0.21</b>	<b>&lt;0.001</b>	<b>0.26</b>	<b>&lt;0.001</b>	<b>0.08</b>	<b>&lt;0.005</b>
MIX vs. BB*	1	<b>0.13</b>	<b>&lt;0.001</b>	<b>0.10</b>	<b>0.001</b>	<b>0.07</b>	<b>0.005</b>

PERMANOVA (+, 9999 permutations) with the factors RZ and DR was applied to saprotrophic, symbiotrophic, and pathotrophic fungal communities separated by treatment. Significant differences within the respective communities between the RZs were determined by paired PERMANOVA (\*; 9999 permutations, Bonferroni adjustment). BB = beech–beech, MIX = beech–spruce, SS = spruce–spruce. Bold numbers indicate significances, and df indicates degrees of freedom.

ECM fungal species of contact and medium-distance exploration types being more abundant in BB and saprotrophic fungi. with an additional root-associated lifestyle being more abundant in SS.

## Discussion

### Drought and recovery reactions of the fine-root system are tree species specific

Spruce fine roots formed before drought release (represented by mesh bag roots) showed positive growth and an increasing vitality after rewatering, which indicates a

reactivation of dormant fine roots. Beech fine roots enclosed in mesh bags, however, did not grow after rewatering, and their vitality was almost without exceptions below the controls. Nevertheless, a consistent mixture effect could not be determined.

Fine-root biomass in the RZ did not significantly differ between the treatments in both species shortly before watering, similar to complementary results on fine-root surface area on the same experimental site (Brunn et al., 2022). Already within the first week after watering, fine-root biomass in all three tree RZs of both treatments increased, which could indicate a fast response of the fine-root growth of both species and corresponds to findings that trees may respond even to very small changes in soil water content (Joseph et al., 2020).

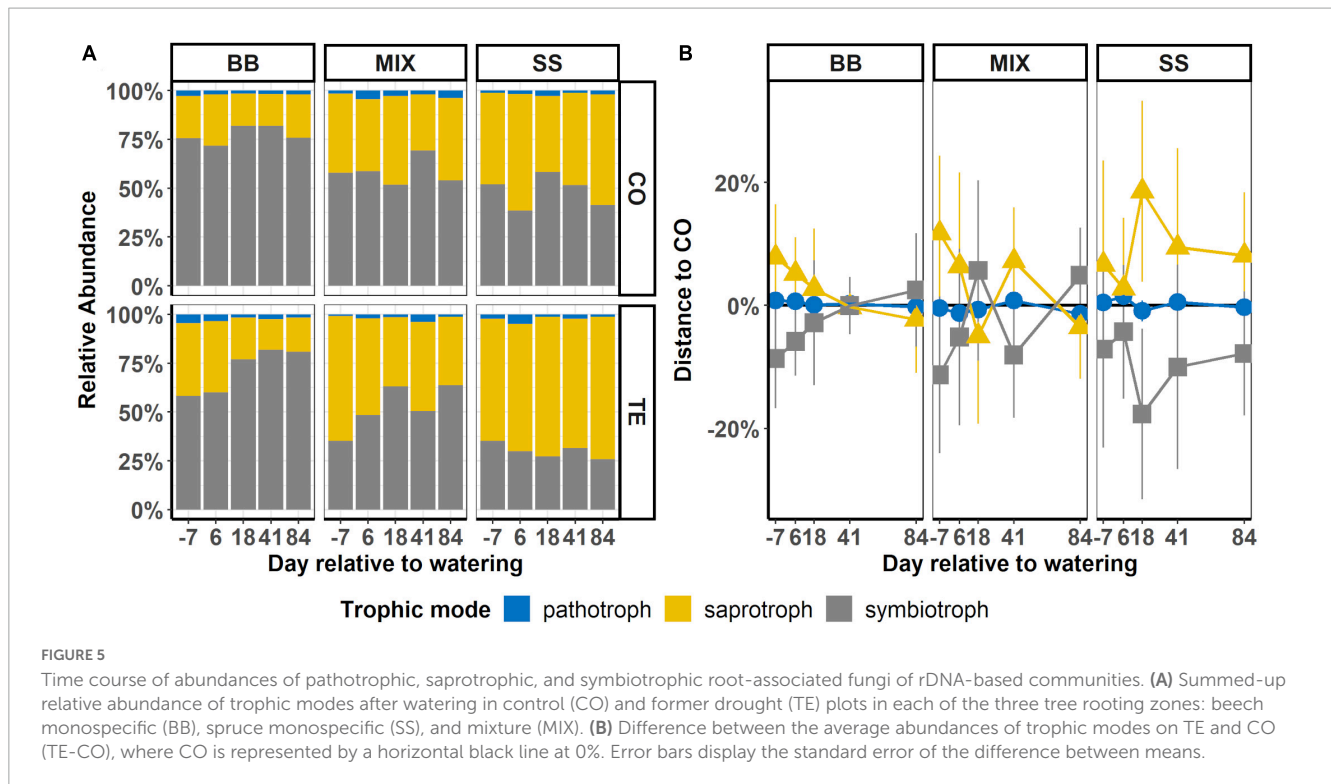


**TABLE 3** Saprotrophic fungal species, which account for  $\geq 10\%$  of the top 10 species after watering, distinguished by tree rooting zone.

Species	Primary lifestyle	Secondary lifestyle	TOP 10 OTU TE	TOP 10 OTU CO
<i>Acephala applanata</i>	Soil saprotroph	Root endophyte, dark septate	MIX (8) SS (19)	MIX (4) SS (12)
<i>Archaeorhizomyces</i> sp.	Soil saprotroph	Root-associated	MIX (15) SS (19)	MIX (29) SS (40)
<i>Cladophialophora</i> sp.	Soil saprotroph	Root endophyte, dark septate	BB (10)	BB (4)
<i>Coccomyces</i> sp.	Litter saprotroph	Plant pathogen	BB (5)	BB (14)
<i>Megacollybia platyphylla</i>	Litter saprotroph	Wood saprotroph		MIX (10)
<i>Oidiodendron</i> sp.	Soil saprotroph	Root endophyte	BB (42) MIX (45) SS (33)	BB (36) MIX (20) SS (19)
<i>Phialocephala</i> sp.	Soil saprotroph	Root endophyte	BB (13) MIX (18) SS (18)	BB (5) MIX (20) SS (14)

Lifestyles are given according to Pölmé et al. (2020), whereby “Primary lifestyle” describes the most commonly occurring lifestyle and “Secondary lifestyle” additional ones. Top 10 OTU describes in which rooting zone the respective fungi are included in top 10 most abundant saprotrophic fungi for former drought (TE) and control (CO) treatment. Values in brackets indicate what percentage they accounted for of the top 10. In the case that species appeared more than once within the top 10, the respective sequence counts were summed up. [Supplementary Table 6](#) contains all as saprotrophic classified species.

**TABLE 4** Pathotrophic fungal species, which account for  $\geq 10\%$  of the top 10 species.

Species	Primary lifestyle	Secondary lifestyle	TOP 10 OTU TE	TOP 10 OTU CO
<i>Cephalotheca</i> sp.	Mycoparasite	-	BB (4) MIX (3) SS (2)	BB (25) MIX (8)
<i>Ilyonectria</i> sp.	Plant pathogen	-	BB (11) MIX (11) SS (10)	BB (18) MIX (11) SS (10)
<i>Lecanicillium primulinum</i>	Animal parasite	Animal decomposer		SS (23)
<i>Mollisia</i> sp.	Plant pathogen	Litter saprotroph	MIX (10)	
<i>Trichoderma</i> sp.	Mycoparasite	Foliar endophyte	BB (81) MIX (70) SS (74)	BB (51) MIX (75) SS (61)

Lifestyles are given according to Pölmé et al. (2020), whereby “Primary lifestyle” describes the most commonly occurring lifestyle and “Secondary lifestyle” additional ones. Top 10 OTU describes in which rooting zone the respective fungi are included in top 10 most abundant pathotrophic fungi for former drought (TE) and control (CO) treatment. Values in brackets indicate what percentage they accounted for of the top 10. In the case that species appeared more than once within the top 10, the respective sequence counts were summed up. [Supplementary Table 7](#) contains all as pathotrophic classified top 10 species.

The vitality of TE spruce roots in mesh bags increased within days after watering and reached a growth rate similar to those of CO, indicating a fast reactivation of existing dormant fine roots after drought, very similar to Scots pine (Joseph et al., 2020).

Nevertheless, those reactivated TE fine roots were more prone to death than CO roots, which is in line with earlier findings of increased fine-root mortality after drought release (Gaul et al., 2008). In contrast, beech fine roots in mesh bags did not show

TABLE 5 ECM fungal species, which account for  $\geq 10\%$  of the top 10 species after watering, distinguished by tree rooting zone.

Species	Exploration type	TOP 10 OTU TE	TOP 10 OTU CO	Drought tolerance	References
<i>Elaphomyces granulatus</i>	Short	MIX (6) SS (34)	MIX (10) SS (20)		
<i>Lactarius</i> sp.	Medium	SS (6)	BB (15) MIX (21) SS (18)	–	Taniguchi et al., 2018
<i>Lactarius subdulcis</i>	Medium	BB (45) MIX (19)	BB (32)	+	Shi et al., 2002
<i>Piloderma</i> sp.	Medium	BB (8) MIX (10)	BB (12) MIX (12) SS (4)		
<i>Russula</i> sp.	Contact	BB (11) MIX (29) SS (18)	BB (8) MIX (9) SS (28)	+	Querejeta et al., 2009; Azul et al., 2010
<i>Russula brunneoviolacea</i>	Contact	MIX (11)		+	Azul et al., 2010
<i>Russula fellea</i>	Contact	BB (16) MIX (11)	BB (19)	+	Azul et al., 2010
<i>Tomentella botryoides</i>	Medium		BB (5) MIX (11)	+	Azul et al., 2010
<i>Tylophilus felleus</i>	Unassigned	SS (10)	SS (6)		
<i>Xerocomellus pruinosus</i>	Long	BB (7) MIX (8) SS (14)	MIX (6) SS (10)		

Exploration types of each ECM fungi were assigned according to Agerer (2001). Top 10 OTU describes in which rooting zone the respective fungi are included in top 10 most abundant ECM fungi for former drought (TE) and control (CO) treatment. Values in brackets indicate what percentage they accounted for of the top 10. In the case that species appeared more than once within the top 10, the respective sequence counts were summed up. “+” and “–” describe whether the respective species were shown to be drought tolerant or not, respectively, according to the publications given in the “References” column. [Supplementary Table 8](#) contains all as ectomycorrhizal classified species.

any growth after watering and only a short peak in vitality in early autumn (d 35 and d 41), a season where the fine-root length tends to increase in beech (Montagnoli et al., 2014). While the results from the beech fine roots within mesh bags suggest that existing fine roots were not reactivated after rewatering, increasing the fine-root biomass of beech outside the mesh bags suggested that beech trees rapidly formed new fine roots. A likely explanation is the short life span of beech fine roots and their high C turnover (Nikolova et al., 2020; Mariën et al., 2021).

The different fine-root recovery patterns in spruce and beech complement the findings of fine-root preservation in spruce and the continuous renewal of low-biomass short life span fine roots in beech during drought (Meier and Leuschner, 2008; Nikolova et al., 2020). For both tree species, the degree of mycorrhization in TE was below CO during the whole period, which corresponds to the findings of Feil et al. (1988), who showed a decreased growth of mycorrhizae in mature spruce during drought periods. In beech, we observed a parallel increase of vitality and degree of mycorrhization after drought, implying that ECM fungi, to some degree, depended more on host root vitality than on abiotic environmental factors. This was also suggested by Shi et al. (2002), who observed that neither the number of ECM types on young beech roots nor the degree of fungal colonization of the roots were affected by a drought treatment. In spruce, though, the degree of mycorrhization decreased after watering and rose 4 weeks later, suggesting that suberisation of fine roots during drought (Nikolova et al., 2020) could contribute to preventing ECM colonization (e.g., Brundrett, 2002; Sharda and Koide, 2008). Consequently, outgrowing fine roots needed to be colonized anew. Reflecting this and the time of full mycorrhizae formation (Ineichen and Wiemken, 1992), we saw increasing mycorrhization from d 28 onward. The sudden and strong variations in the degree of mycorrhization confirmed earlier observed patterns caused by changes in soil temperature and soil moisture (Swaty et al., 1998).

During our 3-month measuring period, only few significant differences were observed with respect to fine-root growth and vitality between monospecific and mixture zones. However, on specific days, growth and vitality were significantly higher in Bmix compared to BB, corresponding to the findings of Zwetsloot et al. (2019) that beech fine roots had lower mortality when growing in mixture zones with spruce. In spruce, growth and vitality were lower in Smix than in SS on some days, possibly reflecting the lower competitive ability of spruce fine roots in mixed stands with beech (Schmid, 2002; Zwetsloot et al., 2019).

## Lasting effects of precedent drought and tree rooting zone on fungal communities after drought release

We found a high agreement between DNA and RNA data regarding the fungal trophic modes, indicating a good representation of the active fungal community by the DNA data and a minor role of inactive fungi and the spores and residues of dead fungi (Pedersen et al., 2015; Carini et al., 2016). According to our data, the root-associated community composition remained stable within 3 months after drought release but differed between the tree species, with ECM fungi being more abundant in beech and saprotrophs in spruce. A higher species richness and increase of ECM fungi after drought indicate a positive effect of tree species mixture. Consequently, H1 can be partially confirmed, which means that the structure of the fungal community after rewatering was lastingly influenced by the previous drought, but its composition highly depends on the development of tree-specific root systems and habitat heterogeneity. A high number of the most abundantly observed ECM fungal species are considered drought resistant, and most saprotrophic species have a facultative root-associated lifestyle, thus confirming H2.

As expected from a previous study on ECM diversity on the KROOF site, the diversity of root-associated fungi was lower in TE than in CO (Nickel et al., 2018). However, alpha diversity and community composition did not change significantly for both tree species within 3 months after drought release. This either indicates that a stable community had established on the treatment plots during drought, which tolerated the changes in soil moisture, or that the drought-surviving fungal communities could not profit from the moisture increase. The majority of the highly abundant fungal species in this study are considered drought tolerant (Table 5; Supplementary Table 8) or have a facultative root-associated lifestyle (Table 3; Supplementary Table 6) that may favor drought survival by easier water access (Querejeta et al., 2003; Hafner et al., 2017). This suggests the emergence of a stable community during drought. Those adapted fungi were closest to newly grown fine roots after rewetting and thus likely the first colonizers (Bruns, 1995), which could explain an unchanged fungal community after drought release.

The tree species RZ was a major driver of the fungal community composition during drought (Nickel et al., 2018) and after watering (our study), which underlines the major influence of tree species on fungal community composition found in many studies (Dickie, 2007; Ishida et al., 2007; Tedersoo et al., 2012; Bogar and Kennedy, 2013; Nacke et al., 2016; Otsing et al., 2021). Furthermore, we observed a higher fungal diversity on spruce compared to beech fine roots irrespective of treatment, which may reflect the higher fungal species richness in the litter layer of spruce compared to beech (Asplund et al., 2019).

In beech, ECM fungi were the most abundant fungal trophic modes in both treatments over time and irrespective of RZ. This suggests that the ECM fungi of beech were better retained through the continuous root growth found in beech under drought as compared to Norway spruce (Nikolova et al., 2020). Moreover, the abundance of ECM fungi increased in mixture after watering but not in the TE SS RZ. Therefore, spruce ECM in mixture may benefit from the continuous renewal of beech fine roots as a more favorable niche to colonize than suberised spruce fine roots, possibly being one aspect of why ECM fungal community compositions of spruce were influenced by neighboring tree species in mixture in other studies, too (Hubert and Gehring, 2008; Otsing et al., 2021). While giving support to the majority of studies that found a positive tree mixture effect on ECM diversity (Gao et al., 2013; Tedersoo et al., 2016), our study adds the aspect of a positive effect of mixtures on fungal diversity under drought. Addressing H1, we further looked at ECM exploration types and found ECM species with contact exploration type were more common in TE compared to CO. Additionally, in spruce, relative abundances shifted with time after watering from dominating contact types to more short- and long-distance types. ECM fungi with rhizomorphs that support water uptake (Duddridge et al., 1980; Cairney, 1992) increased during the first 3 years of experimental drought (Nickel et al., 2018). However, there may be a trade-off between water uptake and carbon costs in which, with the duration of drought, low-cost contact types may become dominant (Castaño et al., 2018). Recently, shifts in ECM exploration types were proposed to rather reflect the fungal C supply by the host (Wasyliv and Karst, 2020). With drought release, spruce in our experiment preferably invested C in fine-root growth within the first month (Hikino et al., 2022), possibly to restore the functions essential for resource uptake (Bardgett

et al., 2014; Solly et al., 2018; Germon et al., 2020), which was not reflected in a higher C sink activity of ectomycorrhizae during this time (Hikino et al., 2022). In beech, the photosynthesis rate was constantly higher during drought and after watering compared to spruce (Goisser et al., 2016), which suggests a better supply of photoassimilates to beech-associated ECM fungi during drought, allowing the maintenance of C-costly medium-distance exploration types (Weigt et al., 2012).

The relatively high shares of saprotrophs in the TE SS RZ remained unchanged over the 3 months. Spruce fine roots become suberised during drought (Nikolova et al., 2020), creating a barrier for ectomycorrhizal colonization (e.g., Brundrett, 2002; Sharda and Koide, 2008), and in addition, a severe root dieback (Nickel et al., 2018) may have increased root necromass. The majority of saprotrophic fungal species found in spruce roots within this study, including the highly abundant *Oidiodendron* sp. and *Phialocephala* sp., were found to have the ability to associate with roots, which corroborates recent studies showing that fungi can occupy multiple ecological niches (Selosse et al., 2018). Thus, some saprotrophic fungi may reveal a facultative root-endophytic lifestyle (Tedersoo and Smith, 2013; Smith et al., 2017) and even show mycorrhizal traits (Jumpponen, 2001; Kohler et al., 2015; Almario et al., 2017). Dark septate endophytes, for example, are shown to better tolerate environmental stresses such as drought (Berthelot et al., 2019), which is why an increased abundance of saprotrophic species with root-associated lifestyles could be an indication of adaptation to a changing climate (Ruotsalainen et al., 2022). Furthermore, the stable shift toward the predominance of drought-resistant ECM species during the 5 years of summer drought, together with a good recovery of the tree fine-root and carbon transport system (Hikino et al., 2021, 2022), may reflect ectomycorrhiza-assisted plant adaptation to drought, as suggested by Cosme (2023). A high litter accumulation in our TE plots (pers. observation), together with a more humid surrounding due to hydraulic redistribution in beech during drought (Querejeta et al., 2003; Hafner et al., 2017), may explain the detection of several litter-degrading saprotrophs (e.g., different species of *Hyaloscypha* and *Mycena*) among the most abundant saprotrophs in BB and MIX RZ. Unlike ECM and saprotrophic fungi, pathotrophs accounted for only a small percentage, highly dominated by *Trichoderma* sp. This genus comprised mycoparasites (Harman, 2006 and literature therein) but also saprotrophic species that produce a plethora of phytohormones, increasing plant and even ECM hyphal growth (Harman et al., 2004; Shores et al., 2010; Oh et al., 2018). Thus, the root-associated unclassified fungal species await further, more detailed studies.

## Conclusion

The present study gives insights into the drought recovery of root-associated fungal communities and the fine-root systems of beech and spruce, suggesting that the composition of root fungal communities is strongly influenced by tree species-specific drought reactions and the restoration of their fine-root systems upon drought release. A positive tree mixture effect of increased total fungal OTU richness underlines the role of diversification in forests from a belowground perspective. Moreover, a comparison

between fungi identified from soil and roots also provides further evidence that an association between saprotrophic fungi and roots may not be an exception but rather a survival strategy of the fungi. However, this study only considered a period of 3 months. Thus, the resilience of fungal communities and fine-root systems needs to be explored at a longer timescale to clarify whether the whole forest system retains its full functional capacity in terms of root recovery, tree growth, root-associated and soil fungi, and other soil biota.

## Data availability statement

The datasets presented in this study can be found in online repositories. The names of the repository/repositories and accession number(s) can be found below: <https://www.ncbi.nlm.nih.gov/>, PRJNA950082.

## Author contributions

FW and KP designed the experiment. JD and RW processed the samples and analyzed and interpreted the data with support from FW. JM provided and compiled data for soil fungi from a parallel study. JD wrote the manuscript with contributions from all the authors. All authors contributed to the article and approved the submitted version.

## Funding

This project was funded by the German Research Foundation (DFG) through grants GR 1881/5-1, MA1763/10-1, PR555/2-1, and PR292/22-1 and by the Bavarian State Ministries of the Environment and Consumer Protection and of Food, Agriculture and Forestry (W047/Kroof II). JM was founded by a scholarship from the Deutscher Akademischer Austauschdienst (DAAD) Grant No. 57507437. Open access publication was supported by the Technical University of Munich (TUM) Publishing Fund.

## References

- Abarenkov, K., Zirk, A., Piirmann, T., Pöhönen, R., Ivanov, F., Nilsson, R. H., et al. (2020). *Full UNITE+INSD dataset for Fungi. Version 04.02.2020*. Tartu: University of Tartu. doi: 10.15156/BIO/786372
- Agerer, R. (2001). Exploration types of ectomycorrhizae. *Mycorrhiza* 11, 107–114. doi: 10.1007/s005720100108
- Allen, C. D., Breshears, D. D., and McDowell, N. G. (2015). On underestimation of global vulnerability to tree mortality and forest die-off from hotter drought in the anthropocene. *Ecosphere* 6, 1–55. doi: 10.1890/ES15-00203.1
- Allen, C. D., Macalady, A. K., Chenchouni, H., Bachelet, D., McDowell, N., Vennetier, M., et al. (2010). A global overview of drought and heat-induced tree mortality reveals emerging climate change risks for forests. *For. Ecol. Manag.* 259, 660–684. doi: 10.1016/j.foreco.2009.09.001
- Almario, J., Jeena, G., Wunder, J., Langen, G., Zuccaro, A., Coupland, G., et al. (2017). Root-associated fungal microbiota of nonmycorrhizal *Arabidopsis thaliana* and its contribution to plant phosphorus nutrition. *Proc. Natl. Acad. Sci. U.S.A.* 114, E9403–E9412. doi: 10.1073/pnas.1710455114
- Anderegg, W. R. L., Kane, J. M., and Anderegg, L. D. L. (2013). Consequences of widespread tree mortality triggered by drought and temperature stress. *Nat. Clim. Change* 3, 30–36. doi: 10.1038/nclimate1635
- Aponte, C., García, L. V., Marañón, T., and Gardes, M. (2010). Indirect host effect on ectomycorrhizal fungi: Leaf fall and litter quality explain changes in fungal communities on the roots of co-occurring Mediterranean oaks. *Soil Biol. Biochem.* 42, 788–796. doi: 10.1016/j.soilbio.2010.01.014
- Asplund, J., Kauserud, H., Ohlson, M., and Nybakken, L. (2019). Spruce and beech as local determinants of forest fungal community structure in litter, humus and mineral soil. *FEMS Microbiol. Ecol.* 95, 1–11. doi: 10.1093/femsec/fiy232
- Azul, A. M., Sousa, J. P., Agerer, R., Martín, M. P., and Freitas, H. (2010). Land use practices and ectomycorrhizal fungal communities from oak woodlands dominated by *Quercus suber* L. considering drought scenarios. *Mycorrhiza* 20, 73–88. doi: 10.1007/s00572-009-0261-2
- Bardgett, R. D., Mommer, L., and De Vries, F. T. (2014). Going underground: Root traits as drivers of ecosystem processes. *Trends Ecol. Evol.* 29, 692–699. doi: 10.1016/j.tree.2014.10.006

## Acknowledgments

We thank our ecology volunteers Valentin Kugler and Sarah Kristen, student helper Laura Pohlenz, and apprentice Isabella Pitzen for their help during the mesh bag preparation, filling, and harvest, as well as their support in the root length analysis. We also thank Susanne Kublik for sequencing, Patrick and Christian Schwaferts for their statistical advice and discussion, Elke Gerstner and Barbara Gross for their reliable lab supply during the COVID pandemic and helping hand for the mesh bag preparation, and Dr. Hans Sanden for taking the time to read this manuscript and providing helpful comments to improve it.

## Conflict of interest

The authors declare that the research was conducted in the absence of any commercial or financial relationships that could be construed as a potential conflict of interest.

## Publisher's note

All claims expressed in this article are solely those of the authors and do not necessarily represent those of their affiliated organizations, or those of the publisher, the editors and the reviewers. Any product that may be evaluated in this article, or claim that may be made by its manufacturer, is not guaranteed or endorsed by the publisher.

## Supplementary material

The Supplementary Material for this article can be found online at: <https://www.frontiersin.org/articles/10.3389/ffgc.2023.1197791/full#supplementary-material>







- Tedersoo, L., Bahram, M., Toots, M., Diédhiou, A. G., Henkel, T. W., Kjøller, R., et al. (2012). Towards global patterns in the diversity and community structure of ectomycorrhizal fungi. *Mol. Ecol.* 21, 4160–4170. doi: 10.1111/j.1365-294X.2012.05602.x
- Unuk, T., Martinović, T., Finžgar, D., Šibanc, N., Grebenc, T., and Kraigher, H. (2019). Root-associated fungal communities from two phenologically contrasting silver fir (*Abies alba* Mill.) groups of trees. *Front. Plant Sci.* 10:214. doi: 10.3389/fpls.2019.00214
- Veach, A. M., Chen, H., Yang, Z. K., Labbe, A. D., Engle, N. L., Tschapinski, T. J., et al. (2020). Plant hosts modify belowground microbial community response to extreme drought. *mSystems* 5:e00092-e20. doi: 10.1128/msystems.00092-20
- Wang, Q., Garrity, G. M., Tiedje, J. M., and Cole, J. R. (2007). Naïve bayesian classifier for rapid assignment of RRNA sequences into the new bacterial taxonomy. *Appl. Environ. Microbiol.* 73, 5261–5267. doi: 10.1128/AEM.00062-07
- Wasyliw, J., and Karst, J. (2020). Shifts in ectomycorrhizal exploration types parallel leaf and fine root area with forest age. *J. Ecol.* 108, 2270–2282. doi: 10.1111/1365-2745.13484
- Weigt, R. B., Raidl, S., Verma, R., and Agerer, R. (2012). Exploration type-specific standard values of extramatrical mycelium—a step towards quantifying ectomycorrhizal space occupation and biomass in natural soil. *Mycol. Prog.* 11, 287–297. doi: 10.1007/s11557-011-0750-5
- Wickham, H. (2016). *Ggplot2: Elegant graphics for data analysis. Use R!*. Cham: Springer International Publishing. doi: 10.1007/978-3-319-24277-4
- Zadworny, M., and Eissenstat, D. M. (2011). Contrasting the morphology, anatomy and fungal colonization of new pioneer and fibrous roots. *New Phytol.* 190, 213–221. doi: 10.1111/j.1469-8137.2010.03598.x
- Zhang, Y., Chen, H. Y. H., and Reich, P. B. (2012). Forest productivity increases with evenness, species richness and trait variation: A global meta-analysis. *J. Ecol.* 100, 742–749. doi: 10.1111/j.1365-2745.2011.01944.x
- Zwetsloot, M. J., and Bauerle, T. L. (2021). Repetitive seasonal drought causes substantial species-specific shifts in fine-root longevity and spatio-temporal production patterns in mature temperate forest trees. *New Phytol.* 231, 974–986. doi: 10.1111/nph.17432
- Zwetsloot, M. J., Goebel, M., Paya, A., Grams, T. E. E., and Bauerle, T. L. (2019). Specific spatio-temporal dynamics of absorptive fine roots in response to neighbor species identity in a mixed beech-spruce forest. *Tree Physiol.* 39, 1867–1879. doi: 10.1093/treephys/tpz086

## *Supplementary Material*

### **Drought legacy effects on fine root associated fungal communities are modulated by root interactions between tree species**

**Jasmin Danzberger\*, Ramona Werner, Joanna Mucha, Karin Pritsch, Fabian Weigl**

**\*Correspondence:** Jasmin Danzberger: [jasmin.danzberger@freenet.de](mailto:jasmin.danzberger@freenet.de)

#### **1 Tables**

**Table S1** Overview of mesh bag samples per sampling day. RZ = rooting zone.

<b>Sampling day</b>	<b>Number of plots</b>	<b>Tree species</b>	<b>RZ per Species</b>	<b>Replicates per RZ</b>	<b>Number mesh bags per day</b>
-7	8	2	2	4	128
10	8	2	2	4	128
17	2	2	2	4	32
28	8	2	2	4	128
35	2	2	2	4	32
42	8	2	2	4	128
89	2	2	2	4	32
<b>Total number of mesh bags</b>					<b>608</b>

**Table S2** Sequences of individual primers for the amplification of ITS2 rDNA, according to Nickel et al. (2018) and Tedersoo et al. (2015). The DNA strand orientation is given in forward (fw) and reverse (rv), black nucleobases in the sequence describe the ITS primer, blue nucleobases the Illumina overhang.

Primer name	Orientation	Sequence	Target
ITS3-Mix1	fw	TCGTCGGCAGCGTCAGATGTGTATAAGAGA CAG CATCGATGAAGAACGCAG	Fungi
ITS3-Mix2	fw	TCGTCGGCAGCGTCAGATGTGTATAAGAGA CAG CAACGATGAAGAACGCAG	Chytridiomycota
ITS3-Mix3	fw	TCGTCGGCAGCGTCAGATGTGTATAAGAGA CAG CACCGATGAAGAACGCAG	Sebacinales
ITS3-Mix4	fw	TCGTCGGCAGCGTCAGATGTGTATAAGAGA CAG CATCGATGAAGAACGTAG	Glomeromycota
ITS3-Mix5	fw	TCGTCGGCAGCGTCAGATGTGTATAAGAGA CAG CATCGATGAAGAACGTGG	Sordariales
ITS4-Mix1	rv	GTCTCGTGGGCTCGGAGATGTGTATAAGAG ACAG TCCTCCGCTTATTGATATGC	Fungi
ITS4-Mix2	rv	GTCTCGTGGGCTCGGAGATGTGTATAAGAG ACAG TCCTGCGCTTATTGATATGC	Chaetothyriales
ITS4-Mix3	rv	GTCTCGTGGGCTCGGAGATGTGTATAAGAG ACAG TCCTCGCCTTATTGATATGC	Archaeorhizomycota
ITS4-Mix4	rv	GTCTCGTGGGCTCGGAGATGTGTATAAGAG ACAG TCCTCCGCTGAWTAATATGC	Tulasnellaceae

**Table S3** Pearson correlation analysis between fine-root vitality, growth and degree of mycorrhisation in spruce and beech.

	CO		TE	
	<i>r</i>	<i>p</i>	<i>r</i>	<i>p</i>
<b>Spruce</b>				
Mycorrhisation ~ Vitality	0.24	<b>0.01</b>	< 0.00	0.99
Mycorrhisation ~ Fine-root growth	0.18	<b>0.05</b>	0.05	0.59
Vitality ~ Fine-root growth	0.40	<b>&lt; 0.00</b>	0.45	<b>&lt; 0.00</b>
<b>Beech</b>				
Mycorrhisation ~ Vitality	0.41	<b>&lt; 0.00</b>	0.30	<b>&lt; 0.01</b>
Mycorrhisation ~ Fine-root growth	0.20	<b>0.03</b>	0.11	0.26
Vitality ~ Fine-root growth	0.19	<b>0.03</b>	0.27	<b>&lt; 0.01</b>

**Table S4** Summary of post-hoc Dunn test for Shannon Index, Simpson Index, Pielou's Evenness and species richness on rooting zone (RZ; BB = beech monospecific, SS = spruce monospecific, MIX = mixture) with Bonferroni adjustment. Only significant results are shown.

Variable	RZ
Shannon Index	BB vs MIX: $p_{adj} < 0.001$ BB vs SS: $p_{adj} < 0.001$ MIX vs SS: $p_{adj} < 0.001$
Simpson Index	BB vs MIX: $p_{adj} < 0.001$ BB vs SS: $p_{adj} < 0.001$ MIX vs SS: $p_{adj} < 0.001$
Pielou's Evenness	BB vs MIX: $p_{adj} < 0.001$ BB vs SS: $p_{adj} < 0.001$ MIX vs SS: $p_{adj} < 0.001$
Species richness	MIX vs BB: $p_{adj} < 0.05$

**Table S5** Pearson correlation analysis between fine-root vitality, growth and fungal community composition using non-metric multi-dimensional scaling (NMDS) axis 1 (NMDS1) separated in all root-associated fungi and ectomycorrhizae in the tree rooting zones (RZ; BB = beech monospecific, SS = spruce monospecific, MIX = mixture). CO represents controls and TE rewatered plots.

RZ	CO		TE	
	<i>r</i>	<i>p</i>	<i>r</i>	<i>p</i>
<b>All root-associated fungi:</b>				
Community composition (NMDS1) ~ vitality				
SS	0.12	0.98	-0.29	0.33
MIX	0.09	0.76	0.51	0.07
BB	-0.15	0.60	0.04	0.90
Community composition (NMDS1) ~ growth				
SS	-0.30	0.33	-0.41	0.24
MIX	0.56	0.05	0.39	0.21
BB	-0.42	0.15	0.01	0.98
<b>Ectomycorrhizae:</b>				
Community composition (NMDS1) ~ vitality				
SS	<b>-0.57</b>	<b>0.04</b>	0.20	0.43
MIX	-0.22	0.44	0.12	0.70
BB	-0.50	0.08	0.24	0.70
Community composition (NMDS1) ~ growth				
SS	-0.20	0.52	0.05	0.90
MIX	0.35	0.24	0.04	0.89
BB	0.04	0.89	0.08	0.80

**Table S6** All saprotrophic fungal species distinguished by tree interaction zone. Lifestyles are given according to Pölme et al. (2020), whereby “Primary lifestyle” describes the most commonly occurring lifestyle and “Secondary lifestyle” additional ones. Top 10 OTU describes in which interaction zone the respective fungi are included in top 10 most abundant saprotrophic fungi for former drought (TE) and control (CO) treatment. Values in brackets indicate what percentage they accounted of the top 10.

Species	Primary lifestyle	Secondary lifestyle	TOP 10 OTU TE	TOP 10 OTU CO
<i>Acephala applanata</i>	soil saprotroph	root endophyte dark septate	MIX (8) SS (19)	MIX (4) SS (12)
<i>Alatospora</i> sp.	litter saprotroph	-		
<i>Alatospora acuminata</i>	litter saprotroph	-		
<i>Amaurodon</i> sp.	litter saprotroph	-		
<i>Ampulloclitocybe clavipes</i>	litter saprotroph	-		
<i>Anthopsis</i> sp.	soil saprotroph	animal parasite		
<i>Apiotrichum</i> sp.	soil saprotroph	-		
<i>Apiotrichum wieringae</i>	soil saprotroph	-		
<i>Archaeorhizomyces</i> sp.	soil saprotroph	root-associated	MIX (15) SS (19)	MIX (29) SS (40)
<i>Armillaria gallica</i>	litter saprotroph	plant pathogen		BB (8) MIX (4)
<i>Ascocorticium</i> sp.	wood saprotroph	-		
<i>Ascocoryne</i> sp.	wood saprotroph	-		
<i>Basidioidendron</i> sp.	wood saprotroph	-	BB (8)	
<i>Botryobasidium</i> sp.	wood saprotroph	-		
<i>Botryobasidium subcoronatum</i>	wood saprotroph	-		
<i>Brachysporium</i> sp.	unspecified saprotroph	-		
<i>Byssonectria</i> sp.	litter saprotroph	dung saprotroph		
<i>Capronia</i> sp.	soil saprotroph	root endophyte dark septate		
<i>Chaetosphaeria</i> sp.	litter saprotroph	wood saprotroph		
<i>Chalara</i> sp.	litter saprotroph	plant pathogen		SS (3)
<i>Chalara angustata</i>	litter saprotroph	plant pathogen		
<i>Chalara aurea</i>	litter saprotroph	plant pathogen		
<i>Chalara hyalocuspica</i>	litter saprotroph	plant pathogen		
<i>Chalara piceae-abietis</i>	litter saprotroph	plant pathogen		
<i>Ciliciopodium brevipes</i>	wood saprotroph	litter saprotroph		
<i>Cladophialophora</i> sp.	soil saprotroph	root endophyte dark septate	BB (10)	BB (4)
<i>Cladophialophora chaetospora</i>	soil saprotroph	root endophyte dark septate		
<i>Coccomyces</i> sp.	litter saprotroph	plant pathogen	BB (5)	BB (14)

<i>Colpoma</i> sp.	litter saprotroph	plant pathogen		
<i>Coniophora</i> sp.	wood saprotroph	-		
<i>Coniophora arida</i>	wood saprotroph	-		
<i>Connersia</i> sp.	wood saprotroph	-		
<i>Cryptosporiopsis</i> sp.	unspecified saprotroph	-		
<i>Davidhawksworthia ilicicola</i>	litter saprotroph	-		
<i>Dictyochaeta</i> sp.	litter saprotroph	wood saprotroph		
<i>Fayodia bisphaerigera</i>	litter saprotroph	-		
<i>Galerina</i> sp.	wood saprotroph	litter saprotroph		SS (5)
<i>Galerina pseudocamerina</i>	wood saprotroph	litter saprotroph		
<i>Geminibasidium</i> sp.	soil saprotroph	-		
<i>Geomyces auratus</i>	soil saprotroph	-		
<i>Hyaloscypha</i> sp.	litter saprotroph	wood saprotroph		BB (4) MIX (3)
<i>Hyaloscypha monodictys</i>	litter saprotroph	wood saprotroph		
<i>Hyaloscypha vraolstadiae</i>	litter saprotroph	wood saprotroph		BB (8) MIX (9)
<i>Hymenopellis radicata</i>	wood saprotroph	-		
<i>Hymenoscyphus</i> sp.	litter saprotroph	plant pathogen	SS (5)	
<i>Hyphodontia pallidula</i>	wood saprotroph	-		
<i>Hypholoma fasciculare</i>	wood saprotroph	-		
<i>Hypochnicium subrigescens</i>	wood saprotroph	-		
<i>Leptodontidium</i> sp.	litter saprotroph	ericoid mycorrhizal		
<i>Leptodontidium irregulare</i>	litter saprotroph	ericoid mycorrhizal		
<i>Leucosporidium</i> sp.	soil saprotroph	-		
<i>Leucosporidium krtinense</i>	soil saprotroph	-		
<i>Lophiostoma corticola</i>	wood saprotroph	litter saprotroph		
<i>Lophium arboricola</i>	litter saprotroph	-		
<i>Luellia</i> sp.	wood saprotroph	-	MIX (4)	SS (3)
<i>Lycoperdon</i> sp.	litter saprotroph	-		
<i>Megacollybia platyphylla</i>	litter saprotroph	wood saprotroph		MIX (10)
<i>Mortierella</i> sp.	soil saprotroph	root-associated		BB (6) SS (3)
<i>Mortierella alliacea</i>	soil saprotroph	root-associated		
<i>Mortierella angusta</i>	soil saprotroph	root-associated		
<i>Mortierella gamsii</i>	soil saprotroph	root-associated		

<i>Mortierella globulifera</i>	soil saprotroph	root-associated		
<i>Mortierella horticola</i>	soil saprotroph	root-associated		
<i>Mortierella longigemmata</i>	soil saprotroph	root-associated		
<i>Mortierella parvispora</i>	soil saprotroph	root-associated		
<i>Mortierella pseudozygospora</i>	soil saprotroph	root-associated		
<i>Mycena</i> sp.	litter saprotroph	root-associated		
<i>Mycena amicta</i>	litter saprotroph	root-associated	BB (7)	BB (7)
<i>Mycena rebaudengoi</i>	litter saprotroph	root-associated		
<i>Mycena sanguinolenta</i>	litter saprotroph	root-associated	BB (5) MIX (5) SS (3)	BB (7)
<i>Oidiodendron</i> sp.	soil saprotroph	root endophyte	BB (42) MIX (45) SS (33)	BB (36) MIX (20) SS (19)
<i>Oidiodendron chlamydosporicum</i>	soil saprotroph	root endophyte		
<i>Oidiodendron echinulatum</i>	soil saprotroph	root endophyte		
<i>Oidiodendron flavum</i>	soil saprotroph	root endophyte		
<i>Oidiodendron pilicola</i>	soil saprotroph	root endophyte		
<i>Orbilia</i> sp.	wood saprotroph	animal parasite		
<i>Penicillium</i> sp.	unspecified saprotroph	foliar endophyte		
<i>Penicillium arianeae</i>	unspecified saprotroph	foliar endophyte		
<i>Phallus impudicus</i>	soil saprotroph	-		
<i>Phialocephala</i> sp.	soil saprotroph	root endophyte	BB (13) MIX (18) SS (18)	BB (5) MIX (20) SS (14)
<i>Phialocephala sphaeroides</i>	soil saprotroph	root endophyte		
<i>Phragmocephala</i> sp.	wood saprotroph	-		
<i>Postia ptychogaster</i>	wood saprotroph	-		
<i>Pseudogymnoascus</i> sp.	soil saprotroph	-		
<i>Pseudogymnoascus appendiculatus</i>	soil saprotroph	-		
<i>Pseudopenidiella piceae</i>	litter saprotroph	-		
<i>Rhinocladiella</i> sp.	soil saprotroph	animal parasite		
<i>Rhodocollybia butyracea</i>	litter saprotroph	-	BB (9)	
<i>Scopuloides hydroides</i>	wood saprotroph	-		
<i>Scytalidium album</i>	wood saprotroph	litter saprotroph		
<i>Serpula</i> sp.	wood saprotroph	-		
<i>Solicoccozyma terricola</i>	soil saprotroph	epiphyte		

<i>Steccherinum</i> sp.	wood saprotroph	-	
<i>Talaromyces</i> sp.	unspecified saprotroph	-	
<i>Trechispora</i> sp.	wood saprotroph	-	SS (8)
<i>Trechispora caucasica</i>	wood saprotroph	-	
<i>Trechispora hymenocystis</i>	wood saprotroph	-	
<i>Trechispora invisitata</i>	wood saprotroph	-	MIX (4)
<i>Trechispora stellulata</i>	wood saprotroph	-	
<i>Tubaria minutalis</i>	litter saprotroph	-	
<i>Tulasnella</i> sp.	litter saprotroph	root-associated	

**Table S7** Pathotrophic fungal species. Lifestyles are given according to Põlme et al. (2020), whereby “Primary lifestyle” describes the most commonly occurring lifestyle and “Secondary lifestyle” additional ones. Top 10 OTU describes in which interaction zone the respective fungi are included in top 10 most abundant pathotrophic fungi for former drought (TE) and control (CO) treatment. Values in brackets indicate what percentage they accounted of the top 10.

Species	Primary lifestyle	Secondary lifestyle	TOP 10 OTU TE	TOP 10 OTU CO
<i>Athelia</i> sp.	lichen parasite	fungus decomposer		BB (5)
<i>Cephalotheca</i> sp.	mycoparasite	-	BB (4) MIX (3) SS (2)	BB (25) MIX (8)
<i>Cryptodiscus</i> sp.	lichen parasite	fungus decomposer	SS (5)	
<i>Ilyonectria</i> sp.	plant pathogen	-	BB (11) MIX (11) SS (10)	BB (18) MIX (11) SS (10)
<i>Lecanicillium primulinum</i>	animal parasite	animal decomposer		SS (23)
<i>Lecanicillium</i> sp.	animal parasite	animal decomposer		BB (2)
<i>Leptobacillium leptobactrum</i>	animal parasite	fungus decomposer	SS (2)	
<i>Metapochonia bulbillosa</i>	animal parasite	animal decomposer	BB (2) MIX (3) SS (4)	MIX (4) SS (7)
<i>Mollisia</i> sp.	plant pathogen	litter saprotroph	MIX (10)	
<i>Monacrosporium drechsleri</i>	animal parasite	Wood saprotroph	MIX (3)	
<i>Pochonia cordycepsociata</i>	animal parasite	animal decomposer	BB (1) MIX (3) SS (2)	
<i>Trichoderma</i> sp.	mycoparasite	foliar endophyte	BB (81) MIX (70) SS (74)	BB (51) MIX (75) SS (61)
<i>Volutella</i> sp.	plant pathogen	-	BB (TE)	



**Table S8** All ECM fungal species after watering distinguished by tree interaction zone. Exploration types of each ECM fungi were assigned according to Agerer, 2001. Top 10 OTU describes in which interaction zone the respective fungi are included in top 10 most abundant ECM fungi for former drought (TE) and control (CO) treatment. Values in brackets indicate what percentage they accounted of the top 10. “+” describes that the respective species was shown to be drought tolerant or not (“-“) according to publications given in the “Citation” column.

Species	Exploration type	TOP 10 OUT TE	TOP 10 OUT CO	Drought tolerance	Citation
<i>Amanita</i> sp.	medium	BB (8) MIX (4)		+	Querejeta et al., 2009, Uroz et al., 2016
<i>Amanita citrina</i>	medium				
<i>Amanita excelsa</i>	medium	SS (5)	SS (4)		
<i>Amanita muscaria</i>	medium				
<i>Amanita porphyria</i>	medium				
<i>Amphinema</i> sp.	medium				
<i>Boletus edulis</i>	long				
<i>Cenococcum</i> sp.	short		SS (4)	+	i.a. Azul et al., 2010, Kerner et al., 2012, Peter et al., 2016
<i>Clavulina</i> sp.	contact				
<i>Cortinarius</i> sp.	medium			+	Boczon et al., 2021, de Jalon et al. 2020, Bodeker et al. 2014
<i>Cortinarius leiocastaneus</i>	medium				
<i>Elaphomyces granulatus</i>	short	MIX (6) SS (34)	MIX (10) SS (20)		
<i>Elaphomyces muricatus</i>	short				
<i>Genea hispidula</i>	Short			-	Taniguchi et al., 2018
<i>Hydnotrya</i> sp.	contact				
<i>Hydnotrya tulasnei</i>	contact				
<i>Hydnum</i> sp.	medium				
<i>Hydnotyra michaelis</i>	contact			(-)	Querejeta et al., 2009
<i>Hygrophorus</i> sp.	contact			-	Taniguchi et al., 2018
<i>Hygrophorus pustulatus</i>	contact				
<i>Inocybe</i> sp.	short			+	Long et al., 2016
<i>Inocybe assimilata</i>	short		MIX (7)		
<i>Lactarius</i> sp.	medium		BB (15) MIX (21) SS (6) SS (18)	-	Taniguchi et al., 2018
<i>Lactarius camphoratus</i>	medium				
<i>Lactarius subdulcis</i>	medium	BB (45) MIX (19)	BB (32)	+	Shi et al., 2002
<i>Leotia lubrica</i>	unassigned				
<i>Melanogaster variegatus</i>	long				
<i>Paxillus involutus</i>	long				

<i>Phaeocollybia</i> sp.	unassigned				
<i>Piloderma</i> sp.	medium	BB (8) MIX (10)	BB (12) MIX (12) SS (4)		
<i>Ramaria apiculata</i>	unassigned				
<i>Russula</i> sp.	contact	BB (11) MIX (29) SS (18)	BB (8) MIX (9) SS (28)	+	Querejeta et al., 2009; Azul et al., 2010
<i>Russula aurora</i>	contact			+	Azul et al., 2010
<i>Russula brunneoviolacea</i>	contact	MIX (11)		+	Azul et al., 2010
<i>Russula chloroides</i>	contact			+	Azul et al., 2010
<i>Russula cyanoxantha</i>	contact			+	Azul et al., 2010
<i>Russula densiflora</i>	contact		MIX (9)	+	Azul et al., 2010
<i>Russula fellea</i>	contact	BB (16) MIX (11)	BB (19)	+	Azul et al., 2010
<i>Russula foetens</i>	contact			+	Azul et al., 2010
<i>Russula heterophylla</i>	contact			+	Azul et al., 2010
<i>Russula nobilis</i>	contact		BB (4)	+	Azul et al., 2010
<i>Russula puellaris</i>	contact			+	Azul et al., 2010
<i>Thelephora</i> sp.	medium			+	Azul et al., 2010
<i>Thelephora terrestris</i>	medium			+	Querejeta et al., 2009; Azul et al., 2010
<i>Tomentella</i> sp.	medium	BB (5) MIX (2)	BB (5) MIX (6)	+	Richard et al., 2011; Gehring et al., 2020; Patterson et al., 2019; Maghnia et al., 2017
<i>Tomentella badia</i>	medium			+	Azul et al., 2010
<i>Tomentella botrydoides</i>	medium		BB (5) MIX (11)	+	Azul et al., 2010
<i>Tomentella ellisii</i>	medium			+	Azul et al., 2010
<i>Tomentella stuposa</i>	medium			+	Azul et al., 2010
<i>Tylopilus felleus</i>	unassigned	SS (10)	SS (6)		
<i>Tylospora asterophora</i>	short	SS (6)	SS (7)		
<i>Xerocomellus chrysenteron</i>	long	SS (5)		+	Shi et al., 2002
<i>Xerocomellus cisalpinus</i>	long				
<i>Xerocomellus pruinatus</i>	long	BB (7) MIX (8) SS (14)	MIX (6) SS (10)		

## 2 Figures

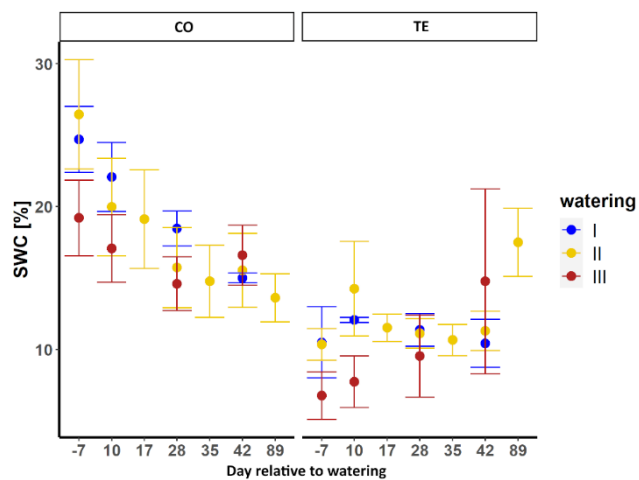


**Figure S1** Average soil water content (SWC) in percent of plots within the different watering campaigns (I = plots 7 & 8, II = plots 3, 4, 11 & 12, III = plots 5 & 6) during the measuring period. CO represents controls and TE rewatered plots. Error bars display the standard error. Data were made available by Grams et al., 2021.

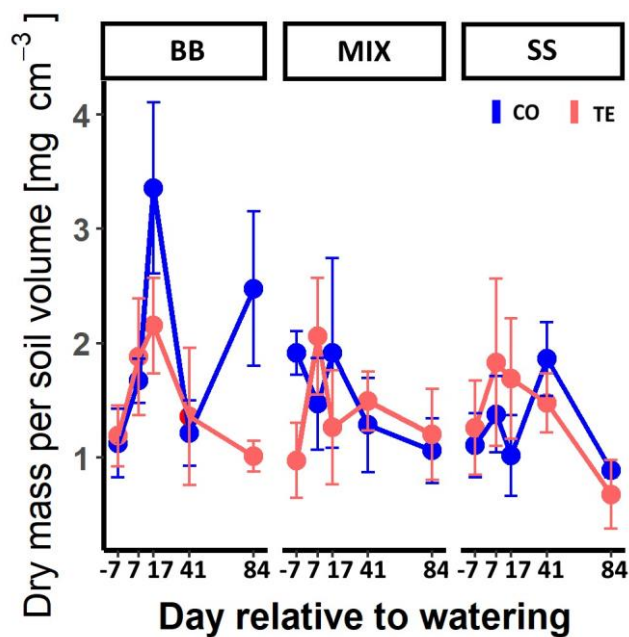


**Figure S2** Fine-root biomass in all rooting zones (BB = beech monospecific, SS = spruce monospecific, MIX = mixture) after drought release. CO represent control roots and TE roots in recovering plots. Mean values with standard errors.

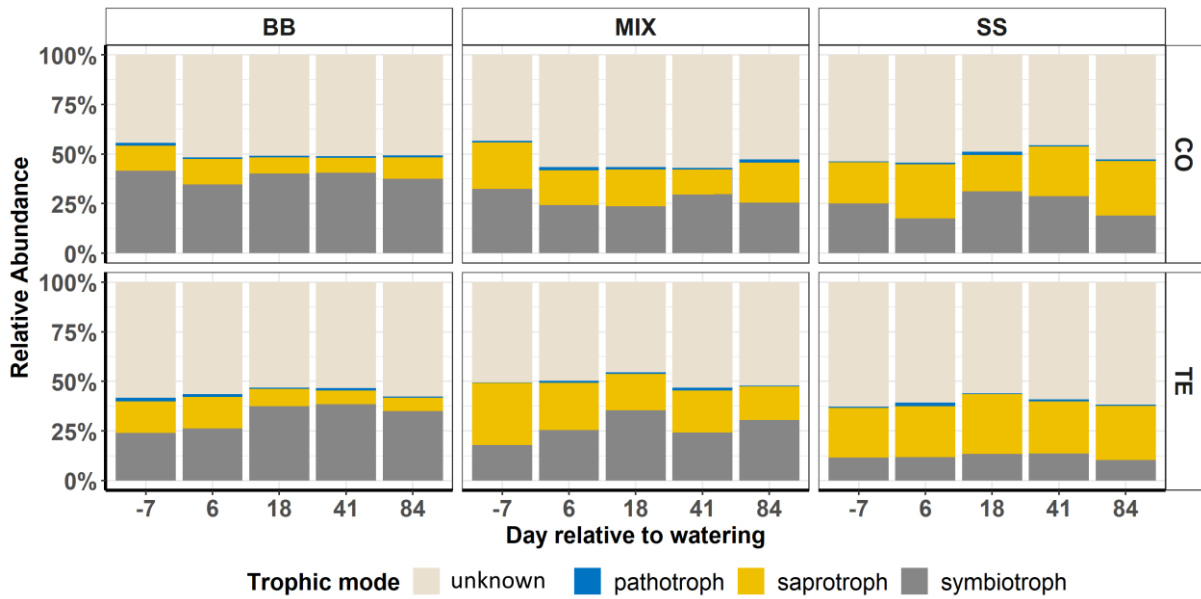


**Figure S3** Summed up relative abundance of unknown, pathotrophic, saprotrophic and symbiotrophic trophic modes of rDNA based root-associated fungal communities after watering in control (CO), former drought (TE) plots, in each of three tree rooting zones: beech monospecific (BB), spruce monospecific (SS) and mixture (MIX).

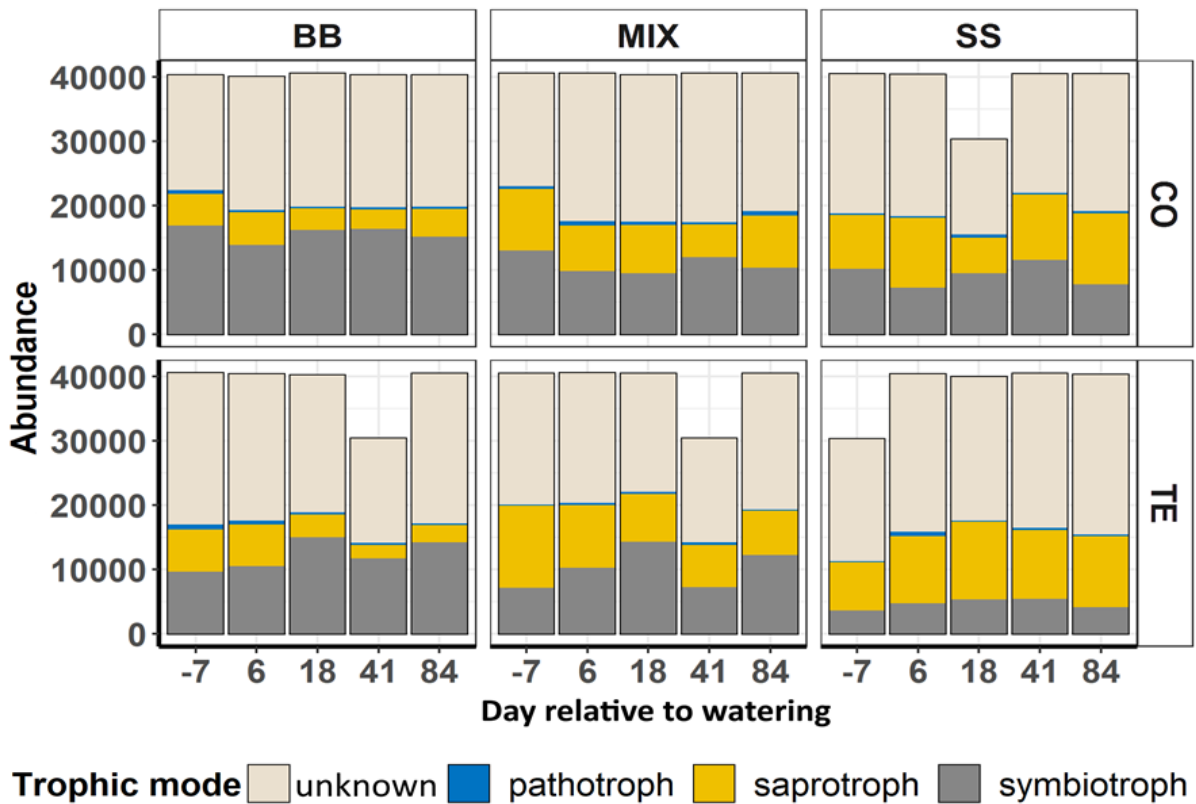


**Figure S4** Summed up abundances of unknown trophic modes, pathotrophic, saprotrophic and symbiotrophic fungi after watering separated by control (CO), former drought (TE),

beech monospecific (BB), spruce monospecific (SS) and mixture (MIX) within the root-associated fungi of rDNA based communities.

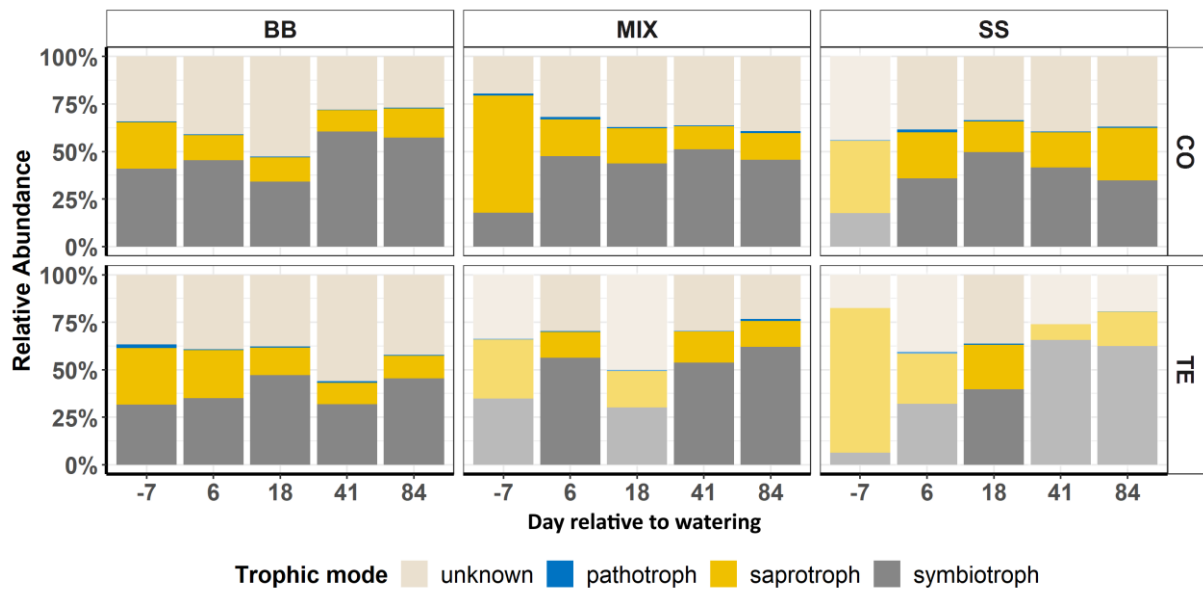


**Figure S5** Relative abundances of unknown, pathotrophic, saprotrophic, symbiotrophic and metabolically active root-associated fungi after watering separated by control (CO), former drought (TE), beech monospecific (BB), spruce monospecific (SS) and mixture (MIX). Light bars indicate results with less replicates.

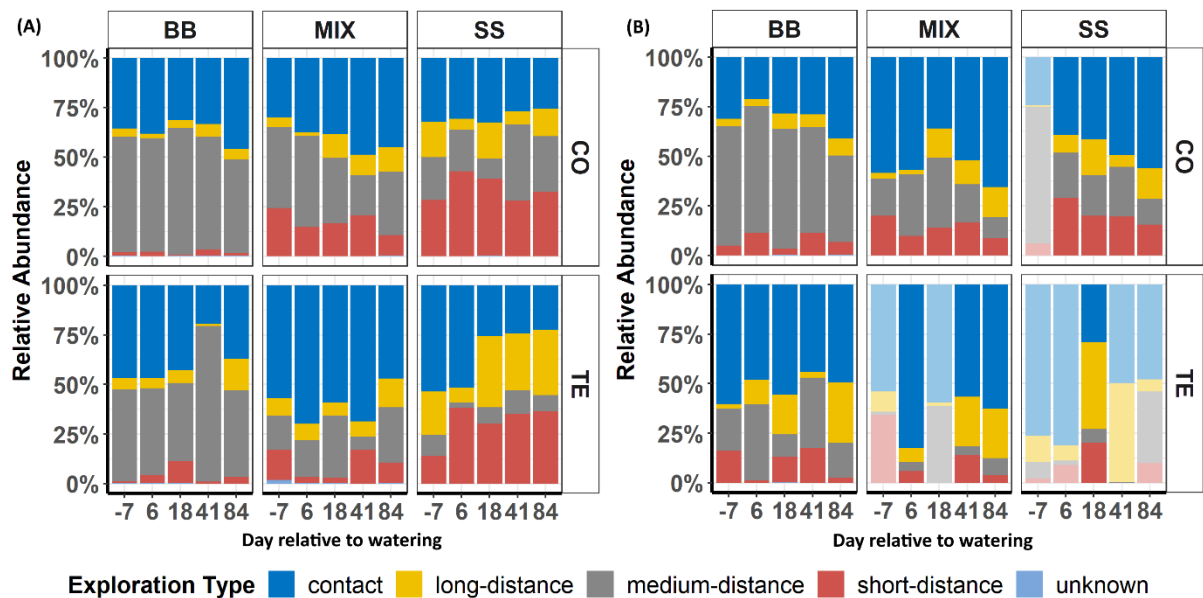


**Figure S6** Summed up relative abundance of contact, long-distance, medium-distance, short-distance and unknown exploration types of root-associated fungi of (A) rDNA based communities and (B) metabolically active root-associated fungi after watering separated by control (CO), former drought (TE), beech monospecific (BB), spruce monospecific (SS) and mixture (MIX). Light bars indicate results with less replicates.

## References

- Grams, Thorsten E.E., Benjamin D. Hesse, Timo Gebhardt, Fabian Weigl, Thomas Rötzer, Benedikt Kovacs, Kyohsuke Hikino, et al. 2021. “The Kroof Experiment: Realization and Efficacy of a Recurrent Drought Experiment plus Recovery in a Beech/Spruce Forest.” *Ecosphere* 12 (3). <https://doi.org/10.1002/ecs2.3399>.
- Nickel, Uwe T., Fabian Weigl, René Kerner, Cynthia Schäfer, Christian Kallenbach, Jean C. Munch, and Karin Pritsch. 2018. “Quantitative Losses vs. Qualitative Stability of Ectomycorrhizal Community Responses to 3 Years of Experimental Summer Drought in a Beech–Spruce Forest.” *Global Change Biology* 24 (2): e560–76. <https://doi.org/10.1111/gcb.13957>.
- Põlme, Sergei, Kessy Abarenkov, R. Henrik Nilsson, Björn D. Lindahl, Karina Engelbrecht Clemmensen, Havard Kauserud, Nhu Nguyen, et al. 2020. “FungalTraits: A User-Friendly Traits Database of Fungi and Fungus-like Stramenopiles.” *Fungal Diversity* 105 (1). <https://doi.org/10.1007/s13225-020-00466-2>.
- Tedersoo, Leho, Sten Anslan, Mohammad Bahram, Sergei Põlme, Taavi Riit, Ingrid Liiv, Urmas Kõljalg, et al. 2015. “Shotgun Metagenomes and Multiple Primer Pair-Barcode Combinations of Amplicons Reveal Biases in Metabarcoding Analyses of Fungi.” *MycKeys* 10: 1–43. <https://doi.org/10.3897/mycokeys.10.4852>.